dsPIC-based Digital Signal Processing Techniques and an IT-Enabled Distributed System for Intelligent Process Monitoring and Management

Raees Ahmed Siddiqui, BSc. MSc.

A thesis submitted in candidature for the degree of Doctor of Philosophy of the Cardiff University

September 2008

Intelligent Process Monitoring and Management (IPMM) Centre, Cardiff School of Engineering, Cardiff University

UMI Number: U585115

UMI

Dissertation Publishing

ProQuest

Declaration

This work has not previously been accepted in substance for any degree and is not concurrently submitted in candidature for any degree.

Signed .... (Candidate)   Date ....25.Sep.2008.
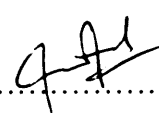
Statement 1

This thesis is being submitted in partial fulfillment of the requirements for the degree of PhD.

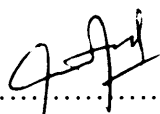Signed .... (Candidate)   Date ..25. Sep 2008.
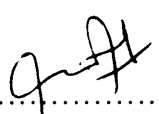
Statement 2

This thesis is the result of my own independent work/investigation, except where otherwise stated. Other sources are acknowledged by explicit references.

Signed .... (Candidate)   Date ...25. Sep 2008.

Statement 3

I hereby give consent for my thesis, if accepted, to be available for photocopying and for inter-library loan, and for the title and summary to be made available to outside organisations.

Signed .... (Candidate)   Date ...25 Sep 2008.

Summary

dsPIC Technology employs a powerful 16-bit architecture into single-chip devices that seamlessly integrate the diverse attributes of a microcontroller with the computation and throughput capabilities of a digital signal processor in a single core. The key element of this dissertation is to explore how dsPIC has influenced the applicability of research in e-Monitoring systems. At the same time dsPIC has offered the opportunity to develop methodologies which were previously not even considered. The dsPIC devices are used, in this research, for front end data acquisition, signal processing and communication tools within a proposed monitoring architecture.

In this work, novel digital signal processing (DSP) techniques are developed for the monitoring of an example application, namely the challenging one of tool breakage in milling operations. The monitoring regime is implemented on the dsPIC and its capabilities for real-time frequency analysis; using overlap FFT and Multiband IIR Filters with dynamic coefficient selection techniques is explored. The developed systems are tested for various cutting conditions using existing machine tool signals and tool breakage is detected reliably in real-time.

In attempting to enhance the accuracy of tool monitoring it is evident that the depth of cut (DOC) is an important parameter and achieving its on-line monitoring provides valuable information for condition monitoring. A systematic approach is adopted for the analysis and selection of ultrasonic sensors for distance measurement. A DOC monitoring system is developed using the dsPIC as the data acquisition and processing core. To achieve reliable results, various DSP algorithms are developed, implemented and verified for their effectiveness.

The system integration stage combines the above elements for robust and reliable decision making and provides communication of the generated information to support management function using the internet and GSM connectivity. This integration enables an enhanced process management system which is capable of identifying all significant events, for offline analysis and subsequent diagnosis in addition to the real time diagnostic mode.

Dedication

To Rameen and Shaheen!

Contents

Acronyms

AC	Alternating Current
ACK	Acknowledge
ADC	Analogue to Digital Converter
AE	Acoustic Emission
AGU	Address Generation Unit
API	Application Programmers Interface
AR	Auto Regressive
ARMA	Auto Regressive Moving Average
ARP	Address Resolution Protocol
ARV	Automatic Voltage Regulator
ASPS	Automated Sensory and Signal Processing Selection System
BP	Back Propagation
CAN	Controller Area Network
CISI	Cutter Insert Self Index
CN	Change Notification
CNC	Computerized Numeric Control
CPU	Central Processing Unit
CRC	Cyclic Redundancy Checksum
CZT	Chirp-Z Transform
DAQ	Data Acquisition
DC	Direct Current
DCS	Distributed Control System
DFT	Discrete Fourier Transform
DHCP	Dynamic Host Configuration Protocol
DLC	Data Length Code
DMA	Direct Memory Access
DOC	Depth Of Cut
DSC	Digital Signal Controller

DSP	Digital Signal Processor/Processing
DWT	Discrete Wavelet Transform
ECG	Electrocardiograph
EEPROM	Electronically Erasable And Programmable Read Only Memory
EOF	End of File/Field
eTCM	Embedded Tool Condition Monitoring System
EWMA	Exponentially Weighted Moving Average
FEN	Front End Node
FFT	Fast Fourier Transform
FIFO	First In First Out
FIR	Finite Impulse Response
FPGA	Field-Programmable Gate Array
FS	Fieldbus Server
FS	Full Scale
FT	Fourier Transform
FTP	File Transfer Protocol
GA	Genetic Algorithm
GSM	Global System For Mobile Communications
GTM	Genetic Tool Monitor
HHT	Hilbert–Huang Transform
HSP	Hardware Signal Processor
HTML	Hypertext Mark-up Language
HTTP	Hypertext Transfer Protocol
IC	Input Capture
ICD	In-Circuit Debugger
ICE	In-Circuit Emulator
ICMP	Internet Control Message Protocol
ID	Identifier

IDE	Integrated Development Environment (MPLAB)
IDE	Identifier Extension Bit (CAN message)
IE	Internet Explorer
IFFT	Inverse FFT
IIR	Infinite Impulse Response
IMF	Intrinsic Mode Frequency
INT	Interrupt
IP	Internet Protocol
IPMM	Intelligent Process Monitoring and Management
ISO	International Standards Organisation
ISR	Interrupt Service Routine
IT	Information Technology
ITDA	Improved Time Domain Averaging
IVT	Interrupt Vector Table
JTAG	Joint Test Action Group
LAN	Local Area Network
LCD	Liquid Crystal Display
LED	Light Emitting Diode
LMS	Local Monitoring System
MAB	Message Assembly Buffer
MAC	Multiply And Accumulate (DSP)
MAC	Medium Access Control (Network)
MCU	Microcontroller Unit
MD	Mahalanobis Distance
MF	Mean Frequency
MIPS	Million Instruction Per Second
MPFS	Microchip File System
NaN	Not a Number
NC	Non Contact

NI	National Instruments
NIC	Network Interface Card
NN	Neural Network
NTP	Network Time Protocol
OA	Orthogonal Array
OEE	Overall Equipment Effectiveness
OSI	Open System Interconnection
OTP	One Time Programmable
PB	Pass Band
PC	Program Counter
PC	Personal Computer
PHY	Physical
PIC	Peripheral Interface Controller
PLL	Phase-Locked Loop
PR3	Timer3 Period Value/Register
PSV	Program Space Visibility
PSVPAG	Program Space Visibility Page
PTSN	Public Switched Telephone Network
RC	Resistor-Capacitor
RCFMA	Recursive Crest Factor Monitoring Algorithm
REI	Relative Energy Index
RISC	Reduced Instruction Set Computing/Computer
RMU	Remote Measurement Unit
RPM	Revolutions Per Minute
RTR	Remote Transmission Request
RTSP	Run-Time Self Programming
S/H	Sample and Hold
SARA	Speed Arrival Signal
SB	Stop Band

SLIP	Serial Line Internet Protocol
SME	Small To Medium Enterprise
SMS	Short Message Service
SNEO	Smoothed Non-Linear Energy Operator
SNR	Signal To Noise Ratio
SoC	System On Chip
SOF	Start Of Frame
SPI	Serial Peripheral Interface
SPS	Samples Per Second
SRAM	Static Random Access Memory
SSTA	Zero Speed (Speed Stationary) Signal
STFT	Short Time Fourier Transform
SU	Subscribed System User
SVM	Support Vector Machine
TCM	Tool Condition Monitoring
TCMS	Tool Condition Monitoring System
TCP	Transmission Control Protocol
TCP/IP	Transmission Control Protocol/Internet Protocol
TDA	Time Domain Averaging
TEEP	Total Effective Equipment Productivity
TFI	Tool Fracture Index
TMAC	Tool Monitor Adaptive Control System
TMR3	Timer 3 Module
TREV	Tool Rotation Energy Variation
TRS	Tool Recognition System
TXREQ	Transmit Request Bit
UART	Universal Asynchronous Receiver Transmitter
VDI	Visual Device Initializer

Sdc	Close Limit of Measuring Range
Sd	Measuring Range =*Sde-Sdc*
TMR_{RISE}	Timer Value at Rising Edge of Pulse
TMR_{FALL}	Timer Value at Falling Edge of Pulse
C_{air}	Speed Of Sound In Air
t_{in}	Time Duration of the Sensor output Pulse
T_c	Temperature in Centigrade
$x(m)$	Input Signal in Discrete Time Domain
$y(m)$	Output Signal in Discrete Time Domain
$h(k)$	Impulse Response of The Filter
K	Length of The Filter

List of Figures

List of Tables

Contents of the Attached CD-ROM

Appendix A

dsPIC30F Family Reference Manual

dsPIC30F Programmers Reference Manual

dsPICDEM1.1 Development Board Users Guide

Microchip TCP/IP Stack Application Note (AN833)

SNMP Agent Application Note (AN870)

Appendix B

Tool Breakage Simulation (AVI file)

Tool Breakage Simulation (Power Point Sideshow file)

Appendix D

UNAM Ultrasonic Analog Sensor Datasheet

PING)))^{TM} Ultrasonic Distance Sensor Datasheet

Appendix G

Full text of Research Publications:

Paper 1 - The Role of Emerging Technologies in eMonitoring

Paper 2 - Adaptable eMonitoring System for Multi-Loop Processes

Paper 3 - Distributed Process Monitoring and Management

Paper 4 - On-Line Measurement of Process Parameter for eMonitoring
Applications

Paper 5 - A Pressure-Based Approach to the Monitoring of a Pneumatic Parallel
Gripper using a dsPIC

Paper6 - Journal Paper- Multi-band Infinite Impulse Response Filtering using
Microcontrollers for e-Monitoring Applications

Chapter 1

Introduction

The manufacturing industry has become highly competitive due to technological growth and companies strive for speed, precision, low cost, and quality. To achieve these goals, components must be produced reliably, precisely, and quickly, with little or no waste and downtime. Manufacturers have to improve the plant machinery or process to stay competitive in the global market. They need to identify and remove defective parts as early in the process as possible and have to avoid introducing new errors in order to improve their process/plant productivity and performance. A machine tool monitoring and management systems can perform a vital diagnostic role in these tasks and help companies remain competitive in the market.

An embedded monitoring system is a monitoring system based on an embedded system which is essentially a special-purpose computer system designed to perform one or a few dedicated functions, often with real-time constraints. Embedded systems can make automated processes more efficient reliable and cost effective by providing close integration, fast response and compact size.

Process and condition monitoring is one of the key elements for improved productivity. In this context e-Monitoring concentrates on the real-time monitoring of industrial machines and processes using automated methods. The principle approach is to detect problems in the early stages when remedial measures are easy to undertake and are cost effective. A tool condition monitoring system (TCMS) monitors the operation of a machine tool so that any deviation from nominal operating conditions can be identified and appropriate correction procedures can be instituted. This capability enables the production of precision, quality, and consistent parts.

The technological breakthrough in embedded technology made in recent years has marked the development of solutions which have seamlessly combined the features of

two contrasting devices such as a microcontroller and a digital signal processor into a single core. Traditionally a microcontroller based system lacked the sophisticated signal processing features and a DSP based system did not have integrated peripherals and communication interfaces.

Digital signal processing (DSP) is one of the most powerful technologies that have shaped science and engineering fields. The application of DSP involves developing and implementing specialized techniques for a particular area of interest. DSP algorithms can be powerful tools that provide algorithmic solutions to different monitoring problems such as the signal analysis of machine tool signals for tool health monitoring. For example, digital filters provide several benefits over their analog counterparts. These algorithms were traditionally implemented using PCs, dedicated digital signal processing (DSP) chips or field programmable grid arrays (PGAs). While these solutions are very efficient for their purpose, they only perform one function in the system and can be both expensive and large. An alternative solution is to utilize dsPIC microcontrollers to implement DSP algorithms in less space and at lower cost.

The research presented in this thesis aims at exploring the feasibility of using dsPIC devices in monitoring systems, by researching and implementing techniques (especially signal processing algorithms) which can be effectively deployed and used for real-time monitoring tasks. It goes on to explore the use of dsPIC devices for improved data analysis with the effective transfer of data using CAN bus communication and Ethernet, and Internet and mobile communication to present the information to concerned users in real-time. The dsPIC devices have been used in this work to their best potential in order to achieve all of these features in the developed monitoring system. The thesis is organized into the following chapters.

Chapter 2 discusses the major motivations behind this research. The importance of digital signal processing for e-Monitoring is identified along with the needs and demands of modern manufacturing industry and a holistic view about the requirements and role of e-Monitoring systems for such applications is presented. The present implementation of the tool condition monitoring techniques is described with a focus on the scarcity of embedded system and limited capabilities of microcontroller based implementations. This narrows down to the requirement of signal processing method

2

implementations at the microcontroller level for achieving an effective Tool Condition Monitoring System (TCMS) to provide a focus on the main objectives of this research.

A literature review is provided in Chapter 3, encompassing tool condition monitoring techniques, methods and systems researched in the past and the capabilities of some commercial tool condition monitoring systems. The review addresses different aspects of the researched system in terms of sensing methods, data acquisition, signal processing and data analysis including decision making. The influence and significance of depth of cut (DOC) information in milling operations is analysed. It further explores the hardware platforms used for implementation of the techniques focusing on embedded and Information Technology (IT) enabled systems. It explores the merits and demerits of different systems with a view to finding their best possible utilization.

Chapter 4 describes the capabilities and features of the dsPIC technology proposed for the e-Monitoring system while describing the tiered system architecture and its operation. It starts with a discussion on the requirements of monitoring systems and the basis of the technology selection. The dsPIC30F6014 microcontroller is explained in detail by describing its enabling features utilized for the realization of required functions at different tiers such as data acquisition, signal processing and CAN and Ethernet communication along with the development tools and libraries utilized in the research. It also explains the operation of various modules designed to achieve such functions and addresses data compression techniques used to handle raw data transfer between different tiers and GSM connectivity for SMS communication to mobile devices.

Next two chapters describe novel signal processing techniques developed for on-line cutting tool breakage detection in real-time. These demonstrate the signal processing capabilities of dsPIC microcontrollers. The two alternative ways of achieving the monitoring system are investigated. These are Multiband Infinite Impulse Response (IIR) Filtering and the Overlap Fast Fourier Transform (Overlap FFT). The IIR Filter technique was developed and tested first because it was a progression on PIC based work which utilized a hardware based analogue filter for the filtering of each frequency component. The Overlap FFT technique utilizes more of the signal processing capabilities of dsPIC and provides real-time frequency analysis. For convenience,

because the frequency spectrum has to be considered first for better understating of milling cutting forces, the Overlap FFT is presented before the IIR Filter technique. It is worth noting that for both techniques the spindle load has been used as source of information thus eliminating the need for any additional sensors.

Accordingly, Chapter 5 explains the novel Overlap FFT technique for real-time frequency analysis of machine tool signals. The basis of tool breakage detection utilizing frequency analysis is discussed with a developed cutting force model. Essential background and theory is provided for the understanding of the technique. The chapter includes the description of designed hardware as well as software used in the implementation of the technique. The selection of different parameters is presented logically along with experimental results. Tool monitoring simulation results confirm the effectiveness of the technique with intelligently chosen parameters. The real-time results of different tests are presented and analysed to extract distinguishing features for the decision making process. The effectiveness of the supporting hardware technology in terms of system requirements is analysed and discussed along with the achieved tool breakage detection speed and the computational capabilities of system for additional signal processing algorithms.

Chapter 6 describes the novel Multiband IIR filtering and dynamic coefficient selection technique for monitoring applications that require simultaneous multiple frequency estimation, such as tool health monitoring. It describes the design, practical implementation and real-time results of a dsPIC based system utilizing this technique. The supporting hardware and software are discussed in detail. It also discusses a time domain analysis technique called Tool Rotation Energy Variation (TREV). Both techniques (IIR Filtering and TREV) are combined to detect and confirm tool breakage and are compared in terms of their efficiency and robustness.

Depth of Cut (DOC) information is very critical in the milling process monitoring. It affects the signals related to tool health. Chapter 7 presents a monitoring system to measure the DOC using ultrasonic sensors and considers the possible advantages of on-line DOC measurement. It discusses the supporting hardware and software for the system design and implementation. The analysis and selection of ultrasonic sensors is presented with comprehensive test results. The developed and deployed signal

processing algorithms (Moving Average, Block Average, Sensor Data Synchronization and Spike Detection & Removal) are also presented. The on-line DOC measurement tests are presented along with the effects of swarf and system's ability to measure the DOC reliably under these conditions.

Chapter 8 presents a structure of the integrated system as an effective and complete e-Monitoring solution enabling a process monitoring system. It also presents the design and implementation of additional features in the system including Ethernet and Internet Connectivity. It also discusses the system's ability to reliably detect tool health using commonly occurring events during the milling process and discusses a process management strategy enabled by the research provided in the thesis.

Chapter 9 presents the important conclusions drawn from this research. These conclusions are based on the results obtained from the implementation of the digital signal processing techniques on the designed hardware with supporting software. It also presents the main contributions of this research work and identifies the needs for the future work emerging from the findings of this research.

The suitability and capability of the dsPIC technology for the e-Monitoring Systems has been investigated thoroughly and been shown to be appropriate for such applications. The research has been focused on the areas where the potential of dsPIC technology can be exploited to achieve a cost effective, robust, efficient and reliable TCMS. However the complexity of the problem does not allow the resolution of all the relevant issues. Therefore this research is presented as a contribution to the overall area of e-Monitoring and embedded signal processing systems. The keywords "author" and "researcher" have been used to refer to the writer of this thesis.

Chapter 2
Research Motivation

The importance of monitoring systems for industrial machines and processes cannot be over emphasized. The efficient and cost effective implementation of such systems not only helps in achieving process reliability but also improves the product quality and system productivity and availability which are directly linked to failure rate, failure detection time and associated repair times. Minimizing these factors through an effective monitoring and maintenance strategy can reduce machine down times and production losses and thus improve the overall equipment effectiveness (OEE). OEE is the product of system availability (dependent on down time losses), performance (dependent on process health) and quality rate (dependent on tool health). These factors are interlinked and if a tooling failure goes undetected due to the absence of an effective monitoring system, it will not only decrease the product quality but also require additional set up costs once detected and rectified.

An effective on-line monitoring system can also support un-manned operations that can enable the machines to be operated round the clock. This may be used to improve the total effective equipment productivity (TEEP), which is the product of machine loading and OEE. Where OEE measures effectiveness based on the scheduled hours, TEEP measures effectiveness against calendar hours. A monitoring system can increase the effective productivity of the system through increased operating times and reduce the cost by providing un-manned maching capabilities.

The tool condition monitoring system designed for the monitoring of tool breakage and associated faults requires sophisticated digital signal processing techniques. The complex nature of the milling operation and involved dynamics require that the identified signal be processed with advanced algorithms such as frequency domain analysis. Researchers have proposed complex signal processing algorithms and have deployed them on PCs. Very few implementations have utilized embedded technology.

Microcontrollers provide flexible solutions combining analog and digital components into one chip. Interrupt driven architectures make them more suitable for monitoring applications where sensing modules can work independently and generate an interrupt when they need the CPU's attention. In this way software is simplified and the system becomes efficient. The Intelligent Process Monitoring and Management (IPMM) group at Cardiff University has used 8-bit PIC microcontroller for monitoring applications and have identified their limitation in terms of processing speed, limited memory, insufficient hardware support to run signal processing algorithms and limited ADC resolution.

The dsPIC microcontrollers can provide enhanced processing power and greater integration as compared to their predecessors. They not only provide higher throughput (while operating at lower clock speeds) but also provide the DSP capabilities in microcontroller architecture. In undertaking this research it was determined that these devices had the potential to not only replace the 8-bit PIC microcontroller but also provide the DSP functionality which was previously achievable with PCs only. This was one of the major motivations behind this research activity. This will harness the microcontroller based embedded monitoring system with the computing power of an advanced DSP processor or a PC. Another motivational factor was that although previous IPMM work has been undertaken on microcontrollers but none had been undertaken using dsPIC.

Previous experience indicates that manufacturing industry is only willing to invest in monitoring systems when they provide low cost to benefit ratios. There has been a vast amount of research in TCMS area but very little practical, reliable and low cost monitoring systems have been realized. Most TCMS utilize expensive sensors such as dynamometers which not only increase the cost but also restrict the working area and hinder machine capabilities. Al-Habaibeh and Gindy [2.1] has suggested that to get sufficiently reliable results, the cost factor may be as high as £19,900, which is almost half of the price of a normal machine tool used in SMEs. This factor has limited the utilization of TCMS in industry. Therefore for a cost effective system the design and management costs need to be minimized. The improvement of cost effectiveness thus provided another motivation behind this research. The dsPIC technology provides features which provide low-cost system development with free software development

tools, integrated features such as high speed, high resolution, and multi channel Analog to Digital Converter (ADC) and CAN and other communication interfaces.

Real-time and reliable tool breakage detection with a minimum number of false alarms is an important factor in automated machining. The generation of false alarm will reduce the machine tool's availability whereas an undetected fault or delayed detection will reduce the product quality and affect the performance rate. Therefore a highly reliable and real-time monitoring system is essential for improving the OEE and TEEP of manufacturing systems. Similarly flexibility of the monitoring system is another important design criterion if the system is to succeed in the competitive industrial world. It is vital that the system can respond to potential internal or external changes affecting its value delivery, in a timely and cost-effective manner. This normally refers to the ability of the system to be used for different conditions especially different applications with changed parameters. To meet these needs any system should have the capability to deal with different signals in different scenarios thus providing more flexibility. To achieve this flexibility, the research is focused on engineering a reliable monitoring system that does not require any hardware infrastructure changes for this purpose.

There has been a vast amount of research activity in estimating tool life and tool wear. Cutting speed and feedrate can be estimated by monitoring the signals related to spindle and axis drive systems respectively. At the moment no viable system has been reported where automated depth of cut (DOC) monitoring or measurement is supported. Researchers monitoring, predicting or modeling tool conditions are assuming that the DOC will be constant through out the tool life cycle. The DOC measurement has been attempted as a challenge and has been another motivation for this research activity.

To exploit the integration capabilities provided by the embedded devices distributed system architecture is considered in this research. Utilizing distributed concepts the monitoring tasks are assigned to different nodes in an intelligent way so that each node is responsible for monitoring a certain aspect of the system. The information between the nodes is shared through message passing and decisions from the nodes are integrated to produce a final decision. Thus a distributed, integrated embedded system design using dsPIC microcontroller has remained an important motivational factor

behind this research. This not only combines the processing power of embedded devices but also enables the system as a whole to accomplish tasks beyond the individual cumulative processing capabilities of these devices.

Embedded devices are getting increasingly connected and are more and more involved in network communications. These devices are now able to communicate using the network/internet protocols that were previously used by PCs. Internet connectivity is widely available and its use is popular with technical as well as non-technical people. It provides an easy method of communication resulting in remote data access. Mobiles have become a basic necessity of modern life and are considered as the most effective way of voice and data communication. The timely communication of the data to the users is a primary requirement of an effective TCMS. The data communication and its presentation in an accurate and desired format were addressed and the dsPIC technology was utilized for this purpose. The designed monitoring system is capable of analyzing the data locally or transferring it to higher tier for further analysis. The final results are presented to the user via the WebPages and urgent information is sent as Text Message via GSM connectivity.

References

[2.1]   A. Al-Habaibeh and N. Gindy, "A new approach for systematic design of condition monitoring systems for milling processes," *Journal of Materials Processing Technology*, vol. 107, Nov. 2000, pp. 243-251.

Chapter 3

Literature Review

3.1. Introduction

The main objective of this research was to explore the feasibility of using dsPIC devices in monitoring systems, by researching and implementing those techniques (especially signal processing algorithms) which can be effectively deployed and used for real-time monitoring tasks. The selected test-bed application was the condition monitoring of a Kondia B500 milling machine. This chapter is therefore not intended to provide an exhaustive review of cutting tool breakage detection and Tool Condition Monitoring Systems (TCMS). There has been a vast amount research published on tool breakage detection. This review does however present the most relevant and recent work in the field in order to highlight the complexity and challenges of the application area. The review covers the broader aspects of the researched techniques, since they can be used for monitoring of machines/processes other than machine tools. With the pace and extent of technological advancements, the computing platforms, used in the past, rapidly become obsolete as much faster equivalents become available. Therefore this review is concentrated on techniques which are deployed on modern platforms such as the dsPIC microcontrollers.

Section 3.2 details general monitoring techniques, with emphasis on the approaches adopted by the IPMM group. An overview of cutting tool condition monitoring system is provided in Section 3.3. A discussion of sensing methods and sensor-less or multi-sensor options is also provided along with a review of the capabilities of some commercial tool condition monitoring systems. Section 3.4 reviews signal processing and analysis techniques commonly used by researches for tool breakage detection along with final decision making techniques. Section 3.5 highlights the significance of depth of cut (DOC) information in milling operations. Tool condition monitoring systems

specifically utilising embedded technology are discussed in Section 3.6 and IT-enabled systems are reviewed in Section 3.7.

3.2 Monitoring Systems

Process and condition monitoring are useful tools for cost reduction and efficiency improvement in a competitive industrial world. One of the major elements affecting the efficiency of equipment is unnecessary downtime which can potentially be avoided if the process is monitored in real-time. The primary purpose of such monitoring is to detect the potential problems in the system, by monitoring the process information generated by different components of the system, at an early stage when remedial measures are more easily and effectively made. In its most complete form, continuous condition monitoring can provide process health information on-line and in real-time.

The term "e-Monitoring" was used by the Intelligent Process Monitoring and Management (IPMM) centre at Cardiff university, to identify an integrated approach to data capture and analysis, decision making and management reporting based upon a distributed set of embedded devices. The approach locates decision making capabilities close to the source of the data being considered whilst providing enhanced, real-time access to the information generated. The evolution of such systems within the IPMM centre was reported by Frankowiak et al. [3.1]. The current research reported in this thesis is aimed at meeting the specification for cost-effective yet powerful monitoring systems. The approaches to securing and managing the data and information generated by such systems within IPMM research has been previously reported by Prickett et al. [3.2].

The IPMM group has been carrying out condition monitoring research for over 20 years. Originally the research concentrated on machine tool applications, used heavily sensor-based techniques, using PC platforms and interfaces, and with large companies such as BAE and Holroyd. For example, Data for use by the modeling, expert system and maintenance partners in a European project was collected for a prolonged period from three industrial installations, all in Germany or Switzerland. The technology, at the time, required a once per week backup of files onto a tape drive, and for the remote hosts to post (snail mail) the tapes back to the centre in Cardiff. In order to make use of

low-cost microcontrollers, IPMM researchers undertook a project aimed at Small to Medium Enterprises (SMEs) in south Wales. In this project distributed, microcontroller-based systems became the main area of research. There has been an accompanying diversification of application areas. The machine tool work continues, but with PLC controlled systems, process and environmental/ energy systems added to the range of monitoring applications.

With the associated logistics and maintenance issues with sensor-based systems, there was a gradual shift towards sensor-less monitoring approach within the IPMM centre. A lot of research was concentrated in using the exiting controller signals for monitoring purposes. Prickett and Grosvenor [3.3] have reported the non-sensor based approach to machine tool and cutting process monitoring. They suggested that a monitoring system should be developed using the existing information, currently generated and used by the machine controller to monitor the cutting process.

Additional knowledge about process parameters may be invaluable for monitoring but extra sensors would be required for that. Companies generally tend to avoid this because of the additional cost and installation issues. Grosvenor and Prickett [3.4] evaluated this situation on the basis of experiences learnt from various machine tool monitoring projects and established that it may now be timely to incorporate more sensor inputs into the distributed monitoring systems. Several possible monitoring applications were identified where this approach would be beneficial.

Whilst meeting the expectations of using industrial network standards to support the successful operation and deployment of DSP based fault detection as identified by Dassanayake et al. [3.5], the IPMM approach is aimed at performing particularly challenging monitoring tasks that need to be supported by diagnostic capabilities that can deliver instantaneous results. In such situations microcontrollers can act as smart sensor systems to play a vital role in real time data acquisition and analysis. The results can be used to report failures, generate alarms when required and provide summative management information with regard to the action of the process or machine being monitored. Such systems must be able to communicate to the outside world, using all available mechanisms, including sending messages on mobiles telephones if required.

The concept of using a "smart sensor" within a distributed data acquisition architecture was proposed by Ehrlich [3.6]. The generic model produced was based upon a "smart sensor" which was defined as a micro-system associated with an individual or group of transducers and capable of signal conditioning, sampling, calculation and communication. An early example of the efficacy of this type of approach can be found in the work of Baccigalupi et al. [3.7]. In this smart sensor area a number of research activities are being reported, including the milling process related work of Baek et al. [3.8]. Building effective monitoring systems based upon these devices also needs the careful consideration of the supporting communication infrastructure.

3.3   Tool Condition Monitoring

Milling is one of the most common and important metal cutting processes. A typical milling machine consists of a motor driven spindle, which holds and revolves the milling cutter, and a reciprocating adjustable worktable, which mounts and feeds the workpiece. These are almost always subject to computer control, with perhaps a supervisory role being played by a human operative. This leads to several operational problems, one of which is the potential for a cutting tool breakage to go undetected. The dangers of continuing to utilize a broken cutter range from damage to the workpiece through to potential damage of the machine tool. For this reason there has been a great deal of effort deployed aimed at detecting tool breakage. This is not however a simple problem, there are many modes of possible tool failure, from minor to catastrophic, and the response of the system to each mode may be further conditioned by the nature of the task being undertaken.

Tool breakage can be classified as shank breakage and tooth breakage. Shank breakage is failure of the cutter across its entire cross-section. It is readily evident and detectable from spindle load measurements, since the load suddenly rises and then drops to an idle load level following the shank breakage. However, tooth breakage, which is failure of a portion of the cutting edge, may go undetected for a certain period. In this case the load will increase, which may lead to additional tooth fractures and potentially and ultimately to shank breakage. It also degrades the surface finish of the workpiece [3.9].

14

In this research tool breakage will refer to tooth breakage and shank breakage is not considered.

San [3.10] has defined a tool condition monitoring system (TCMS) as "essentially an information flow and processing system in which the information source selection and acquisition (sensors and data collection), information processing and refinement (signal processing and feature extraction), and decision-making based on the refined information (condition identification) are integrated." Any comprehensive TCMS can be sub-divided into three major activities as shown in Figure 3.1. These cover: signal retrieval and data acquisition, signal processing and analysis (feature extraction) and final decision making and classification.
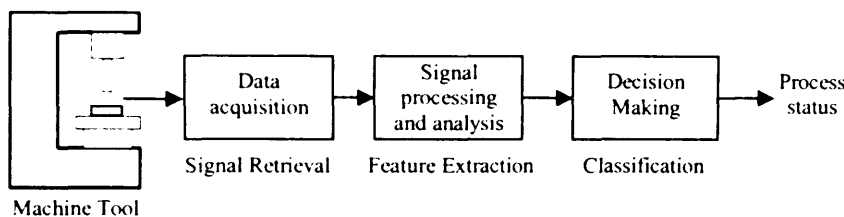
Figure 3.1: Generic representation of a TCMS

TCMS deployed to support these activities are generally based on one of two main techniques: direct monitoring or indirect monitoring [3.11]. The direct monitoring techniques deal with the actual direct sensing of the health of the tool. Examples of these include the use of optical sensors, proximity sensors and touch trigger probes etc. The major practical problem with direct sensing is that since the cutting area is normally inaccessible during cutting, the development of on-line TCMS is not practical. These techniques (as will be discussed in section 3.3.1) normally require the tool to be brought to reference position away from the cutting area. These systems provide in-process measurements when the tool is not cutting by waiting for the current cutting cycle to be completed and for the tool to be positioned at predefined location which means that tool breakage detection is deferred until cycle completion.

Indirect monitoring techniques rely on data retrieved from other sources. These methods make it possible to monitor the cutting tool condition on-line [3.12]. They can

be sub-divided into two further categories: sensor-based and sensor-less techniques. For the former, many monitoring techniques have been developed to detect tool breakage and to estimate tool wear by evaluating the most important characteristics of signals coming from sensors such as dynamometers, accelerometers, acoustic emission sensors, thermocouples, and microphones, and relating them to the predetermined tool conditions. The main disadvantage is that each machine tool needs to be fitted with a sensor system, which often makes this method very expensive and logistically difficult to install [3.12]. Multi-sensor TCMS usually employ sensor-fusion techniques to combine the features from different sensors [3.13].

Sensor-less techniques make use of existing machine controller signals [3.14] along with any sensor signals already available on the machine or process. A review of the approaches for end milling tool monitoring was presented by Prickett and Johns [3.15]. It described the investigation of different sensing techniques, feature extraction methods and decision-making approaches. Indirect measurement methods were considered the most appropriate for tool monitoring, since they allow dynamic assessment, without requiring the stopping of the cutting process. An up-to-date review was provided by and Amer et al. [3.16] which considered the indirect sensing method better than other methods. It reviewed frequency based techniques for tool breakage detection A critical review of the sensors and signal processing methodologies is provided by Rehorn et al. [3.17]. They suggested that end milling tool condition monitoring is the least researched area as compared to turning, drilling or face milling.

The practical ability and success rate of any TCMS relies on two basic elements: first, the number and type of the sensors used and second, the associated signal processing and analysis methods utilised to extract the necessary important information from acquired signals. The first element typically involves expensive hardware which influences the cost of the system, whereas the second element affects the efficiency and the speed of the system. It is worth noting that there exists a balance between two elements; as the number of sensors increases and provides better information retrieval and higher diagnostic reliability so does the overall cost of the system. While extensive research has already been done in this area, no definitive system has been developed for monitoring machines and tools under all cutting conditions.

The required process information for milling operations can be extracted via a variety of methods. These include the measurement of cutting forces, acoustic emission (AE) and/or machine vibrations and the utilization of control signals from spindle and axis drive systems. Spindle system signals typically include load/power, speed and current while axis drive systems usually provide current, position and velocity signals. As a starting point for the review of such approaches, a non exhaustive list of reported research is summarized in Table 3.1. The summary shows that the cutting force signal is the most popular choice. Normally the cutting forces are obtained using a 3-axis dynamometer, fixed between the workpiece and the bed of the milling machine. A small number of researchers have adopted the approach to calculate the cutting force from other signals like axis drive motor current signals, thus eliminating the need for the dynamometer.

Table 3.1: Indirect Sensing Methods

Cutting Force:	[3.8,3.9,3.11,3.18-3.29,3.13,3.30]
Indirect Force:	[3.20,3.23-3.25,3.29]
Acoustic Emission:	[3.26,3.31,3.32]
Vibrations:	[3.11,3.23,3.26,3.33-3.35]
Spindle System Signals:	[3.9,3.14,3.16,3.26,3.34,3.36-3.38]
Axis Dive System Signals:	[3.13,3.20,3.24,3.25,3.27,3.29,3.39-3.42]
Multi-sensor Systems:	[3.9,3.11,3.13,3.26,3.34]
Sensor-less Systems:	[3.24,3.25,3.36,3.37,3.14,3.16]
Vision Sensors:	[3.43]

Lee and Tang [3.18] describe cutting force analysis using the discrete wavelet transform (DWT). The DWT performs a multi-level signal decomposition of the cutting force allowing cutter breakage features to be extracted. It was reported that the use of a second order Daubechies wavelet was sufficient to detect the occurrence of cutter breakage. The DWT was primarily used to de-noise the signal with its output being similar to the signal variations obtained via DC component removal and low pass filtering. No further processing or automatic decision making is described. The workpiece material consisted of gray cast iron blocks mounted on a table type dynamometer (Kistler 8144B). The dynamometer signal was transmitted through a charge amplifier (Kistler 4996) from which the cutting force signal was obtained and

17

recorded at a PC workstation. The level to which the signal should be decomposed was stated to depend on the number of teeth for a given cutting tool. The sampling rate used was selected to be proportional to spindle speed and gave 72 samples per revolution in each case.

Tang et al. [3.19] describe tool failure diagnosis using a neural network (NN). Cutting force signals were obtained from a dynamometer and acquired by a data acquisition card installed in a PC. A cutting force model was derived to establish the relationship between spindle speed and various frequency components present in the frequency spectrum for both healthy and broken cutters. The details of the signal analysis are reported in section 3.4. The system was tested under varying cutting conditions including tool entry and exit but with constant spindle speed. In the opinion of the author, the system would require training if the spindle speed is to be changed.

Baek et al. [3.8] report a tool breakage detection system for face milling that used cutting forces acquired through a dynamometer. The system was developed on a DSP board. An 8th order Auto Regressive (AR) model and a method using calculated band energy were used to extract the features of cutting forces that changed with tool condition. A comparison in terms of accuracy and computation times was presented. Neural networks (NN) were used to classify the tool state as either normal or broken. In each case, the NN was trained with data sets from 240 cutting tests that covered different cutting and tool conditions. Its input included spindle speed, feedrate and DOC in addition to cutting force features. This shows the dependence on these parameters. Baek et al. stated that Fast Fourier Transform (FFT) methods were not used since the signal processing time was not fast enough to allow an FFT to be performed. The AR model was found to be more accurate although it was slower than the band energy method. The system required data equating to 1 tool rotation and 0.17 sec for computation. This represents more than one tool rotation for breakage detection when the spindle speed is 370 RPM or higher. Thus the author anticipates that it can potentially produce an alarm output typically after 2 or more tool rotations post a tool breakage event.

Lee et al. [3.20] measured the cutting force indirectly by monitoring the feed drive AC motor current. The feed drive system was modeled and calibrated, with a tool force dynamometer in place, showing sufficient sensitivity (of the feed drive motor current)

to characterize tool breakage. The work claimed to be an improvement on the work of Altintas [3.21] since it eliminated the need for a dynamometer. A cutter insert self index (CISI) parameter was proposed and used. The index value decreases at tool breakage and then returns to previous normal value even when cutting with broken tooth.

Bhattacharyya et al. [3.22] reported on using combinations of signal processing techniques for the real-time estimation of tool wear in face milling, using cutting force signals. Three different strategies, based on linear filtering, time-domain averaging and wavelet transformation techniques were adopted for extracting relevant features from the measured signals. A sensor fusion technique at a feature level was used in search of an improved and robust tool wear model. It is important to note that one insert tool was used which simplified the algorithms and the tool wear relationships established may not be applicable to multi toothed cutters.

Cao et al. [3.31] proposed a method based on a lifting scheme and Mahalanobis Distance (MD) calculation for detection of tool breakage. The AE signals, generated in end milling process, were acquired from an AE sensor connected to a PC. A bi-orthogonal wavelet with impact property was constructed using a lifting scheme, and the wavelet transform separated AE components from the original signals. Then a Hilbert transform was adopted to demodulate the signal envelope for selected wavelet coefficients allowing salient features, indicating the tool state, to be extracted. Finally, tool conditions were identified directly through the recognition of these features by means of MD. The major advantage of using AE to monitor tool conditions was described as the frequency range of the AE signals. This range is much higher than that of the machine vibrations and environmental noises, and thus, AE can provide a good representation of the material removal process of cutting. The algorithm ultimately extracted tool rotation, its second harmonic and tooth passing frequency components for tool breakage detection purposes. The method relied on finding the MD vectors for all faults to be detected, by performing test cuts. Its accuracy depended on the correctness of the MD vectors. It also required thresholds to be set based on the prevailing cutting parameters, to be adjusted whenever parameters changed. This demonstrated the dependency of the method on cutting parameters such as DOC and feedrate.

Zhang and Chen [3.23] collected vibration signals from a milling machine using a microcontroller-based data acquisition system and development board-based accelerometers. The acquired data was analysed on a PC Laptop using software developed in Visual Basic. FFT and time domain analyses have been used and the results were interpreted visually. Any tool entry and exit events were avoided by programming a delay into the system. The frequency analysis of the vibration signals was reported to show that there was a large rise in the amplitude of the tool rotation frequency component for a damaged tool. The sampling rate was 100 to 300 Hz and was made dependent on spindle rotational speed. Zhang and Chen did not report about data acquisition or processing time

Jun and Suh [3.33] have discussed the analysis of vibration signals in NC milling. The system fed the time-domain vibration signal from a sensor attached to a spindle bracket on the CNC machine, into a PC at a sampling rate of 1KHz. Statistical process control methods were used for monitoring tool breakage where control limits or thresholds were automatically calculated independently of cutting conditions. The performance of a number of proposed statistical process monitoring methods, including the X-bar control scheme, the exponentially weighted moving average (EWMA) scheme, and the adaptive EWMA scheme was compared. The proposed monitoring system was stated to have an expected reliability/success rate of 94% with a 3% false alarm generation rate which is very high in the opinion of the author. Moreover the results presented indicate that tool breakage detection regime is shank breakage detection one.

Yesilyurt [3.34] described the acquisition of vibration signals from spindle mounted accelerometers. The signals were analysed using a scalogram method and the obtained mean frequency was proposed as a distinguishing feature for defect detection at different feedrates. Data for 40 cutter rotations was acquired at 12.5 KHz and stored in a PC. A shaft encoder was used to produce a pulse-per-revolution reference to facilitate analysis. Feedrate was measured by rotary encoders mounted on the feed drive motors. It was observed that the feedrate was significantly influential on the mean frequency. Its variations are relatively responsive to the presence of fault even when the severity of fault is low. A trend indicator was defined to reflect the progression of fault severity

and was reported be very sensitive to any change in the feedrate particularly when the severity of fault is small. This showed a high dependence on the cutting conditions.

Franco-Gasca et al. [3.36] used a spindle motor current-based system deployed on a hardware signal processing unit. The latter was implemented via a field-programmable gate array (FPGA) that was used for acquisition, conditioning, and basic signal monitoring. The system was used to monitor several types of machining process such as drilling, milling, hobbing and turning. The system model was described as being reconfigurable and scalable so that it may be adapted to diverse conditions. It was said to be an economical standalone unit since it did not require either computers or microprocessors. The sampling rate was user-defined (and depended predominantly on the spindle speed) to give the optimum feature set of change in the output of the wavelet transform based data compression stage. The mean value of the feature signal was compared with three fixed thresholds which were selected during training cuts. For the milling process the speed of the system operation was such that it required 3-4 tool rotations to detect tool breakage.

Li and Guan [3.39] describe a minor cutting edge fracture detection algorithm using the feed-motor current signals. The algorithm (reported in Section 3.4) consisted of wavelet-based de-noising, discrete time-frequency analysis, FFT and second differencing. Some typical experiments, the cutter run-out, entry/exit cuts and cutting parameters-variation, have been performed to confirm the robustness of algorithm which was implemented on a PII PC. It required 4 tool rotations (twice the target set in this research) post tool breakage to generate and alarm output at typical settings.

Li et al. published a number of papers on tool breakage detection using feed motor current signals [3.40,3.41,3.44,3.45]. These use different signal processing techniques (including time domain averaging (TDA), permutation entropy and fuzzy logic) and will be more fully discussed in Section 3.4

Bassiuny and Li [3.42] proposed a flute breakage detection method for end milling using feed-motor current signals which were acquired into PC by attaching additional current sensors on the motors. They used a Hilbert–Huang transform (HHT) analysis and a smoothed non-linear energy operator (SNEO) to extract crucial characteristics

from the measured signals to indicate tool breakage. The SNEO output was compared to a threshold which was selected experientially during cutting operation with a healthy cutter. A segment of 64 samples of feed motor current acquired at 1 KHz was captured for processing. Bassiuny and Li recommended that the sample selection should consider a number of cutter teeth and prevailing spindle speed. Wavelets were used for de-noising purposes. The algorithm repeatedly calculated intrinsic mode frequency (IMF) components until a near DC component is obtained. However the most informative IMF depends on the cutting conditions. There was a delay of 0.35 seconds (equivalent to 3.5 tool rotations at 600prm and more on higher speeds) between fracture and the output indicating a broken tool.

Although vision sensor based systems for tool monitoring have been investigated by a large number of researchers, their industrial applications are still in their infancy, because of their high complexity. Lanzetta [3.43] has described a vision system (as part of a tool monitoring system). He identified the advantages of vision sensing as: natural human-like operation, ability to recognize different morphologies, high information content in images, high availability of algorithms, independence from the cutting conditions and sufficient accuracy. An exhaustive classification of the defects in cutting inserts was researched and reported along with the design of automated system to recognize the defects and to measure tool wear. The quantitative parameters required to be used as threshold values were selected from internationally established standards. A defect detection and wear measurement flow chart was then proposed which dealt with a variety of cutter conditions and scenarios. An auto-focus zoom lens was used to maintain uniformity when dealing with different tool sizes and varying distances.

Although the application of vision system has great potential, no results in this particular area have performed to sufficient levels. In the opinion of the author, the reasons behind this may include: sensitivity to normal industrial disturbances, influence of chips, fluids and dirt, the high maintenance requirement for such systems leads to unnecessary downtime, and high investment costs.

Jesús et al. [3.24,3.25,3.46] have published papers relating to different aspects of a sensor-less monitoring system using axis motor driver current signals. Three hardware

signal processors (HSP), based on FPGA were used and the algorithm used was simplified to three equations (Sum of Squares, Wavelet in the form of a multirate FIR filter and Asymmetry) to enable it to be implemented on a one time programmable (OTP) FPGA. They report that time domain signal variations are extremely small for different tool conditions, making it hard to draw solid conclusions. Thus autocorrelation was performed, in the form of asymmetry between two insert forces, to detect different cutter conditions. The asymmetry weighing function was then indicative of the damage to the tool. This assumes that both/all insets cannot have same level of wear or breakage. In [3.25], they discussed the axis motor current and its basic components. In particular the frequency range for the band pass filter was suggested such that it could be successfully used for tool breakage detection.

Tseng and Chou [3.14] interfaced a PC based system to a machine tool and extracted the workload of the spindle motor (from the machine controller) and transmitted the data using an I/O card for further processing. The spindle load fluctuations were used as an indicator for the determination of the machine tool health. They introduced a monitoring index, based on the workload variations and the diameter of the cutter. The variations in spindle load monitored were up to 1.5% of maximum load in case of a worn cutter and 2-4% when the cutter was chipped or broken. Observation of the data indicated that when the tool was about to break, these variations rose to 15-29% of the work load during normal cutting. Depending upon the variations of motor load signal, Tseng and Chou derived three rules to categorize the operation as normal, semi-normal or abnormal states. However it is felt that the designed system may encounter practical problems of generating false alarms, because of the absence of any counter verification strategy before generating any alarm or stopping the process.

In parallel to sensor-less or single sensor based TCMS there has been ongoing research into multi-sensor TCMS. The tool breakage signal from a single measurement may make a misjudgement due to the complicated dynamic characteristics of the cutting process and instability of machine tool itself [3.43]. To counter this issue, integrated approaches based on measurements from several sensors have been proposed by various researchers.

Fu and Hope [3.26] have used force, AE, vibration and current sensors to measure machine parameters and have designed an intelligent monitoring system for the online classification of tool wear. The sensors signals were pre-amplified and filtered. The filtered signals were acquired, and input into a PC, at different sampling rates. The PC was used to extract the statistical and frequency spectrum features from the signals representing different wear values. They suggested mean value calculations for power consumption, standard deviation for vibration and power spectra for the AE and X cutting force component signals respectively. Tool wear was estimated by application of a neural-fuzzy pattern recognition technique and classified into three (new, normal and worn) states of the tool condition.

Cho et al. [3.9] used a support vector machine (SVM) learning algorithm to recognize process abnormalities. Their system utilized multiple sensors to record cutting forces and power consumption. The main element reported was the training of the proposed system for performance improvement and detecting tool breakage. The performance of the developed system was compared to the results from an alternative detection system that was based on a multiple linear regression model. They claim to have achieved a success rate of 75% when using only force signals and 99% when it was used in combination with the power signal.

Although the multi-sensor machine tool monitoring system may be very effective; the additional cost involved in installation of these sensors adds to the overall system cost. As is clearly evident from the research reported by Al-Habaibeh and Gindy [3.11] to get sufficiently reliable results, the cost factor may be as high as £19,900, which is almost half way to the price of a normal machine tool used in SMEs.

3.3.1 Commercial Systems

In today's manufacturing environment there is an increasing demand for tool condition monitoring systems. Many different sensor types, coupled with signal processing technologies are now available, and many sophisticated signal and information processing techniques have been invented and presented in research papers. There has been a considerable research activity and academic work in this area but very few have found their way to commercial applications [3.47]. The reasons are believed to be

either the high cost associated with implementation of suggested techniques or the time required by certain systems to achieve the diagnostics rendering then unsuitable for real-time analysis. Often the inflexibility of the models and algorithms used means that a system will work with a particular tool under certain cutting conditions but will fail to achieve correct diagnostics if the cutting conditions change.

Most commercial systems employ direct sensing methods for tool breakage detection, for example in systems provided by Renishaw Plc (UK), TPS International (USA), and Techna-Tools (USA). They either use touch probes or laser based non-contact methods to verify the tool size and integrity and hence to detect breakage. In either case the tool has to be moved to a reference position where the sensor is installed. These methods as stated provide the in-cycle tool breakage detection but can not detect tool breakage whilst the tool is actually cutting. As a consequence of this, many commercial systems typically work in-cycle rather than providing full in-process, on-line diagnostics.

Renishaw has two different products for detecting tool breakage [3.48]: NC4 (non-contact tool setting and tool breakage system) and TRS2 (tool recognition system). Both systems are laser based but differ in the mode of operation. NC4 (and previous versions NC2 and NC3) projects a laser beam (as shown in Figure 3.2(a)) to the sensor element and the tool has to break the beam. The TRS2 (as shown in Figure 3.2(b)) shines a laser beam onto the tool which reflects the light back to the built-in sensor. The tool must be rotating at 200, 1000 or 2000 rpm to generate a pattern that TRS2 can detect within 2 seconds. It sends a positive integrity signal to controller. It requires 30 seconds to confirm a broken tool.

(a) NC4   (b) TRS2
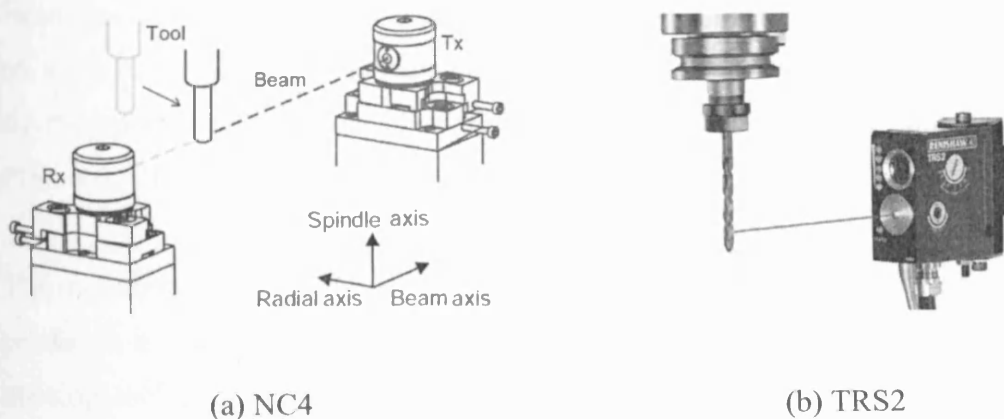
Figure 3.2: Non contact tool breakage systems [adopted from [3.48])

TPS International [3.49] provides "positive contact sensors" PCS 100 and PCs 250 which use a rotating needle to sweep around the machine until needle touches the tool. Similarly Ciro Products [3.50] and Techna-Tool [3.51] provide tool breakage detection products that use wands to check tool position to detect the tool breakage as shown in Figure 3.3. Techna-Tool's BK Mikro 8 is mainly designed for broken tool detection inside the tool changers of machining centers.
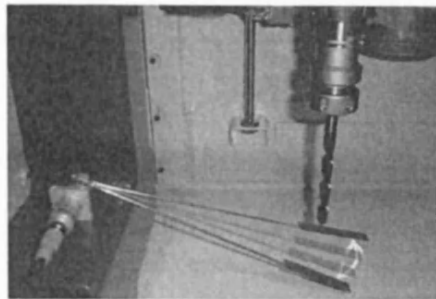
Figure 3.3: Contact-type tool breakage detection systems (adopted from [3.51])

The other category of commercial tool monitoring systems utilizes indirect sensing methods to determine the health of the process. The most common sensing method for tool breakage in commercial systems is spindle power. A power sensor measures the spindle or axis drive power by measuring current and voltage. Power is linearly related to the cutting force load and is preferred to current sensing since current is less sensitive at small loads.

Most of the commercial monitoring systems focus on turning operations and claim to treat the milling operation in a similar way. Jemielniak . [3.52] has compared monitoring systems developed by various suppliers including Artis, Brankamp, Kitstler, Nordmann and Prometec. He found that most systems perform basic monitoring based on static limits or thresholds which are learnt during the teach-in tests or manually set by the operator. Few utilize dynamic limits however. This is the approach used in Prometec's PROMOS [3.53].

The monitoring system offered by Techna-Tools 'Techna-Check 3200', measures true power on a machine spindle or axis motor to determine if there is a broken, dull or missing tool [3.54]. Figure 3.4 shows a typical measured power profile during a machining cycle.
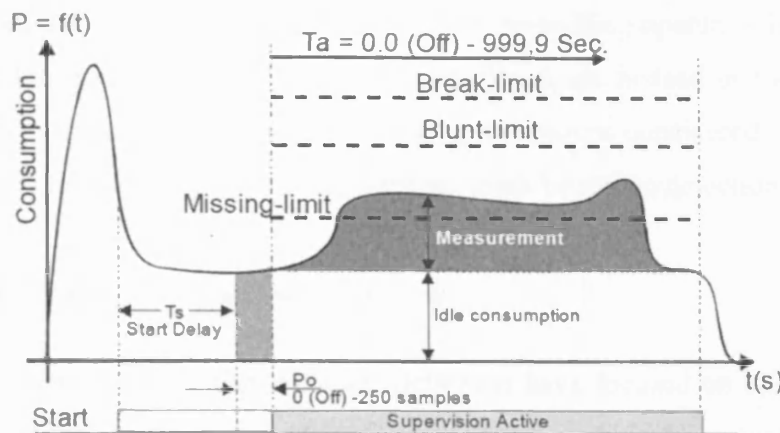
Figure 3.4: Spindle Power profile and limits for tool monitoring (taken from [3.55])

The monitoring starts after the initial peak power has passed and load drops below the missing limit. A start delay is introduced to let the system settle to the idle power consumption level. The idle consumption is the power used just to turn the spindle. High and low limits on idle power determine if a belt has broken or bearings are going bad in the spindle. The measured true power shows the tool condition. For example more power is required as the tool becomes blunt (dull). When the tool breaks a short energy peak or spike is created and if no tool is present or the part has already been cut, the power consumption drops back to idle level. If any of these situations occur the Techna-Check will output a fault alarm and will immediately stop the machine. Other limits such as missing-limit, blunt-limit and broken-limit shown on Figure 3.4 are used for the tool condition monitoring. If the power exceeds the blunt-limit the tool is declared blunt and if exceeds broken-limit it means the tool is broken. A similar approach has been used in 'Power Monitor' system offered by Marposs Ltd [3.56].

The Tool Monitor Adaptive Control System (TMAC) offered by Caron Engineering [3.57] operates on the principle that the horsepower required to cut a part increases as the tool's cutting edges deteriorate. It measures true motor horsepower for spindle and/or feed axes and regulates the feedrate in order to maintain a constant spindle motor horsepower during cutting. It is believed that tool life is extended when a tool cuts continually at its optimum horsepower. This feature is stated to optimize cycle times whilst still providing limits to protect the machine and tool. BranKamp and Artis also offer multi-sensor based monitoring systems with similar adaptive control options.

The review of commercial TCMS revealed the scarcity of the on-line monitoring systems for milling operations. Most systems treat the milling operation like turning or drilling operation and mostly focus on the shank breakage instead of tooth breakage. The next section reports on the signal processing techniques considered by researchers for tool condition monitoring mainly focusing on tooth breakage detection.

3.4   Digital Signal Processing and Analysis

The most recent methods of tool breakage detection have focused on the development of signal processing techniques that can enhance the sensitivity to tool breakage of measurements such as cutting force, acoustic emission and spindle motor current. The effect of tool breakage is usually revealed by an abrupt change in these enhanced measurements, which then for example, exceed a decision threshold. Signal processing thus plays a key role in feature extraction, from the acquired and filtered data, before final decision making. Signal processing methods can be divided into two main categories: Model based and feature based approaches. Table 3.2 presents an overview based on relevant published research, with the research activities grouped according to signal processing methods they used. The Feature based approaches can further be divided into three main categories:

a.   Real time series signal analysis

b.   Frequency domain analysis including filters/band energy methods

c.   Combined time-frequency analysis including wavelets

Mathematical models are used to describe the behaviour of a physical system based on physical laws. Their use enables the calculation of some time dependent quantity, nearly exactly, at any instant of time. The reliability of a model based system is dependent on the capability of the model to accurately and fully represent the dynamic behaviour of the system under all conditions. The model based TCMS approaches then use the difference between calculated and measured cutting forces to detect tool breakage. The modelling of cutting forces in milling has been attempted by various researchers [3.58 - 3.62] and is the subject of on-going research. An alternate approach is to use an auto regressive model, which estimates the output based on the past values of the monitored parameter [3.63].

Table 3.2: Signal Processing Techniques

Model based analysis	[3.8,3.20,3.29,3.21,3.64,3.27,3.58-3.62]
Time Series Analysis	[3.9,3.14,3.20,3.21-3.24,3.27,3.29,3.32,3.33,3.36-3.38,3.13,3.41,3.65,3.30]
Frequency Domain (FFT)	[3.11,3.13,3.23,3.19,3.35],[3.30,3.31,3.34,3.39]*
Time-Frequency	[3.26,3.34,3.39,3.42]
Wavelets	[3.11,3.24,3.18,3.22,3.28,3.31,3.34,3.36,3.39,3.40]
Filters/Band Energy	[3.8,3.16,3.22,3.32,3.34,3.65]

* used as secondary processing method

Since every TCMS employs some form of signal processing techniques, different example applications of these techniques are presented and discussed in this review. In terms of structure, there is an overlap with previous section 3.2 which focused on sensing methods.

Zheng el al. [3.58] have proposed a generalized analytical model for cutting force calculation based on the relationship between the local cutting forces and the instantaneous chip load and integration of the local cutting forces. The model was adopted for face and end milling. The model estimated the frequency spectrum and calculated the cutting forces in angle domain through inverse FFT operation. The model used force constants which were calculated for a particular type of cutter and work piece material using 27 cutting tests in each case. Experimental testing was performed to verify the cutting-force models in the context of angle domain waveform and frequency domain components using cutting force measured form another 6 tests. A Kistler platform dynamometer was used to measure cutting forces at a sampling rate of 2 Ksps. The reported average and maximum absolute percentage errors were 4.4 and 18.2, respectively.

Ritou et al.[3.27] analysed three process-based indicators; tool fracture index (TFI), peak rate (B_m) and relative eccentricity rate (K_m); for tool breakage detection by using a cutting force model. TFI (proposed by Kim and Chu [3.66]) is the ratio of peak-to-valley cutting forces between adjacent teeth, divided by its own past average. The average ratio is intended to prevent the TFI from cutting conditions changes. As proposed by Deyuan et al. [3.67], K_m is the ratio of the difference to the sum between peak forces of adjacent teeth and B_m is similar to the ratio of tooth eccentricity to

maximum chip thickness. The indicators were claimed to be independent of cutting conditions. Experiments were carried out in industrial conditions to check the dependability of the indicators on instantaneous feedrate and DOC. Specific transient cutting conditions encountered during the machining of test parts revealed the indicators to be unreliable in this respect. Consequently a versatile in-process monitoring method was suggested. Based on experiments carried out under a range of different cutting conditions; a new indicator, termed relative radial eccentricity of the cutters, was proposed. This was estimated at each instant and characterized the tool state. It was then compared with the previous tool state in order to detect cutter breakage or chipping. The new approach was reported to be reliable when implemented during machining tests. Cutting forces from a dynamometer were measured at 64 Ksps and a PC was the monitoring platform used. Signals from x and y position encoders were sampled at 500sps. The approach determined the relationship between resultant peak force (for each tooth) and chip thickness by performing trail cuts. The relationship was used to calculate parameters which allowed to the system to avoid false alarms by pausing the monitoring during changes in the tool path. In the opinion of the author this approach may be beneficial in achieving automated machining of one-off components.

The model developed by Long et al. [3.61] described the dynamics of milling processes with variable time delays associated with each cutting tooth. The source of these variable time delays was reported to be the feedrate. The system dynamics were described by a set of delay differential equations with periodic coefficients and variable time delays. Good agreement was claimed to be found between the numerical results obtained from the model and cutting experiments. In the opinion of author this model may be useful when measuring the surface finish of the workpiece.

Tansel et al. [3.64] have proposed a Genetic Tool Monitor (GTM) to identify problems in milling operations by using an analytical model for micro-end-milling operations and an associated Genetic Algorithm (GA). They used the components of cutting force in a horizontal plane to support process related decision-making. Their program requires that all the known parameters including operating conditions and tool geometry are provided as inputs. Depending on operating conditions, one or more unknown parameters can then be estimated. In the opinion of the author this system might only be useful if on-line monitoring of machining was considered and became available.

The second main category represented in Table 3.2 is time series signal analysis and this has been widely used in tool condition monitoring. These techniques rely on calculating the properties of time domain signals such as average, maximum, minimum and peak-to-peak values. Statistical methods (mean, variance etc) used with time varying signals are also usually considered as time domain techniques. These also include time domain averaging, trend analysis, control limits, and energy variations. Time domain methods are being used in commercially available TCMS. Some CNC controllers (including the Kondia B500) provide the facility to set a maximum limit for the spindle load to facilitate tool monitoring. These systems monitor the spindle power and if it exceeds a preset threshold an alarm is generated. Although these methods may be effective in detecting the shank breakage, they may not detect tooth breakage.

Li [3.41] used an improved time domain averaging (ITDA) technique with a floating threshold, for detecting tool breakage using feed drive motor current signals. It was stated that cutting force based methods normally require complex signal processing methods, (higher order time series models, FFT, time-frequency analysis etc) which became a hindrance to real-time application because of the required computation times. ITDA was reported to reduce the errors due to the difference in the period of the signal and the period of the averaging kernel. It used a floating threshold, which was calculated using the average current over last three tool rotations and incorporated a risk factor (which defined the sensitivity of the detection). A large risk factor value would make the detection of breakage less sensitive. The system was shown to detect tool breakage under various cutting conditions. In considering this method the author deems that the threshold is only crossed once on the occurrence of tool breakage. The floating threshold then adjusts to a new value which is larger than the feature value. Thus cross verification of tool breakage is not likely to be possible.

Altintas [3.29] has used an AR model (AR time series filter) to detect tool breakage for milling process monitoring. Cutting forces were predicated from the feed drive motor current. A model of the feed drive control system was used to analyze cutting force measurements from the armature current suggesting its use as a cutting force measurement sensor. The importance of periodicity of milling forces at tooth passing frequencies was highlighted. Average current was sampled by an analog circuit which was triggered and synchronized to the tooth passing interval, by an encoder mounted on

the spindle shaft, using a PC. It was highlighted that tool failure in milling can be detected by adaptively filtering the average current signals at tooth passing periods. It was suggested that whenever a tooth breaks, it doesn't remove any metal and the drive motor current will drop. The next tooth will remove more metal than usual and the current will increase. This pattern of variations will indicate tool breakage. The algorithm compares the residual terms of a first order AR model against a dynamically set threshold. The breakage algorithm was claimed to be independent of cutting conditions and the friction in the drive system. In the opinion of the author the sampling rate for the system was set to match the tooth passing frequency, which seems to be very low for such a critical monitoring task.

The application of AR modeling has been reported by Lee et al. [3.20] in order to determine tool breakage. An indirect cutting force calculated from the feed drive motor current was used. The relationship between the cutting forces and the average motor current was established using linear regression. Lee et al. report the implementation of an algorithm on a DSP board. There are no reported details of the type of DSP used or its computation performance. The main claimed contribution from Lee et al. in terms of signal processing is introduction of a new cutter health index CISI. This index monitors the health of each insert individually. In this way effects of cutter-runout are minimized.

The third category of Table 3.2 namely frequency domain analysis has gained research attention in recent years. The milling operation is well suited application for frequency analysis because of the particular cutting dynamics. Normally machine load is periodic and directly related the tooth passing frequency. When a tooth is broken, the load pattern changes as broken tooth exerts less force and tooth after it has to exert extra force to cut material left by broken tooth. This decrease and increase in load will occur once per tool rotation. The time domain analysis of the load signal can be deceived by cutting operations such as tool entry, exit or change in DOC. However, frequency analysis will be more robust in such circumstances. In the research reported in this thesis the frequency spectrum of the signal is calculated via Fast Fourier Transforms (FFT) and overlap FFT (discussed in Chapter 5) and digital filters (discussed in Chapter 6).

Normally FFT or Time-Frequency analysis has been used in conjunction with wavelets. The wavelets have been used by the researchers mainly for de-noising purposes and the resultant signal is similar to the signal which is obtained after removing the DC and passing the signal through a low pass filter. Normally some additional signal processing methods are required to exploit wavelets for tool breakage detection.

Kasashima et al. [3.62] discussed a milling force model based on the individual radii of the teeth. The model was shown to be in good agreement with experimental results. They used this model to verify a tool breakage algorithm based on discrete wavelets transforms. Data equating to one tool rotation was analysed and it was concluded that for a broken cutter the wavelet coefficients (which were equal to number of teeth) exhibited a "zigzag pattern", the amplitude of which depends on the amount of chipping. The cutting force model was deemed to be directly relevant to the current research and the author carried out further investigations based on it. The model was adapted in Matlab code and was used to verify and justify time-frequency results obtained in this research. The details are reported with in Chapter 5.

Li and Guan [3.39] reported a signal processing method which consisted of wavelet-based de-noising, discrete time-frequency analysis, FFT and second differencing algorithms for the detection of minor cutting edge fracture during end milling. Algorithms when applied sequentially, extracted marked features from the (AC 3-phase) feed-motor current signals which were acquired and stored into a PC. In the process of extracting a marked feature, 64 samples, from current sensors on each phase, were sampled at 1 Ksps. Time-frequency plane calculations, after de-noising of the segment using wavelets, were used to extract the signal features (primary frequency components). The main frequency of interest was calculated based on spindle speed and the number of cutter flute/teeth. A feature point, which was the maximum amplitude value from the frequency domain was then calculated via FFT, with second differencing used to provide a marked feature. Tool breakage was determined to have occurred when the marked feature crossed the threshold value. The computation time of the system was 0.315sec (using a PII PC). It was stated to require 0.379 sec to generate an output (excluding the time required to compute previous two feature points). This equates to 4 tool rotations at typical cutting parameters. Since processing time is much larger than the acquisition time, the author believes that some data is not being analysed

or its computations must be lagging behind. Li and Guan [3.39] have mentioned some limitations including the limited bandwidth of the current sensing system and poor sensitivity of the current system at light loads.

Tang et al. [3.19] used FFT to compute the spectrum of the cutting force signal for tool failure diagnosis. They suggested that, after establishing the relationship between spindle speed and frequency spectrum for a healthy and broken cutter, the frequency components in the spectrum can indicate the tool failure. A NN was used to analyze the outputs from the FFT. The NN was trained using the simulated FFT spectrum under varying cutting conditions. The FFT Spectrum of the acquired force signal is fed into a NN with 25 inputs. The system was reported to be reliable under varying cutting conditions.

The use of scalogram and its mean frequency analysis was proposed by Yesilyurt [3.34] for analyzing the vibration signals of the cutting process. The method also utilized wavelets, Digital filters, FFT and time-Frequency Analysis. The mean frequency was in the range of 800-1800Hz. An energy distribution around 200Hz becomes apparent when defective tooth was cutting. The variations in mean frequency were periodic with tool rotation frequency requiring further analysis if the tool breakage is to be automatically detected.

Chen and Chen [3.35] report the frequency analysis of vibration signals measured using an accelerometer. A vibration sensor model was developed and the effect of a broken cutter was highlighted. Based on the model results, they decided to use FFT. One FFT spectrum was calculated for each test and in particular the tool rotation frequency and its second harmonic were used as key features. The ratio of amplitudes between the features increased at tool breakage. Chen and Chen suggested using both current and past FFT calculations in order to avoid false alarms.

Li et al. [3.40] proposed a method to analyze feed motor current, which composed of the estimation of permutation entropy and wavelet-based de-noising. A 128 point segment of the signal from current sensors was acquired by an ADC operating at 1KHz. A PC, with P4 1.66GHz CPU, was used for analysis. The permutation entropy of a time series is a simple, robust and extremely fast complexity measurement method for

distinguishing the different conditions of a physical system. The normalized entropy $Hp=Hp(n)/\ln(n!)$ with $n=5$ was selected as the feature used to determine tool condition. Two thresholds were calculated from analysis of a series of tests with either no cutting, normal cutter or broken cutter status under various machining conditions. If the Hp value was between the two thresholds then the tool was taken as broken. As this method relied upon two level thresholds, the sensible time to confirm tool breakage was in the order of 0.395 seconds. This equates to 6 tool rotations at the selected spindle speed. The author thinks that it may be prone to DOC variations as a linear trend of Hp is observed with DOC variations.

Al-Habaibeh and Gindy [3.11] proposed an automated sensory and signal processing selection system (ASPS) approach where appropriate sensors and signal processing techniques are selected using Taguchi's method and an orthogonal array (OA). The approach was shown to reduce the cost and complexity of the resultant monitoring system without compromising its ability to detect cutter faults. The technique uses n number of sensory signals and m number of signal processing methods. This gives rise to $m \times n$ possible solutions. In their experiments, they used 15 different sensory signals and 23 different signal processing and feature extraction systems. The signal processing methods were in the categories of: wavelets, average value, standard deviation, power value, kurtosis value, FFT and skew value. The process variables investigated were: normal cutter, broken cutter, 3 levels of DOC, table feedrate and spindle speed. The analysis showed that the system with lowest error, of 8.89%, had a cost of around £19900. The cost could be brought down to under £3000, at an expense of a 3.11% increase in error (12% total error).

The features obtained from the signal processing techniques need to be classified in an automated way for an on-line tool breakage detection. The techniques used for this purpose are termed as decision making techniques which include neural networks, fuzzy logic, control limits and static and dynamic thresholds.

Tansel et al. [3.68] investigated the use of a back propagation (BP) type neural network in monitoring tool wear in a micro-end-milling operation. They investigated the relationship between tool usage and the cutting force by presenting data to a NN in two

35

different encodings. One of the encodings was based on simple force-variation and the second encoding was based on a more complicated segmental-average. Experiments were performed on aluminum and steel to include the effects of the material being cut on the process. They observed that the optimization of the NN parameters was extremely difficult but extensive training would create a compact and representative model. They claimed to get excellent wear estimations using this approach.

A support vector machine (SVM) learning algorithm has been reported by Hsueh and Yang [3.37]. Spindle displacement was measured by two displacement sensors and the average defection per tooth and per rotation was calculated. These features were input to the SVM for analysis. Like NN, SVM algorithms also require training before they can begin working. The system was shown to be reliable under various cutting conditions.

3.5 Depth of Cut Monitoring

A reliable TCMS should allow the optimum utilization of a tool life cycle. Normally tools are replaced based on a conservative valuation of tool life [3.69]. Timely and accurate estimation of the tool life is critical. Over-estimation of tool life can result in degraded product quality and damaged parts (in case of early tool breakage), while under-estimation leads to frequent stoppages (of the machining process) and increased cost of production [3.22]. Thus real-time tool life estimation is deemed to be the key to automated machining.

There has been a vast amount of research activity in estimating tool life and tool wear. Some researchers have modeled the tool life and tool wear taking into account various cutting conditions namely cutting speed, feedrate and depth of cut. [3.70,3.71]. Cutting speed and feedrate can be estimated by monitoring the signals related to spindle and axis drive system respectively. At the moment no viable systems were reported where automated DOC monitoring or measurement is supported. Researchers monitoring, predicting or modeling tool conditions are either accessing DOC information (by other measurement means) or assuming that the DOC will be constant through out the tool life cycle [3.72].

Tasi et al. [3.71] presented a method based on an abductive network for predicting tool life in high-speed milling operation. They have shown that once cutting speed, feedrate and axial depth of cut is provided, tool life can be predicted reliably. Results from a large number of tool life experiments, performed for the training of the network, were reported in a tabular form, which listed the tool life for different cutting speeds, feedrate and depth of cuts. Since it was not explicitly contained in the cited reference, the author has analysed the data for dependence of tool life on depth of cut. The relationship between DOC and tool life (for two cutting speeds of 471 and 628 m/min) is shown in Figure 3.5. It is evident from the Figure 3.5 that tool life decreases as depth of cut increases. Therefore if the DOC changes during the life cycle of a tool its effective life will be affected and assuming a constant DOC is not always a viable option.
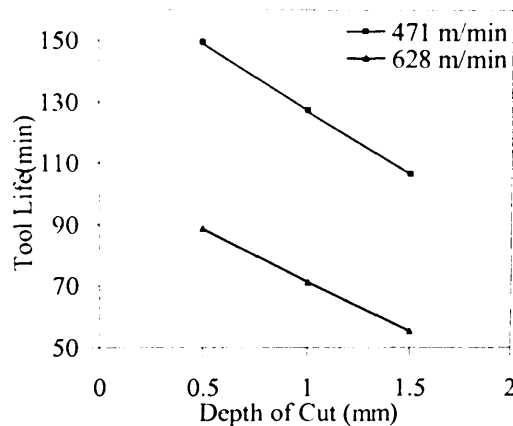
Figure 3.5: Relationship between tool life and depth of cut (derived from [3.71])

Gogfrey et al. [3.70] report an approach to predictive modelling for tool wear estimation which requires depth of cut and other cutting conditions to be provided. They have reported tool wear values obtained from tests carried out for different cutting conditions (including DOC). The reported results suggest that tool wear increases with any increase in DOC. Similarly, Shao et al. [3.12] describe a cutting power model for tool wear monitoring. The model requires the cutting conditions (including DOC) and average flank tool wear to be input to the model for effective monitoring.

Prickett and Grosvenor [3.73] suggest measuring and accumulating the work during different cuts performed by the tool, in order to update and track the total work performed. This information would be useful if the system can predict the residual life,

which depends on the DOC and other cutting conditions that the tool will be subjected to in the future.

Szwajka [3.72] reports that one of the drawbacks of most research work is that constant cutting parameters have been used for entire tool life. In industrial practice, this not the case, where typically the same tool is used at different feeds and depth of cuts in sequential passes. Szwajka has demonstrated through various cutting experiments, that there is a weak dependence of main cutting force on tool wear. On the other hand feed force is only effected by depth of cut and tool wear. Therefore to use feed force for tool wear estimation, the depth of cut must be identified directly or implied by the using the weak dependence of cutting force on tool wear. Based on his test results obtained from a deployed industrial force sensor, he suggests that depth of cut must be measured directly.

Alauddin et al. [3.64] proposed a model for estimating cutting force in end milling and discussed the influence of different cutting conditions on the cutting force. It was concluded that cutting forces increase with feedrate and depth of cut. Similarly Li and Li [3.60] proposed a model using a dynamic sheer length and reported the experimental verification of results. They observed that the maximum cutting forces are proportional to depth of cut. This effectively means that to predict any cutting forces, the depth of cut information will be required and any unexpected change in depth of cut will affect the estimation process.

In considering the non-measurement sources, it would be possible to pre-calculate the depth of cut at any particular in time, for the present job at hand from the CNC programme, provided that the workpiece initial dimensions are exactly known. This holds true for cases where machining cycles are repeated and exactly the same workpiece is being fed for machining. However when machining one-off components or where the workpiece is coming from a casting process or being otherwise selected from available stock on the shop floor, it will not hold true. Then the DOC will not be predetermined and it will be impossible to calculate the DOC using CNC programme information.

In the opinion of the author, therefore, the only viable option appears to be a system which can provide real-time DOC information for both tool wear and tool life estimation. Although previous work in the IPMM group has indicated that the tool breakage system will not be fooled by moderate changes in depth of cut, any attempt to monitor the tool force will inevitably be improved when depth of cut monitoring is included. As far as is known there are no commercially available systems to measure depth of cut.

3.6 Embedded Tool Condition Monitoring Systems

The majority of tool condition monitoring systems is based on a PC while very few have been implemented on an embedded platform. The main reason for this seems to be that flexibility and computational power provided by PC is far better than embedded counterparts. Another reason seems to be the availability of large number of advanced signal processing software packages for PC platforms.

There is some diversity in the use of the term embedded. For the current research embedded is ultimately taken to refer to the use of distributed single-chip solutions such as microcontroller devices. This section of the review will however also refer to embedded, small footprint and limited peripherals, PC platforms.

Li et al. [3.74] developed an embedded tool condition monitoring system (eTCM) based on an embedded PC platform with 300MHz processor running Windows CE. They suggest that eTCM can be used as the required third level feedback loop, additional to the normal feedback loops of velocity and position, to provide the machining process data for process control. Their system utilizes a multi-sensor approach for data acquisition using a data acquisition card installed in the embedded PC. The sensors used included an accelerometer, a dynamometer, a microphone, and an AE sensor. A recursive crest factor monitoring algorithm (RCFMA) was reported for tool breakage detection. The crest factor is the ratio of the peak value to RMS value of a waveform. Although the system is actually based on a PC platform, it was claimed to be an embedded TCM on the basis of the chosen hardware.

Baek et al. [3.8] used a DSP (TMS320C40) development board for implementation of a TCMS with an 8th order AR model and a band energy method coupled with a neural network. The neural network used the following inputs: spindle speed, feedrate and DOC in addition to cutting force features. The detail of the signal processing algorithm used has already been reported in section 3.3. The AR model was found to be more accurate but slower than the band energy method.

The only FPGA implementation which could be found in the literature was reported by René de Jesús et al. [3.24,3.46]. Three hardware signal processors (HSP) based on FPGA were used and simplified algorithms were implemented on a one time programmable (OTP) FPGA. The detail on signal processing and sensing methods has already been reported in section 3.3. A suggested cost for the processing system was $300.

More recently (in 2008) René de Jesús has co-authored with Franco-Gasca et al. [3.36] to describe an FPGA based tool condition monitoring system using similar algorithms to detect tool breakage using spindle motor current. Their system was shown to be adaptable for different machining processes. It compared the mean value of the feature signal (output from wavelet) with three fixed thresholds (hi, lo, and max) which were calculated during "teach-in" cutting cycles. The user could also manually enter the max thresholds. The system displayed the condition of the tool on a 7-segment LED (light emitting diode) display as GOOD when the mean value was between the hi and lo threshold, and FAIL when the mean value exceeded the max threshold. It also displayed LO and HI status depending upon the crossing of hi or lo thresholds. The system functionality looks very similar to the commercial system Techna-check as discussed in Section 3.3.1.

3.6.1 Microcontroller-based Monitoring Systems

Microcontroller based monitoring systems can be much cheaper than PC based systems [3.75]. However the implementation of digital signal processing techniques using microcontrollers is neither simple nor straight forward. This has been largely due to limitations in the device's ability to provide the mathematical capabilities required. This situation is however changing, with the evolution of products such as dsPIC microcontrollers which are able to acquire and process the signals needed in monitoring

applications. Due to the cost effectiveness of the devices it is economically feasible to embed any required number of them within a machine or process. They can then be linked together to form a distributed sensor network.

The characteristics of such systems have been identified by authors such as Bolic et al. [3.75]. They correctly propose that, when designing installations where considerations such as cost, size and power consumption are especially critical, microcontrollers would increasingly represent a viable solution. The potential of approaches based upon embedded microcontrollers can be demonstrated by a large body of work including the case study describing the distribution of sensors and their associated data processing and analysis tools within mail sorting machinery presented by Al-Habibeh et al. [3.76]. The approach used was based upon low-cost infrared sensors which reported the status of equipment. (Further details on the system are reported in Section 3.7)

The benefits of deploying decision making modules close to the source of the information were identified by Kandasamy et al. [3.77]. They considered that the use of multiple nodes provided enhanced monitoring functions and proposed that each node could be equipped with a specific behavioral model. The fault detection process then becomes a collective operation; the use of multiple independent detection points provides a degree of redundancy that can support fault detection even with the loss of elements of the system.

Although in a wider sense, there is vast amount of research reported on microcontrollers, their application in tool condition monitoring has been much more limited. The IPMM group has reported their use for monitoring of milling machine operations such as tool changer and cutting process. The review of following 2 papers in intended to summarize the research of the IPMM group that is specific to machine tool applications.

Frankowiak et al. [3.78] describe a tool condition monitoring system which is based on the Petri-net concept, and used PIC microcontrollers for its implementation. It was designed to monitor a tool changer operation and was further developed and extended to provide information pertaining to individual tool utilisation, thus offering additional functionality relating to tool-life. A Petri-net model was developed and deployed in the

microcontroller node which them monitored the tool changer operations. The Petri-net developed for this application required 170 transitions and 104 places. A total of 17 digital and 2 analogue signals were interfaced. It was reported that the majority of the data is dealt with locally and only small amounts of data would need to be sent for more advanced analysis on a server-side PC.

Amer et al. [3.16] have reported a tool breakage monitoring system based on distributed set of PIC microcontrollers and based on frequency analysis of the spindle load signal using hardware-based reconfigurable filters. These microcontrollers were connected to each other via controller area network (CAN) communications. Each microcontroller controlled a filter which filtered a particular frequency component. Thus by separately monitoring the frequencies related to tool and tooth rotation frequencies respectively, tool breakage was monitored. The results from all the nodes were combined to provide a decision on the overall tool condition.

Zhang and Chen [3.23] reported the use microcontroller for data acquisition of vibration signals from accelerometers for tool condition monitoring. They have acquired the signal into a PC laptop and performed the analysis using computer based software.

3.6.2   dsPIC-based Monitoring Systems

The dsPIC technology is quite new and there are very limited research activities reported using it. The reported research that exists mainly deals with control system applications.

Capua et al. [3.79] describe the implementation of a smart-sensor based on a dsPIC microcontroller. This was a measurement system used to monitor voltage RMS values and to extract the index values which were transmitted to software located on an external peripheral via serial communication for subsequent data processing. They described the conditioning of the signal to make it suitable for the ADC of a dsPIC device. An external zero-crossing detector was used as the trigger for sampling of signal. The sampling rate was 10Ksps. The RMS algorithm was optimized to use less data memory.

Jayabarathi and Devarajan [3.80] report a reactive power compensation technique using NN based on a dsPIC microcontroller. The system consisted of three parts: A/D converter, NN controller and Threshold comparator. The input signals to the dsPIC were DC voltages proportional to the sending end real power, reactive power, sending end voltage and far end bus voltage. The voltages measured were input to the NN which produced 4 outputs corresponding to 4 different conditions. It was proposed that these outputs will be used for compensation of the reactive power.

Caner et al. [3.81] report the development of a dsPIC-based electrocardiograph (ECG) simulator intended to be used in the testing, calibration and maintenance of ECG equipment, and for educational purposes. The developed system has a parameterized signal generator, a low pass filter, a summation block and interference introduction block. A D/A converter was used to generate an analog version of an ECG signal. The simulated ECG signals were perfectly produced and controlled for a very wide range of conditions. It was reported that since standard commercially available electronic components were used to construct the prototype simulator, the proposed design was also relatively inexpensive to produce.

Zhang et al. [3.82] reported a dsPIC-based excitation control system for a synchronous generator. They stated that the functionality provided by dsPIC is ideal for the design of next generation of Automatic Voltage Regulators (AVRs). The CAN bus was used to communicate with other modules in the system and TCP/IP Ethernet communication was used to communicate with a Distributed Control System (DCS) within a modern power plant. For this purpose a stand-alone Ethernet controller ENC28J60 with an SPI interface was used. It was concluded that dsPIC based excitation control systems are suitable for modern power plants.

3.7 IT-enabled Monitoring Systems

With the advancement of information technology new means of communications such as mobile, email and internet communication are taken for granted these days. Internet connectivity is widely available and its use is popular with technical as well as non-technical people. It provides an easy method of communication resulting in remote data access. Mobiles have become a basic necessity of modern life and are considered as the

most effective way of voice and data communication. This section of the review looks at research related to IT-enabled monitoring systems.

Bartolomeu et al. [3.83] present a distributed monitoring system based upon Bluetooth technology. This technique is useful for particular applications where wired access is not possible or not feasible such as coastal sea water quality monitoring. The system is designed on the principal of dividing the complexity in multiple subsystems which simplifies the addition of extra monitoring capability to the system. Each of the subsystems was called a local monitoring system (LMS) and acquired local information and sent it to subscribed system users (SUs) through a Bluetooth network. SUs were connected to internet in order to publish the information, allowing any user with internet connection to access them. They recommended the implementation of an authentication mechanism to deny access to non-registered users.

Frankowiak et al. [3.78] reported a PIC microcontroller based distributed monitoring system for monitoring the tool changer in a milling machine. The system has data communication features such as CAN bus and Internet connectivity. Petri-nets have been used to monitor the discrete events in tool changer activity. The Microcontrollers were connected to each other and higher layer via a CAN bus. The UDP protocol was used to communicate with a server over Ethernet. The events were recorded in a server-side database for analysis and process information was displayed through a dynamic webpage.

The use of web-based technology to help manufacturers with organisational challenges, such as geographically spread out manufacturing plants, was reported by Ong et al. [3.84]. Information was identified in this work as a strategic resource that becomes essential in such a situation. The employment of monitoring tools based on Internet technologies is a way in which manufacturing activities in many regions and even in different countries can be integrated and monitored. Among the many benefits cited, perhaps the most relevant here is that the performance of a machine or process can be monitored and accessed from anywhere in the organisation. It was also proposed that productivity information, diagnosis and staff training on the effective operation of manufacturing systems could be shared among partners at different locations. Internet technology was praised by Ong et al. due to its rapid development, and its capacity of

providing access to the most remote locations all over the world. A prototype system was developed and used for remote fault diagnostics of tool wear in CNC machining.

Bucci and Landi [3.85] proposed a distributed measurement system using three hierarchical communication levels (fieldbus, intranet and Internet). Remote measurement units (RMUs) acquired the signal, performed necessary processing and provided it to a fieldbus server (FS). Each RMU had three modules each responsible for one task: signal acquisition, processing, and the fieldbus interface. The FS acted as master for communication with RMUs and obtained data from each of them sequentially. A 32-bit microcontroller from Hitachi with external memory was used for the RMU implementation. It was attached to a 20 x 4 lines display and a 16-key keyboard that formed a local user interface. Several RMUs connected with a fieldbus server formed a measurement site. An FS handled the tasks of data storage and analysis, display and report generation, and data sharing. Several measurement sites were interlinked using a LAN where PCs were used for the required processing power and management applications. A measurement server at LAN level performed advanced data analysis and logging. A PC-based Gateway connected the LAN to the Internet and provided the security layer. The system was designed with the aim of supporting dynamic web pages managed by an Apache server, so that remote users could access the latest information. The fieldbus interface was based on the RS-485 protocol with a data transfer rate of up to 38.4 Kbps. The system performance was evaluated, for power quality in an electrical distribution network and was found to be well suited for such applications in terms of cost and performance.

Al-Habaibeh et al [3.75] reported on a remote monitoring and diagnostic system for royal mail automatic sorting machines designated as Integrated Mail Processors (IMP). IMPs are complex systems which include large number of rollers, bearings, belts, gears, motors, electronic systems, etc. The Royal mail delivers about 82 million items of mail and parcel post every day. Accordingly, IMPs do an enormous amount of work and generate a lot of heat. A microcontroller based monitoring system was developed to check the generated heat and any abnormal patterns were detected. Infrared imagers were interfaced with microcontrollers connected to the Internet. PIC16F877 microcontrollers were used in this application along with a PICDEM.NET development board from Microchip Ltd used to provide Internet connectivity. UDP/IP protocol was

used to relay acquired data on Ethernet for processing by remote computers. The use of microcontrollers provided a low-cost acquisition system in this application.

The implementation issues of the TCP/IP stack protocols on microcontroller-based systems were discussed by Eady [3.86]. It was highlighted that resources, within a microcontroller are normally very limited, are heavily burdened by the TCP/IP stack required for communicating on the internet. Various options were described for the microcontrollers in this regard and Eady emphasized that a simplistic TCP/IP stack might suffice for small systems. He proposed that the stack should be a modular one and only the modules required for a specific application should be included. He used CMX-MicroNet, which is a TCP/IP stack designed for use with microcontrollers. It supports up to 127 UDP or TCP sockets. However, its high cost (starting from $5500) may be an issue for small system developers. Microchip has come up with their own TCP/IP stack which freely available from their website. It however works only with Microchip microcontrollers.

Although the internet provides a very effective and fast way of communication, it also renders the connected devices vulnerable to hackers. Proper security is required against unauthorized users to minimize malicious attacks. Hackers may intrude into an Internet-based monitoring system and change the settings for causing undesirable effects. Embedded systems normally don't have enough processing power to employ full-blown encryption techniques for security over internet. [3.87]. As first line of defense, an embedded system may be placed behind a firewall provided by the company LAN. Besides security reasons, this is often the case of network implementation in a company. The firewall provides security by hiding the local processors' IP addresses from the Internet and by allowing only the required services. It was also argued on restricted access, based on username and password authentication to provide further security, or in case a firewall was not available. This kind of authentication can be implemented using simple HTML code with a HTTP POST request.

Ciancetta et al. [3.88] described architecture for a web-enabled distributed monitoring system based on a smart sensor and a web service. The developed smart sensor consisted of three dsPIC microcontrollers and a networking embedded system based on

46

Fox-board hosting ETRAX LX100 32bit CPU with on-chip Ethernet interface. The dsPIC microcontroller in this application has been utilized only for data acquisition and pre-processing of the voltage signal from a three phase power network. The Fox-board controls (through a single control line) and communicates with dsPIC microcontrollers on a shared data bus. It also connects to internet on Ethernet. Ciancetta et al. also discussed the need for a synchronization clock on the network and decided the use of Network Time Protocol (NTP) which provided synchronization accuracy of 10 msec. Measurement results were made available as web service so that all users could built their own applications to use the data.

3.8 Summary

This review has shown that majority of research on tool condition monitoring is still based on a PC platform and very few have utilized the embedded platforms for such systems. Although the PCs allow very sophisticated analysis of the signal, they are not designed for real-time mission-critical operations. Embedded systems provide integration of the monitoring system within the process and can monitor the process in real-time. Normally embedded system have limited computational power requiring the algorithms to be simplified and fine-tuned to work on embedded devices such as dsPIC microcontrollers. This seems to be the main reason for researchers to use PC based platforms.

The IPMM group has researched the use of PIC microcontrollers for tool condition monitoring and reported the limitations of such devices in-terms of memory and computational power. The introduction of devices such as the dsPIC has opened the possibilities of deploying advanced signal processing algorithms (which were previously deployable on PCs only), on an embedded level. The distributed monitoring system combines the processing power of small embedded devices in a coherent way providing scalability and enhanced processing capabilities close to the machine. The industrial networks such as CAN bus form the backbone of the distributed system where different nodes exchange process information to make better and robust decisions about the process health. Internet communications and GSM connectivity provide the facility to transfer the process information across the borders in real-time.

This review has highlighted the need for deploying the advanced signal processing algorithms on embedded devices such as dsPIC microcontrollers in order to realize a low cost embedded distributed monitoring system which will monitor the tool condition in real-time and provide the diagnostic information for process management system.

References

[3.1]   M. Frankowiak, R. Grosvenor, and P. Prickett, "A review of the evolution of microcontroller-based machine and process monitoring," *International Journal of Machine Tools and Manufacture*, vol. 45, 2005, pp. 573-582.

[3.2]   P. Prickett, R. Grosvenor, and A. Jennings, "Intelligent process monitoring and management using the Internet," *International Journal of Condition Monitoring and Engineering Management*, Vol. 6(4), 2003, pp. 9-17.

[3.3]   P.W. Prickett and R.I. Grosvenor, "Non-sensor based Machine Tool and Cutting Process Condition Monitoring," *Condition Monitoring and Engineering Management*, vol. 2, 1999, pp. 31-37.

[3.4]   R.I. Grosvenor and P.W. Prickett, "Intelligent Process Monitoring and Management - Time for a Return to Sensor-based Methods?," *Sensors and their Applications* , Sep. 2003, pp. 497-502.

[3.5]   H. Dassanayake, C. Roberts, and C. Goodman, "An architecture for system-wide fault detection and isolation," *Journal of Systems and Control Engineering*, vol. 215, 2001, pp. 37-46.

[3.6]   J. Ehrlich, A. Zerrouki, and N. Demassieux, "Distributed architecture for data acquisition: A generic model," *IEEE Instrumentation and Measurement Technology Conference*, 1997, pp. 1180-1185.

[3.7]   A. Baccigalupi, A. Bernieri, and A. Pietrosanto, "A digital-signal-processor-based measurement system for on-line fault detection," *Instrumentation and Measurement, IEEE Transactions on*, vol. 46, 1997, pp. 731-736.

[3.8]   D.K. Baek, T.J. Ko, and H.S. Kim, "Real time monitoring of tool breakage in a milling operation using a digital signal processor," *Journal of Materials Processing Technology*, vol. 100, Apr. 2000, pp. 266-272.

[3.9]   S. Cho, S. Asfour, A. Onar and N. Kaundinya, "Tool breakage detection using support vector machine learning in a milling process," *International Journal of Machine Tools and Manufacture*, vol. 45, Mar. 2005, pp. 241-249.

[3.10]   W.Y. San, "Effective Tool Condition Monitoring for Automated Machines," *National University of Singapore*, Oct. 2003, [WWW] <URL http://www.eng. nus.edu.sg/ERcsnews/0310/rd/rd_7.html> (accessed on 10 Jun. 2007)

[3.11]   A. Al-Habaibeh and N. Gindy, "A new approach for systematic design of condition monitoring systems for milling processes," *Journal of Materials Processing Technology*, vol. 107, Nov. 2000, pp. 243-251.

[3.12]   H. Shao, H. Wang, and X. Zhao, "A cutting power model for tool wear monitoring in milling," *International Journal of Machine Tools and Manufacture*, vol. 44, 2004, pp. 1503-1509.

[3.13]   K.T. Chung and A. Geddam, "A multi-sensor approach to the monitoring of end milling operations," *Journal of Materials Processing Technology*, vol. 139, Aug. 2003, pp. 15-20.

[3.14]   P.C. Tseng and A. Chou, "The intelligent on-line monitoring of end milling," *International Journal of Machine Tools and Manufacture*, vol. 42, Jan. 2002, pp. 89-97.

[3.15]   P.W. Prickett and C. Johns, "An overview of approaches to end milling tool monitoring," *International Journal of Machine Tools and Manufacture*, vol. 39, Jan. 1999, pp. 105-122.

[3.16]   W. Amer, R. Grosvenor, and P. Prickett, " Machine tool condition monitoring using sweeping filter techniques," *Journal of Systems and Control Engineering*, vol. 221, 2007, pp. 103-117.

[3.17]   A.G. Rehorn, J. Jiang, and P.E. Orban, "State-of-the-art methods and results in tool condition monitoring: a review," *The International Journal of Advanced Manufacturing Technology*, vol. 26, Oct. 2005, pp. 693-710.

[3.18]   B.Y. Lee and Y.S. Tarng, "Milling cutter breakage detection by the discretewavelet transform," *Mechatronics*, vol. 9, Apr. 1999, pp. 225-234.

[3.19]   Y.S. Tarng, S.T. Hwang, and Y.W. Hseih, "Tool failure diagnosis in milling using a neural network," *Mechanical Systems and Signal Processing*, vol. 8, Jan. 1994, pp. 21-29.

[3.20]   J.M. Lee, D. K. Choi, J. Kim, C. N. Chu, "Real-Time Tool Breakage Monitoring for NC Milling Process," *CIRP Annals - Manufacturing Technology*, vol. 44, 1995, pp. 59-62.

[3.21]   Y. Altintas, "In-process detection of tool breakages using time series monitoring of cutting forces," *International Journal of Machine Tools and Manufacture*, vol. 28, 1988, pp. 157-172.

[3.22]   P. Bhattacharyya, D. Sengupta, and S. Mukhopadhyay, "Cutting force-based real-time estimation of tool wear in face milling using a combination of signal

processing techniques," *Mechanical Systems and Signal Processing*, vol. 21, Aug. 2007, pp. 2665-2683.

[3.23] J. Zhang and J. Chen, " Tool condition monitoring in an end-milling operation based on the vibration signal collected through a microcontroller-based data acquisition system," *The International Journal of Advanced Manufacturing Technology*, 2007; http://dx.doi.org/10.1007/s00170-007-1186-6.

[3.24] R.R.D. Jesu's, , H.R. Gilberto, T.V. Ivan, and J.V.J. Carlos, "FPGA based on-line tool breakage detection system for CNC milling machines," *Mechatronics*, vol. 14, May. 2004, pp. 439-454.

[3.25] R.R.D. Jesu's, , H.R. Gilberto, T.V. Ivan, and J.V.J. Carlos, "Driver current analysis for sensorless tool breakage monitoring of CNC milling machines," *International Journal of Machine Tools and Manufacture*, vol. 43, Dec. 2003, pp. 1529-1534.

[3.26] Pan Fu and A. D. Hope, "A Neural-fuzzy Pattern recognition Algorithm based Cutting Tool Condition Monitoring Procedure," *ISNN 2007*, 2007, pp. 293-300.

[3.27] M. Ritou, S. Garnier, B. Furet and J.Y. Hascoet, "A new versatile in-process monitoring system for milling," *International Journal of Machine Tools and Manufacture*, vol. 46, Dec. 2006, pp. 2026-2035.

[3.28] X. Hongjian, Y. Kechong, and Y. Rong, "The shape characteristic detection of tool breakage in milling operations," *International Journal of Machine Tools and Manufacture*, vol. 37, Nov. 1997, pp. 1651-1660.

[3.29] Y. Altintas, "Prediction of cutting forces and tool breakage in milling from feed drive current measurements," *Journal of engineering for industry*, vol. 114, 1992, pp. 386-392.

[3.30] G Dini and F Tognazzi, "Tool condition monitoring in end milling using a torque-based sensorized toolholder," *Journal of Engineering Manufacture*, vol. 221, 2007, pp. 11-23.

[3.31] H. Cao, X. Chen, Y. Zi, F. Ding, H. Chen, J. Tan and Z. He, "End milling tool breakage detection using lifting scheme and Mahalanobis distance," *International Journal of Machine Tools and Manufacture*, vol. 48, Feb. 2008, pp. 141-151.

[3.32] I. Tansel, A. Nedbouyan, C. Velez, W.Y Bao and T.T. Arkan, "Micro-end-milling--III. Wear estimation and tool breakage detection using acoustic

emission signals," *International Journal of Machine Tools and Manufacture*, vol. 38, Dec. 1998, pp. 1449-1466.

[3.33] C. Jun and S. Suh, "Statistical tool breakage detection schemes based on vibration signals in NC milling," *International Journal of Machine Tools and Manufacture*, vol. 39, Nov. 1999, pp. 1733-1746.

[3.34] I. Yesilyurt, "End mill breakage detection using mean frequency analysis of scalogram," *International Journal of Machine Tools and Manufacture*, vol. 46, Mar. 2006, pp. 450-458.

[3.35] J.C. Chen and W. Chen, "A tool breakage detection system using an accelerometer sensor," *Journal of Intelligent Manufacturing*, vol. 10, Apr. 1999, pp. 187-197.

[3.36] L.A. Franco-Gasca, R.R.D. Jesu's & G. Herrera-Ruiz and R. Peniche-Vera, "FPGA based failure monitoring system for machining processes," *The International Journal of Advanced Manufacturing Technology*, Jan. 2008; http://dx.doi.org/10.1007/s00170-008-1386-8.

[3.37] Y. Hsueh and C. Yang, "Tool breakage diagnosis in face milling by support vector machine," *Journal of Materials Processing Technology*, In Press, Corrected Proof, 2008, [WWW] <URL http://www.sciencedirect.com/ science/article/B6TGJ-4RRFN8G-5/2/39eec0a3fd5fa40986221bfbf1638ece> (accessed on 11 Aug. 2008)

[3.38] B. Y. Lee, H.S. Liu, and Y.S. Tarng, "Monitoring of tool fracture in end milling using induction motor current," *Journal of Materials Processing Technology*, vol. 70, Oct. 1997, pp. 279-284.

[3.39] X. Li and X.P. Guan, "Time-frequency-analysis-based minor cutting edge fracture detection during end milling," *Mechanical Systems and Signal Processing*, vol. 18, Nov. 2004, pp. 1485-1496.

[3.40] X. Li, G. Ouyang, and Z. Liang, "Complexity measure of motor current signals for tool flute breakage detection in end milling," *International Journal of Machine Tools and Manufacture*, vol. 48, Mar. 2008, pp. 371-379.

[3.41] X. Li, "Detection of tool flute breakage in end milling using feed-motor current signatures," *Mechatronics, IEEE/ASME Transactions on*, vol. 6, 2001, pp. 491-498.

[3.42] A. Bassiuny and X. Li, "Flute breakage detection during end milling using Hilbert-Huang transform and smoothed nonlinear energy operator,"

International Journal of Machine Tools and Manufacture, vol. 47, May. 2007, pp. 1011-1020.

[3.43] M. Lanzetta, "A new flexible high-resolution vision sensor for tool condition monitoring," *Journal of Materials Processing Technology*, vol. 119, 2001, pp. 73-82.

[3.44] X. Li, S. Dong, and Z. Yuan, "Discrete wavelet transform for tool breakage monitoring," *International Journal of Machine Tools and Manufacture*, vol. 39, Dec. 1999, pp. 1935-1944.

[3.45] X. Li, S.K. Tso, and J. Wang, "Real-time tool condition monitoring using wavelet transforms and fuzzy techniques," *Systems, Man, and Cybernetics, Part C: Applications and Reviews, IEEE Transactions on*, vol. 30, 2000, pp. 352-357.

[3.46] R. de Jesús Romero-Troncoso and G.H. Ruiz, " FPGA Implementation of a Tool Breakage Detection Algorithm in CNC Milling Machines," *Field Programmable Logic and Application*, Springer Berlin / Heidelberg, 2004, pp. 1142-1145.

[3.47] D. Dimla Snr., "Sensor signals for tool-wear monitoring in metal cutting operations - a review of methods," *International Journal of Machine Tools and Manufacture*, vol. 40, 2000, pp. 1073-1098.

[3.48] Renishaw Plc (UK), "Tool setting and broken tool detection," [WWW] <URL http://www.renishaw.com/en/6079.aspx> (accessed 15 Jun. 2008)

[3.49] TPS International, "TPS International," [WWW] <URL http://www.tpsintl. com/home.htm> (accessed on 15 Jun. 2008)

[3.50] CIRO Products Ltd, "Broken Tool Detectors" [WWW] <URL http://ciro.com/ middtool.htm#Middex%20BKS1S> (accessed on 10 Apr. 2008)

[3.51] Techna Tools Inc, "BK Mikro 8", [WWW] <URL http://www.techna-tool.com/?id=bk_mikro_8> (accessed on 10 May. 2008)

[3.52] K. Jemielniak, "Commercial Tool Condition Monitoring Systems," *The International Journal of Advanced Manufacturing Technology*, vol. 15, 1999, pp. 711-721.

[3.53] PROMETEC Ltd. "PROMOS Modular Process Monitor System," [WWW] <URL http://www.prometec.com/download/datasheets_machining/PROMOS_ TDM.GB.pdf> (accessed on 11 May. 2008)

[3.54] Techna Tools Inc, "Techna-Check 3200"; [WWW] <URL http://www.techna-tool.com/?id=techna_check_3200> (accessed on 11 May. 2008)

[3.55] Techna Tools Inc, "Techna-Check TC3200 Manual," [WWW] <URL http://www.techna-tool.com/fileadmin/technatool/webassets/assets/techna_check/models/model_3200/TC3200Manual.pdf> (accessed on 11 May. 2008)

[3.56] Marposs Ltd, "Mida Power Monitor System" [WWW] <URL http://www.midaprobing.com/Documents/controllopotenza_G.pdf > (accessed on 20 May. 2008)

[3.57] CNC Engineering Inc. "Tool Monitoring Adaptive Control," [WWW] <URL http://www.cnc1.com/pdfs/Tool%20Monitoring%20Adaptive%20Controls.pdf > (accessed on 21 Jun 2008)

[3.58] L. Zheng, Y. Li, and S.Y. Liang, "A generalised model of milling forces," *The International Journal of Advanced Manufacturing Technology*, vol. 14, Mar. 1998, pp. 160-171.

[3.59] M. Alauddin, M. El Baradie, and M. Hashmi, "Modelling of cutting force in end milling Inconel 718," *Journal of Materials Processing Technology*, vol. 58, 1996, pp. 100-108.

[3.60] H. Li and X. Li, "Milling force prediction using a dynamic shear length model," *International Journal of Machine Tools and Manufacture*, vol. 42, 2002, pp. 277-286.

[3.61] X. Long, B. Balachandran, and B. Mann, "Dynamics of milling processes with variable time delays," *Nonlinear Dynamics*, vol. 47, 2007, pp. 49-63.

[3.62] N. Kasashima, K. Mori, G. Herrera Ruiz and N. Taniguchi, "Online failure detection in face milling using discrete wavelet transform," *CIRP Annals - Manufacturing Technology*, vol. 44, 1995, pp. 483-487.

[3.63] Peter Chi and C. T. Russell, "Statistical Methods for Data Analysis in Space Physics: AR model," *Institute of Geophysics and Planetary Physics, UCLA*, [WWW] <URL http://www-ssc.igpp.ucla.edu/personnel/russell/ESS265/Ch9/autoreg/node9. html> (accessed on 24 Feb. 2008)

[3.64] I. Tansel, W.Y. Bao, N.S. Reen and C.V. Kropas-Hughes, "Genetic tool monitor (GTM) for micro-end-milling operations," *International Journal of Machine Tools and Manufacture*, vol. 45, 2005, pp. 293-299.

[3.65] W. Amer, R. Grosvenor, and P. Prickett, " Sweeping filters and tooth rotation energy estimation (TREE) techniques for machine tool condition monitoring,"

International Journal of Machine Tools and Manufacture, vol. 46, Jul. 2006, pp. 1045-1052.

[3.66] G. Kim and C. Chu, "In-Process Tool Fracture monitoring in Face Milling Using Spindle Motor Current and Tool Fracture Index," *The International Journal of Advanced Manufacturing Technology*, vol. 18, 2001, pp. 383-389.

[3.67] Z. Deyuan, H. Yuntai, and C. Dingchang, "On-line detection of tool breakages using telemetering of cutting forces in milling," *International Journal of Machine Tools and Manufacture*, vol. 35, Jan. 1995, pp. 19-27.

[3.68] I. Tansel, T.T. Arkan, W.Y. Bao, N. Mahendrakar, B. Shisler, D. Smith and M McCool, "Tool wear estimation in micro-machining. Part I: Tool usage-cutting force relationship," *International Journal of Machine Tools and Manufacture*, vol. 40, 2000, pp. 599-608.

[3.69] P.N. Botsaris and J.A. Tsanakas, "State-of-the-art in Methods Applied to Tool Condition Monitoring (TCM) in Unmanned Machining Operations: A Review," *Proceedings of 21st International Congress on Condition Monitoring and Diagnostoc Engineering Management*, Prague, Czech Republic: 2008, pp. 73-87.

[3.70] G. Onwubolu, P. Buryan, and F. Lemke, "Modeling tool wear in end-milling using enhanced GMDH learning networks," *The International Journal of Advanced Manufacturing Technology*, Dec. 2007; http://dx.doi.org/10.1007/s00170-007-1296-1.

[3.71] M. Tsai, B. Lee, and S. Yu, "A predicted modelling of tool life of high-speed milling for SKD61 tool steel," *The International Journal of Advanced Manufacturing Technology*, vol. 26, Oct. 2005, pp. 711-717.

[3.72] K. Szwajka, "Laboratory versus industrial cutting force sensor in tool condition monitoring system," *Journal of Physics: Conference Series*, vol. 13, 2005, pp. 377-380.

[3.73] P.W. Prickett and R.I. Grosvenor, "A Microcontroller-Based Milling Process Monitoring and Management System," *Proceedings of the Institution of Mechanical Engineers, Part B: Journal of Engineering Manufacture*, vol. 221, 2007, pp. 357-362.

[3.74] H. Z. Li, X. Q. Chen, and H. Zeng, "*An Embedded Tool Condition Monitoring System for Intelligent Machining*," 2004; [WWW] <URL

http://www.simtech.a-star.edu.sg/Research/TechnicalReports/TR0307.pdf >
(accessed on 25 May. 2008)

[3.75] M. Bolic, V. Drndarevic, and B. Samardzic, "Distributed measurement and control system based on microcontrollers with automatic program generation ," *Sensors and Actuators A: Physical*, vol. 90, May. 2001, pp. 215-221.

[3.76] A. Al-Habaibeh, D.R. Whitby, R. M. Parkin and M.R. Jackson, "The development of an Internet-based mechatronic system for remote diagnostic of machinery using embedded sensors," *International Conference on Mechatronics, ICOM 2003*, 2003, pp. 297-302.

[3.77] N. Kandasamy, J. Hayes, and B. Murray, "Time-constrained failure diagnosis in distributed embedded systems: application to actuator diagnosis," *Parallel and Distributed Systems, IEEE Transactions on*, vol. 16, 2005, pp. 258-270.

[3.78] M.R. Frankowiak, R.I. Grosvenor, and P.W. Prickett, "A Petri-net based distributed monitoring system using PIC microcontrollers," *Microprocessors and Microsystems*, vol. 29, Jun. 2005, pp. 189-196.

[3.79] C. D. Capua, S.D. Falco, A. Liccardo and E. Romeo, "A dsPIC-based measurement system for the evaluation of voltage sag severity through new power quality indexes," *Proceedings of the 2005 IEEE International Conference on VECIMS*, Italy, Jul. 2005, pp. 2-6.

[3.80] R.A. Jayabarathi and N.B. Devarajan, "ANN Based dsPIC Controller for Reactive Power Compensation"; *American Journal of Applied Sciences*, vol. 4 (7), 2007, pp. 508-515

[3.81] C. Caner, M. Engin, and E. Engin, "The Programmable ECG Simulator," *Journal of Medical Systems*, vol. 32, 2008, pp. 355-359.

[3.82] W. Zhang, Y. Yang, and J. Wang, "A dsPIC-based Excitation Control System for Synchronous Generator," *Mechatronics and Automation, 2007. ICMA 2007. International Conference on*, 2007, pp. 3844-3848.

[3.83] P. Bartolomeu, J. Fonseca, and O. Pacheco, "Distributed monitoring subsystems based on a Bluetooth implementation," *Emerging Technologies and Factory Automation, 2003. Proceedings. ETFA '03. IEEE Conference*, 2003, vol. 2, pp. 121-124.

[3.84] S. Ong, N. An, and A. Nee, "Web-based fault diagnostic and learning system," *International Journal of Advanced Manufacturing Technology*, vol. 18, 2001, pp. 502-511.

[3.85]   G. Bucci and C. Landi, "A distributed measurement architecture for industrial applications," *Instrumentation and Measurement, IEEE Transactions on*, vol. 52, 2003, pp. 165-174.   57

[3.86]   F. Eady, " TCP/IP Stack Solution," *Circuit Cellar*, Nov. 2004, pp. 54-61.

[3.87]   Jan Axelson, " Network Security for Small Systems," *Circuit Cellar*, Nov. 2004, pp. 62-69.

[3.88]   F. Ciancetta, B.D. Apice, D Gallo and C. Landi, "Architecture for Distributed Monitoring based on Smart Sensor and Web Service," *IMTC 2006*, Sorrento, Italy: 2006, pp. 2054-2059.

Chapter 4

e-Monitoring and dsPIC Technology

4.1. Introduction

4.1.1. Definition of e-Monitoring

The field of e-monitoring concentrates on real-time monitoring of industrial machines and processes using automated methods. The backbone of e-monitoring, in the development process for different applications, is the data acquisition of the process signals from various machine systems. Different sensing systems may require development in order to achieve the appropriate data acquisition. Sensors provide continuous data about a particular aspect of a process such as pressure, voltage, current, temperature etc. which needs to be collected and compiled in a desirable format so that it can be used in a fruitful way. The data is then processed and analysed using different techniques to extract features, which represent the process/machine condition. Based on the output of the analysis, recommended action is then taken to keep the process/machine running at maximum efficiency or to alarm and trigger timely process stops. The obtained data should be communicated to an expert for further analysis when the monitoring system is unable to make a robust decision to required confidence levels.

4.1.2. Monitoring System Requirements

A monitoring system is conventionally based on an industrial or a commercial PC which is equipped with a data acquisition system. With associated proprietary software and data acquisition cards, it becomes an expensive solution. Although such a system is superior to its embedded counterpart in terms of computational power, it is sometimes not deployable in industrial environments because of space constraints. It also requires a complex wiring network, from the sensors to the central data collection point, which is often difficult to install and may be cumbersome to maintain. The cost associated with such complex wiring is also very high. Different noise factors may also affect the

measured signal before it reaches the collection point. Since monitoring depends upon the quality of the obtained signal, its effectiveness is directly related to the signal accuracy. The deployment of a centralized system is therefore often impracticable and not an ideal solution.

A more ideal solution would be to collect and (if possible) analyze the process signals close to the sensors. In this way accuracy will be very high and the resulting monitoring will be effective. The obtained (analysed/processed) data may then be transmitted on a digital bus to the central processing unit for further analysis. Digital transmission is more immune to noise than analog data from the sensors. The problem of wiring is also tackled effectively, with the added advantage of reduced cost. The overall size of the monitoring system will be more compact making it more suitable for industrial process/machines. The latest embedded devices incorporate impressive processing power, computational speed, integrated peripherals and communication modules on a single chip such as the dsPIC Digital signal controller. This makes the development of a distributed, process monitoring system a desirable solution to a wide variety of applications.

Tanenbaum has defined the distributed system as "A collection of independent computers (microcontrollers/microprocessors in the case of embedded systems) that appear to its users as a single coherent system" [4.1]. Various devices in a distributed system can operate concurrently and tasks are undertaken independently. Actions however are coordinated at well-defined stages by exchanging messages [4.2] through a digital communication medium such as Controller Area Network (CAN) bus, which is widely used in many industries, as is available on the dsPIC chip.

Due to the advancements in information technology it is now expected that a monitoring system should provide the ability to monitor the process conditions remotely. The acquired/processed data may be transferred to each recipient. The information requirement may be different for different parties depending upon the interaction with the process. The accumulated data may be sent to remote users electronically through WebPages, pagers, email, fax, SMS etc. The system must intelligently decide the status of the process and send appropriate alarm messages to

concerned parties. Considerable work has been done on this approach in the IPMM group at Cardiff [4.3, 4.4]

A monitoring system should be reliable, able to meet the application requirements and provide a low cost to benefit ratio to be accepted by the manufacturing industry [4.5]. It should also fit in the limited space. It should be able to withstand the harshness of industrial environments. It should provide a suitable user interface to interact with.

4.1.3. Introduction to Technology Selection

The remaining of this chapter describes the various aspects of a distributed tool condition monitoring system based solely upon Microchip's dsPIC Digital Signal Controllers. These are 16-bit microcontrollers with on-chip digital signal processing (DSP) engine. The dsPIC has a built-in digital signal processor along with typical microcontroller features. Computational speed makes it superior to previous generation of microcontrollers. The latter provides additional benefits to the front-end processing capabilities. In addition these devices are equipped with various peripherals and communication interfaces making them suitable for distributed applications. The following sections describe the architecture of the researched system, the technology selection for the different tiers and major system operations (data acquisition, signal processing and communication) with a focus on enabling features of the dsPIC Technology.

4.2   Monitoring System Architecture

The main objective of this research was to develop and implement data processing techniques capable of monitoring various systems, including the particular applications pertaining to condition of machine tools, whilst deploying minimal electronic components and sensors. To achieve this it was decided to use a 16-bit dsPIC microcontroller platform. The hardware architecture of the proposed distributed monitoring system is shown in Figure 4.1.

The monitoring system is based on a three-tier architecture that enables flexibility & data integration and provides resource sharing capabilities. This architecture uses different dsPIC microcontroller based (embedded) 'Front End Node' (FENs) for data acquisition and signal processing at the first tier. The desired variable (parameter) can

be analysed in a FEN for any fault symptoms. Signal acquisition and processing are performed in this tier of the monitoring system to take advantage of the processing capabilities of dsPIC and to explore its potential in tool condition and other monitoring tasks. The need for a reliable and effective system demands that information be shared, through CAN bus communications (for the proposed system) between different dsPIC microcontrollers at this tier so that a more informed decision can be made about the health of the process in hand. This can minimize the number of false alarms being made. The performance of CAN bus in noisy environments is known to be robust and superior to other methods, therefore it is being used to provide the communications between devices. Based on the results obtained within the IPMM group using 8-bit PIC devices (where an 80% expectation at the FEN level was in operation) and noting the increased processing capability of the dsPIC, it was expected that more than 90% of faults may be identified at this tier.
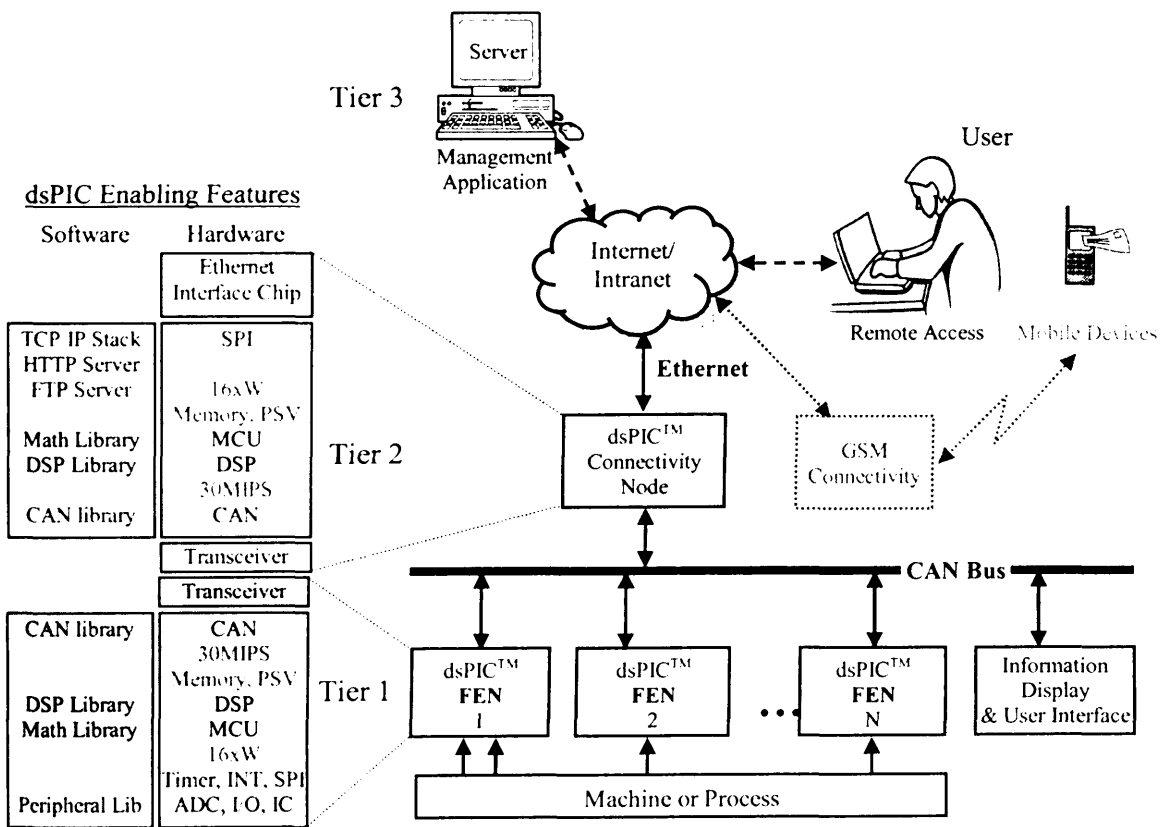

Figure 4.1: Hardware architecture of proposed monitoring system.

The second tier in the proposed hierarchy consists of a synchronisation-connectivity node also based on the dsPIC platform. This acts as the interface for FENs and provides Ethernet connectivity and Global System for Mobile communications (GSM)

connectivity. The GSM connectivity to users can be achieved via internet protocols, in particular using the SMS messaging API [4.6]. Thus this node acts as a bridge between different communication interfaces. The second tier is also an additional source of data processing (when conditions require it) and adds to the system capabilities. At this stage, when required, data from various FENs are combined and analysed. It is proposed that 8% of faults can be detected (with 90% already handled by the FENs directly). This tier also links the FENs to a server-side PC via the internet, where further analysis tools can be used on a personal or industrial computer to identify the remaining 2% of faults.

The 90/8/2% split was set as an operating principle, with the hope that even more significant proportion of faults can be detected within the distributed nodes. The selected application for system development and testing was the monitoring of a cutting tool condition monitoring on milling machines.

The top tier 'management application' is a software implementation based on a PC that provides a common interface to databases. The accumulated data is sent to remote users electronically. Web sites, pagers, email, fax, SMS etc. may be used for this purpose [4.3]. This architecture also supports the acquisition of data from selected modules as designated by condition monitoring systems that function at the management level. In this way, should a monitoring module find that it cannot identify potential faults with its embedded processing capabilities it is able to initiate actions that capture and package data and deliver it to more powerful analysis tools [4.7, 4.8]. The server-side analysis (tier 3) is not explicitly considered in this research. It is part of the proposed architecture and both possible enhancements and future work are detailed later in the thesis, drawing upon the results of the implemented and tested application.

4.3   Technology Selection

Research has been reported in recent years supporting the development of an alternative cost-effective way of using microcontrollers [4.9]. An embedded monitoring system is usually small in size and can be located close to signal source, thus improving the signal-to-noise ratio (SNR). In a distributed system there is a need to process the signal, in real time, so that only useful information is sent to any higher layers in the deployed

architecture rather than sending the raw data. This will not only make the data acquisition more meaningful but will also reduce the network traffic allowing more devices to be incorporated without exceeding the network capacity / bandwidth.

For example, the IPMM research group has exploited the capabilities of Microchip's 8-bit PIC microcontrollers, whilst evaluating and reporting their limitations particularly in processing power, on-chip memory and computational speed [4.7-4.9]. PIC microcontrollers were used mainly for data acquisition and provided limited local processing such as calculation and the comparison of thresholds, average signal values, finding maximum and minimum values and determination of time delays. Sophisticated signal processing methods such as FFT could not be fully or successfully implemented because of limited memory, processing and computational power constraints. The PIC microcontrollers used have 10-bit Analog to Digital (A/D) Conversion; however the analog data acquisition had in effect been limited to 8-bit resolution because of 8-bit architecture and limited on-chip memory [4.10]. The author carried out the current research within the IPMM group and the expertise already established in the IPMM centre with Microchip's products and the available resources deemed the now available and superior Microchip's 16-bit dsPIC devices as the best choice for the implementation of this research. Figure 4.1 shows various enabling features of dsPIC devices for proposed system architecture. The following sections will summarize and justify the selection of dsPIC devices.

4.3.1 The dsPIC Microcontroller

The new generation (available since about 2004) of Microchip's dsPIC digital signal controllers claim to close the performance gap by providing easy migration from microcontroller (MCU) to Digital Signal Processor (DSP) performance. In simple terms they integrate the MCU functionality with DSP capabilities. This provides a complete system-on-chip (SoC) fully equipped with the necessary modules to enable an effective monitoring solution. Their reported performance in comparison with other 16-bit embedded systems is summarised in Table 4.1.

Table 4.1: The dsPIC30F family as compared to other 16-bit devices (adopted from [4.11])

Company	MCU Family	Instruction Cycle Rate (MHz)	Number of Cycles per Instruction	Average Throughput (MIPS)[1]
Microchip	**dsPIC30F**	**30**	**1-2**	**28**
Infineon	XC161/166	40	1-6	28
TI	320LF240x	40	1-4	21
Motorola	56F80x	40	1-8	19
Hitachi	H8S/26xx	33	1-7	15
Infineon	C16xx	25	2-4	12
ST Micro	ST10F269	20	2-4	9
Mitsubishi	M16C	20	1-8	9
Motorola	MC9S12D	25	2-6	6

1. dsPIC30F actual, other estimated based on instruction frequency analysis
2. Preliminary results for calendar year 2004

Devices such as the dsPIC30F contain a rich set of peripherals, have reasonably sized on-chip data memory, a significant program memory space (which can also be used for data storage), CAN bus communication capabilities and I/O ports. They also contain an oscillator, which can be configured, using a Phase-Locked-Loop (PLL) technique, to achieve 30 MIPS (Million-Instructions-Per-Second), making them suitable for many industrial applications.

In particular the evaluation of capabilities and suitability of dsPIC for monitoring systems lead to various options for deployment of the dsPIC in the tool condition monitoring system. The dsPIC could not only effectively replace the PIC based monitoring modules but was also expected to provide a significant step forward by opening the possibility of employing sophisticated DSP algorithms such as FFT and Multiband Filters for real-time signal analysis. This could be done at FEN level, where more than one signal can be acquired and processed simultaneously. Its selection would help to reduce the overall system size and cost. It can also be used at the second, connectivity module, tier where it can interface the CAN bus communications to internet/Ethernet connections. In particular a dsPIC can be used as an internet server, which can take some functionality of the management tier and send top priority messages (in cases of extreme emergency) to the user without waiting for the management application's response.

The dsPIC has facilities well-suited for signal acquisition, processing, and communication with the outer world. It has a fast 12-bit ADC, large memory, 16- and

32-bit timers, and large number of external interrupts, input capture module, digital I/O ports, and multiple communication modules including CAN, SPI (Serial Peripheral Interface), and UART (Universal Asynchronous Receiver Transmitter). The latter can be used to implement the RS-232 standard for communication with a PC COM port. The UART and SPI modules helped in the initial development of the proposed system. This evaluation of these devices, led the author the choice of dsPIC digital signal controllers (DSC) for implementation of the monitoring system in this research. In the next section, a general overview of dsPIC30F families is provided along with a more insight into the capabilities of the particular dsPIC30F6014 digital signal controller.

4.3.2 The dsPIC30F6014 Digital Signal Controller

The dsPIC architecture has a full-featured DSP engine, C compiler friendly design, and familiar microcontroller-like platform and allows easy migration of existing code for PIC18 devices [4.12]. The dsPIC30F have three device families namely: (1) General Purpose Family, (2) Motor Control and Power Conversion Family and (3) Sensor Family. Of these, the author has investigated General Purpose Family platform and subsequently many features were utilized in the development of the proposed monitoring system. Different variants of the General Purpose Family are listed in Table 4.2.

Table 4.2: dsPIC30F General Purpose Family variants (adopted from [4.13])

Device	Pins	Program Memory Bytes	Program Memory Instruction	SRAM Bytes	EEPROM Bytes	Timer 16-bit	Input Capture	Output Compare / Standard PWM	Codec Interface	A/D 12-bit 100/200Ksps	UART	SPI	I²C	CAN	I/O Pins (Max)[1]
dsPIC30F3014	40/44	24K	8K	2048	1024	3	2	2	-	13 ch	2	1	1	-	30
dsPIC30F4013	40/44	48K	16K	2048	1024	5	4	4	AC'97,I2S	13 ch	2	1	1	1	30
dsPIC30F5011	64	66K	22K	4096	1024	5	8	8	AC'97,I2S	16 ch	2	2	1	2	52
dsPIC30F6011 dsPIC30F6011A²	64	132K	44K	6144	2048	5	8	8	-	16 ch	2	2	1	2	52
dsPIC30F6012 dsPIC30F6012A²	64	144K	48K	8192	4096	5	8	8	AC'97,I2S	16 ch	2	2	1	2	52
dsPIC30F5013	80	66K	22K	4096	1024	5	8	8	AC'97,I2S	16 ch	2	2	1	2	68
dsPIC30F6013 dsPIC30F6013A²	80	132K	44K	6144	2048	5	8	8	-	16 ch	2	2	1	2	68
dsPIC30F6014 dsPIC30F6014A²	80	144K	48K	8192	4096	5	8	8	AC'97,I2S	16 ch	2	2	1	2	68

1. Maximum I/O pin count includes pins shared by the peripheral functions.
2. ADC sampling rate up to 200Ksps.

65

The dsPIC30F6014 DSC was selected for both the front-end and connectivity nodes of the distributed monitoring system. The basis for selecting the dsPIC30F6014 MCU was that it had the largest number of features with maximum amount of data and program memory, allowing flexibility and many opportunities to explore the potential of such a new device throughout the process to develop the system proposed in this research.

An important fact to be considered is that Table 4.2 presents a brief summary of Microchip dsPIC30F General purpose Family variants which were available at the start of this research in 2004. Concurrently with the research, Microchip expanded its portfolio to include compatible families of 16-bit PIC24 microcontrollers, high speed dsPIC33F DSC and 32-bit PIC32 microcontrollers. These offer a new level of performance and even higher integration. Recognizing that this was bound to occur, the author designed the monitoring system operation and supporting architecture in such a way so as to allow these new devices to be integrated into the system, if required in future developments.

4.3.3   The CPU Architecture [4.13, 4.14]

The CPU of dsPIC30F is based on a 16-bit (data) modified Harvard architecture with an enhanced instruction set, including significant support for DSP. Its instruction word is 24-bits wide, whilst its program counter (PC) is 23-bits wide and can address up to 4M x 24 bits of user program memory space. It is possible to execute all instructions in a single cycle, thus providing very fast predictable execution of the developed programs. The only exceptions are the instructions that change the program flow, such as the double-word move and table instructions. Overhead free program loop constructs are supported using DO and REPEAT instructions, both of which are interruptible at any point. Major elements forming the dsPIC core and its peripherals are shown Figure 4.2 (adapted from [4.15]) where as detailed diagram is provided in "Appendix A". The grayed blocks in Figure 4.2 show the peripherals, present in the motor control and power conversion family, which replace the 12 bit ADC and standard PWM module.

There are sixteen 16-bit working registers (W0-W15) available as compared to one 8-bit working register in PIC microcontrollers. Each of these registers can act as a data, address or address offset register. The 16th working register (W15) in particular operates as a software stack pointer for interrupts and subroutine/function calls. The

instruction set for these devices has two classes of instructions: the MCU and DSP class of instructions. Both classes are seamlessly integrated into the architecture and execute from a single unit. The instruction set includes many addressing modes and is designed for optimum C compiler efficiency.
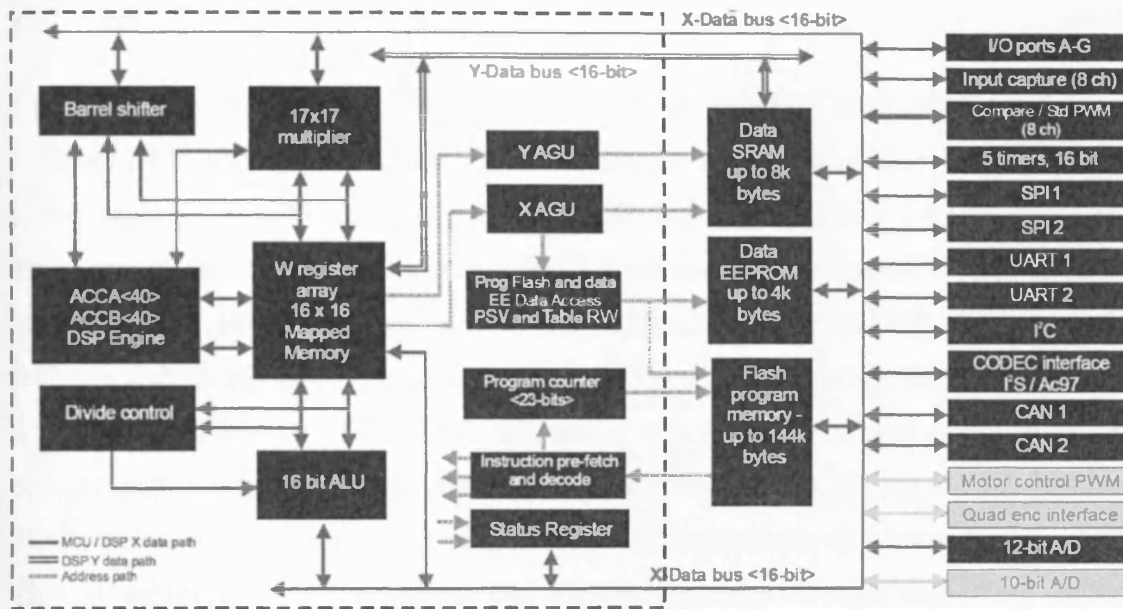

Figure 4.2: The dsPIC core (enclosed by dashed line) and peripherals of dsPIC family

The dsPIC30F6014 has 8Kbyte of data memory which is 16-bit wide and directly linearly addressed as a contiguous data space. The entire data space can be addressed as 32K words or 64 Kbytes and is split into two blocks, referred to as X and Y data memory. Each memory block has its own independent Address Generation Unit (AGU). The MCU class of instructions operates solely through the X memory AGU, which accesses the entire memory map as one linear data space. Certain DSP instructions operate through the X and Y AGUs to support dual operand reads. The upper 32 Kbytes of the data space memory map can optionally be mapped into program space at any 16K program word boundary defined by the 8-bit Program Space Visibility Page (PSVPAG) register. This feature allows any instruction access program space as if it were data space.

Overhead free circular buffers (modulo addressing) are supported in both X and Y address spaces. This removes the software boundary checking overhead for DSP algorithms. The X AGU circular (modulo) addressing can be used with any of the MCU class of instructions. The X AGU also supports bit-reverse addressing to greatly simplify input or output data reordering for radix-2 FFT algorithms. The CPU supports

67

various flexible addressing modes to meet the compiler needs. For most instructions, the dsPIC30F is capable of executing a data (or program data) memory read, a working register (data) read, a data memory write and a program (instruction) memory read per instruction cycle. As a result, three operand instructions can be supported, allowing A+B=C operations to be executed in a single cycle.

The DSP engine of the dsPIC devices features a high speed, 17-bit by 17-bit multiplier, a 40-bit ALU, two 40-bit saturating accumulators and a 40-bit bi-directional barrel shifter capable of shifting a 40-bit value up to 16 bits left or right in a single cycle. The DSP instructions operate seamlessly with all other instructions and have been designed for optimal real-time performance. The basic instruction for most DSP operation is the multiply and accumulate (MAC) instruction, which multiply the two operands and adds it to the accumulator. The MAC instruction and other associated instructions can concurrently fetch two data operands from memory while multiplying two W registers. This requires that the data space be split for these instructions and linear for all others. This is achieved in a transparent and flexible manner through dedicating certain working registers to each address space.

The dsPIC30F supports 16/16 and 32/16 divide operations, in both fractional and integer formats. All divide instructions are iterative operations which can be interrupted during any of those 19 cycles without loss of data. Furthermore, the dsPIC30F6014, used in the proposed monitoring system, features 5 external interrupts, and an interrupt vector table (IVT) that supports up to 54 interrupt sources. Any source of interrupt can be programmed for one of 7 priority levels, thus providing flexibility and control of target applications. In addition it is possible to interrupt the CPU through an implementation scheme on the rise or fall of a signal level of up to 24 digital I/O pins, adding more potential to deploy this device in all kind of applications. The above features of the CPU architecture of such devices enhance the efficiency (in terms of code size and speed of execution) of the C compiler.

The system requirement analysis for first tier revealed that data acquisition tasks will require ADC and an Input Capture (IC) module in addition to standard timers, interrupts and digital I/O. The CAN controller module will be utilized for CAN bus communications. The SPI module will be used to communicate to the LCD controller

for information display and user interface implementation. The DSP class of instructions will be utilised to access the DSP Engine of dsPIC for different DSP algorithms implementation

4.3.4 Development Tools and Libraries

The easy-to-learn development tools for the dsPIC30F families provided by Microchip are well-suited for embedded monitoring solutions. These tools and software libraries were very influential in the decision of selecting this device. The following tools and libraries were utilized in this research.

Hardware Tools

The main hardware tools of dsPIC30F devices utilized include:

- Demonstration boards, allowing the designer the opportunity to have hands-on examples of emerging technologies with which they intend to work.

- In-Circuit Debugger 2 (ICD2); this device can be enabled for emulation to test the developed software on the target hardware circuits and to download it onto the dsPIC DSC.

Software Tools

The software tools available for the dsPIC30F families can be summarized as follows:

- MPLAB IDE (Integrated Development Environment) includes a text editor, software simulator, assembler and Visual Device Initializer (VDI) which can be utilized for peripherals configuration. MPLAB IDE is powerful software, yet it has a simple and user-friendly interface. It is available free of charge.

- MPLAB C30 C Compiler provides code efficiency and a cost-effective, ANSI-compliant option for writing C or mixed C and Assembly code modules.

- Digital Filter Design and dsPICworks for data analysis of DSP algorithms.

Software and Device Libraries

Microchip offers the libraries designed especially for the dsPIC30F families including:

- Math library providing functions to perform various math operations like trigonometric, hyperbolic, logarithmic, root and power etc.

- Peripherals library providing functions to access the on board-peripherals

- DSP library: all DSP routines are developed and optimized in dsPIC30F assembly language and are callable from both Assembly and C language.

- Microchip TCP/IP Stack Protocol support library for Ethernet Connectivity.

4.3.5 dsPICDEM1.1 Development Board

The dsPICDEM1.1 development board (as shown in Figure 4.3) supports a dsPIC30F6014 device. It provides a CAN bus communication interface (with on-board CAN transceiver) to allow communication between devices on the Controller Area Network. It also has RS-232 (used in this research to provide a data link to PC) and RS-485 communication channels. There is a 122x32 dot addressable Liquid Crystal Display (LCD) which is controlled by a on-board PIC microcontroller, which is connected to dsPIC30F6014 via SPI [4.16]. The LCD along with switches and potentiometers provides a significant tool for user interface and information display. It can be used to display the process signal or messages to inform the operator about the health of the system.
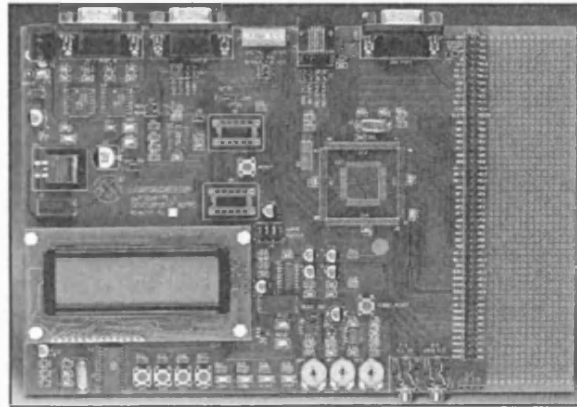

Figure 4.3: dsPICDEM 1.1™ General Purpose Development Board [4.17]

4.4 Data Acquisition

An effective monitoring system relies heavily on the efficient data collection system. The dsPIC30F has powerful modules: External Interrupts (INT), Change Notification (CN) on I/O pins, timers/counters, Input Capture (IC), and a 12-bit Analog to Digital Converter (ADC). These enabled data acquisition (both digital and analog) in an efficient manner.

4.4.1 Digital Data Acquisition

Digital signals are discrete in nature and possess one of a pre-determined range of values at a given time. Normally digital computers/ microcontrollers deal with the binary signals, which have only two states i.e. high or low. Voltage levels used to

represent high or low state vary amongst different representation schemes and platforms and appropriate signal conditioning is required to make them TTL compatible (0-5V) before their interfacing with the MCU. Using digital signals, information can be represented in different formats such as state (high or low), timing information (rising or falling edge or both), event (pulse), quantity (number of pulses), frequency/rate (number of pulses in a unit time) and pulse width modulation (duty cycle).

The dsPIC30F features (IC, timers/counters; External INT and CN on I/O pins) make digital signal acquisition an efficient task. The change in a signal can be detected by using CN or External INT functionality which generate an interrupt when the signal changes. Distinct from PIC18 microcontrollers, the dsPIC provides the facility to define an Interrupt Service Routine (ISR) for each interrupt. Each interrupt can be given priority level from 1 to 7 (with 7 being the highest priority). This feature decreases software overheads making the system much faster and more efficient.

Input Capture Module

The Input Capture module (IC) is used to capture a timer value upon an event on an input pin. The IC features are useful in applications requiring frequency (time period) and pulse measurements [4.18]. Figure 4.4 shows a simplified block diagram of the IC module.
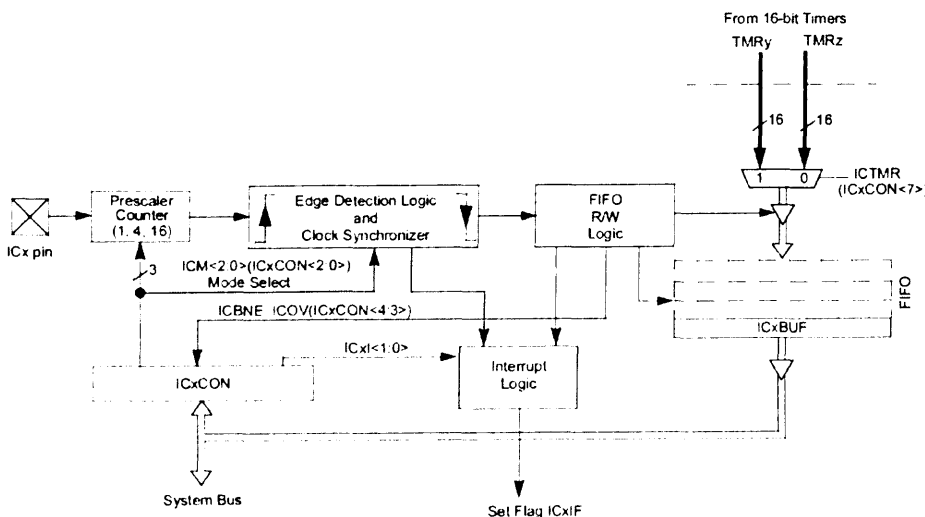

Figure 4.4: Block diagram of the Input Capture Module of dsPIC30F [4.18]

It has multiple operating modes (for example it can be used for the selection of a capture event on rising, falling or each edge) selectable via ICxCON register. The IC works with timer 2 or 3 which is selectable for each IC module. It reads the associated

71

timer value at the selected event and stores in a four-level First In First Out (FIFO) buffer (ICxBUF). The IC module has the ability to generate an interrupt based upon a selected number (1 to 4) of captured events. In particular, this module was used for measuring the width of the output pulse from an ultrasonic distance sensor (PING)))^TM) (Chapter 7). The module was set to capture at appropriate stages both the rising and falling edges of the input signal pulse and store the timer 3 in ICxBUF. A CPU Interrupt was generated after 2 capture events. The pulse width of the echo pulse from the sensor was determined by the difference in successive reading from the IC buffer register.

The resolution of the digital signal acquisition is dependent upon the system clock frequency (F_{CY}) and setting of the Timer module which can be configured to run at fractions of the overall processor rate by configuring the prescaler register. With a prescaler value of 1, the best time resolution which can be achieved is equal to $1/F_{CY}$. i.e. 33.9 nsec at 29.49MIPS (the maximum throughput with installed oscillator)

4.4.2 Analog Signal Acquisition

Most machine tool signals, typically those representing load, current, voltage, speed, or temperature are analog in nature . These signals have to be converted into digital format before processing by a computer or microcontroller. The dsPIC devices are equipped with a fast 12-bit Analog to Digital Converter (ADC) which provides this transformation. Analog to digital conversion is a very important step towards the digital signal processing and analysis. If correct signal is not acquired, correct analysis are not possible. It is effectively a three step process: sampling, quantization and conversion as shown in Figure 4.5. Sampling is the conversion of a continuous-time signal $x_a(t)$ into a discrete-time signal $x(n) = x_a(nT)$ obtained by taking samples of the continuous time signal at discrete-time instants [4.19]. If sampling is done at a Nyquist rate i.e. twice the highest signal frequency or higher, the full signal information can be retrieved from sampled signal [4.20]. The difference between discrete time signal $x(n)$ and quantized signal $x_q(n)$ is called quantization error and is irreversible. The precision and resolution of the ADC depends on the number of quantization levels. In the coding process, each discrete valued $x_q(n)$ is represented by a b-bit binary sequence which is the ADC output. A 12-bit coder is required for a 4096 quantization level ADC. The dsPIC has

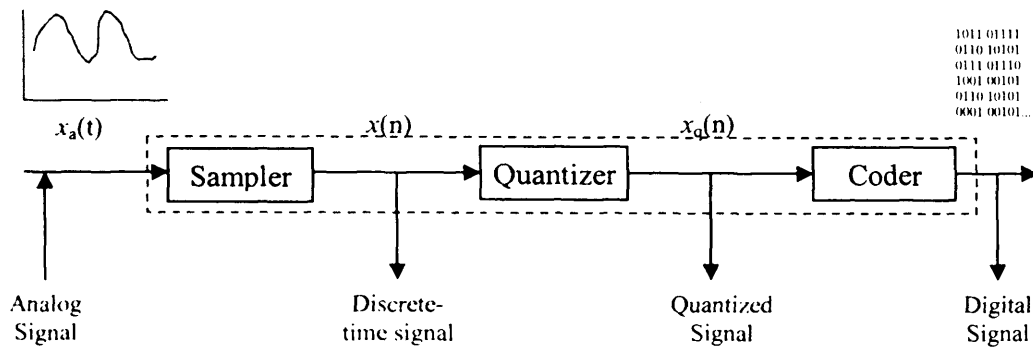12-bit ADC which provides 4 times more resolution as compared to 10-bit ADC of previous PIC microcontrollers.

Figure 4.5: Basic parts of an ADC (Adopted from [4.19])

12-bit ADC Module

The 12-bit Analog-to-Digital Converter (ADC) allows conversion of an analog input signal to a 12-bit digital number. This module provides a maximum sampling rate of 200Ksps. The block diagram of the 12-bit ADC is shown in Figure 4.6.
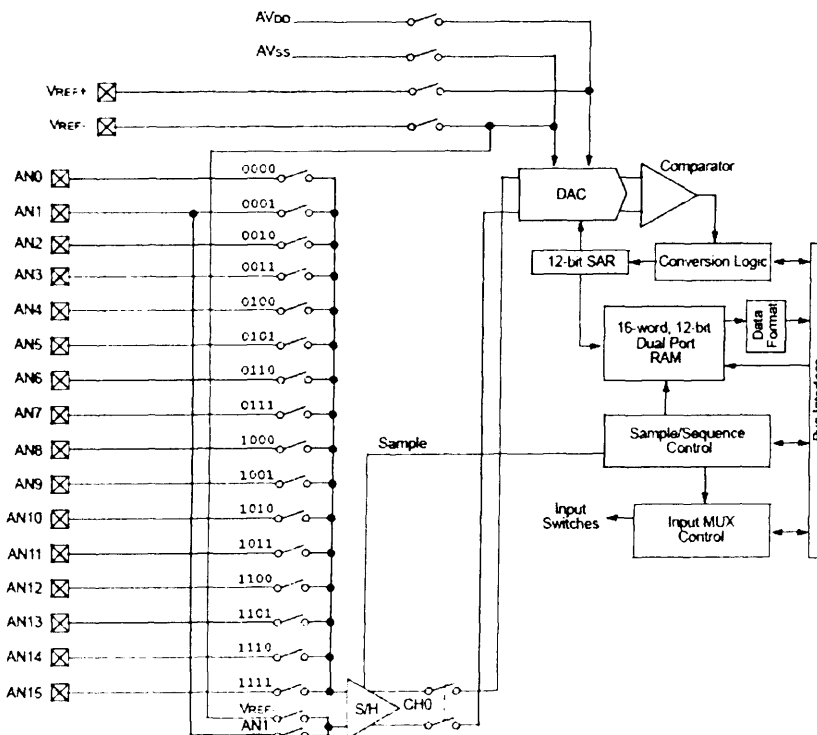

Figure 4.6: Block Diagram of 12 bit ADC module (taken from [4.21])

The ADC module has up to 16 analog inputs which are multiplexed into a sample and hold (S/H) amplifier. The output of S/H is the input into the converter which generates the result. The analog reference voltage is software selectable to either the device

supply voltage (AVDD/AVSS) or the voltage level on the (VREF+/VREF-) pin. For a typical 0-5volt range, one quantization step (resolution) is equal to $5/2^{12}=1.22mV$. The resolution can be improved by selecting the reference voltages such as to provide a smaller input voltage range. The ADC has a unique feature of being able to operate while the device is in Sleep mode with RC oscillator selection. It can convert an input signal manually (under software control) or automatically (the conversion trigger is under ADC clock control. The conversion trigger can also come from an external Interrupt (INT0) or Timer 3 (TMR3) modules, providing flexible sampling rates.

The operation of the ADC module is controlled by three control resisters ADCON1-3 and configuration registers (ADCHS, ADPCFG and ADCSSL). ADCHS selects the input channels to be converted; ADPCFG configures the port pins as analog inputs or as digital I/O and ADCSSL selects inputs for scanning. The module contains 16-word dual-port read only buffer called ADCBUF0...ADCBUFF. Sampling per Interrupt can be set between 1 and 16. In this way the frequency at which ADC interrupt occurs can be decreased. This allows more time for the processing of a signal using sophisticated algorithms like FFT which require longer computation time. This feature was used while implementing the overlap FFT algorithm for real-time frequency analysis outlined in Chapter 5.

Variable Sampling Rate

A variable sampling rate was required to be used for the real-time frequency analysis (Chapter 5) and Multiband IIR filter analysis (Chapter 6) for the tool condition monitoring. Therefore it was necessary to setup the ADC in a fashion that allowed the sampling rate to be easily changed. The on-chip Timer 3 module (as shown in Figure 4.7) was used for this purpose. The system clock pulse (T_{CY}) was divided with a Prescaler to generate the timer trigger pulse and the timer incremented with each pulse. Timer 3 was set to generate an ADC Event Trigger, whenever the timer value (TMR3) matched timer period (PR3), which can be calculated as follows [4.22]:

$$PR3 = F_{CY} / (f_s \times Prescaler) \qquad (4.1)$$

Where F_{CY} is the system clock frequency and f_s is the required sampling rate in Hz.

The prescaler was set to minimum to obtain maximum frequency resolution as PR3 was rounded to an integer during calculations.
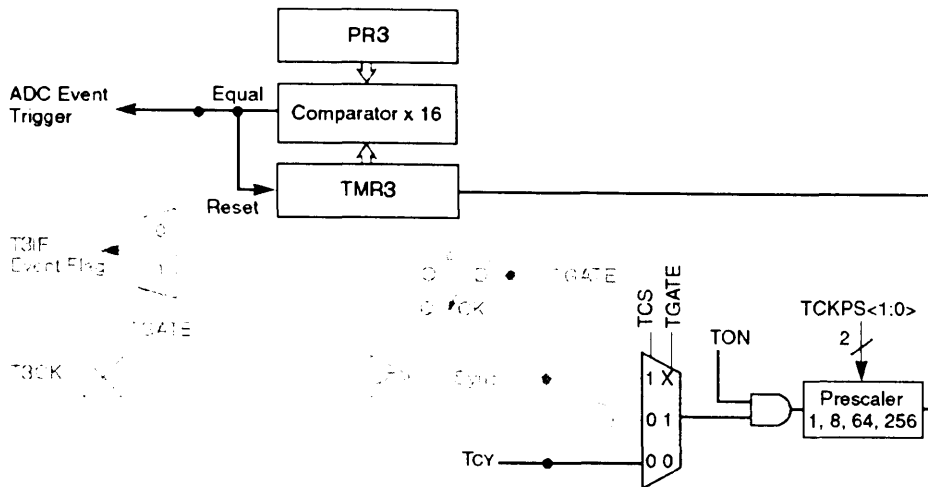
74

Figure 4.7: Timer 3 operation to generate ADC event trigger (adopted from [4.22])

Now simply updating the timer period value changed the sampling rate of the timer. The ADC was set to acquire a sample on the ADC event trigger from timer 3 becoming true. In this way variable sampling rates were realized without requiring any modification to the ADC registers, which would have required stopping the ADC before modifying any control registers. The timer period register can be update without stopping the timer; this method thus provided very fast updating of the sampling rate. This novel technique, which utilizes the ADC feature to vary sampling rate on the go, will enable the monitoring of tool breakage with varying spindle speed.

4.5   Second Tier Technology

The second tier of the system provides an additional source of data and signal processing to the system capabilities. It deals with cases where processing and analysis is found to be challenging and require that information from various FENs be shared, to reach a conclusive decision about the health of the system being monitored. This layer acts as a bridge between different communications interfaces to connect the first tier to Ethernet and GSM connectivity solutions. It needs extra resources for example communication interfaces and memory to perform the intended tasks of CAN bus, Ethernet and GSM connectivity.

The design analysis for the proposed monitoring system under research revealed that the hardware of the second tier should be based on 16-bit or higher architecture. Extra data memory was required to store data communicated by FENs for further analysis and

75

decision making. After a survey of commercially available technologies to support the aims of second tier, the author selected the dsPICDEM.net platform. This platform, provided by Microchip Technology Inc., can deliver the processing power and multiple communication interfaces as required by the application. Moreover, the well-established experience and knowledge amongst the IPMM research group with Microchip's hardware and software as well as the immense resources available deemed this platform a sensible option. A brief summary of supporting factors and more detailed insight into CAN controller, Ethernet connectivity and internet Protocols are presented in the following sections.

4.5.1 The dsPICDEM.net Connectivity Board

The dsPICDEM.net 1 connectivity development board (as shown in Figure 4.8) provides a basic platform for developing and evaluating both connectivity and non-connectivity based requirements. The dsPICDEM.net board provides the hardware circuitry for supporting the Public Switched Telephone Network (PSTN) and 10-Base T MAC/PHY interfaces. Its hardware schematic diagrams are provided in "Appendix A". The selection of dsPICDEM.net platform as the second tier is supported by many factors. The key features and attributes are listed below [4.23]:

- It hosts a dsPIC30F6014 high performance digital signal controller (DSC). The processing capabilities of installed dsPIC30F6014 DSC at this level when combined with functionality and power provided by FENs may eliminate the need for third level in many applications (i.e. processing and analysis at server level may not be required)

- An Ethernet interface is provided using the Realtek RTL8019 Ethernet controller. This is accessed via the bidirectional bus on PORTD. The availability of a 10-Base T Ethernet Network Interface Card (NIC) provides a link between second tier and internet making the monitoring system accessible from anywhere.

- Different libraries for TCP/IP stack, FTP and HTTP web server implementation are available from Microchip Inc. This would allow remote users to interact with the monitoring application.

- Serial Communication Channels Interface (UART and CAN) provide with other devices. CAN bus is used for communication with FENs as shown in Figure 4.1.

- 64 Kbytes external I^2C EEPROM memory is provided for storing constants such as Web pages, linearization tables for sensors and custom data tables.

- External 64K words (128Kbytes) SRAM memory is provided and can be used to store temporary data from FENs for advanced analysis and diagnostic purposes. This memory is accessible via PORTD on dsPIC30F6014.

- General Purpose Prototyping Area with Expansion Header enabling the enhancement of the development board such as increasing the external memory or connecting the header for different peripherals.

- A 2-line LCD Display along with provided LEDs, switches and potentiometers, is useful for status display and user interface implementation.

- Supports MPLAB ICD 2 and ICE 4000 emulator for device programming and emulation respectively.
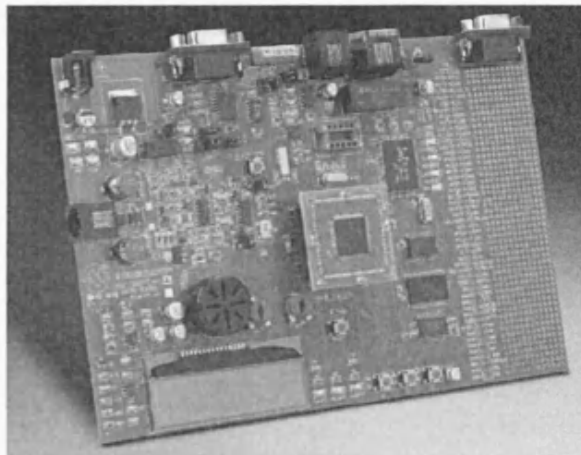

Figure 4.8: The dsPICDEM.net Development Board [4.23].

4.5.2   A Stand-alone Monitoring System

With the above mentioned features, the dsPICDEM.net development board, shown in Figure 4.8, can in fact act as a stand-alone monitoring system, by which a small application can be monitored and controlled via the internet. The dsPIC30F6014 device has all the capabilities to acquire signals and process them, and make decisions about the process. Ethernet connectivity can then be implemented in conjunction with the TCP/IP stack software (provided from Microchip at no cost) to send data to interested remote users (clients). As mentioned earlier, GSM connectivity can also be provided

via sending an HTTP message using SMS messaging APIs eliminating the need of having a separate dedicated SMS connectivity module.
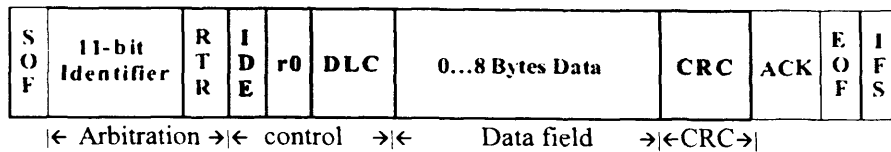
4.5.3 Communication using CAN Bus

The CAN is the leading serial bus system for embedded control which was internationally standardized (ISO 11898–1) in 1993 [4.24]. The protocol was originally developed for automotive applications. Today CAN bus has gained widespread use and is used in industrial automation as well as in automotive and mobile machines. It is based on a message broadcast mechanism where every node gets the message transmitted by any node on the bus. It uses message-content-based addressing scheme unlike other protocols which rely on source and destination address. This feature makes it suitable for open ended system in which different modules can be plugged in and out as required without affecting the overall operation of the system.

Every message has a unique message identifier, which defines the content and the priority of the message. The message identifer with smallest value has the highest priority. Unlike Ethernet, which uses collision detection at the end of the transmission, CAN uses collision detection with resolution at the beginning of the transmission. When a collision occurs during arbitration between two or more CAN nodes that transmit at the same time, the node(s) with the lower priority message(s) will detect the collision. The lower priority node(s) will then switch to receiver mode and wait for the next "bus idle" condition to attempt transmission again.

The CAN protocol supports two message frame formats, with different identifier (ID) length. In standard format the ID is 11 bit long providing 2048 different message identifiers, and in the extended format it has 29 bits providing 537 million identifiers [4.25]. The two CAN message formats are shown in Figure 4.9. The standard message always has higher priority over the extended message.

There are some trade-off considerations when using message in extended format: higher bandwidth requirements, longer bus latency times, and less powerful error detection capability.

Standard Frame

S O F	11-bit Identifier	R T R	I D E	r0	DLC	0...8 Bytes Data	CRC	ACK	E O F	I F S

|← Arbitration →|← control →|←   Data field   →|←CRC→|

Extended Frame

S O F	11-bit Identifier	S R R	I D E	18-bit Identifier	R T R	r1	r0	DLC	0...8 Bytes Data	CRC	ACK	E O F	I F S

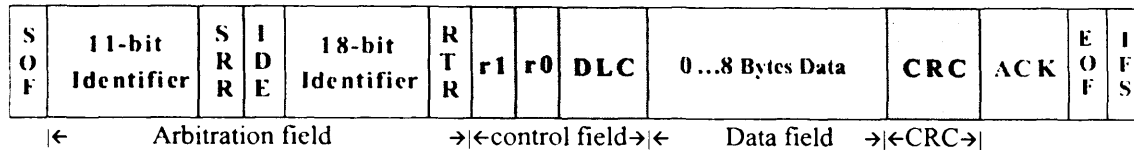|←   Arbitration field   →|←control field→|←   Data field   →|←CRC→|

Figure 4.9: CAN data frame formats according to ISO 11898-1 (Adopted from [4.25])

A CAN frame message starts with the Start of Frame (SOF) bit, which is followed by the arbitration field including the 11-bit Identifier (ID) and the Remote Transmission Request (RTR) bit. The RTR bit differentiates between "data frame" and "remote frame" (a request frame without any data bytes) [4.26]. The Identifier Extension (IDE) bit indicates if it is standard format or extended format. For extended frames it is followed by the remaining 18 bits of the 29 bit ID. The control field also contains one reserved bit (two in case of the extended frame), and at least 4 bits count of data bytes in the data field. In the remote frame Data Length Code (DLC) corresponds to the length of the requested data. Data field ranges from 0 to 8 bytes in length depending upon the DLC and is followed by Cyclic Redundancy Checksum (CRC) field, which is used as frame security check for detecting bit errors [4.27]. The ACK slot bit is sent as a recessive bit and is overwritten as a dominant bit by those receivers that have not detected any CRC failure at this time. Correct messages are acknowledged positively regardless of the result of the acceptance filtering. The end of the message is indicated by EOF field (7 recessive bits). "Intermission" is the minimum number of bit periods separating consecutive messages. If there is no following bus access by any station, the bus remains in an idle (recessive) state. [4.28].

The dsPIC30F has two on-chip CAN modules [4.28] and the dsPICDEM1.1 and dsPICDEM.net development boards each have one Microchip CAN Transceiver with CAN connector ready to form a CAN communication network. Figure 4.10 shows the interconnection of different nodes of the monitoring system connected to CAN bus. Each dsPIC's CAN controller is connected to CAN bus through a transceiver which converts the TTL signal in to CAN bus compatible signal.
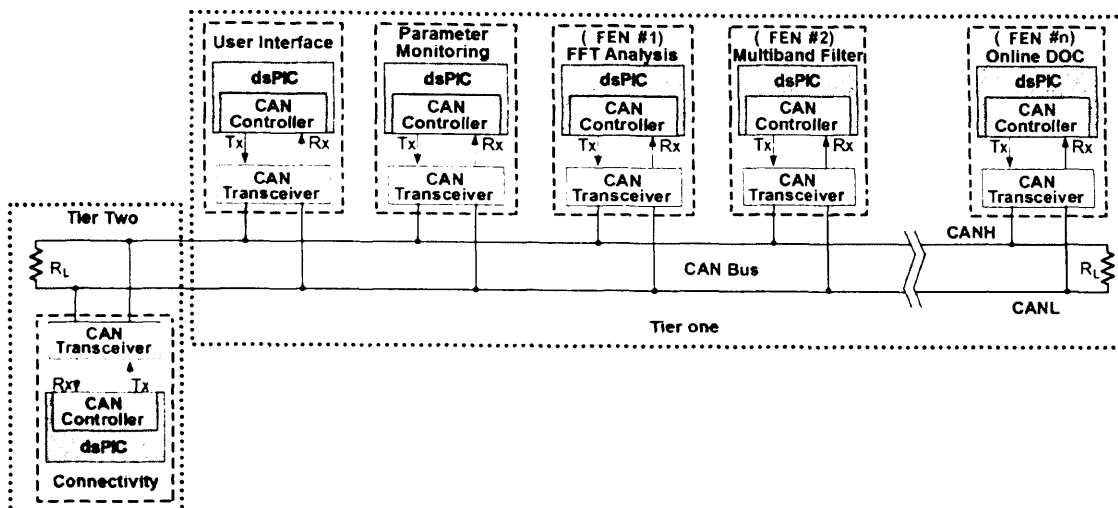
Figure 4.10: Block Diagram of CAN connections, shown for a 6 node network.

4.5.4 dsPIC30F CAN Controller

The CAN module is a communication controller implementing the CAN 2.0 A/B protocol, as defined in the BOSCH specification. The module implementation is a full CAN system [4.14]. A block diagram of CAN controller is posted in "Appendix A". The on-chip CAN controller consists of a protocol engine, set of buffers and filters. The CAN protocol engine handles all functions for receiving and transmitting messages on the CAN bus. It supports data transfer with built-in hardware error detection, a sophisticated message prioritisation scheme, and has the ability to set filters that allow only messages of interest to be received. Each CAN module has two receive buffers and three transmit buffers.

CAN Message Reception

The CAN protocol engine receives all bits of transmitted messages and places them into the Message Assembly Buffer (MAB). Once a message is completely placed into the MAB, its identifier field (specified by the user) is matched against a filter value, in conjunction with a mask value, and if there is a match it's then moved into the corresponding receive buffer. The module will subsequently generate an interrupt and set the receive buffer full (RXFUL) bit, located in a particular receive buffer control register (C1RX0CON). The application software can then clear this bit, indicating that the module has read the buffer and it is ready to receive the next message. There are two receive (or acceptance) filters associated with receive buffer 0 (RXB0), and four associated with receive buffer 1 (RXB1). One mask is also designated for each receive buffer.

If buffer 0 happens to be full when a message is accepted, it has the capability to store that message in buffer 1, assuming that buffer 1 is available. This feature is enabled by setting the DBEN bit in its control register (C1RX0CON). Additionally, if every bit of received identifier field either matched the corresponding filter bit or was ignored, the message is automatically sent to the appropriate receive buffer, otherwise it is rejected as indicated by the truth Table 4.3 below.

Table 4.3: Filter/Mask Truth Table [4.28]

Mask Bit	Filter Bit	Message Identifier Bit	Accept or Reject Bit
0	X	X	Accept
1	0	0	Accept
1	0	1	Reject
1	1	0	Reject
1	1	1	Accept

CAN Message Transmission

There are three transmit buffers in the module, only one of which is allowed to send data at any given time. A message to be transmitted is written onto one of the buffers and CAN controller is instructed when the message is to be transmitted. For example for tool breakage alarm, a message can be assembled/ prepared in advance and put in transmit buffer and when tool breakage CAN controller can be instructed to transmit the required message by setting the transmit request bit (TXREQ) in the associated control register (C1TX0CON). On receiving this command it initiates a transmission procedure.

Whenever the module initiates a transmission from a specific buffer, the bits of that buffer are sent to CAN protocol engine to begin transmission on the bus and perform error checking. If the bus is busy, the module will wait until the bus is idle before attempting transmission. When the module completes transmission, it automatically clears the TXREQ bit and generates an interrupt. Only then, the application software can request another transmission. It is possible for all transmit buffers to request transmission, at any time. When the bus is free, the module will then decide the order in which messages are sent based on a user-specified priority level for each buffer. One of four transmit priority levels (0 to 3) can be assigned for each buffer, with 3 being the highest and 0 the lowest, thus providing an additional degree of flexibility to the user

application. Meanwhile, if two buffers have the same priority level, their indices will then resolve the issue. In simple terms, buffer 2 (TXB2) is given the highest priority over buffer 0 (TXB0). This mechanism enhances the module capability to ensure that messages are delivered to intended nodes and no message is lost, and hence proving CAN protocol a more reliable serial network well-suited for monitoring and control applications.

4.5.5 Data Compression Techniques

This section describes the proposed data compression techniques which increase the effective bandwidth of the CAN bus by compressing the data into fewer bytes. These techniques especially focus on 12-bit ADC data which will be required to be transmitted in case of an abnormal condition as discussed in Chapter 8.

The data acquired by 12bit ADC requires 2 bytes to store each sample. The fact, that it could be represented by 12 bits only, is the basis of the first compression algorithm. In this case only 12 bits per sample are utilized to send the data using CAN message. As each CAN message can carry 8 bytes (64 bits), it would be possible to fit 5 data samples (60 bits) in a message as shown in Figure 4.11(b) as compared to 4 messages when no compression is used (Figure 4.11(a)). For example 20 samples require 4 CAN message instead of 5; thus providing a compression ratio of 20%.

(a) Without Data Compression

Byte1	Byte2	Byte3	Byte4	Byte5	Byte6	Byte7	Byte8
Sample1		Sample2		Sample3		Sample4	

(b) With Data Compression Technique 1 (20%)

Byte1	$\frac{Byte2}{2}$	$\frac{Byte2}{2}$	Byte3	Byte4	$\frac{Byte5}{2}$	$\frac{Byte5}{2}$	Byte6	Byte7	$\frac{Byte8}{2}$	$\frac{Byte8}{2}$
Sample1		Sample2		Sample3		Sample4		Sample5		X

(c) With Data Compression Technique 2 (50%)

Byte1	Byte2	Byte3	Byte4	Byte5	Byte6	Byte7	Byte8
Sample1	Sample2	Sample3	Sample4	Sample5	Sample6	Sample7	Sample8

X =not used

Figure 4.11: CAN message data field for different compression techniques

The second compression algorithm relies on the fact that the first difference (difference between consecutive samples acquired) is normally small as compared to the whole

ADC range as shown in Figure 4.12. It is evident from Figure 4.12 that the first difference exceeded the limits of ±119, only 0.25% of the time (i.e. 5 out of 2000 samples). This strongly suggests that same information can be transmitted with fewer amounts of data at the expense of some processing power.
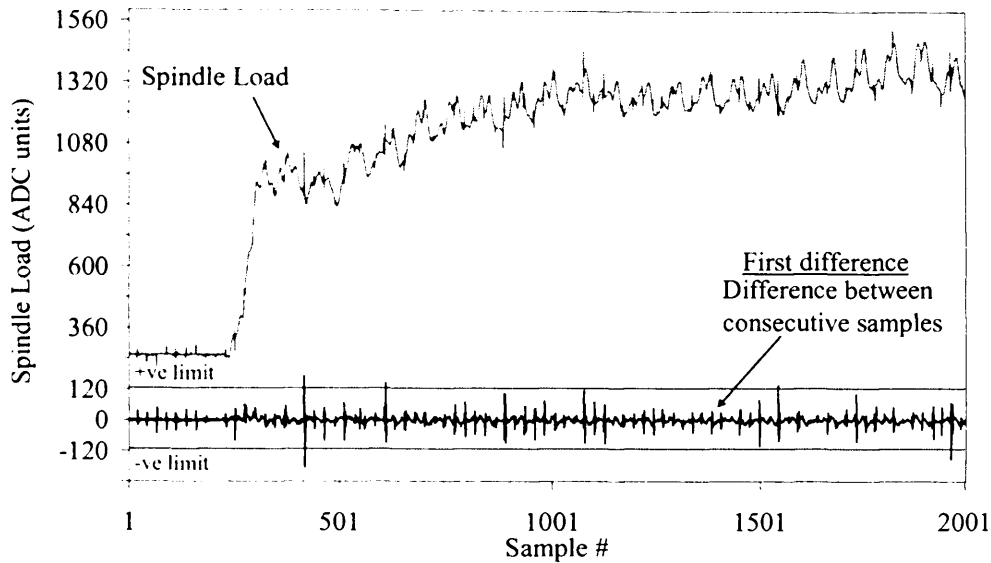

Figure 4.12: First difference of spindle load signal

In this algorithm only the difference from the last sample is transmitted using only 1 byte. Thus one CAN message can accommodate 8 bytes of data (as shown in Figure 4.11(c)) which provides a compression ratio of 50%. If the first difference is with in ±119, then 1 byte is used to store it by adding 120 to the first difference. It requires 2 bytes when the first difference is greater than ±119. In this situation the first byte will contains a value greater than 239, acting as flag and carrying higher 4-bits of the sample. The lower 8-bits of the sample are sent in the second byte. Thus an extra byte will be required whenever the first difference is larger than ±119. For a particular example as shown in Figure 4.12, only 5 extra bytes or one extra CAN message will be required to be sent for transmitting of 2000 samples. In total 251 CAN messages will be required instead of 500, providing a compression ratio of 49.8% and hence helping in reducing the network traffic. This means that the CAN bus will be available for additional time for other nodes to communicate while data is being sent to second tier.

4.5.6 Ethernet Connectivity

Ethernet is described by [4.29] as "the dominant cabling and low level data delivery technology" used in local area networks (LANs), and is commonly known as IEEE 802.3 standard. It forms the lower two layers of the Open System Interconnection (OSI) model [4.30] adopted by the International Standards Organisation (ISO). OSI model is a 7 layer protocol architecture representing information in a network. Using Ethernet, the data can be transmitted at different rates, which depend on the cabling of the communication network. For instance, a network built with a twisted-pair cable is supported by 10BASE-T Ethernet, where data is transmitted or received at up to 10 Mbps. It is most widely deployed network and some of its embedded applications include industrial monitoring, security systems and automation. [4.31]. It supports a wide array of data types such as TCP/IP, UDP and Apple Talk. It provides scalable networks, thus providing flexibility to system installation. IEEE 802.3 standards ensure reliability mainly in terms of network connection and data transmission. It detects data collisions, when more than one devices attempt to send data at the same time, so as preventing loss of information [4.32]. A device can be monitored or controlled through the internet once it is connected to an Ethernet network. Moreover, data collection and data sharing are also benefits from deploying Ethernet in embedded applications.

Internet Protocols

There are various internet protocols, but the most commonly employed protocol today is the Transmission Control Protocol/Internet Protocol (TCP/IP protocol). During the 1970s, the need to share computer resources in a cooperative way led to the development of this software-based protocol [4.33]. This protocol is reliable, thus data delivery is guaranteed [4.34]. Many implementations follow a software structure known as "TCP/IP reference model" in which software is divided into multiple layers stacked on top of each other and each layer accesses services from one or more layers directly bellow it.

The Microchip TCP/IP Stack

Microchip developed its own "TCP/IP stack", that provide services to TCP/IP-based applications such as HTTP and FTP servers, suitable for the deployment of its devices in embedded solutions. It is implemented in a modular fashion. Unlike the reference

model, one layer can access services from one or more layers not directly below it as illustrated in Figure 4.13.
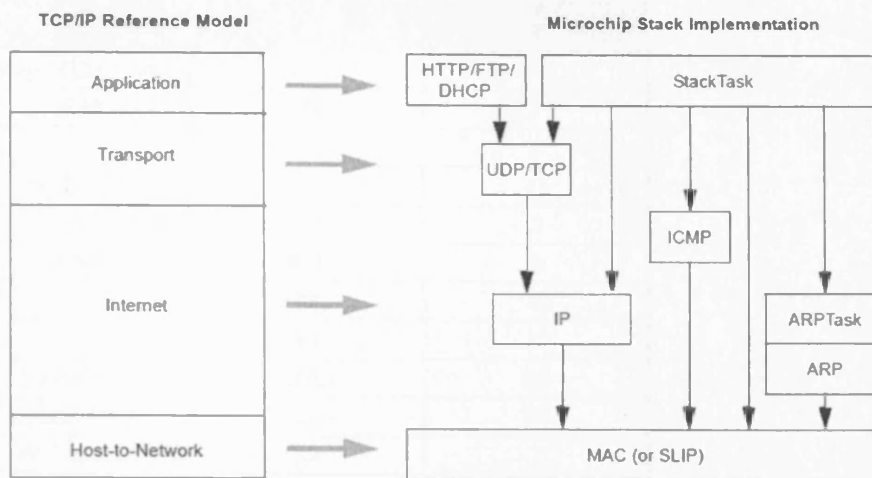

Figure 4.13: Illustration of Microchip TCP/IP stack software [4.33].

The Microchip TCP/IP protocol is designed to be independent of operating systems and is capable of cooperative multitasking [4.33]. It is written in C programming language and is designed to run on the dsPICDEM.net internet/Ethernet development board that is equipped with dsPIC30F6014 DSC and Realtek Ethernet controller. An in-depth discussion about this software is available in application notes AN833 and AN870 on the company's web site. It is portable across different Microchip microcontroller families including dsPIC30 and it provides support for Microchip C18, C30 compilers. It is based on modular design allowing new components to be added easily. It Implements complete TCP state machine and provides multiple TCP and UDP sockets with simultaneous connection / management. It can be used as a part of HTTP Server which is included with TCP/IP stack. It also includes Microchip File System (MPFS) and PC based program to convert PC files into MPFS image. Above all it is freely available and there are not royalty or license fees which may be a major consideration while implementing low cost system.

The total amount of memory used for the Microchip TCP/IP Stack depends on the compiler and modules being used. Typical sizes for the various stack modules are shown in Table 4.4. The Microchip TCP/IP Stack provides a space efficient and modular version of TCP/IP in a small footprint. Without getting into further details about the Microchip TCP/IP stack, its implementation with HTTP server was considered in this research.

Table 4.4: Memory Usage for various TCP/IP Stack Modules [4.33]

Module	Program Memory (words)	Data Memory (bytes)
MAC (Ethernet)	906	5[1]
SLIP	780	12[2]
ARP	392	0
ARPTask	181	11
IP	396	2
ICMP	318	0
TCP	3323	42
HTTP	1441	10
FTP Server	1063	35
DHCP Client	1228	26
IP Gleaning	20	1
MPFS[3]	304	0
Stack Manager	334[4]	12+ICMP Buffer

1. As implemented with the RTL8019AS NIC
2. Does not include the size of transmit and receive buffers which are user defined.
3. Internal program memory storage.
4. Maximum size. Actual size may vary.

4.5.7 GSM Connectivity

There is an increasing demand for real-time message communication on personal mobile devices. In recent times different products and services have become available which can be integrated into a monitoring system and SMS messages can be sent directly to the concerned person by the monitoring system. A SMS messaging hardware is basically a scaled and stripped down version of a mobile phone which provides only the SMS features. This can be interfaced with a microcontroller based system through a UART port and messages can be sent by following the specialized AT commands. This method has been tested in previous research [4.35] within the IPMM group. The main requirement for this system is the availability of GSM signals where the system is to be deployed. This method is however not suitable for places which are sensitive to GSM transmission and block are restrict these signals.

The other option is a subscription based service which hosts above mentioned hardware on a larger scale and provide internet interface to their system. Users can install SMS software on PC which sends HTTP request to the service provider specifying all the

information required for sending a text message. The automated system on the service provider side parses the HTTP message and prepares and sends the message immediately. One such service provide, ClickSMS also provides SMS messaging API which can be used to implement personalized application for sending SMS on an embedded platform which are connected and can run TCP/IP protocol. This functionality is implemented on the dsPIC based connectivity node in the integrated system.

4.6   Signal Processing and Analysis

There is great need to be able to process the signal in real time so that only useful information is sent to the higher layer instead of sending the raw data. This will not only make the data acquisition more meaningful but reduce the network traffic allowing more devices to be incorporated in a network without exceeding the network capacity /bandwidth.   Appropriate signal processing can provide an effective base for fault prediction. The first stage is to differentiate between normal and abnormal conditions. When an abnormal condition is detected then deeper analysis and monitoring can be triggered. DSP algorithms have been used for such purpose [4.36]. Even when the process is with in control limits different analysis of the various parameters can predict a potential developing (soft) fault at an early stage before it actually occurs. This will help to avoid catastrophes and fatal accidents as well as financial losses.

Math and DSP algorithm libraries provided by Microchip enable the mathematical computations to be performed with great speed and accuracy. The dsPIC30F Math Library is the compiled version of the math library that is distributed with MPLAB C30 compiler. It contains advanced single and double-precision floating-point arithmetic and trigonometric functions from the standard C header file <*math.h*>. The library delivers small program code size and data size, reduced cycles and high accuracy. The Math functions are callable from either MPLAB C30 or dsPIC30F assembly language. These functions are IEEE-754 compliant, with signed zero, signed infinity, NaN (Not a Number) and denormal support and operated in the "round to nearest" mode. The DSP library supports multiple filtering, convolution, vector and matrix functions. There are total of 49 functions. Some DSP functions use double precision and floating point arithmetic. All DSP routines are developed and optimized in the dsPIC30F assembly

language and are callable from both assembly and C language. Among the supported functions which are utilized in this research are:

- Infinite Impulse Response (IIR) Filters
- Finite Impulse Response (FIR) Filters
- Complex Fast Fourier Transform (FFT)
- Vector Operations: Addition, Subtraction, Dot Product and Power
- Support for Program Space Visibility

4.7   Summary

The dsPIC technology has introduced a new level of integration at the embedded level by combining the power of DSP with the rich set of peripherals and communication facilities of an MCU. These features can greatly contribute to the development of a reliable distributed monitoring system. A distributed system based on the 16-bit dsPIC digital signal controllers is proposed. A general overview of the proposed system was provided along with various aspects in signal acquisition, processing and communication. Efficient and reliable communication protocols such as CAN have become a necessity to enable the integration of distributed devices. Microchip has developed a TCP/IP protocol designed to ensure optimal performance requirements of the dsPIC devices, and this was implemented in this research, in conjunction with Ethernet Protocol, to enable access via the Internet. In this way a common interface was established for process management and communication of the real-time process status to the users remotely.

The technology requirement to enable the deployment of a three tiered distributed monitoring system based entirely on dsPIC modules and aiming at the monitoring of the machine tool was established in this chapter. To test the applicability and effectiveness of the system, the Kondia B500 milling machine will be monitored for tool breakage and several algorithms will be developed and implemented (chapter 5 and 6). In Another application, the depth of cut (DOC) is to be measured on-line using ultrasonic sensors and various techniques and algorithms (chapter 7). Finally these systems will be integrated to form a coherent TCMS (chapter 8) using technologies and techniques discussed in this chapter. These will be presented in the following chapters.

References

[4.1] A. S. Tanenbaum, M. V. Steen, "Distributed Systems: Principles and Paradigms," 2nd Edition, *Prentice Hall* 2007, ISBN: 0132392275, p2.

[4.2] G. Couloris, J. Dollimore, T. Kinberg, "Distributed Systems: Concepts and Design," 4th Edition, *Addison Wesley/Pearson Education* June 2005, ISBN: 0321263545, p1.

[4.3] V. R. Kennedy, A. D. Jennings, R. I. Grosvenor, J. R. turner, P.W. Prickett, "Monitoring using WebPages (e-Monitoring)," *In the proceeding of COMADEM 2000, 13th International Congress on Condition Monitoring and Diagnostic Engineering Management.* Huston USA 2000. MFPT Society, pp 877-883.

[4.4] J. R. Turner, A. D. Jennings, R. I. Grosvenor, P.W. Prickett, "The Design and Implementation of a Data Acquisition and Control system using Field bus Technologies", *In the proceeding of COMADEM 2001, 14th International Congress on Condition Monitoring and Diagnostic Engineering Management. Manchester*, UK 2001. Elsevier Science, pp. 391-398.

[4.5] S. Dunn, "Condition Monitoring in the 21st Century," *Plant Maintenance Resource Center*, [WWW] <URL:http://www.plant-maintenance.com/articles/ConMon21stCentury.shtml> (accessed on 20 Aug. 2006)

[4.6] Click SMS Ltd, "SMS Messaging API (XML/HTTP)", Click SMS Ltd (UK) [WWW]<URL:http://www.clicksms.co.uk/docs/ClickSMS-STD-SMS-API.pdf> (accessed on 3 Aug. 2008)

[4.7] M.R. Frankowiak, R.I. Grosvenor, and P.W. Prickett, "A Petri-net based distributed monitoring system using PIC microcontrollers," *Microprocessors and Microsystems*, vol. 29, Jun 2005, pp. 189-196.

[4.8] M. R. Frankowiak, R.I. Grosvenor, P.W. Prickett and A.D. Jennings, Distributed monitoring system using PIC microcontroller technologies," *International Conference on Mechatronics*, ICOM 2003, 2003, pp. 415-420.

[4.9] Q. Ahsan, W. Amer, R.I. Grosvenor, and P.W. Prickett, "A compact monitoring system for process valves," *IEEE Symposium on Emerging Technologies and Factory Automation*, ETFA, 2005, pp. 1043-1046.

[4.10] Q. Ahsan, W. Amer, R. I. Grosvenor, A. D. Jennings, P. W. Prickett, M. R. Frankowiak, "Design of a Process & Condition Monitoring System using PIC based Analogue Data Acquisition", *In the proceeding of COMADEM 2003*,Växjö, Sweden: Växjö University, ISBN 91-7636-376, pp. 227-235.

[4.11] P. Sinha, "The dsPIC30F Web Seminar: What is a dsPIC®DSC? (Part 1)" *Microchip Technology Incorporation*, [WWW] <URL: http://techtrain. microchip.com/webseminars/documents/dsPICIntro_111204.pdf (accessed on 20 Jul. 2005)

[4.12] Microchip Technology Inc., "dsPIC® Digital Signal Controllers" [WWW] <URL: http://www.microchip.com/1010/promos/dspic/ > (accessed on 15 Dec. 2004)

[4.13] Microchip Technology Inc., "The dsPIC30F Family Overview", [WWW] < URL: http://ww1.microchip.com/download/en/DeviceDoc/70043F.pdf > (accessed on 15 Dec. 2004)

[4.14] Microchip Technology Inc., "The dsPIC30F6011/6012/6013/6014 Data Sheet", [WWW] <URL: http://ww1.microchip.com/downloads/en/DeviceDoc/70117F .pdf> (accessed on 19 Dec. 2004)

[4.15] Matrix Multimedia Ltd UK "Teaching computing and electronics: dsPICs are coming." [WWW]<URL: http://www.matrixmultimedia.com/datasheets/dsPICs %20article.pdf> (accessed on 10 Jan. 2008)

[4.16] Microchip Technology Inc, "dsPICDEM1.1 General Purpose Development Board" [WWW] <URL: http://www.microchip.com/stellent/idcplg?IdcService= SS_GET_PAGE&nodeId= 1406& dDocName=en023537&part=DM300014 > (accessed on 23 May. 2005)

[4.17] Microchip Technology Inc, "dsPIC® Development Tools" [WWW] <URL: http://www.microchip.com/stellent/idcplg?IdcService=SS_GET_PAGE&nodeId =2035> (accessed on 24 May. 2005)

[4.18] Microchip Technology Inc., "dsPIC30F Family Reference Manual: High performance Digital Signal Controllers", Section 13, Document DS70046C, 2004.

[4.19] J. G. Proakis, D.G Manolakis, "Digital Signal Processing, principles, algorithms and applications", 3rd Edition, *Prentice Hall* 1996, ISBN: 0133737624, pp. 5-35

[4.20] S. W. Smith, "The Scientist and Engineer's Guide to Digital Signal Processing", *California Technical Publishing* 1999, ISBN: 0966017668, pp.40-42

[4.21] Microchip Technology Inc., "Section 18- 12-bit A/D Converter (dsPIC30F Family)" [WWW] <URL: http://ww1.microchip.com/downloads/en/DeviceDoc/70065D.pdf > (accessed on 10 Jul. 2008)

[4.22] Microchip Technology Inc., "Section 12- Timers (dsPIC30F Family)" [WWW] <URL: http://ww1.microchip.com/downloads/en/DeviceDoc/70065D.pdf > (accessed on 02 Jul. 2008)

[4.23] Microchip Technology Inc., "dsPICDEM.net 1 and dsPICDEM.net 2 Connectivity Development Board User's Guide", [WWW] <URL: http://ww1.microchip.com/downloads/en/DeviceDoc/51471a.pdf> (accessed on 02 May. 2007).

[4.24] CAN in Automation, "Controller Area Network (CAN)", [WWW] <URL: http://www.can-cia.org/> (accessed on 12 Jul. 2008).

[4.25] Steve Corrigan, "Introduction to the Controller Area Network (CAN)", Application Report Number SLOA101A, Texas Instruments 2008, [WWW] <URL http://focus.tij.co.jp/jp/lit/an/sloa101a/sloa101a.pdf> (accessed on 10 Jul. 2008)

[4.26] CAN in Automation, "CAN made easy" [WWW] <URL: http://www.can-cia.org/pg/can/additional/can_basics_print.pdf> (accessed on 17 Sep. 2006)

[4.27] Microchip Technology Inc., "Ease into the Flexible CAN bus Network," [WWW] <URL: http://ww1.microchip.com/downloads/en/DeviceDoc/adn004 .pdf > (accessed on 10 Sep. 2006)

[4.28] P. Sinha, "The dsPIC30F Web Seminar: Serial Communication using the dsPIC30F CAN module", Microchip Technology. Inc., [WWW] < URL: http://techtrain.microchip.com/webseminars/ArchivedDetail.aspx?Active=92 > (accessed on 25 May. 2005)

[4.29] Indiana University, "University Information Technology Services", [WWW] <URL: http://kb.iu.edu/data/aesi.html> (accessed on 8 May. 2007)

[4.30]   C.E. Spurgeon, "Ethernet," *O'Reilly* 2000, ISBN: 1565926609, pp. 12-13

[4.31]   Cisco Systems, "Internetworking Technologies Handbook", [WWW] <URL: http://www.cisco.com/univercd/cc/td/doc/cisintwk/ito_doc/index.htm> (accessed on 5 May. 2007)

[4.32]   Microchip Technology Inc., "Embedded Ethernet Made Easy", [WWW] <URL: http://techtrain.microchip.com/webseminars/ArchivedDetail.aspx?Active=126> (accessed on 15 Apr. 2007)

[4.33]   Microchip Technology Inc., "Microchip TCP/IP Stack Application Note", [WWW] <URL: http://www.microchip.com/stellent/idcplg?IdcService=SS_ GET_PAGE&nodeId=1824&appnote=en011993> (accessed on 10 Apr. 2007)

[4.34]   Microchip Technology Inc., "Connectivity Solutions for the dsPIC30F", WWW] <URL: http://techtrain.microchip.com/masters2004/(m4klpwnelumu 3o3dth10rnqb)/downloads/classes/857/857.htm> (accessed on 7 Jul. 2005)

[4.35]   Q. Ahsan, "Compact Information Technology Enabled Systems for Intelligent Process Monitoring", PhD Thesis, *Cardiff School of Engineering, Cardiff University* 2006, pp. 113-114

[4.36]   P.R. Drake, R.I. Grosvenor and A.D. Jennings, "Review of Data Acquisition System Developed for the MIRAM Project", *The seventh conference on Sensors and their Applications VII*; Institute of Physics Publishing, 1995, pp. 433-437.

Chapter 5

Real-Time Frequency Analysis for Tool Monitoring

5.1.   Introduction

This chapter describes the development and testing of dsPIC digital signal controller algorithms both in a general sense and for a specific application. The latter used real-time frequency analysis of machine tool signals as a basis for a tool health monitoring system. Frequency analysis reveals information about the overall signal content which can be otherwise hidden in time domain signals. Time domain signals containing complex patterns are broken apart into their various frequency components, which act as a feature set for tool condition monitoring. Normally, for frequency analysis, a signal is sampled in the time domain and its frequency response is calculated using different mathematical techniques such as the Discrete Fourier Transform (DFT). The Fast Fourier Transform (FFT) is a well known algorithm used to compute the DFT of a signal a much faster speed [5.1]. However FFT is normally only suitable for stationary signals (signals whose properties are unaffected by change in the time domain) and is not very effective for non-stationary signals; it cannot reveal information about transients occurring in non-stationary signals [5.2]. FFT can be used for machine tool monitoring through a modified algorithm known as Short Time Fourier Transform (STFT) which computes FFT for a small portion of signal at a time as will be discussed in Section 5.2.

The primary aim was to investigate the suitability and capability of dsPIC devices for monitoring the health of cutting tools using digital signal processing algorithms. This was intended to provide a practical low cost system as an alternative to the majority of the reported research, where a PC based analysis under laboratory conditions were carried out (as reported in Chapter 3). The author has, in published work, successfully demonstrated the capability and accuracy of such devices in performing different signal processing algorithms such as digital filters and FFT [5.3].

The new research here used an overlap FFT algorithm which was initially tested using a simulation model developed in Matlab/Simulink software. After verifying the effectiveness of the algorithm with systematically selected parameters, this was programmed into the dsPIC microcontroller.

The IPMM group has created a large database of recorded signals from a variety of cutting tests on a known milling machine. For testing purposes the recorded spindle load signals were selected and in each test the analog signal was recreated from the pre-recorded files, containing data acquired, using Matlab software and National Instruments Data Acquisition (DAQ) card with analog output capabilities. In order to simplify the test and to concentrate on the overlap FFT algorithm, the required signal conditioning stages were implemented in the Matlab code whilst re-generating the signal. The generated signal was then input to the dsPIC based system, which processed the acquired data and stored the results in its memory. The stored results were communicated to a PC after completion of the test, for display and reporting purposes. Various aspects, related to the design and implementation of the system, are discussed in the following sections.

5.2   Frequency Analysis

There are various techniques available for the frequency analysis of a signal such as filter banks, wavelets, power spectral density and Fourier based transforms including Fourier Transform (FT), FFT and STFT.

5.2.1   Fourier Transform

The Fourier transform (FT) needs no introduction as a tool for analysis, and full discussion of it is beyond the scope of this thesis. However it is still the most important signal processing tool, and as such warrants a brief overview. It is also necessary background for understanding of the Short Time Fourier Transform (STFT). Using Fourier theory, one can mathematically relate the time domain with the frequency domain. The Fourier transform is given by [5.4]:

$$X(f) = \int_{-\infty}^{\infty} x(t)e^{-j2\pi ft}dt \qquad (5.1)$$

where $x(t)$ is a signal represented in the time domain and $X(f)$ is its Fourier transform in the frequency domain. Normally the Fourier transform is defined for continuous

signals whereas digital systems are discrete in nature and the signal acquired is also discrete. The Discrete Fourier Transform (DFT) is thus one of the specific forms, which requires an input that is discrete and whose non-zero values have a limited (*finite*) duration. Such inputs are often created by sampling a continuous signal, such as the spindle speed and load signals for machine tool application. An input sequence of N complex numbers x_n, $n=0,...N-1$ is transformed into a sequence X_k of N complex numbers via the DFT according to Equation 5.2.

$$DFT_N\{x_n\} \equiv X_k = \sum_{n=0}^{N-1} x_n e^{-j\frac{2\pi}{N}kn} \qquad 0 \le k \le N-1 \qquad (5.2)$$

The DFT provides enough frequency components to only reconstruct the finite segment that was analyzed. Its inverse transform cannot reproduce the entire time domain signal, except when the input is periodic. Thus the DFT is often described as the a transform for the Fourier analysis of finite-domain discrete-time functions. Since the input function is a finite sequence of real or complex numbers, the DFT is ideal for processing information stored in computers. In particular, the DFT is widely employed in signal processing and can be computed efficiently in practice using a Fast Fourier Transform (FFT) algorithm. FFTs are of great importance to a wide variety of applications, from digital signal processing and solving partial differential equations to algorithms for quick multiplication of large integers. Calculating the DFT directly is known to take take $O(N^2)$ arithmetical operations, where as the FFT algorithm will compute the same result in only $O(N.logN)$ operations. Since the inverse DFT is the same as the DFT, but with the opposite sign in the exponent and a $1/N$ factor, any FFT algorithm can easily be adapted for inverse transforms.

To summarize, the main parameters of an FFT are as follows:

The FFT operates on a block of data to produce a corrosponding frequency spectrum as a set of data . If f_s is the sampling frequency of the input signal x_n and an N-point FFT is performed, then the resulting spectrum will have N values from 0 to f_s equally spaced on the frequency scale at Δf. Frequency components from $f_s/2$ to f_s are in fact mirror images of the 0 to $f_s/2$ components and the useful frequency output range is normally considered as 0 — $f_s/2$. The Frequency resolution Δf of the DFT is defined as follows :-

$$\Delta f = \frac{f_s/2}{(N/2)-1} \qquad Hz \qquad (5.3)$$

$$\text{or } \Delta f \cong \frac{f_s}{N} \qquad \text{for large values of } N \qquad (5.4)$$

Further if $Y = \text{DFT}_N\{x_n\}$ is the N point Discrete Fourier Transform (DFT) of input a signal x_n then [5.5]

$$\text{Amplitude of the DFT} = |Y| \qquad (5.5)$$

$$\text{Power of the DFT} = \frac{|Y|^2}{N} \qquad (5.6)$$

As a comparasion, two other specific transforms are reported here, since these were considered in terms of compactness and effectiveness of the code required for the eventual dsPIC implementation. Zoom-FFT and Chirp-Z transform (CZT) can be used for calculating the spectrum of a signal over a small range of frequencies. Details of the zoom FFT and the chirp-Z transform can be found in [5.6] and [5.7] respectively. Figure 5.1 shows a typical spectrrum for the spindle load signal (of a milling machine) obtained, whilst cutting with a broken tool. Figure 5.1(a) shows the version of the spectrum obtained using CZT and Figure 5.1(b) shows results of an FFT performed on the same data. The CZT provides much better, and arbitrary, frequency resolution. However CZT algorithm requires two FFT operations, one Inverse FFT (IFFT) operation and two array multiplication operations. As a direct consequence, the FFT calculated the required feature set with much less computation time. This was deemed to be a significant requirement for the dsPIC microcontroller-based system that was to form the heart of a real-time tool conditioin monitoring system.

(a) Chirp z Transform
250 data points, Δf=0.31Hz

(b) FFT
240 data points, Δf=4.16Hz
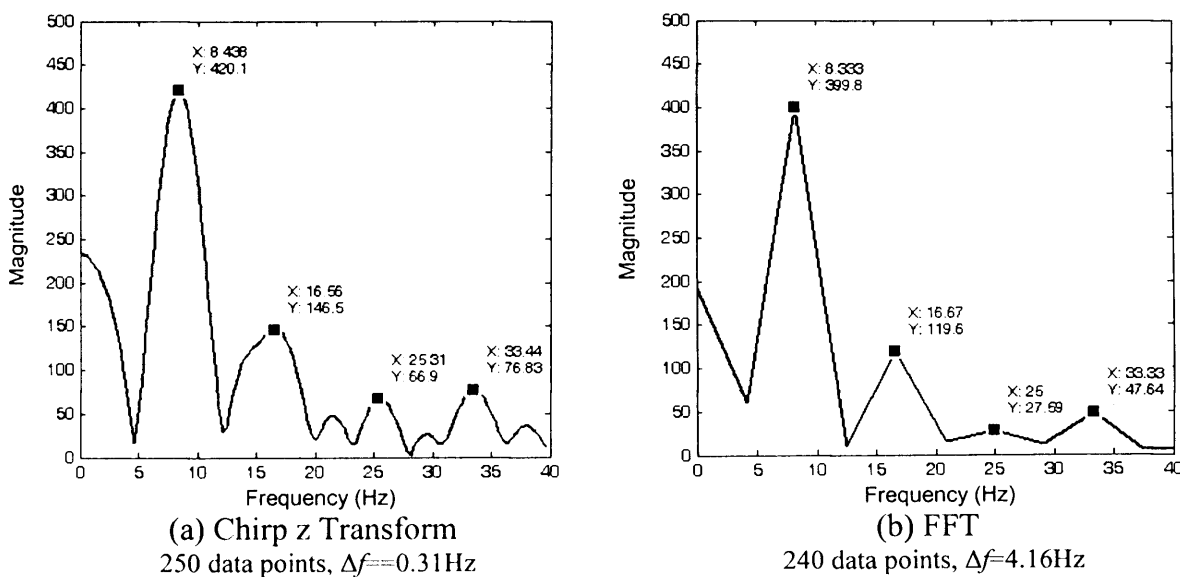
Figure 5.1: Comparison of Chirp Z transform and FFT

5.2.2 Short Time Fourier Transform

Although the Fourier transform is the standard spectral analysis technique, it performs poorly at analyzing non-stationary signals, since the frequency content is considered for the complete block of input data. To see how the frequency contents of a signal change over time, the signal can be 'cut' into blocks or frames of contiguous data and the spectrum of each frame computed. This provides a time resolution equal to the selected length of frame. This technique is called Short Time Fourier Transform (STFT). Usually, in STFT analysis, the signal $x(t)$ is windowed using some window function $w(t)$, which is nonzero for only a short period of time, before the Fourier transform is applied. The complete time-frequency transform is then acquired by translating this window along the signal and repeatedly applying the Fourier transform at each location. In this way a 2D transform is created, with values defined at translation points τ and spectral points f. mathematically, this is written as [5.8]:

$$STFT\ \{x(t)\} \equiv X(\tau, f) = \int_{-\infty}^{\infty} x(t)w(t - \tau)e^{-j2\pi ft} dt \qquad (5.7)$$

The simplest type of window function is the rectangular window, which in effect simply selects the signal frame whose length is equal to window size. Other window functions include the Hanning window, the Hamming window and the Gaussian ("hill" centered around zero) window. $X(\tau, f)$ is essentially the Fourier Transform of $x(t)w(t - \tau)$. In order to demonstrate the benefits of STFT for a non-stationarry signals, a simple example is provided in the following paragraph.

Figure 5.2 shows the analysis of two different combinations ($x_1(t)$, $x_2(t)$) of two specific sine waves (with frequencies f_1=5 and f_2=20 Hz), such that:-

$$x_1(t) = sin\ (2\pi f_1 t) + sin(2\pi f_2 t) \qquad (5.8)$$

$$x_2(t) = [1 - u(t-1)]sin(2\pi f_1 t) + u(t-1)sin(2\pi f_2 t) \qquad (5.9)$$

In the left hand column the additive combination, $x_1(t)$ (Equation 5.8), of the two sine terms applies for whole of the example 2 second timeframe. However, the right hand column results of Figure 5.2 use $x_2(t)$ (Equation 5.9) where f_1 sine wave exists initially and is then replaced with the f_2 frequency. The plots thus show up the limitation of the FT, since the power spectrum for both cases are essentially the same. The reason for

this can be seen in Equation 5.1 - the terms of the integral are in this case, for the full 2 second duration. On the other hand, the STFT correctly identifies the switch over between the two sections of the signal $x_2(t)$.
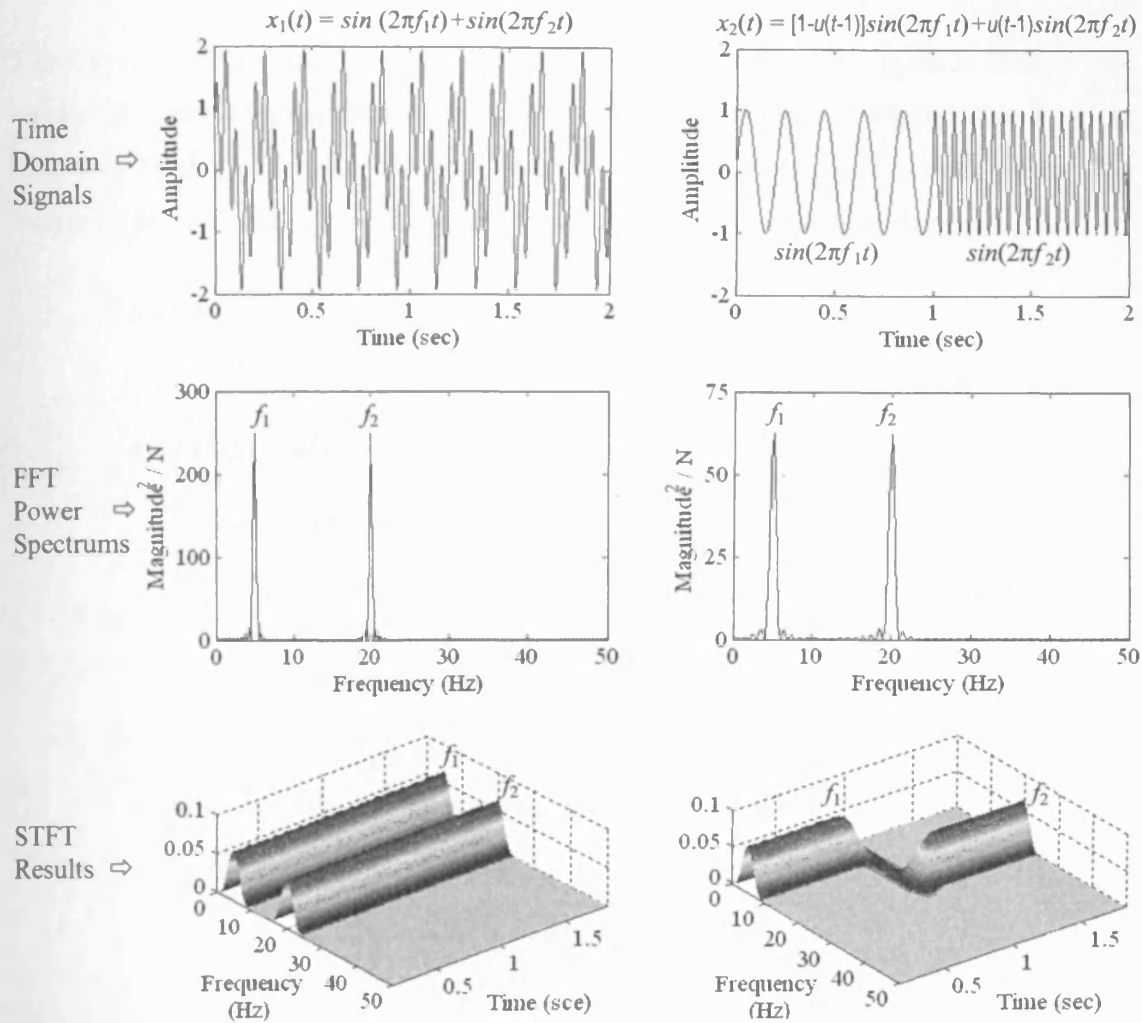

Figure 5.2: Signals presented in different domains: the time domain (top), the power spectrum from the FFT (middle), and the spectrogram from the STFT (bottom)

In the most direct application of the discrete Time STFT, as defined below, is in its use to calculate sampled STFT for discrete time signals sampled at fixed intervals.

$$STFT\{x_n\} \equiv X_{k,m} = \sum_{n=0}^{M-1} x_{n-L,m} w_n e^{-j\frac{2\pi}{N}kn} \qquad 0 \le k \le N-1 \qquad (5.10)$$

$$STFT\{x_n\} \equiv X_{k,m} = DFT_N\{x_{n-L,m}(w_n|_0^{M-1}, zeros(N-M))\} \qquad (5.11)$$

Where

$zeros(N-M)$ is the zero padding to make the length of the signal equal to FFT length N,

98

M is window length or block/frame size and

Lapse time L is number of samples the signal is shifted between consecutive FFT calculations.

There is no overlap between consecutive data frames, when the signal is broken into blocks of length M then shifted M samples at a time along the window i.e. $L=M$ as shown in Figure 5.3(a). In this case one FFT result is obtained for each frame. The following section and Figure 5.3(b) introduce the use of overlapping data sections.

Figure 5.3 (a): STFT with no overlap

Figure: 5.3 (b) Overlap FFT
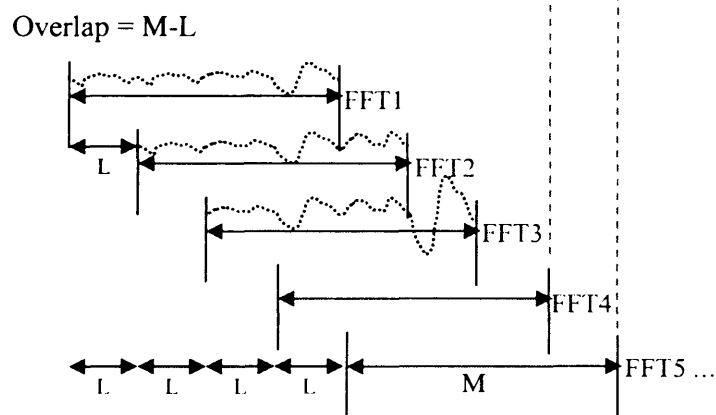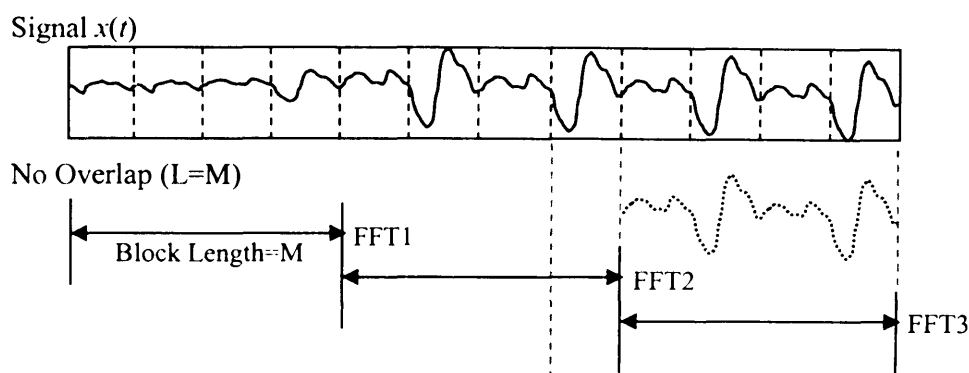
5.2.3   Overlap FFT

The window function has a dual purpose in the STFT: to isolate a block of data from the signal and to minimize the spectral frequency leakage resulting from sharp signal cutoffs (discontinuities) at the data block ends/edges. If there is a transient signal at the edge of the block, this will not be visible in the FFT spectrum because signal will be attenuated to zero due to windowing. To overcome this problem and to reduce time between successive FFTs, the overlap parameter (lapse time) L should be shorter than the window length M, thus providing an *overlap=M-L* between two connective frames, as shown in Figure 5.3(b).

In defining the details of the STFT/overlap FFT to be used for a given application, there are several parameters which must be considered. Briefly these parameters are as follows:

- Type of window.
- Block/window length, M.
- FFT size
- Frequency Resolution
- Amount of zero padding, if any.
- Lapse time L or Amount of overlap between blocks (M-L)

The specifics of parameter selection for the cutting tool application will be discussed in Section 5.5.

There are other transforms which can also be used for time-frequency analysis such as the Gabor transform, wavelet transform, chirplet transform and transforms based on Wigner, Wigner-Ville and Choi-Williams distribution functions. These are not considered in this thesis.

5.3 Cutting Forces / Spindle Load Signal Analysis

A typical milling machine consists of a motor driven spindle, which holds and revolves the milling cutter and a movable worktable, which mounts and feeds the workpiece. These are almost always controlled by a computerized controller, with perhaps a supervisory role being played by a human operator [5.9]. This leads to several operational problems, one of which is the potential for a cutting tool breakage to go undetected. The dangers of continuing to utilise a broken cutter range from damage to the workpiece through to potential damage of the machine tool. For this reason there has been a great deal of effort deployed aimed at detecting tool breakage.

The end milling process exhibits a period generation mechanism, perturbed by spindle speed variations, tool conditions and effects of chip [5.10]. The cutting force/spindle load signal varies periodically with tooth passing frequency f_p which is the product of the spindle rotational frequency and the number of cutting teeth (n_t).

$$f_p = \frac{n_t N_s}{60} \quad \text{[Hz]} \qquad \text{where } N_s \text{ is spindle speed in revolutions/min} \qquad (5.12)$$

The basic assumption made considers that, under normal cutting conditions, the cutting force is periodic, with f_p being the dominant frequency. The characteristics of the cutting force signal and its frequency components may then be assumed to change with (usually deteriorating) tool condition. Thus it is proposed that the tooth passing frequency and its harmonics are dominant for a healthy tool/cutter. The definition used for 'healthy' is that each tooth removes approximately the same amount of material per cut. In the event of a tooth breakage, since one of the teeth is missing and next one has to do extra cutting, a clear indication of the rise in the cutting force for that particular tooth is seen. This in turn is responsible for a change in overall frequency spectra. In simple terms, the cutting force signal decreases and then increases once every revolution compared to healthy levels and a tool rotation frequency f_r will appear in the spectrum.

$$f_r = N_s / 60 \text{ [Hz]} \tag{5.13}$$

This introduces frequency components which are the same as those arising due to tool rotation and its higher harmonics. These frequency components get stronger when the tool breaks and can be used to give clear indication of the breakage.

In a separate, more theoretical analysis a cutting force model was developed in Matlab. This model was based on equations provided in [5.11] and modeled forces for both a 4-tooth healthy tool and for a tool with a broken tooth. In each case the cutting tool rotational speed was 500 rpm. The modeled cutting forces are shown in Figure 5.4.

(a) Healthy tool   (b) Tool with 1 tooth broken
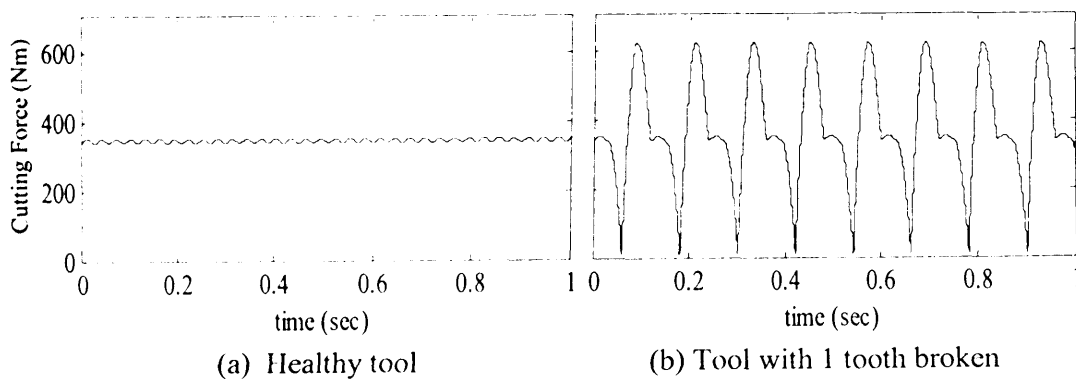
Figure 5.4: Modeled cutting forces

The FFT spectrums (of the modeled cutting forces) obtained are shown in Figure 5.5. This specific case illustrates the previously assumed behavior. The tool rotation frequency f_r was 8.33 Hz and the tooth passing frequency f_p was 33.3 Hz. From Figure

5.5 it can be seen that components of the tooth passing frequency f_p (and to a lesser extents its harmonics) are prominent in the frequency spectrum for healthy tool. For the broken cutter case, the tool rotation frequency f_r and its harmonics now dominate the spectrum, noting that f_p is itself a multiple of f_r. This analysis confirms that frequency domain analysis can be used to indicate tool breakage.

(a) Healthy tool   (b) Tool with 1 tooth broken
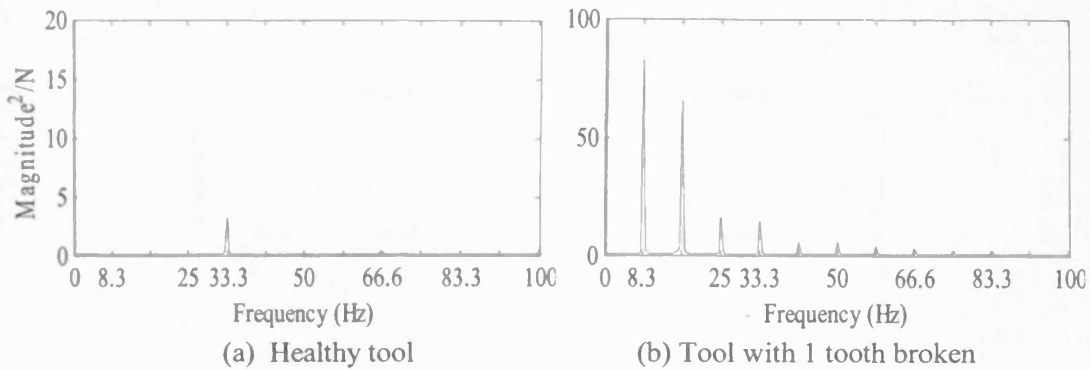
Figure 5.5: FFT spectrums of the modeled cutting forces

By analyzing the magnitude and pattern of these key frequencies present in the spectrum and having selected the algorithm (to resolve the harmonics of tool rotation) for real-time analysis on a dsPIC, and using limited amount of data, it is possible to monitor the health of the cutting tool in real time.

Figure 5.6 shows the spindle load signal re-constructed from cutting cycles undertaken in the IPMM laboratory, for a simulated tool breakage. Signals for healthy and broken tool were 'stitched' together to simulate tool breakage profile. The corresponding spectrogram from a STFT, performed in Matlab using built spectrogram function is also shown. For this offline test, the tool breakage occurs around 1 second into the time profile. Prior to this the tool is in healthy condition and the spectrogram is relatively flat. Tool breakage can easily and almost immediately be identified from the increasing amplitude of the tool rotation frequency f_r and its harmonics (again 8.33Hz and multiples for results shown).

The spindle speed signal was processed in the same way and the results are shown in Figure 5.7. This confirms that these assumptions can equally be applied to spindle speed signal as well. This shows the suitability of the STFT for real-time tool breakage detection using associated signals.
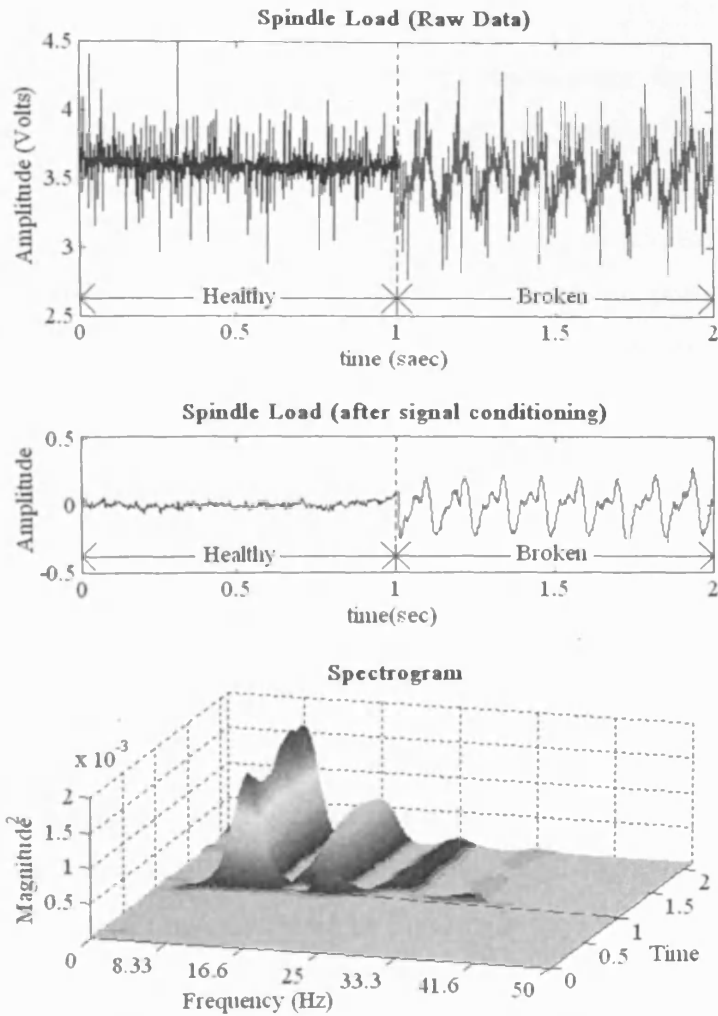
Figure 5.6: Spindle load signal (top and middle) and spectrogram from STFT (bottom)
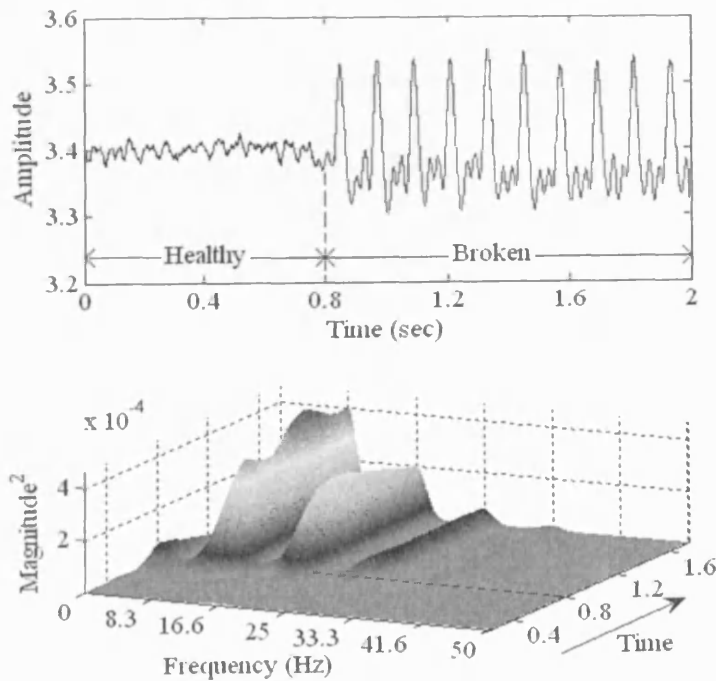
Figure 5.7: Spindle speed signal (top) and spectrogram from STFT (bottom)

103

5.4   Selection of Parameters

This section describes the selection of different parameters for the overlap FFT algorithm. These needed to be set to make the method computationally efficient and hence fast enough for tool health monitoring whilst providing sufficient robustness and resolution. In comparison to other appropriate published research, the ambitious target of achieving tool breakage detection in under 2 tool revolutions post breakage was set an objective. For the numerical example provided this equals to detection of tool breakage with in 0.24 seconds.

5.4.1   Window Type and Block Length

The first parameters considered were the window type and block length M. This was approached via consideration of the ability to resolve 2 close frequencies. For effective tool condition monitoring, the harmonics of the tool rotation frequency f_r present in the spindle load signal are those that must be resolved. The time resolution of STFT is inversely proportional to window length i.e. the window with minimum length M will provide best time resolution while separating the harmonics. The Fourier transform of two windowed sinusoids with frequency f_1 and f_2 summed together is the sum of two overlapping window transforms, as shown in Figure 5.8 for a rectangular window.
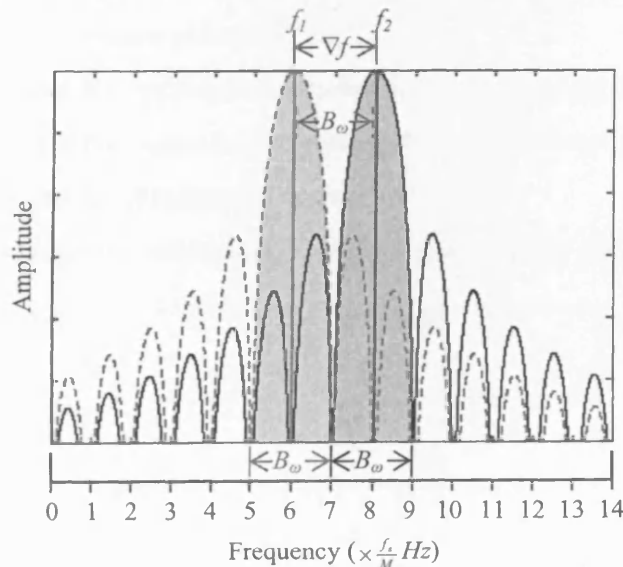
Figure 5.8: Two rectangular window transforms displaced by $\nabla f = \frac{2f_s}{M}$ Hz

A simple sufficient requirement for resolving two sinusoidal peaks spaced ∇f Hz apart is to choose a window length long enough so that the main lobes are clearly separated [5.12]. To obtain this separation, it is required that

$$B_\omega \leq \nabla f \text{ Hz} \tag{5.14}$$

where $\nabla f = |f_2 - f_1|$ is the minimum sinusoidal frequency separation in Hz and B_ω is the main lobe width of the window's transform in Hz given by $B_\omega = W (f_s / M)$. Here W is the main-lobe width in terms of frequency bins (when critically sampled i.e. FFT size N is equal to the window length M).

Requiring $B_\omega \leq \nabla f$ Hz thus implies that:

$$M \geq W \frac{f_s}{|f_2 - f_1|} \tag{5.15}$$

More specifically, the harmonic components of tool rotation frequency f_r (Hz) occur at integer multiples of f_r, and have spacing $\nabla f = f_r$. Thus to resolve these particular harmonics requires that:

$$M \geq W \frac{f_s}{f_r} \text{ or } M \geq k \cdot W \tag{5.16}$$

where $k = f_s / f_r$ is the number of samples in the fundamental period of the signal with fundamental frequency f_r, which is sampled at a sampling rate of f_s. The sufficient resolution requirement on window length M, for periodic signals with period of k samples, is $M \geq Wk$. This is shown diagrammatically in Figure 5.9, for 2 of the considered window types. Resolving the harmonics of a periodic signal with period k samples is assured if there are at least [5.12]

- 2 periods under the rectangular window ($M = 2k$), [shown in Figure 5.9(a)]
- 4 periods under the Hamming window ($M = 4k$), [shown in Figure 5.9(b)]
- 6 periods under the Blackman window ($M = 6k$),
- 2L periods under the Blackman-Harris L-term window ($M = 2L.k$).
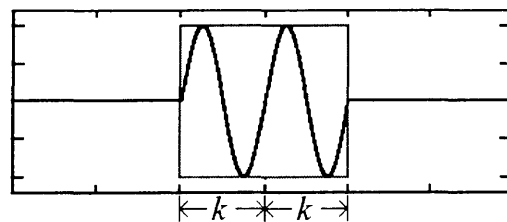
(a) Rectangular Window: Length $M=2k$
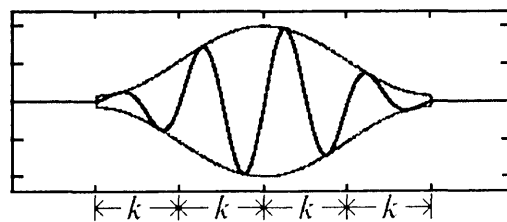
(b) Hamming Window: Length $M=4k$

Figure 5.9: (a) Rectangular and (b) hamming windows applied to a sinusoidal signal

These analysis show that using a rectangular window can provide harmonic separation with the least amount (2 tool rotations) of data being required. For example, if the spindle load signal is sampled at 1066Hz for a tool revolving at 8.33 Hz (spindle speed of 500 rpm), the minimum number of samples (equal to window length) required for Fourier analysis will be 256.

As well as providing the minimum window/block length, the rectangular window has added advantage of having a constant amplitude (in its active region) which can be safely assumed unity. The implications for the dsPIC implementation are that there is no need for array multiplication of the window and the shifted signal. Although rectangular window provides spectral leakage but this can be minimized by making the sampling rate proportional to the spindle speed, whereby f_r and its harmonics are located in the centre of the main lobe of the window transform.

5.4.2   FFT Length and Resolution

The next parameter considered was the FFT length (N) and in particular the effect on the achievable resolution in the resulting spectrums. To facilitate this spindle load signals (for healthy and broken cutters) were analysed using N values of 128, 256, 512, 1024, 2048 and 4096. Fourier transforms were compared in terms of the clarity of the required and prominent frequencies. Figure 5.10 shows a typical set of results.

It can be seen in the Figure 5.10 that the tool rotation frequency f_r (8.33 Hz) and its harmonics are prominent in the broken cutter transform for each N value case. The components between each harmonic have almost zero amplitude. For the 128 point FFT the prominent frequencies exist but the resolution is limited and no information is present for between harmonic frequencies. The 256 point FFT (broken cutter) shows prominent frequencies and at least one frequency component between them which are all very small in magnitude. The information provided by FFTs with larger N values confirms the choice of the 256 point FFT for the tool condition monitoring application. With N=256 and signal sampling 1066 Hz (for spindle speed = 500 RPM) the tool rotation frequency was 8.333 Hz. The frequency resolution thus would be:-

$$\Delta f = \frac{f_s}{N} = \frac{f_r}{2} = 4.165 Hz \qquad (5.17)$$
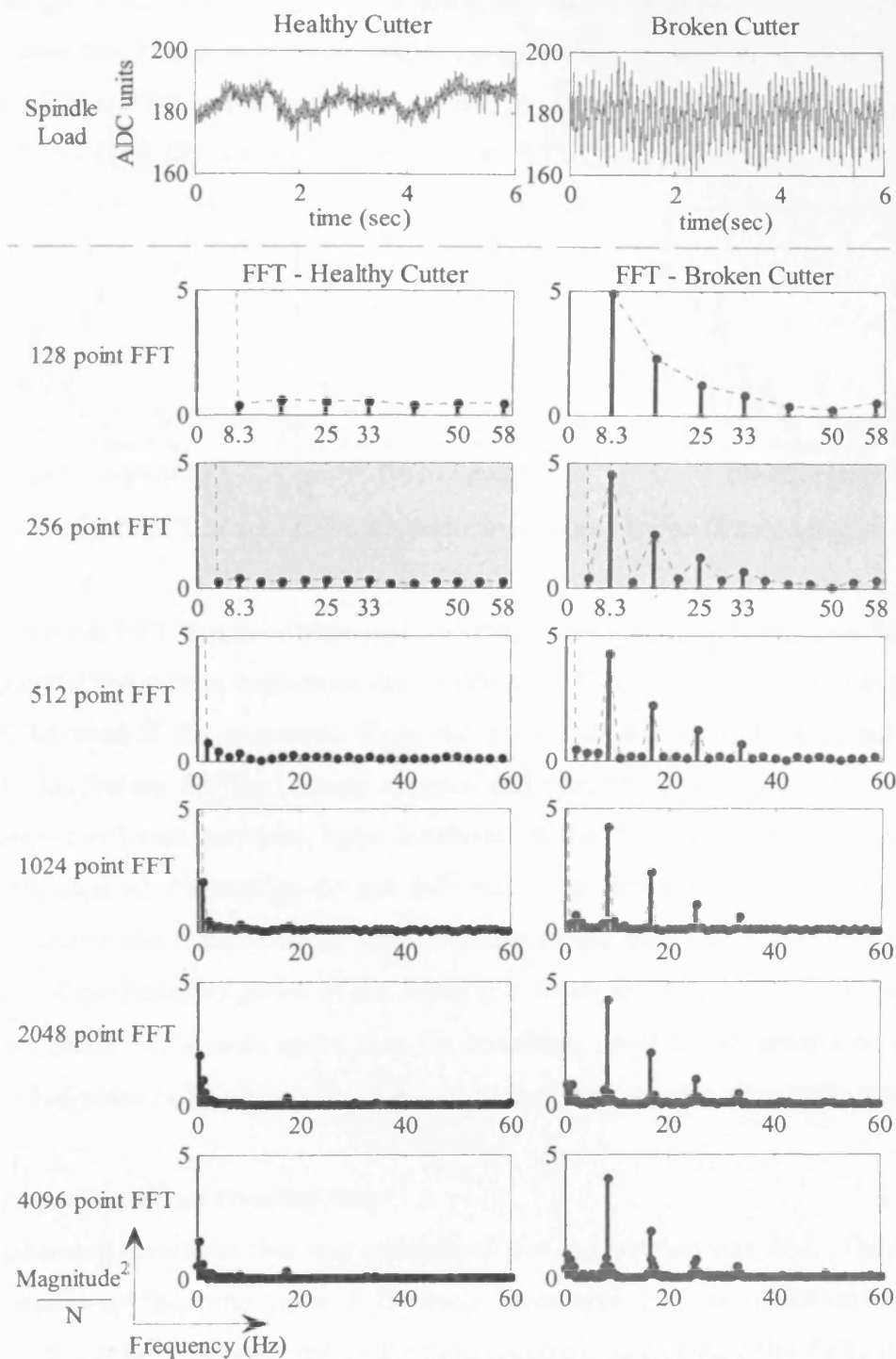
f_s=1065Hz, ASS= 500rpm, DOC=2mm, feedrate= 100mm/min, 4 teeth cutter, tool dia=15mm

(Left: Healthy Cutter, Right: Broken Cutter, Row 1: Spindle Load, Row 2 to7: FFT)

Figure 5.10: Comparison of Spindle Load Signal for different FFT Lengths (N)

Frequency resolution can be increased by increasing the FFT length and zero padding the signal with *N-M* zeros. However it will not provide better frequency separation as this is limited by the window length. Tests and analysis were calculated using a fixed

block length of 256 and filling the remaining FFT buffer with zeros. The sampling rate in this case was 1KHz, providing frequency resolution of Δf=3.91, 1.95 and 0.98 Hz for the FFTs shown in Figure 5.11 (a, b and c). Figure 5.11(a) has no zero padding, Figure 5.11(b) has 256 zeroes added and Figure 5.11(c) has 768 zeroes.

(a) 256 point FFT   (b) 512 point FFT   (c) 1024 point FFT
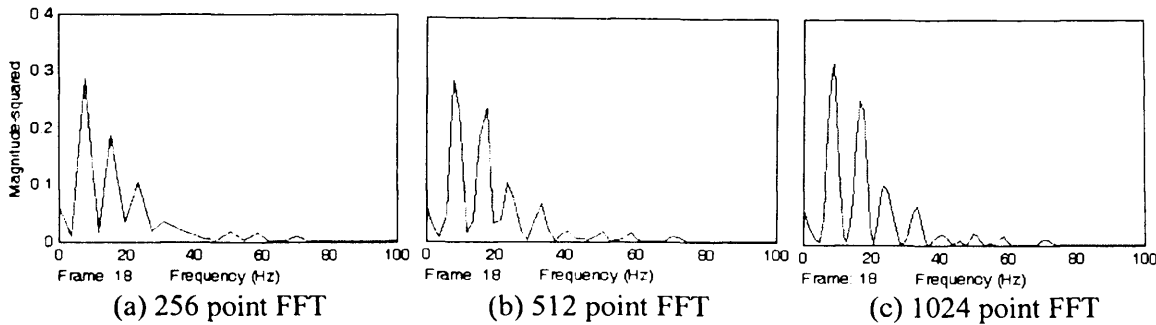
Figure 5.11: FFT of zero padded spindle load signal frame (frame length=256)

As the overall FFT length is increased, increased frequency resolution provides more spatial detail and correct harmonics can be detected. Thus the highest possible FFT size should be used if the resources allow the computation and processing sufficiently quickly i.e. before the next frame appears and requires processing. This increased frequency resolution provides better estimate of the frequency spectrum especially when the desired frequencies do not fall exactly in the centre of the main-lobe of window transforms because of the frame/window length not exactly matching with any multiple of fundamental period of the signal (i.e. $M{\neq}W.k$). However if sampling rate is in proportion to the spindle speed then the condition, $M{=}W.k$, will always be satisfied and the 256 point FFT will be able to detect the tool breakage for all spindle speeds.

5.4.3 Lapse Time and Overlap Size

The remaining parameter that was considered was the overlap size M-L. The Overlap size determines the time lapse L between successive FFT computations. Overlap processing can only be achieved if the time required, to calculate the FFT, is shorter than the frame length [5.13]. The overlap between frames has the effect of magnifying the time resolution of the STFT. Overlap is normally defined as a percentage or fraction of the frame/block length. In the tool monitoring application the frame length is fixed to correspond to 2 tool rotation periods. The lapse time L is thus referred to as a fraction of tool rotation. For example, when $L{=}\frac{1}{2}$ (of a tool rotation), the overlap is 75% or if $L{=}\frac{1}{4}$, the overlap is 87.5% of frame length. Ideally one FFT computation should be

performed for each tooth period, in order to achieve the optimum fault detection time. This means that for a cutter with n_t teeth, L should be $1/n_t$ and the overlap should be $2 - 1/n_t$ revolutions or $(1 - 1/2n_t) \times 100\%$.

As sampling rate is linked to spindle speed (justified in Section 5.5.3) for this application, any increase in spindle speed will decrease the frame acquisition time and there will be less time available to compute the FFT. Considering the processing power of dsPIC microcontroller, it will not always be possible to compute and process an FFT in $1/n_t$ tool revolutions. Taking into consideration the computing power of the dsPIC and the targeted breakage detection time of less than 2 revolutions, it was decided to compute the FFT every half tool rotation thus providing a 75% overlap with lapse time of 64 samples for selected buffer size of 256 samples.

5.5   Tool Monitoring Simulation

The Time-Frequency analysis technique for monitoring the spindle load signal was simulated in Matlab/ Simulink software. This process was performed to assess the suitability of the STFT/overlap FFT (with the selected parameters) for tool condition monitoring before implementation on a dsPIC microcontroller and to address any issues arising during this simulation. The developed simulation model is shown in Figure 5.12 in the form of a screen shot. The spindle load signal was acquired (at a sampling rate of 8Ksps) from actual cutting tests and was stored in an excel file. Data was then imported into the Matalb workspace using built-in functions and converted into a voltage signal representing spindle load and stored as a 2-dimentional variable (with the first column containing simulation time and the second column containing the signal). The simulation model then read the modified spindle load signal from the workspace and ran the simulation. The simulated signal (shown in top left plot of Figure 5.12) was passed through an anti-aliasing filter before being fed to the ADC block (consisting of S/H with sampling ate of 1066sps and ADC quantizer to simulate 12bit ADC of the dsPIC microcontroller). The output from the quantizer is shown in top right plot of Figure 5.12. This simulates the A/D conversion using a 12 bit ADC with a justified 16 bit result (equivalent to the behaviour of the ADC module on the dsPIC microcontroller) with sampling rate of 1066Hz. This sampling rate was selected so that

the tool rotation frequency and tooth passing frequency are in the centre of the main lobe of the rectangular window transform.
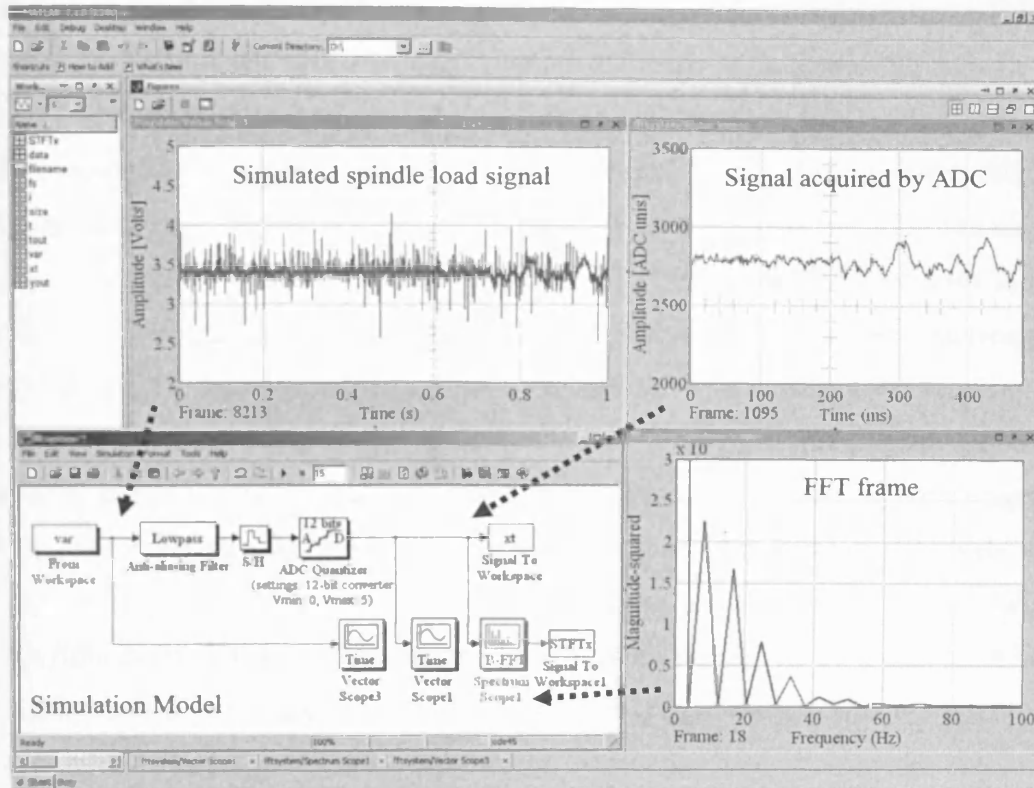
Simulated spindle load signal (top-left) Signal acquired by ADC (top right) FFT frame (bottom right)

Figure 5.12: Screenshot of the simulation model with generated plots

The spectrum scope block was used to simulate the STFT as it provided all the options required to set and adjust the selected parameters discussed in the previous section. Parameters for this block were thus set as follows:-

- Buffer (frame) size   M = 256
- Buffer overlap   M-L= 265-64 =192 samples = 75%
- Window type   Boxcar (rectangular window)
- FFT length   N=256
- Sampling rate f_s=1066 Hz
- Amplitude scaling   Magnitude-squared (linear)

The FFT frame calculated by the model is shown in the bottom right plot of Figure 5.12. This is updated every 64 samples (or 60msec at the given settings), which is equal to ½ tool rotation for a spindle speed of 500 rpm.

110

5.5.1 Simulated tool breakage Monitoring

This section describes the build up of spectrum as the system computes successive FFT frames for a simulated tool breakage scenario. Figure 5.13 shows the spindle load signal in the left hand column and the FFT frames in the right hand column while the middle column shows the data acquired by the ADC block of the system after anti-aliasing filter stage. Figure 5.13(a) shows the FFT of the signal just after the required settling down time. When the system starts, the FFT buffer is initialized with zeros. A stable FFT result is obtained when this buffer is full and the system subsequently provides an FFT frame after each ½ tool revolution. The settling time required is at least 2 tool rotations and to be sure it was set to 2.5. The FFT frame (Figure 5.13(a)) for a healthy cutter shows that tool the rotation frequency f_r has almost zero magnitude whilst the tooth passing frequency f_p and its harmonics have a relatively small magnitude. Figure 5.13(b) shows the FFT frame when the tool has just broken (evident in the right hand section of the acquired time domain data). The FFT spectrum begins to change and it continues to change in Figure 5.13(c and d), which shows the FFT frames after ½ and 1 revolution respectively. Although there is a change observed in these frames, the FFT spectrum does not show the regular and final signature for a broken tooth. The time domain signals of corresponding frames show that the FFT buffer still has data from healthy operation. This causes partial frequency spectra of healthy and broken tooth to appear in the FFT frames.

As the cutting continues, another FFT frame is computed at 1½ revolution after breakage, as shown in Figure 5.13(e), f_r and its harmonics have become more prominent and a clear signature of tool breakage is given by the FFT. At this point tool breakage is detected from the unique spectrum related to broken tooth. Figure 5.13(f) shows that magnitude of the prominent frequencies continues to increase and than stays there while the broken cutter is cutting. The FFT for the broken tooth long after breakage is shown in Figure 5.13(g) and, importantly, is identical to the FFT at 2 revolutions after breakage. From the spindle load data directly it is very difficult to identify the broken tooth as signal is corrupted by noise. The STFT has not only calculated the FFT spectrum of the signal but had also provided the information about the breakage within the targeted aim of 2 tool revolutions. In this case the FFT has been analysed visually where as in an automated monitoring system, it will be processed further with different

Spindle Load Signal   **Acquired data** (1066Hz)   **256pt FFT**
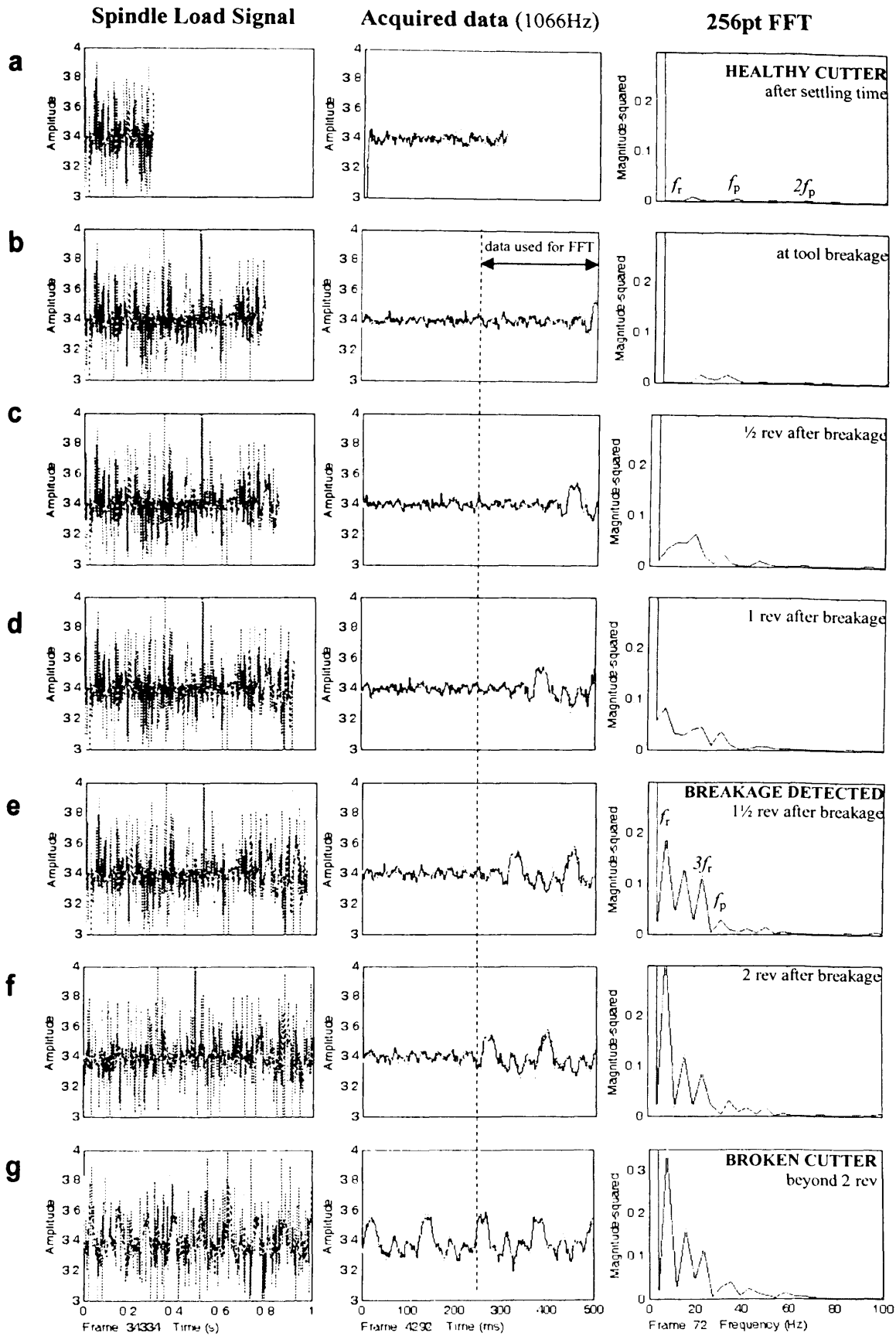
(a) Healthy cutter after settling time (b) At tool breakage (c) ½ rev after breakage (d) 1 rev after tool breakage (e) 1½ rev after breakage (f) 2 rev after breakage (g) Beyond 2 rev after tool breakage

Figure 5.13: System results for a healthy and broken cutter at different tool revolutions

112

algorithms e.g. threshold detection, pattern matching and mean frequency to classify the tool condition and generate alarm in case of tool failure/breakage. An animation of the monitoring simulation is provided in an electronic "Appendix B".

5.5.2 Monitoring for different Depth of Cuts

Machine tool cutting forces are affected by changes in depth of cut (DOC). DOC itself can change according to the workpiece geometry and required tool path during the milling process. Therefore it was necessary to test the monitoring system with DOC changes present. Cutting tests were carried out with different DOCs (0.5, 1.0, 1.5, 2.0 mm) and the resulting spindle load was then simulated and analysed as discussed in Section 5.5.1. The results from these tests are shown in Figure 5.14(a—d). Plots in the left hand column show the FFT for a healthy cutter and plots in the right hand column show the obtained FFT for a broken cutter two revolution after breakage. The centre column plots again show the time domain signal for reference.
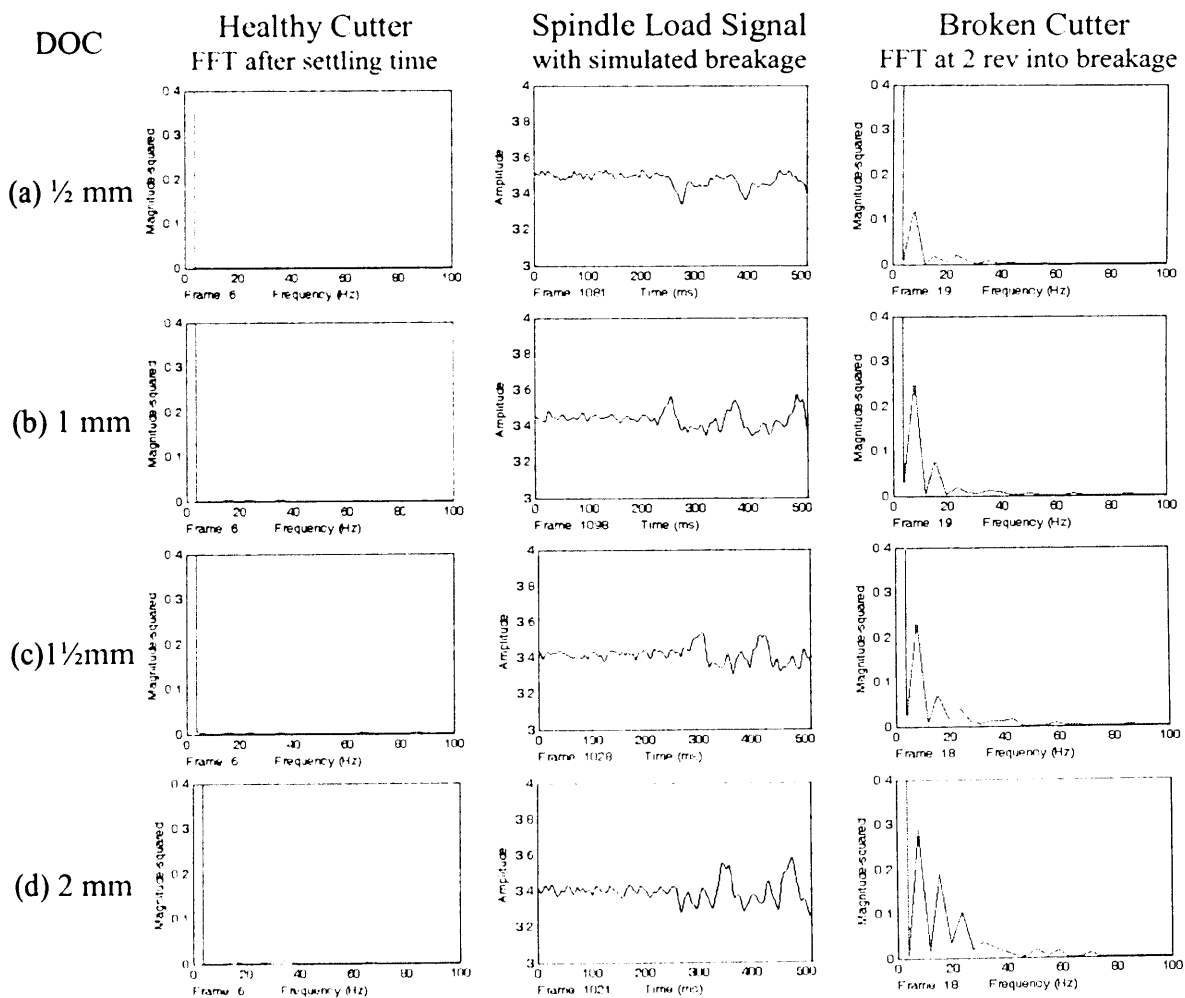
Figure 5.14: 256 pt FFT Analysis for cutting tests at different DOC

The broken cutter FFT in all cases shows f_r and its harmonics. Also the magnitude of f_r and its harmonics increase as the DOC increases. For healthy cutter spectrums, the magnitude of f_r is almost zero for all cases. Therefore it is suggested that a threshold should be set in relation to DOC.

5.5.3 Monitoring for variable Spindle Speeds

Another machining parameter that typically changes from one operation to another is the spindle speed. The spindle speed is set by the operator according to material and cutting parameters. For example different values will be selected for roughing and finishing operations. To evaluate the effective estimation of spindle speed tests were carried out at different spindle speeds (300 -2500 RPM) without any cutting and the spindle speed voltage signal was captured. The average ADC value for each test was calculated and plotted against spindle speed as shown in Figure 5.15. It is clear that there is a linear relationship between spindle speed and the captured ADC values.
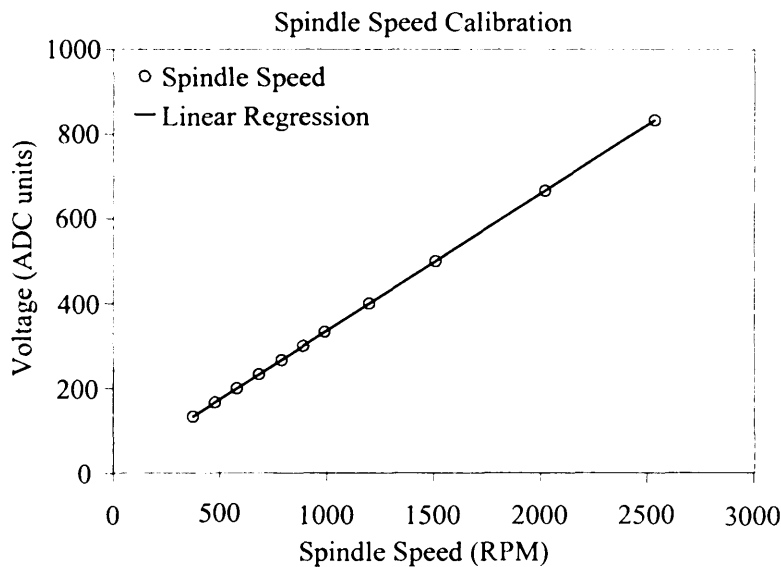
Figure 5.15: Relationship between ADC values and spindle speed.

As explained in Section 5.3, when using a healthy cutter, the spindle load signal varies periodically with tooth passing frequency f_p, which is product of spindle rotational frequency and number of cutting teeth as given in Equation 5.12. When the tooth is broken there is a change in the spindle load variation pattern. Now Spindle load decreases and increases (as explained in Section 5.3) once every revolution generating a tool rotation frequency $f_r = N_s / 60$. Tool frequencies (f_r, f_p) and their harmonics are

114

proportional to the average spindle speed and are bound to change with spindle speed variation. The relationship between these frequencies and spindle speed is shown in Figure 5.16. Here f_p and f_r can be calculated according to Equations 5.12 and 5.13, if average spindle speed is known (or measured) during the milling operation.
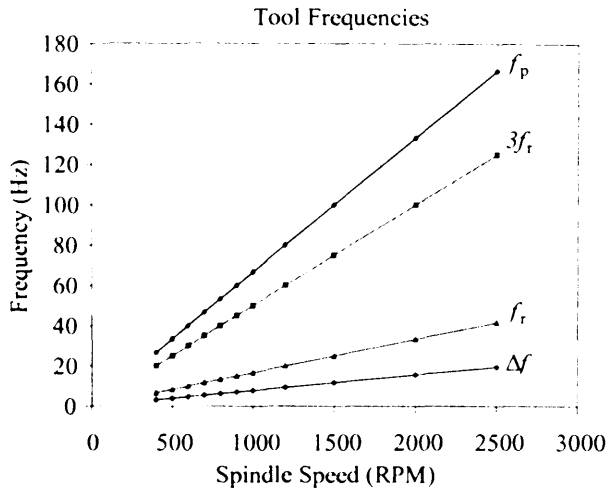
Figure 5.16: Relationship between Tool frequencies and Spindle speed

If the signal is sampled at a constant sampling rate, the values of the monitored frequencies (f_r and f_p) need to be selected according to the spindle speed and the FFT has to cover the entire range of f_r and f_p (0-400Hz for spindle speed range of 0-6000 RPM for a 4 teeth cutter). For an 8 teeth cutter this range would be 0-800 Hz and so on. The minimum frequency f_{min} to be monitored depends on minimum value of spindle speed while maximum frequency f_{max} would be dependent on number of teeth n_t and maximum value of spindle speed which can be calculated according to following equations.

$$f_{min} = f_r\Big|_{min} = \frac{N_s}{60}\Big|_{min} \tag{5.18}$$

$$f_{max} = f_p\Big|_{max} = \frac{N_s}{60}\Big|_{max} \times n_t \tag{5.19}$$

The required frequency resolution is also dependent on spindle speed necessitating opting for a 1Hz or better resolution. With the processing power of the current dsPIC microcontroller this is not a viable solution. To handle this situation a new technique is proposed to make the sampling rate in proportion to the spindle speed such that:

$$f_s = k \times N_s / 60 \tag{5.20}$$

where k is number of samples to be acquired in one tool rotation.

For suggested value of $k=128$, the sampling rate f_s is 1066.6Hz (for $N_s=500$ RPM). If sampling rate is made proportional to spindle speed then f_r and f_p can be expressed in terms of f_s and k according to following equations:-

$$f_r = f_s / k \tag{5.21}$$

$$f_p = n_t f_s / k \tag{5.22}$$

The frequencies f_r and f_p can be normalized in terms of sampling rate f_s or spindle speed. Normalized frequencies have constant values over entire range of spindle speed as shown in Figure 5.17.
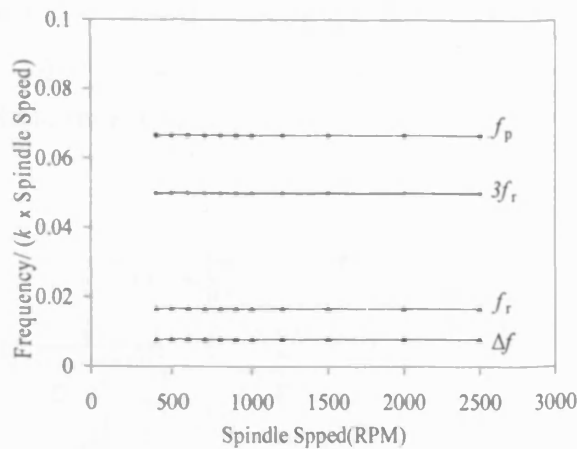
Figure 5.17: Normalized Tool frequencies vs. Spindle Speed

The proposed technique ensures that frequencies of interest always lie in the same frequency bin and provide constant computation time irrespective of the spindle speed. The time period of the timer (controlling the ADC sampling rate as discussed in Section 4.4.3 (*Variable Sampling Rate*) is adjusted according to the spindle speed and all the calculation are automatically normalized to the operational spindle speed.

5.6 Implementation on dsPIC

The capabilities of a dsPIC in performing FFT computations were tested and compared with Matlab computations as reported by the author in the Comadem 2005 conference [5.3]. Based on these successful analyses, the algorithms were enhanced to compute the suggested overlap FFT which is suitable for real-time monitoring applications requiring frequency domain analysis of non-stationary signals.

5.6.1 System Description

The researched machine tool condition monitoring system is based on the three tier architecture as described in previous chapter and the system described in this chapter forms a FEN at first tier. Figure 5.18 shows the block diagram of the developed monitoring node. The spindle speed and spindle load signals are obtained from the machine controller via an isolation card. This card provides high voltage protection between the machine tool signals and analogue inputs to the system. A signal conditioning stage is implemented prior to the signal being fed to the dsPIC microcontroller for analysis. Spindle speed and load signal are also acquired by the parameter monitoring node (discussed in Chapter 8) for calculating operational parameters for the whole monitoring system and this information is communicated to FENs.
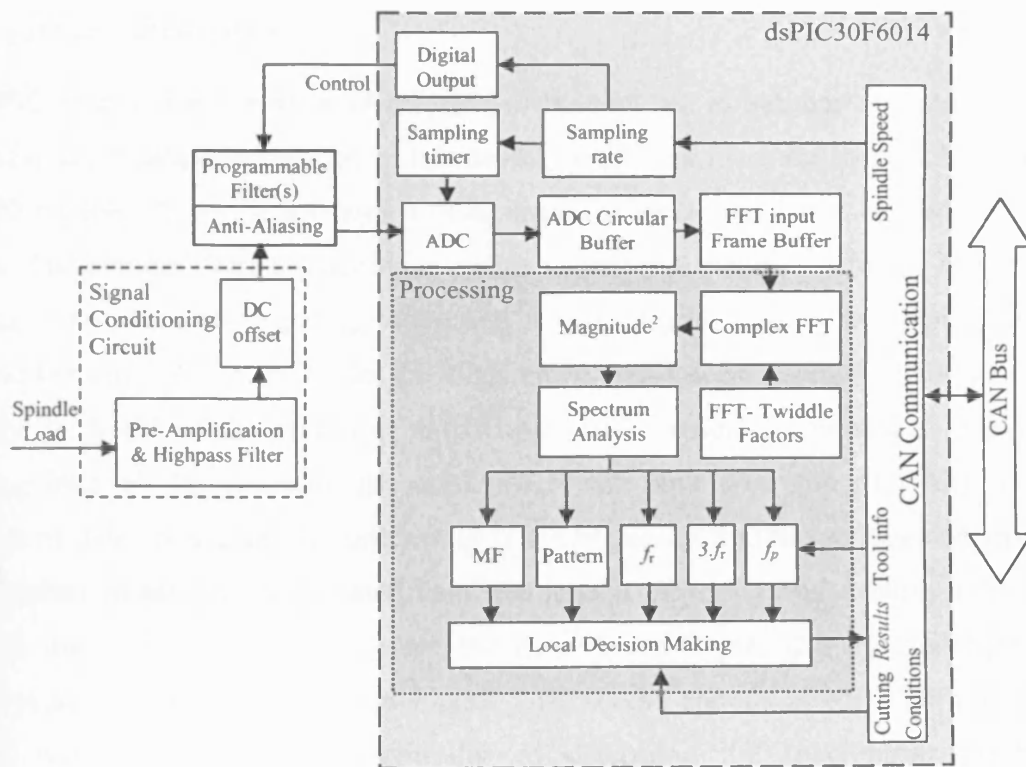
Figure 5.18: Block Diagram of the monitoring node

The spindle load signal conditioning for this FEN consists of; a pre-amplification stage which removes the DC offset (and frequencies below 2Hz) from the machine tool signals to increase the overall resolution in the implementation of digital filtering stage, the addition of a DC offset to make the signals compatible with microcontroller's inputs

117

and an anti-aliasing filtering stage. The output from this block is fed to the dsPIC microcontroller's analogue input via anti-aliasing filter whose pass band frequency is set in accordance with the current sampling rate being used by the system. The acquired data stored in a circular buffer which is translated into an input Frame buffer and processed according the processing block (as shown in Figure 5.18) which will be discussed in the following sections.

The dsPIC30F6014 microcontroller used for this activity can be linked to other microcontrollers undertaking related monitoring functions using a Controller Area Network (CAN) bus communications. Other functions which can be integrated in this may include the monitoring of the tool changer, the coolant system, the DOC measurement system etc.

5.6.2 System Initialization

The dsPIC microcontroller has a 24-bit wide instruction set. A number of instructions are available for data manipulation in this device, which are ideal for this application. The A/D module allows the conversion of an analogue input signal to a corresponding 12-bit digital number. Data acquisition is enabled using initialization software that sets the microcontroller into operating mode and selects and configures the digital and analogue I/O pins. Next it initialises the CAN activity and does essential handshaking to verify the health of the system at initialization. This action is repeated at regular operating intervals (to announce the existence of the node over the network). The initiation of data acquisition and processing is controlled by a message received from the parameter monitoring node based upon the receipt of predefined existing signals from the machine controller. These are the Zero Speed Signal (SSTA) and Speed Arrival Signal (SARA) as shown in Figure 5.19. These signals along with a CNC demand signal allow the microcontroller to determine the machining process parameters. The parameter monitoring node sends messages to start and suspend monitoring based on spindle load monitoring as will be discussed in Chapter 8.
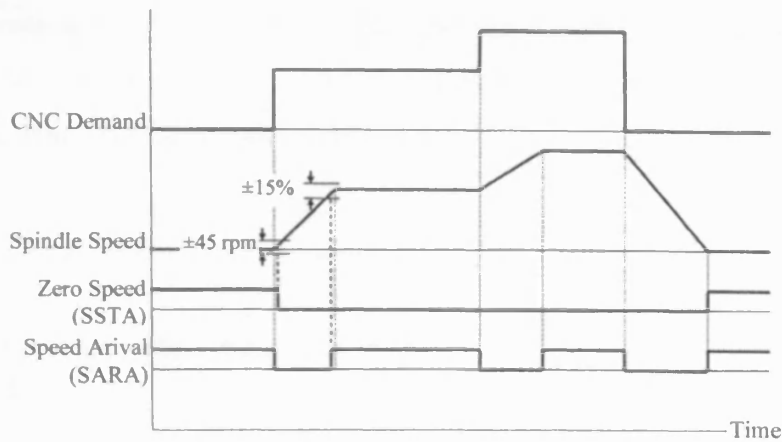
118

Figure 5.19: Relationship between CNC demand and spindle signals.

5.6.3 System Operation

The spectrum analysis using STFT provides several advantages over other frequency analysis techniques developed earlier by the group [5.14] which utilized hardware based switched capacitor filter for calculating the frequency spectrum of the signal. To achieve a spectrum, the entire frequency range was swept one by one by tuning the filter at each frequency and calculating the peak-to-peak value of filtered signal. This scanning technique required a much longer time and assumed the signal to be stationary. FFT was used in the second layer of the system as an advanced diagnosis tool in earlier applications. This section describes the implementation of suggested overlap FFT algorithm and related spectrum analysis and decision making on dsPIC microcontroller for real-time monitoring of tool breakage. The implementation of the said algorithm was divided into three sub systems: (a) data acquisition and windowing (b) FFT computation and (c) spectrum analysis and decision making.

5.6.4 Data acquisition and windowing

The dsPICDEM1.1 general purpose development board with a dsPIC30F6014 microcontroller has been used for this application. The development board has a 7.3728 MHz crystal oscillator, which is sufficient to achieve 29.49 MIPS performance by using the built-in clock multiplier in the microcontroller [5.15]. This microcontroller has a 12bit ADC module which can acquire data at sampling rates up to 100Ksps. As discussed and suggested in earlier sections of this chapter, variable sampling rates were to be used for this application. It was thus necessary to setup the ADC in a fashion that allowed the sampling rate to be easily and quickly changed. The onboard Timer 3

module as described in Section 4.4.3 was used for this purpose. Timer 3 was set to generate an ADC Event Trigger, whenever the timer value (TMR3) matched timer period (PR3), which can be calculated as follows:

$$PR3 = \frac{F_{CY} \times 60}{k \times N_s} \tag{5.23}$$

where F_{CY} is the system clock frequency in Hz

When a change in spindle speed (N_s) was communicated by the parameter monitoring node, a new value of the timer period was calculated according to Equation 5.23 (which incorporated the sampling rate f_s) and PR3 was updated accordingly. This would change the sampling rate of the ADC. Since the timer period register can be update without stopping the timer; this method thus provided the very fast updating of the sampling rate.

There are 16 ADC buffer registers ADCBUF0-ADCBUFF to hold the data after conversion. The ADC can generate to an interrupt so that the acquired data can be processed. To reduce the ADC interrupt rate, it was set to generate an interrupt after 16 samples are acquired. This was necessary to gain time for the FFT algorithm and thus the key timing requirement to be met when programming the dsPIC.

Since spindle load data for the previous two tool rotation periods is required for FFT analysis, a circular data buffer was created, to store 256 samples acquired by the ADC. Figure 5.20 shows the operations involved in manipulating this circular buffer to store ADC values. At each interrupt the data from ADC buffer was copied into the data buffer and when the ADC buffer index reached the set upper limit (256) it was reset to 0 and hence the ADC started overwriting the oldest block of data. In this way last 256 samples were always available. After every 64 samples (½ tool rotations), a *frame_flag* was set to indicate that data required for computing the FFT was available. This flag was monitored in the main programme and data was transferred to the FFT Frame buffer according to the sequence shown in Figure 5.21. This ensured that the values in the FFT frame buffer were correctly ordered and was equivalent to applying rectangular window to the data. The spectral leakage was minimized since each frame/window was arranged to contain data for complete two rotations. Typically the edge points had

almost identical values and the waveform progressed seamlessly from one frame to the next.
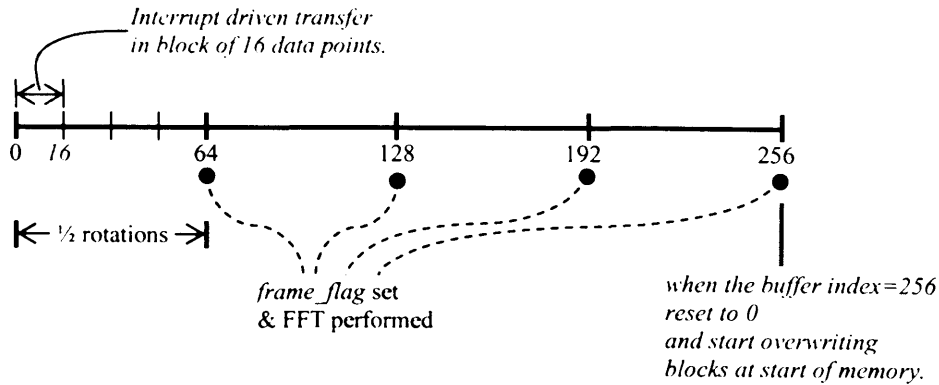

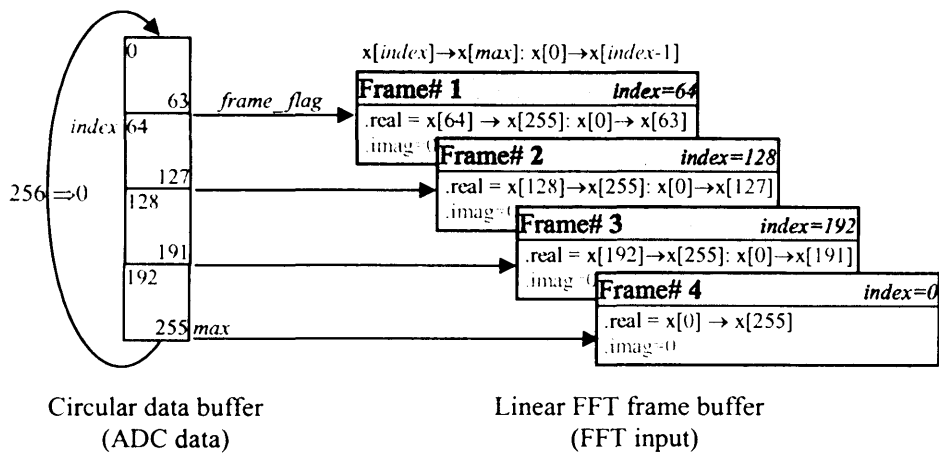Figure 5.20: ADC interrupt and *frame_flag* timings

Figure 5.21: Translation of circular data buffer into FFT input frame buffer

The methodology resulted in an overlap between successive frames of data, with each frame containing 192 samples from the previous frame and 64 new samples. The copying of data from the ADC data buffer to the FFT frame buffer was required to avoid overwriting of the current input frame to the FFT function's storage space. This was required since the ADC was acquiring data in a background process whilst the FFT was being computed.

5.6.5 FFT Computation

The 'in-place' complex FFT algorithm of the dsPIC was used to compute the DFT of the signal frame. In each case the imaginary part of input complex frame was set to zero. In-place algorithms are memory efficient and replace the input vector with the output results once computation is completed. Equation 5.2, to compute FFT, can be rewritten as follows:-

$$FFT_N\{x_n\} \equiv X_k = \sum_{n=0}^{N-1} x_n (w_k)^n \qquad 0 \le k \le N-1 \qquad (5.24)$$

$$\text{with} \qquad w_k = \begin{cases} e^{-j\frac{2\pi}{N}k} & 0 \le k \le \frac{N}{2} \\ w_{N-k}^{*} & \frac{N}{2}+1 \le k \le N-1 \end{cases}$$

where w_k (primitive roots of unity) are known as the "twiddle factors" used in the FFT algorithm. Since these factors are not dependent on the input signal, they can be pre-calculated to speed up the FFT algorithm. Only $\frac{N}{2}$ factors are required, to be calculated and stored, as second the half of the factors are complex conjugate of the first half. These factors (which are required by the FFT algorithm) were programmed into the program memory providing manifold benefits:-

- Extra data memory was made available which would have been used up by these factors.
- The coefficients/twiddle factors were preserved when system was powered off.
- Faster system availability was achieved by saving computation time for calculating them, every time system was powered on or reset.

The Program Space Visibility (PSV) functionality was used to access the twiddle factors. This PSV functionality mapped program space/memory into data space/memory when required and the DSP algorithms could treat it as data available in data memory. The output of the FFT was arranged in the correct order using Bit-reversed addressing. The power (squared-magnitude) of the output was calculated using the function provided in the library provided by Microchip and it was transferred into another array which was accessible to spectrum analysis and decision making subsystems. This array could store results of the past 32 FFT computations (equivalent to holding the history for last 16 tool rotations).

5.6.6 Spectrum Analysis and Decision Making

The power spectrum of the relevant frame shows the contribution of each frequency in the signal. The FFT algorithm computes the frequency components (termed as frequency bins) separated by Δf. As was discussed in Section 5.5.2, the tool rotation frequency f_r is dependent on spindle speed and sampling rate f_s was arranged to be proportional to the spindle speed. The frequencies of interest were thus directly proportional to the sampling rate and could be directly mapped to specific frequency bins for the entire range of spindle speed. For example, a spindle speed N_s=500 rpm and sampling rate = 1066.6 Hz thus gave Δf =4.166 Hz, for a selected 256 point FFT, which is half of the tool rotation frequency f_r. Hence, for a cutting tool with n_t cutting teeth, the tool related frequencies are given by

$$f_r = f_s / k = 1066/128 = 8.33 \text{Hz and harmonics } (n\,f_r) \text{ at } 16.67, 25, 33.3 \ldots$$

$$f_p = n_t\,f_r = 8.33 \cdot n_t$$

Since n_t is an integer, the value of f_p will also be one of the harmonics of f_r. For example for a 4 tooth cutter (n_t=4) it is 33.3 Hz, which is the 4th harmonic of f_r. Frequency bin 0 represents the DC gain of the signal and is not used in the analysis. As shown in Table 5.1, f_r and its harmonics occupy even frequency bins while f_p and its harmonics occupy frequency bin $2n_t$ and its multiples. (i.e. 8, 16, 24 etc for 4 a teeth cutter). Thus the tool frequencies can be directly mapped to specific frequency bins which remain constant for all cutters with the same number of teeth.

Table 5.1: Mapping of frequency bins to tool frequencies for a 4 tooth cutter

Frequency Bin (Number)	Frequency (Hz)			Tool rotation frequency f_r & harmonics	Tooth passing frequency f_p & harmonics
	N_s=100 Δf=0.833	N_s=500 Δf=4.165	N_s=1000 Δf=8.33		
0	0	0	0	0	0
1	0.83	4.16	8.33		
2	1.67	8.33	16.67	f_r	
3	2.50	12.50	25.00		
4	3.33	16.67	33.33	$2f_r$	
5	4.16	20.83	41.66		
6	5.00	25.00	50.00	$3f_r$	
7	5.83	29.17	58.33		
8	6.67	33.33	66.67	$4f_r$	f_p
16	13.33	66.67	133.33	$8f_r$	$2f_p$
24...	20.00	100.00	200.00	$12f_r$	$3f_p$

The following features may then be considered:

Thresholds

Thus the even frequency bins (2, 4, 6 etc) correspond to tool rotation frequency components which are prominent for a broken tool. Thus any decision about the health of the cutter can be made by observing the magnitude of these frequency bins (especially f_r and $3f_r$). These values can be compared against a set of thresholds to generate a tool breakage alarm.

Mean Frequency

Mean frequency (*MF*) (adopted from [5.16]) provides a single measure about the distribution of frequencies in the spectrum. It provides the frequency trend in the whole spectrum. Mean frequency is calculated as follows:

$$MF = \sum_{k=1}^{N/2} f_k \times X_k \bigg/ \sum_{k=1}^{N/2} X_k \qquad (5.25)$$

where f_k and X_k are the frequency and magnitude of kth bin of the spectrum respectively. This algorithm was implemented on dsPIC microcontroller and it was found that MF of a broken cutter less than that of a healthy cutter. Thus MF can be compared against a threshold to detect a tool breakage.

Pattern Matching

A consistent pattern in the frequency spectrum of the broken cutter was observed during the machining tests (both during Matlab simulation and dsPIC implementation). For each FFT frame the pattern is calculated by assigning a '1' to the bin if its magnitude is above the threshold or '0' otherwise. The pattern in Figure 5.22 shows the relative amplitude of the frequency bins 1-7, which alternates between high and low magnitude and crosses the threshold shown by dotted line providing a "0101010" pattern. This pattern coupled with MF and threshold is used to confirm the tool breakage.

Frequency Bin #	1	2	3	4	5	6	7	8	9
Pattern	0	1	0	1	0	1	0	f_p	
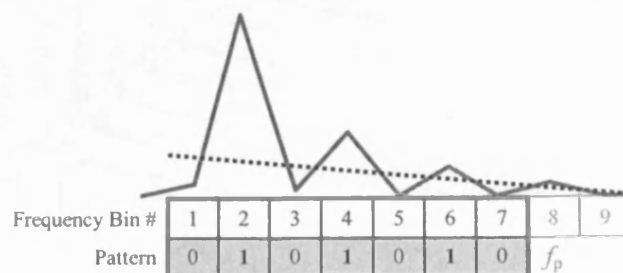
Figure 5.22: Pattern relating to broken tool

The above mentioned features of the signal were combined for decision making about the condition of the tool, which will be described in the following section along with actual machining tests and their results.

5.7 Machining Tests and Results

The system and algorithm initially simulated via Matlab was deployed on the dsPIC microcontroller and fully tested. For convenience the pre-recorded signals from the database of actual tests, with known/pre-determined parameters, were used. As discussed previously, the appropriate signals were re-created using Matlab and a National Instruments Data acquisition card, installed in a PC. The Matlab program read the recorded signal from an excel file and processed the signal to perform the signal conditioning steps including removing DC components by using a RC high pass filter, amplifying the signal and applying DC offset of 2.5V. After processing the signal, the sampling rate was increased by using an interpolation filter and the final data was fed to the DAQ card which generated an analogue spindle load signal. This was fed to the dsPIC based frequency analysis system.

Since it was impossible to achieve on an actual machine tool in a controlled way, tool breakage was simulated by combining the data for healthy and broken cutters and tests were performed to detect tool breakage at different depth of cuts. An example spectrum of successive overlapped frames (obtained by FFT computations), pre and post tool breakage, are shown in Figure 5.23 as a waterfall diagram.
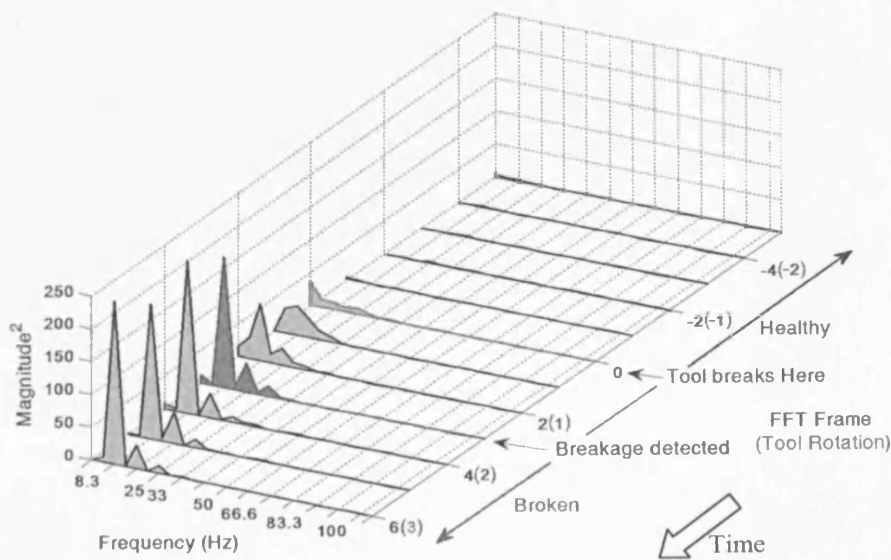
Figure 5.23: Tool breakage detection using overlap FFT analysis

125

In the case of Figure 5.23, the most recent frame is shown at front and oldest frame at the back of the waterfall plot. The time axis is labelled with both FFT frames and tool rotations (in brackets) with zero denoting the frame where tool breakage occurred. Frames, before and after this point, represent healthy and broken tool frames respectively. For a healthy cutter all frames are similar with almost zero power (magnitude^2) at f_r and its harmonics. When tool breakage occurred the power of these components began to increase, as clearly seen in frames 0, 1 and 2. As shown in Figure 5.24, at this stage the calculated mean frequency (MF) decreases rapidly and crosses the threshold at frame 1 or 2, hence providing an early warning of a possible tool breakage.
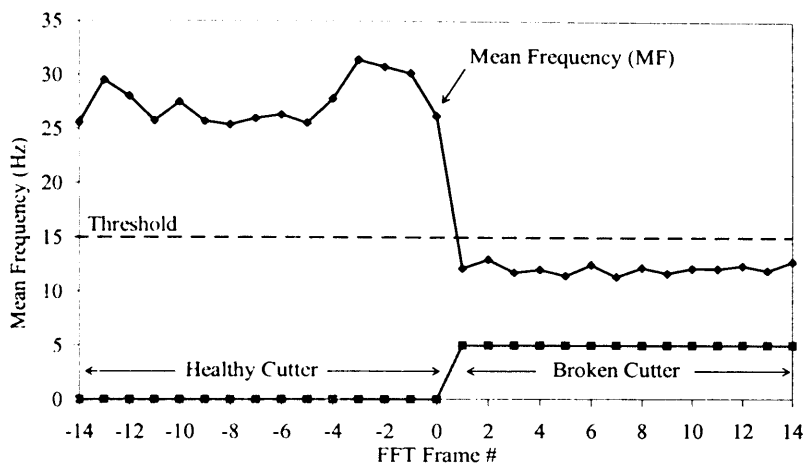
Figure 5.24: Mean Frequency for tool breakage detection

A distinct pattern (as described previous section and shown in Figure 5.22) in the spectrum for f_r and its harmonics (relating to the broken tool) is confirmed in Frame 3. Since frames are computed after every ½ tool rotation, frame 3 represents 1½ tool rotations since the broken tool engaged. After this point the overlap FFT consistently provides a stable broken tool power spectrum. In this way tool breakage can potentially be detected and confirmed in 1½ tool rotations, so tool breakage is detected within the aimed for 2 tool rotations period.

Figure 5.25 shows the 3D view of the FFT of spindle load signal computed by the dsPIC system for a simulated tool breakage. The DOC was 1.5mm for Figure 5.25a and 2.0mm for Figure 5.25b. The Power (magnitude^2) of f_r and its harmonics for broken tool are clearly identifiable in the 3D view. The FFT frames for the healthy, broken cutter after 1.5 revolutions into breakage and a broken cutter are shown separately for clarity and analysis in each DOC case. Data shown in the 3D plot is that, which was held in

dsPIC memory and was thus accessible to analysis and decision making algorithms. The last 32 frames of computed FFT spectrum are always available for analysis and diagnosis purposes.
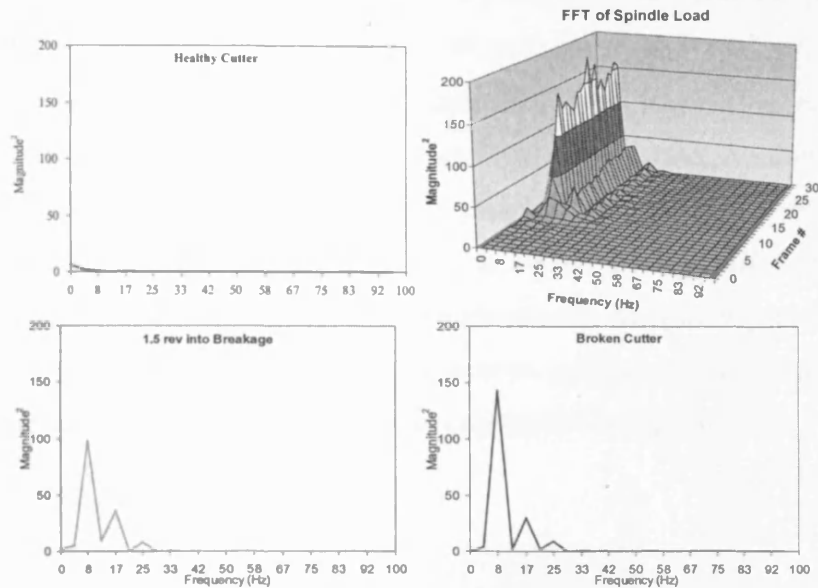
(a) 1.5mmDOC
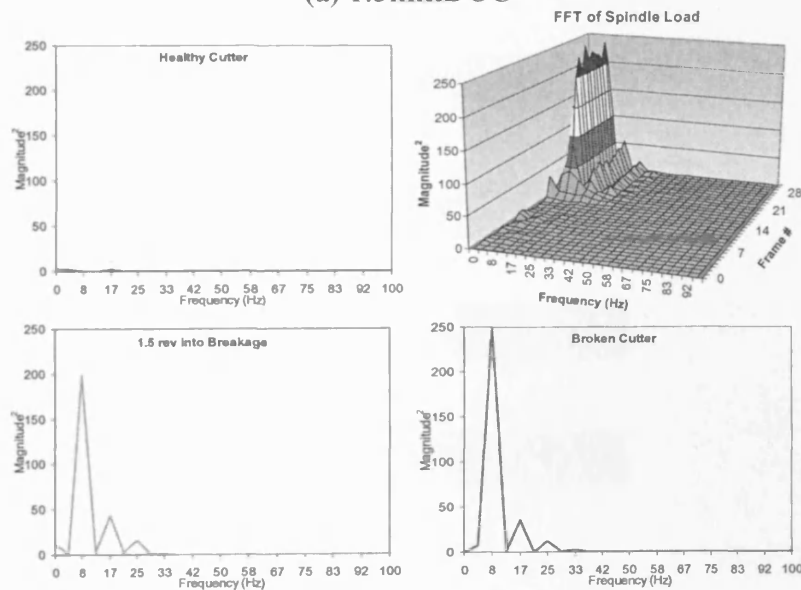
(b) 2mm DOC

Figure 5.25: Over lap FFT analysis of simulated tool breakage

Similar tests were carried out on other combinations of machining parameters and results are posted in "Appendix C".

5.8 Decision Making

The overlap FFT algorithm implemented on dsPIC microcontroller provided the frequency domain data enabling the extraction of key features; Mean Frequency (MF), Pattern and Thresholds on magnitude of key frequencies (f_r, $3.f_r$ and fp); which were found sensitive to tool breakage and tool condition. MF monitoring indicated tool failure earlier than other features. This was combined with other features for counter verification to avoid any false alarms. The simplest way of combining them was sequential cascaded decision making as shown in Figure 5.26. In this case tool failure was considered only when MF dropped below threshold and pattern was matched with the broken tooth pattern. If any the frequency components magnitude crossed threshold the tool was declared broken otherwise it was considered a chipped tool.
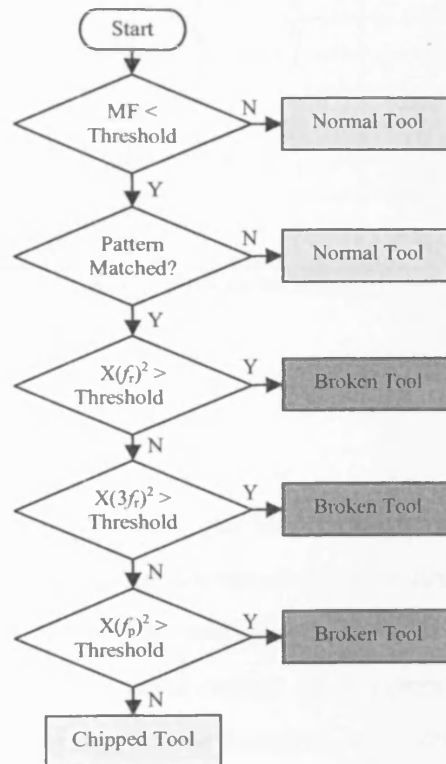
Figure 5.26: Decision making Flow Chart.

This method worked for all the tests reported in this research. A more elaborate decision making process is given in Table 5.2, these features can indicate more than tool breakage for example a blunt tool when magnitude of f_p exceeds the threshold but MF and pattern would treat it as normal tool. In this table '1' indicates that the threshold has been crossed and 'X' denotes "don't care" condition. An advanced

diagnosis can also be requested for unrecognised cases. In this case the parameter monitoring node will initiate an advance diagnosis sequence and send the acquired data to the second tier for analysis. When a broken tooth is detected a message is sent to parameter monitoring node which then combines this decision with decisions from other FENs and make a final decision about the health of the tool. Upon a possible blunt tool detection a blunt flag message is sent which is used for process management function and the tool can be checked after the machining cycle finishes.

Table 5.2: Decision making Table

Mean Frequency	Magnitude^2			Pattern	Decision
	f_r	$3f_r$	f_p		
0	0	0	0	0	Healthy
0	0	0	1	0	Blunt Tool
0	1	X	X	0	?
0	X	1	X	0	?
1	0	0	0	0	Wait for next Frame
1	0	0	0	1	Chipped Tool
1	1	X	X	1	Broken Tooth
1	X	1	X	1	Broken Tooth
1	X	X	1	1	Broken Tooth

? = Unexpected : request for advanced diagnosis

5.9 Discussion

This chapter has outlined the design and implementation of a real-time frequency domain signal analysis technique for monitoring the milling machining process. The dsPIC microcontroller took about 5.6 msec to perform all the FFT computations with the deployed algorithm (including windowing) when operating at 7.37MIP. Some time was required for decision making, house keeping, and communication of results. The system was tested with spindle speeds upto 3000 rpm and it provided correct and timely results. At 3000 rpm the time interval between successive FFT frames was 10 msec. The performance rate can be increased 29.49MIPS at which it would take 1.4msec to perform entire computation and the cycle time can be reduced to 2.5msec. This would enable the module to monitor cutting processes with spindle speeds up to 12000 rpm, which exceeds the maximum requirement of 6000 rpm considered in this research. At a maximum spindle speed of 6000 rpm the FFT cycle time would be 5 msec which is twice the required cycle time with the deployed algorithms. This effectively means that

the dsPIC can handle some additional processing algorithms if required in future. These can be downloaded from higher tier using the CAN communication and programmed into the dsPIC microcontroller using the run time self programming (RTSP) capability.

The variable sampling rate and intelligent manipulation of the overlap FFT has enabled tool breakage detection and confirmation in less than 2 revolutions under all operating spindle speeds. In effect, the detection time decreases (as shown in Figure 5.27(a)) as the spindle speed increases providing a constant detection time in terms of number of revolutions (as shown as Figure 2.57(b)). Similarly the settling time, at the start up, is also fixed in terms of tool rotations for all spindle speeds.
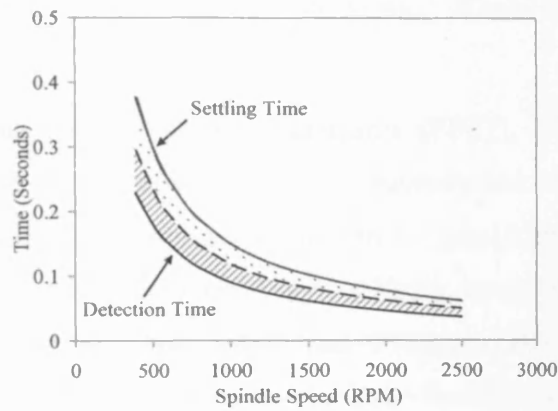
(a) Detection and Settling Time
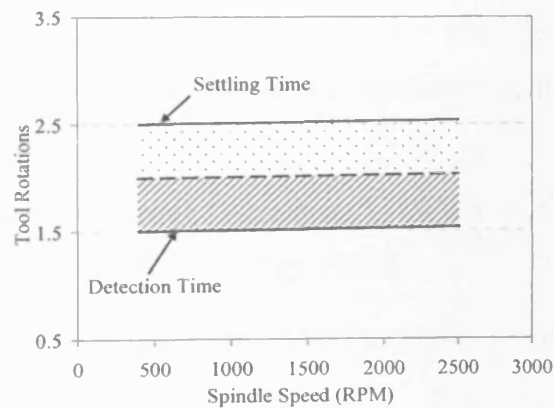
(b) In terms of Tool rotations

Figure 5.27: Detection and Settling Time vs. Spindle Speed

References

[5.1] "Frequency Analysis of Electronic Signals," [WWW] < URL http:// physics.ust.hk/penger/n1-7.doc> (accessed on 15 May. 2008)

[5.2] M. Cerna, A.F. Harvey, "The Fundamentals of FFT based Signal Analysis," National Instruments Corporation, July 2000, Application Note 340555B-01.

[5.3] R.A. Siddiqui, Q. Ahsan, R.I. Grosvenor, P.W. Prickett, "The role of emerging technologies in eMonitoring", *In the proceedings of 18th International congress on Condition Monitoring and Diagnostic Engineering Management (COMADEM),* Cranfield, 2005, pp. 263–271.

[5.4] R. Priemer, "Introductory Signal Processing," *World Scientific* 1991, ISBN: 9971509199, p 165.

[5.5] MathWorks Inc., "Fast Fourier Transform (FFT)", Matlab Documentation, [WWW]< http://www.mathworks.com/access/helpdesk/help/techdoc/index.html ?/access/helpdesk/help/techdoc/math/brentm1-1.html&http://www.mathworks.c om/cgi-bin/texis/webinator/search/?db=%20MSS&prox=page&rorder=750&rpr ox=750&rdfreq=500&rwfreq=500&rlead=250&sufs=0&order=r&is_summary_ on=1&ResultCount=10&query=Fast+Fourier+Transform > (accessed on 21 May. 2008)

[5.6] Bores Signal Processing, "The Zoom FFT," [WWW] < URL http://www. dewtronics.com/tutorials/dspintro/advanced/files/zoomfft.pdf > (accessed on 10 May. 2007)

[5.7] Douglas L. Jones, "Chirp-z Transform", [WWW] < http://cnx.org/content/ m12013/latest/> (accessed on 10 May. 2007)

[5.8] K. Gröchenig, "Foundations of Time-Frequency Analysis," *Springer* 2001, ISBN: 0817640223, p 37.

[5.9] "Fundamentals of Machine Tools: Milling Operations," Training Circular 9-524, Headquarters, *Department of the Army, Washington DC,* 29 Oct. 1996, Chapter 8, p 1.

[5.10] X. Li and X.P. Guan, "Time-frequency-analysis-based minor cutting edge fracture detection during end milling," *Mechanical Systems and Signal Processing*, vol. 18, Nov. 2004, pp. 1485-1496.

[5.11] N. Kasashima, K. Mori, H. Ruiz, G. and N. Taniguchi, "Online failure detection in face milling using discrete wavelet transform," *CIRP Annals - Manufacturing Technology*, vol. 44, 1995, pp. 483-487.

[5.12] Julius Orion Smith III, "Choosing Window Length to Resolve Sinusoids", [WWW] <URL http://www.dsprelated.com/dspbooks/sasp/?urlkeywords= Choosing_Window_Length_Resolve > (accessed on 10 Apr. 2007)

[5.13] DLI Engineering Corporation, "Overlap Processing", [WWW] < URL http://www.dliengineering.com/vibman/overlapprocessing.htm> (accessed on 25 May. 2008)

[5.14] W. Amer, R. Grosvenor, and P. Prickett, "Machine tool condition monitoring using sweeping filter techniques", *Journal of Systems and Control Engineering*, vol. 221, 2007, pp. 103-117.

[5.15] Microchip Technology Inc, "dsPIC® Development Tools" [WWW] <URL: http://www.microchip.com/stellent/idcplg?IdcService=SS_GET_PAGE&nodeI d=2035> (accessed on 24 May. 2005)

[5.16] I. Yesilyurt, "End mill breakage detection using mean frequency analysis of scalogram," *International Journal of Machine Tools and Manufacture*, vol. 46, Mar. 2006, pp. 450-458.

Chapter 6

Multiband Infinite Impulse Response Filters

for Tool Monitoring

6.1. Introduction

The aim of this part of the research was to investigate the DSP capabilities of dsPIC microcontroller for another important DSP algorithm. This chapter describes the design, practical implementation and results of a dsPIC based dynamic digital filtering technique. This technique can be used for monitoring applications requiring simultaneous multiple frequency estimation such as tool health monitoring where amplitude of certain frequencies increase for broken cutter (as discussed in Section 5.3). Signal conditioning and anti-aliasing filtering are used to condition the signal, making it suitable for interfacing with the microcontroller. The technique simultaneously uses variable data sampling rates and a table of predefined filter coefficients to dynamically adjust its pass band characteristics to match the range of interest. In the system development process, a time domain feature was observed to be responsive to tool breakage and it is named as Tool Rotation Energy Variation (TREV). The signal analysis required for the monitoring of a machine tool in a manufacturing environment is again catered for by the enhanced power of the dsPIC microcontroller.

6.2 Digital Filters

Digital filters are a very important part of DSP. In fact, their 'extraordinary performance' is one of the key reasons that DSP has become so popular [6.1]. They not only provide a cheap alternative to analog filtering, but they can perform functions which are almost impossible to implement with analog filters such as pure linear phase response and the reuse of the filter for different applications (by merely changing the coefficients or sampling rate). There have been many reported comparative analyses of analogue and digital filters. In general these have indicated that analogue filters are

normally cheap, fast and have a large dynamic range in both amplitude and frequency [6.2]. When using analogue filters, the emphasis is often on addressing any limitations in performance arising from the lack of stability of active and passive components. In comparison, the performance of digital filters is generally superior and the emphasis normally shifts to theoretical issues regarding their efficient implementation in terms of achieving the required processing capabilities.

6.2.1. Frequency Response of a Digital Filter

Filters are usually defined by their responses to the frequency components that constitute the input signal. A filter's response to different frequencies is characterized into the following three bands [6.3]:-

- *Pass band.* The pass band response is the filter's effect on frequency components that are passed through (largely) unchanged.
- *Stop band.* Frequencies within a filter's stop band are highly attenuated.
- *Transition band.* The transition band represents frequencies in the middle, which may receive some attenuation but are not completely removed from the output signal.

An Ideal filter will have zero width transition bands, no attenuation in the pass band frequencies and infinite attenuation of the stop band frequencies. These parameters for a good but not ideal filter implementation are shown in Figure 6.1.
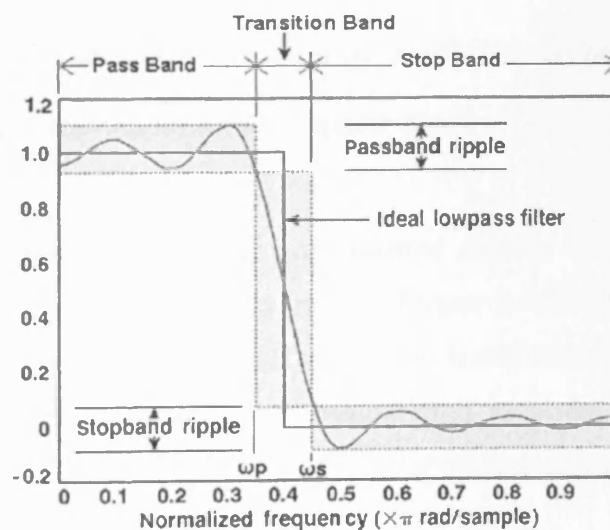
Figure 6.1: Frequency Response of a low pass filter

There are four types of filters based on the relative locations of pass band (PB) and stop band (sb) namely: low Pass (PB—sb), high pass (sb—PB), band pass (sb1—PB—sb2) and band stop (PB1—sb—PB2) filters. Band pass filters are discussed in this chapter.

6.2.2   Infinite Impulse Response Filter

Infinite impulse response (IIR) filters have an impulse response function which has non-zero (but decreasing values) over an infinite length of time. This contrasts to finite impulse response (FIR) filters which have fixed-duration impulse responses. IIR filters may be implemented as either analog or digital filters. In digital IIR filters, the output feedback is immediately apparent in the difference equations defining the output. IIR filter structures must be recursive (use feedback); an infinite number of coefficients could not otherwise be realized with a finite number of computations per sample. The general time-domain difference equation for an IIR filter is

$$y(n) = -a_1 y(n-1) - a_2 y(n-1) + \ldots - a_N y(n-N) + b_0 x(N) + b_1 x(n-1) \ldots + b_M x(n-M) \quad (6.1)$$

or more consisely

$$y(n) = -\sum_{i=1}^{N} a_i y(n-i) + \sum_{j=0}^{M} b_i y(n-j) \quad (6.2)$$

where:

M and *N* are the feedforward and feedback filter order respectively,

Bj and *ai* are the feedforward and feedback filter coefficients respectively,

x(n), y(n) are the input and output signal respectively.

The difference equation 6.1 is usually implemented directly as written by the Direct-Form-I IIR Filter Structure as shown in the Figure 6.2(a). There are other filter structures which minimize the memory (Direct form II and Transpose form as shown in Figure 6.2 (b and c) respectively) and computation requirements (Transpose form structure). The IIR filter function in dsPIC DSP library implements the Transpose form structure.
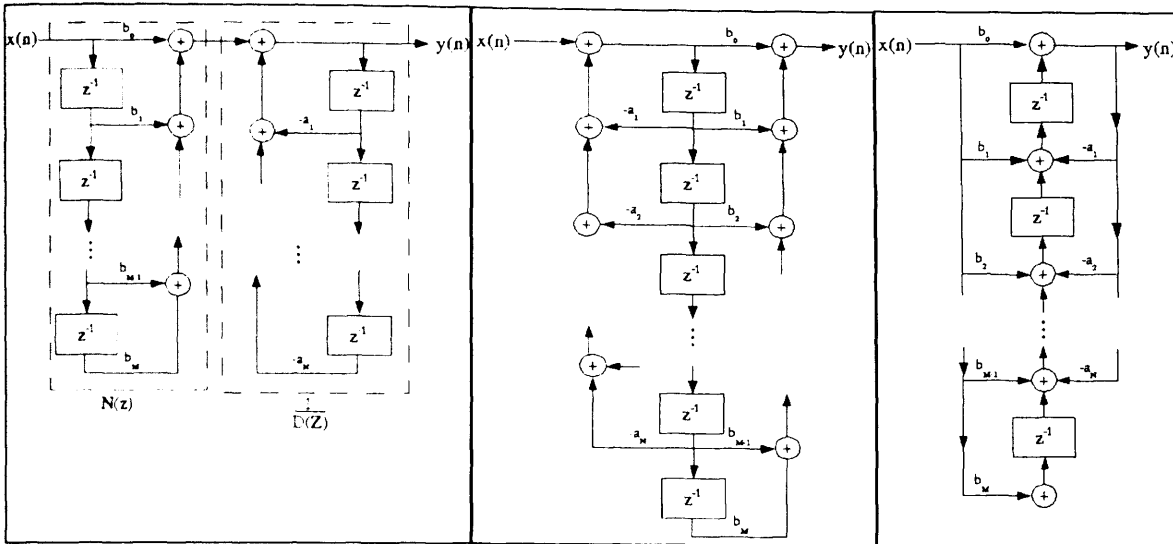
(a) Direct Form I   (b) Direct Form II   (c) Transpose Form

Figure 6.2: IIR Filter Structures (adopted from [6.4])

6.2.3 IIR Filter on dsPIC

The Digital IIR filters used in this research are C-callable functions provided in the dsPIC30F DSP library software. Such digital filters are typically implemented in software using the Multiply-Accumulate (MAC) class of DSP instructions. The MAC-class of instructions requires input data to be presented in 1.15 signed-fractional number format. This poses some limitations on the input signal which needs to be conditioned accordingly. Figure 6.3 shows a general architecture of a dsPIC microcontroller based signal processing system utilizing multiple digital filters.
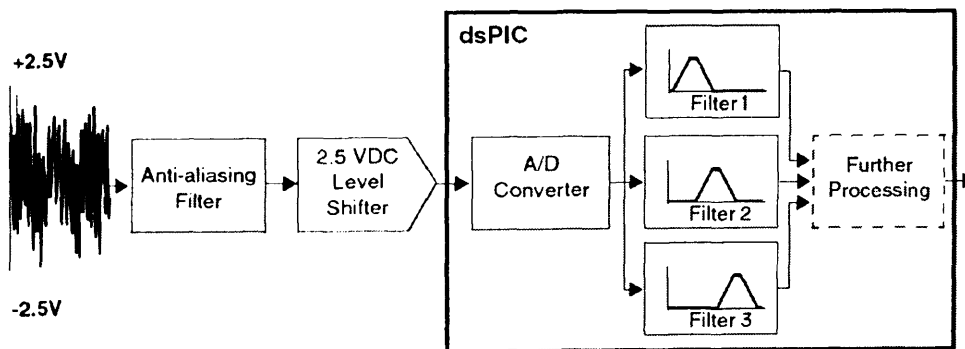
Figure 6.3: Signal processing system using multiple filters

The input signal needs to be conditioned to lie with in ±2.5V. After that the signal is passed through the anti-aliasing filter to fulfill the Nyquist criteria. The DC level shifter adds 2.5VDC to the signal thus making it compatible with the ADC which can measure

136

between 0 to 5 volts. The ADC is configured to provide a signed fractional digital result to the IIR filter. Depending upon the application, more than one filter can be implemented which can filter different signal components which are processed further to extract related features. The following sections describe the design and implementation of such signal processing system for tool condition monitoring utilizing Multiband IIR filters.

6.3 Monitoring Task

There has been extensive research on applying time domain and frequency domain analysis techniques in the context of machining process monitoring. Some of the frequency domain signal analysis techniques adopted by different researchers for designing TCMS have been reported in Chapter 3 providing an insight into the nature of the problem being considered and to the effectiveness of the e-Monitoring approach developed in this research. The basic assumption made by IPMM researchers, others and in this research consider that (under normal cutting conditions) the cutting force is periodic with tooth passing frequency f_p (as explained in Chapter 5). The characteristics of the cutting force signal and hence its frequency components may then be assumed to change with deteriorating tool condition.

Drawing in work in the IPMM group and to further developing the frequency analysis techniques mentioned above, filtering methods (both analogue and digital) have been considered. A sweeping filter technique for machine tool signal analysis was developed by Amer et al. [6.5] using programmable analogue filters. A precision programmable bandpass filter was used with a microcontroller based embedded system to analyse existing machine tool signals (spindle speed and load). The programmable gain and control settings of the filter IC were managed using a PIC microcontroller in order to optimise the frequency analysis for an anticipated range of frequencies of interest. The entire frequency range of interest was scanned to generate a total profile of the signal. The main drawback to the approach was the need to introduce and manage the required programmable analog filters. The features such as DSP engine and 12-bit ADC provided on dsPIC and the increased processing speed allow the development of digital filters which can be managed with the software. The dsPIC-based developed system

137

eliminated the analog filters which reduced the hardware component count resulting in a more compact and reliable monitoring system.

6.4 System Description

The proposed machine tool condition monitoring system is based on the three tier architecture shown in Figure 6.4. The spindle speed and spindle load signals were obtained from the machine controller via an isolation card. Spindle speed signal was monitored by a parameter monitoring node for the calculation of operational parameters which were communicated to other FENs when a signal change was detected. A signal conditioning stage was implemented prior to the signal being fed to the dsPIC microcontroller for analysis. This consisted of a pre-amplification stage which removed the DC offset (and frequencies below 2Hz) from the machine tool signals to increase the overall resolution in the implementation of digital filtering stage, the addition of a 2.5VDC offset to make the signals compatible with microcontroller's input range, and an anti-aliasing filtering stage. The output was fed to the dsPIC microcontroller's analogue input.
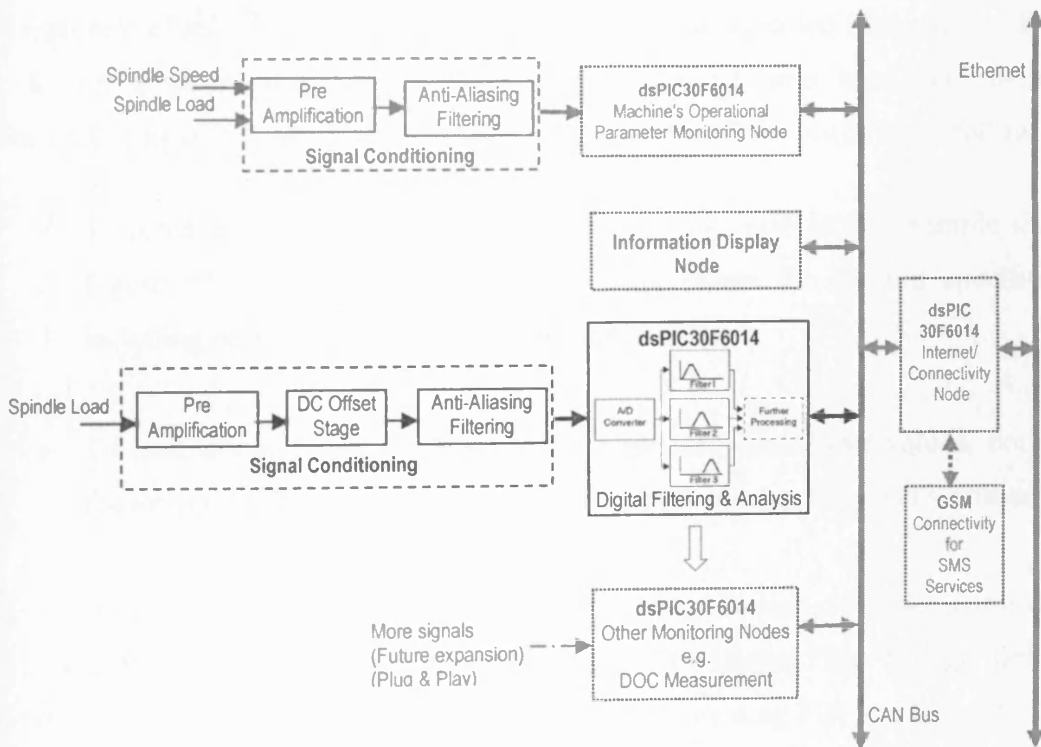
Fig. 6.4: Monitoring system architecture

138

In the initial set up there were three different Infinite Impulse Response (IIR) bandpass filters simultaneously implemented in the microcontroller. Each filter's pass band was dynamically determined and the filter coefficients adjusted in real time by the microcontroller depending upon the cutting parameters. In the "tool breakage detection mode" the centre frequencies for these bandpass filters were the machine tool rotation frequency (f_r), its third harmonic ($3f_r$) and tooth passing frequency(f_p). For a example spindle speed of 500 rpm, these frequency were 8.33,25 and 33.3 Hz respectively. The logic behind choosing these frequencies relates to the assumptions made regarding the effect that a broken tooth has on the overall frequency spectra.

The spindle speed information provided by the parameter monitoring node was used by the microcontroller in determining the working coefficients for the bandpass filters and the sampling rate for the ADC module. The microcontroller used 7.3728 MHz crystal oscillator which was sufficient to achieve a rate of 29.49 MIPS performance by using the built-in clock multiplier in the microcontroller.

6.5 Digital Filter Design

The process of selecting a filter's length and coefficients is called filter design. The goal is to set those parameters such that certain desired stop band and pass band characteristics will result. The main aims of the design effort should be as follows:

- To achieve and verify a frequency response plot, such as the example shown in Figure 6.5(b). This verifies that the filter meets the desired specifications, including ripple levels and transition width.

- To establish and consider the filter's length and coefficient values, noting that the longer the filter (more taps) the more finely the response can be tuned.

In this research, the dsPIC FD Lite, Digital Filter Design software (provided by Microchip), was used to design the desired filters. The Digital Filter Design tool for the dsPIC devices makes designing, analyzing and implementing FIR and IIR digital filters relatively easy through a menu-driven and intuitive user interface. The filter design tool performs the complex mathematical computations, provides graphical displays and

generates various design reports. Desired filter frequency specifications are entered while designing the filters and the tool automatically generates the code and coefficient files ready to use in the MPLAB Integrated Development Environment (IDE). System analysis of the filter transfer function is supported via multiple plots including magnitude, phase, group delay, log magnitude, impulse response and pole/zero location plots [6.6]. Figure 6.5(a) shows the dialog boxes for entering the required filter parameters and Figure 6.5(b) shows a screenshot of the multiple graphs. The example plots are for a 4th order inverse Tschebycheff bandpass IIR filter for 8.33Hz centre frequency and a sampling rate of 500sps.
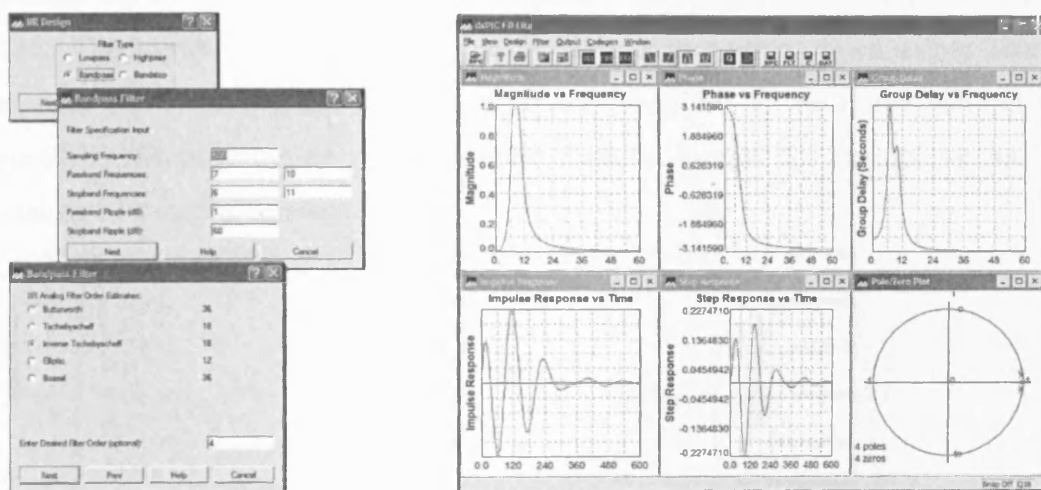
(a) Filter Design Sequence   (b) Main Screen with generated graphs

Figure6.5: dsPIC Digital Filter Design Software with the designed 8.33 Hz IIR Filter

6.5.1 System Response

To detect the tool breakage using the spindle load signal, the frequency components of the signal relating to tool rotation frequency, its 3rd harmonic and the tooth passing frequency need to be monitored. For a typical spindle speed of 500 RPM, these components are at 8.33Hz, 25Hz and 33.3Hz respectively. IIR Filters for these frequencies were designed as described using the dsPIC FD Lite software and the coefficients were exported to MPLAB IDE where these were programmed into the dsPIC microcontroller. The parameters used for these 4th order Inverse Tchebbysheff bandpass filters are summarised in Table 6.1.

Table 6.1: Parameters used for filter design

Design Frequencies			Passband parameters			Stopband parameters		
Sampling Rate f_s (Hz)	Tool	Frequency (Hz)	Frequencies (Hz)		Ripple (dB)	Frequencies (Hz)		Ripple (-dB)
500	f_r	8.33	7	10	1	6	11	60
500	$3.f_r$	25.00	23	27	1	12	26	60
500	f_p	33.33	32	35	1	30	36	60

Figure 6.6 shows the system responses for the filters. Frequency, Phase and Impulse responses are compared for the 3 key frequency components of 8.33Hz, 25 Hz and 33.3Hz. The impulse responses show that the filter output settles down within 280msec (less than 3 tool rotations). This is important since this is the initial settling time required by the filter before it can provide a useful output, for example at the very beginning of a cutting operation.

(a) Frequency Response   (b) Phase Response   (c) Impulse Response
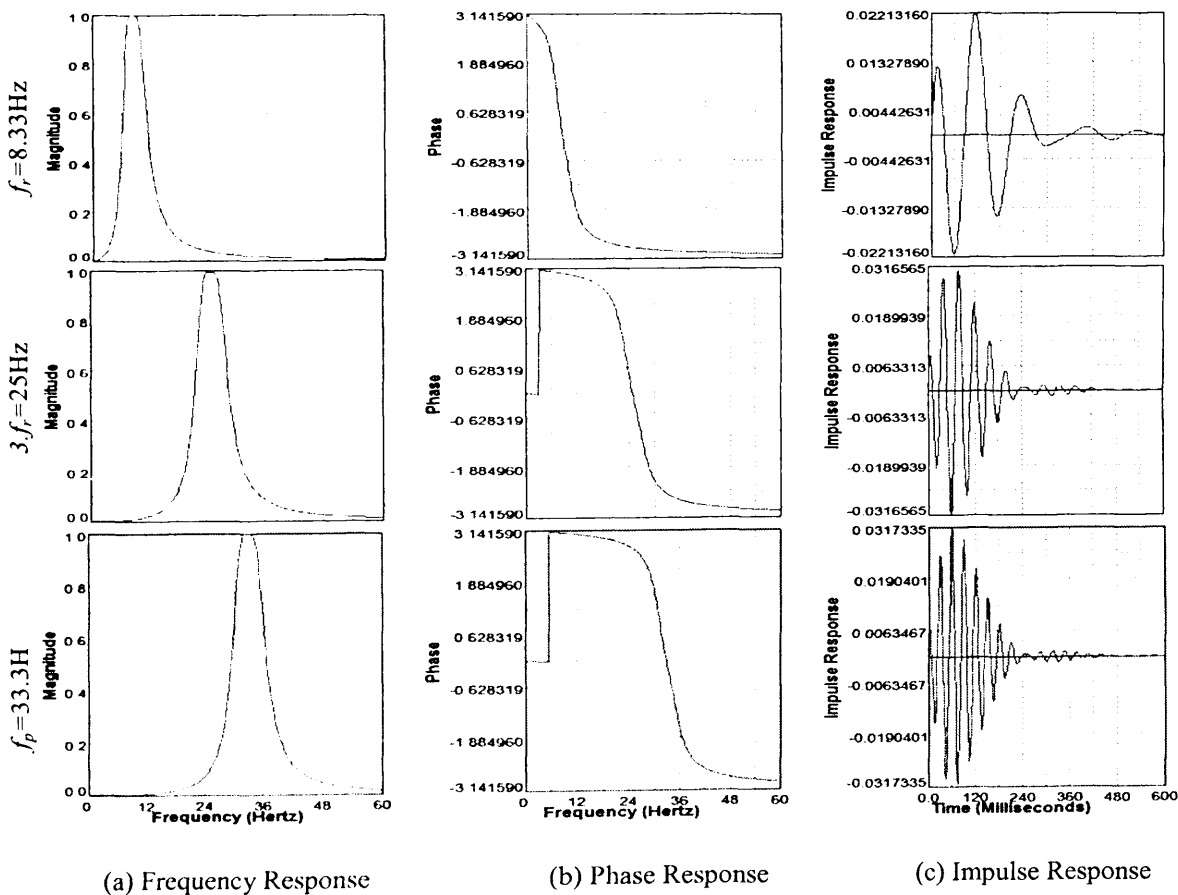
Figure 6.6: IIR Filter/System Response at 500sps (for Spindle Speed = 500rpm)

141

6.5.2 Relative Energy Index (REI)

The output of the IIR filter is a time domain sinusoidal signal of the centre frequency of the filter whose amplitude varies in accordance with the energy contained by that frequency component. Since direct amplitude varies periodically between maximum and minimum, it cannot be used directly. To effectively utilize the filter output, Relative Energy Index (REI) is calculated by taking the difference between maximum and minimum output value for 60 consecutive samples which equates to one tool rotation. REI is calculated after each tool rotation i.e. every 60 samples. A separate REI value is calculated for each filter output. Therefore three different REI values corresponding to f_r, $3f_r$ and f_p, are available for every tool rotation.

6.5.3 Tool Rotation Energy Variation (TREV)

Tool Rotation Energy Variations (TREV) is calculated along the same lines as the calculation of Relative Energy Index (REI), using the acquired spindle load signal which is processed directly, instead of using the filtered signal(s). TREV shows the effect of the all frequency components present in the signal. A detail discussion on TREV is provided in section 6.8.4 along with cutting tests.

6.6   Dynamic Coefficient Selection Technique

The key element in flexibly configuring the filtering function to suit specific machining process parameters is referred to, in this research, as the Dynamic Coefficient Selection Technique which is diagrammatically illustrated in Figure 6.7. This uses the spindle speed signal as reference to determine the sampling rate for the spindle load signal and allows the set-up to be automatically tuned to the parameters being monitored. A fixed sampling rate is used for the spindle speed signal to determine the actual spindle speed by the parameter monitoring node. The required sampling rate of spindle load signal is then set, since it is directly proportional to the spindle speed. For example; for a spindle speed of 500 rpm a sampling rate of 500 samples per second is selected and for a speed of 1200 rpm the sampling rate is 1200 samples/s. At any spindle speed, there are 60 samples of spindle load for each tool rotation available for analysis and decision making after the filtering stage.

System frequency response for desired frequency components
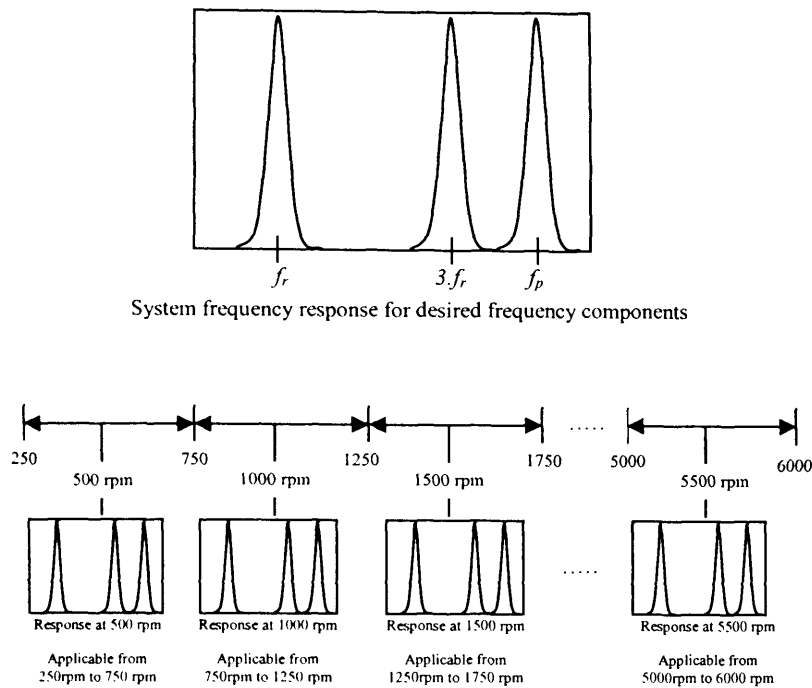
Figure 6.7: System Response for spindle speed range of 250-6000RPM

The proposed monitoring system has been designed to make the necessary adjustments to the filter coefficients as spindle speed varies from 250 to 6000 rpm. The monitoring technique uses two different parameters as a basis to achieve the dynamic set-up of the filters. A fixed set of banded coefficients has been defined for a number of predefined frequency ranges. For example for spindle speeds between 250 and 750 rpm, the filter coefficients for all of the IIR bandpass filters remain unchanged. Sampling rate then acts as a variable, and depending upon the actual spindle speed, can be used to establish the centre frequency of the pass band to the frequency of interest. This technique ensures that, whenever the spindle speed shifts from one range to another, the filter coefficients change to that particular band's settings dynamically. Within every band of spindle speeds the sampling rate stays variable to ensure that the pass band stays where required. The filter coefficients for different speed bands are pre-calculated and pre-programmed in a look up table within the microcontroller memory for ease of use

Filter coefficients for different ranges of sampling rate/spindle speed were calculated using the parameters given in Table 6.2. Each filter's coefficients required 10 words (20 bytes) storage space. The complete set of coefficients required 270 words (540 bytes) of storage space.

Table 6.2: IIR filter design parameters for sampling rates of 250-6000 sps

Spindle Speed (RPM)	Design Frequencies		Passband		Stopband		
Sampling Rate f_s (Hz)	f_s (Hz)	f_r (Hz)	Frequencies (Hz)	Ripple (dB)	Frequencies (Hz)		Ripple (dB)
250-750	500	8.33	7	10	1	6	11	60
750-1250	1000	16.67	14	18	1	13	19	60
1250-1750	1500	25.00	23	27	1	21	29	60
1750-2250	2000	33.33	30	36	1	27	39	60
2250-2800	2500	41.67	38	44	1	35	47	60
2800-3500	3150	52.50	49	55	1	46	58	60
3500-4200	3850	64.17	60	68	1	56	72	60
4200-5000	4600	76.67	72	80	1	68	84	60
5000-6000	5500	91.67	87	95	1	83	99	60

It is possible to use larger ranges to reduce the number of coefficients to be stored in the microcontroller memory with compromise being made on the larger bandwidth for higher side of the range. Figure 6.8(a) shows the spread of the frequencies for tool rotation frequency component for entire range of spindle speed. The frequency spread is much smaller than that of a single normalized filter designed for entire range as shown in Figure 6.8(b).
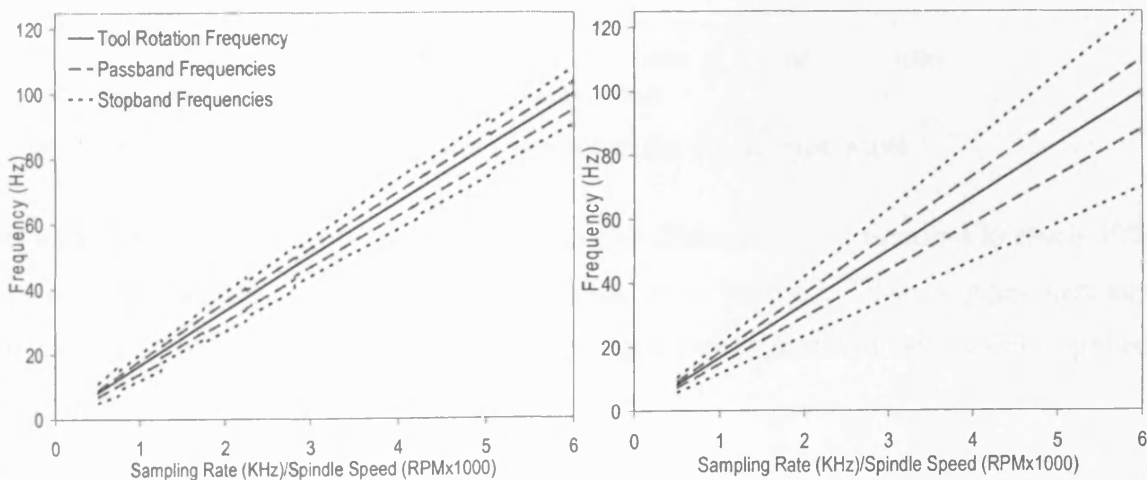
(a) Dynamic Coefficient Selection Technique

(b) One set of coefficients normalized for all frequency range

Figure 6.8: Filter Frequencies (Bandwidth) of the IIR Filter

6.7 Preliminary Filter Testing

Preliminary tests were performed to confirm the performance levels of the designed filters, and the associated signal conditioning stage. The tests were designed to enable the analysis of the system response time, the effect of amplification on system output, the response to a chirp signal test and the response to a single individual frequency component test.

6.7.1 System Response Test

According to the impulse response of the designed filter, the settling time was estimated to be 280msec for the tool rotation frequency case (8.33Hz at 500sps). To confirm this, an 8.5Hz (being the centre frequency of designed filter) sinusoidal signal was fed to the system and output shown in Figure 6.9 was obtained.
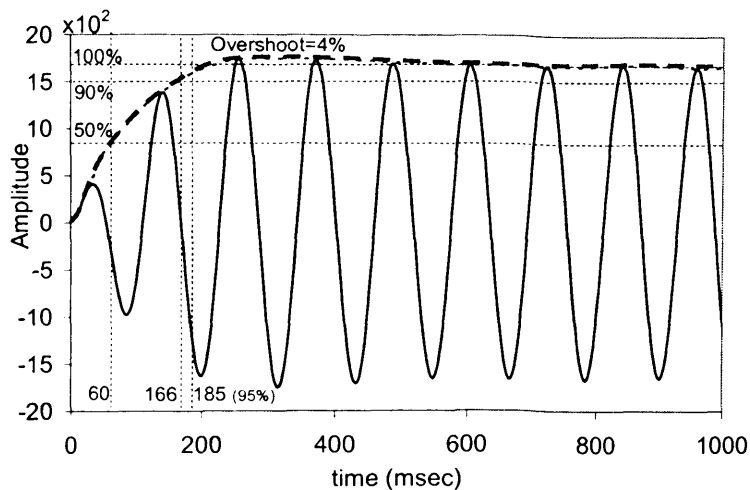
Figure 6.9: System Response for 8.5Hz Sine wave

It took 185msec to reach 95% of final value and 60msec (½ tool rotation) to reach 50% level. After one tool rotation a 72% level had been reached. These suggest that any threshold level subsequently used to detect tool breakage could be sensibly applied within 1-2 tool rotations time frame.

6.7.2 Chirp Signal Test

The frequency of a chirp signal increases or decreases lineally with time and this signal can be used to calculate the frequency response of a system. A chirp sinusoidal signal was generated in Matlab and fed to the system. The chirp signal frequency varied from

0 to 50Hz in 5 seconds and acquisition started slightly before the signal was generated by the DAQ. The system output is shown in Figure 6.10(a) which shows that settling time for all three frequency components is 3 tool rotations. The system output was adjusted to represent the REI for the frequency range 0-45Hz and is shown in Figure 6.10(b). This is effectively the measured frequency response of the system.
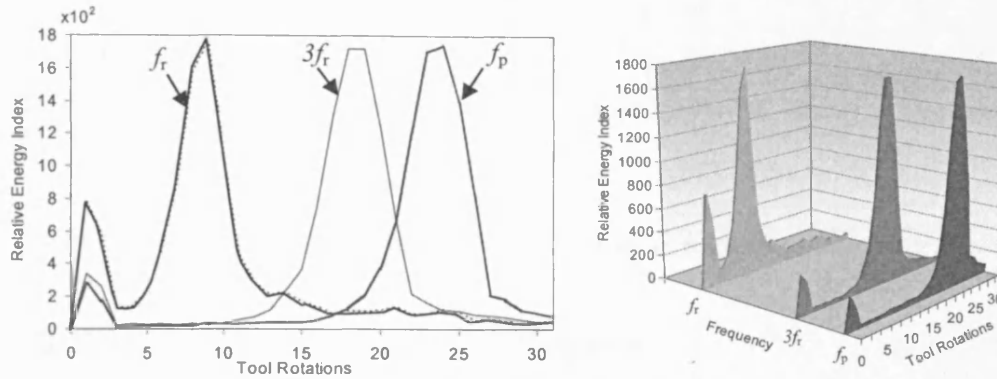
Figure 6.10(a): System output in response to the chirp signal input
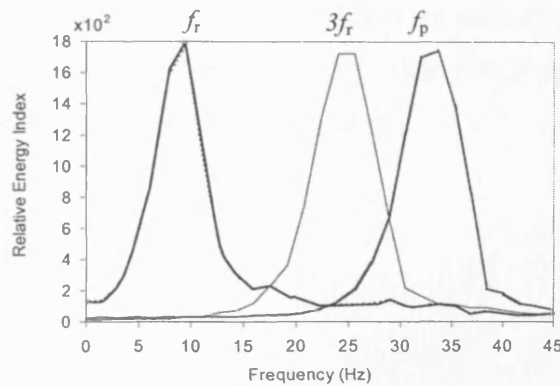
Figure 6.10(b): System frequency response obtained using chirp signal as input

6.7.3   Effect of amplification at signal conditioning stage

For this test a recorded spindle load signal from a cutting test performed at 2.0mm DOC with a spindle speed of 500RPM was input via the signal conditioning circuit board to the 25Hz filter with and without the amplification applied to signal. REI for 3rd harmonic of the tool passing frequency was monitored. The results are shown in Figure 6.11 from which it can be seen that amplification at the signal conditioning stage improved the system response. The separation between REI (for 25 Hz) for healthy and broken tooth cases became more distinct when amplification was used and it was possible to apply a threshold after the settling time (3 tool rotations) to distinguish between healthy and broken cutters.

(a) Output without any gain   (b) Output with gain
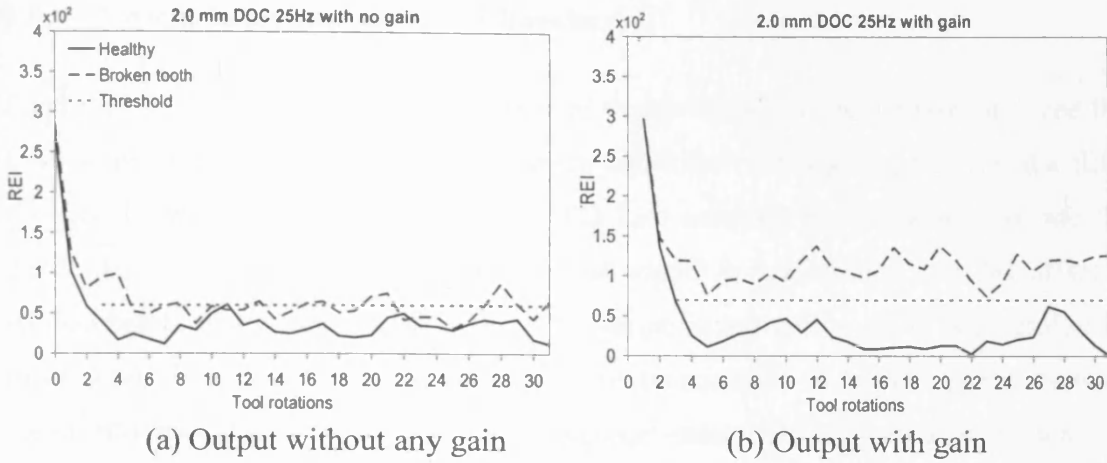
Figure 6.11: Effect of amplification of the signal at signal conditioning stage

6.7.4   Individual Frequency Component Response

For this test individual frequency sinusoidal signals were applied to the system and the time domain responses are shown in Figure 6.12(a). In each case the appropriate centre frequency has large amplitude compared to the other two frequencies. Figure 6.12(b) shows the system output in frequency domain plots.
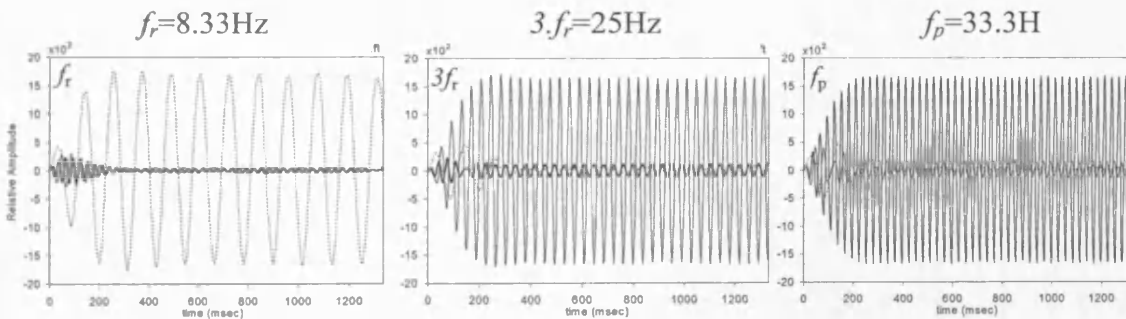
(a) Time Domain Output (Relative Amplitude)
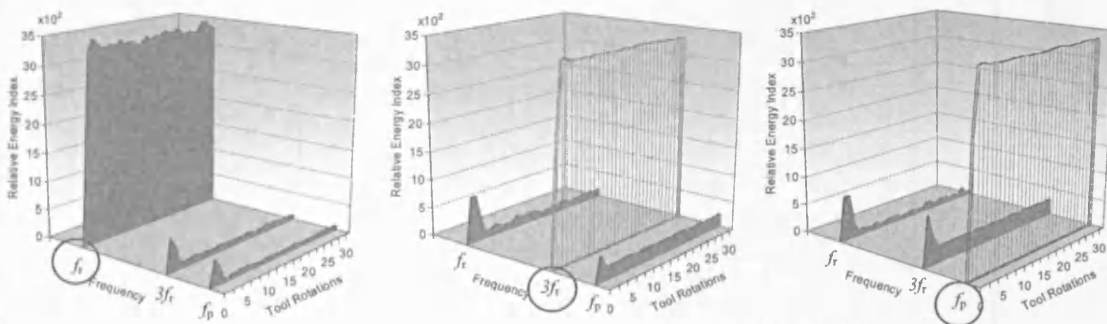
(a) Frequency Domain Output (REI)

Figure 6.12: System output for Individual Frequency sinusoidal input signals

147

6.8 System Implementation and Results

Figure 6.13 shows the schematic diagram of the developed system based on three IIR Filters implemented on dsPIC30F6014 microcontroller. As discussed earlier the filter coefficients were calculated using dsPIC FD Lite software and programmed into the dsPIC using MPLAB IDE. The spindle load signal is conditioned and DC offset is applied before being input to the ADC. The sampling rate of the ADC is controller by timer 3 which provides variable sampling rate proportional to spindle speed. Spindle speed information is obtained via CAN message transmitted by parameter monitoring node which monitors the operational parameters and controls the monitoring process based on the spindle load. The filter coefficients of filters for f_r, $3f_r$ and f_p are dynamically selected based on the sampling rate as discussed in section 6.6. Filters are executed at each sample to produce the output which is used to calculate the REI after each tool rotation. Unfiltered spindle load data is used to calculate tool rotation energy variation (TREV). The calculated parameters (TREV and REI for each filtered frequency component) are input to local decision making module which determines the health of the tool and communicates the results on CAN bus. The detail operation of the system will be discussed in the following section.
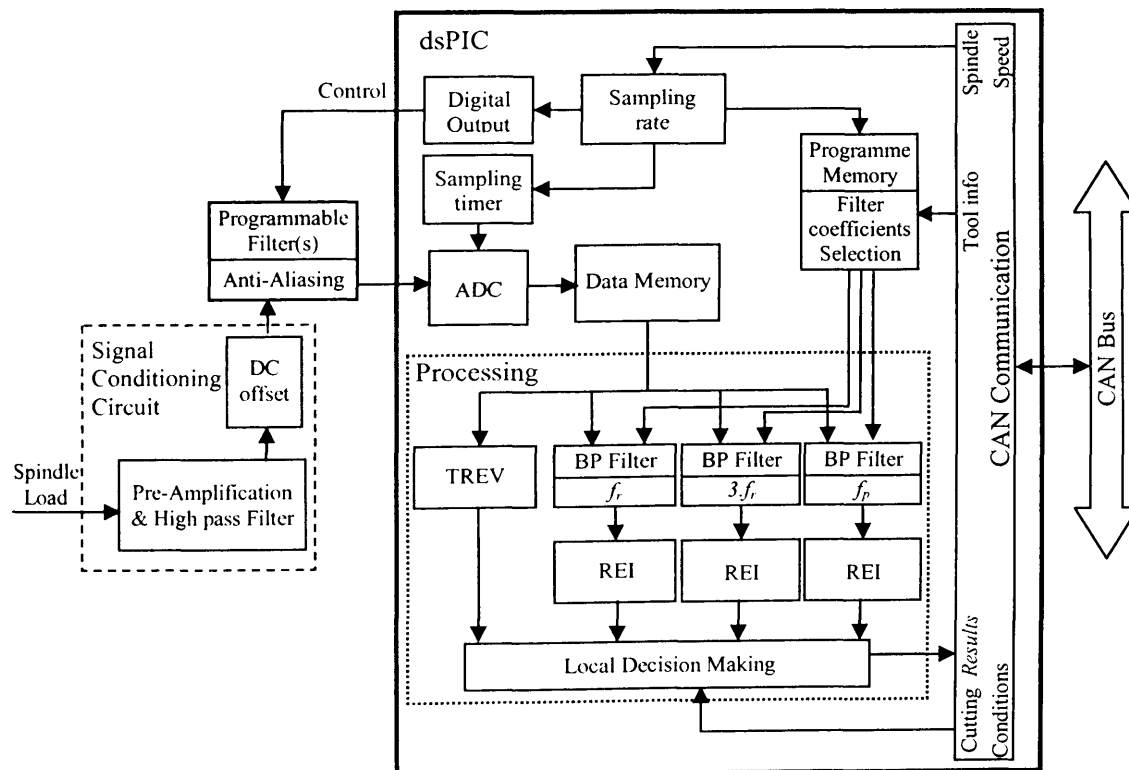
Figure 6.13: Schematic diagram of developed system

6.8.1　System Operation

The main frequencies of interest in the frequency spectrum of a spindle load signal are the tool rotation frequency and the tooth passing frequency. The observation of these frequency components in terms of their relative strength can be used to dynamically monitor cutting tool health. This technique observes thee frequencies (f_r, $3f_r$ and f_p) in parallel using 3 IIR filters implemented on a single dsPIC microcontroller. The data memory allocation space for each tooth rotation has been kept constant by directly linking the sampling rate to the spindle speed. During any cutting process the spindle load data is acquired and buffered in segments of one tool rotation. During the data acquisition stage of the next sample, the processing of previously acquired sample is completed. The processing includes digital filtering and updating the minimum and maximum values. After a segment of data is acquired and processed; the peak to peak difference (REI indicator for that revolution) is calculated by taking the difference of maximum and minimum values and local decision making is performed using indicators to confirm the health of the tool. This technique ensures that data processing is completed in shortest possible time and results are available immediately after the revolution is completed.

To illustrate the basis of this method consider the action of a four toothed end mill. A healthy cutter will register four even cuts per revolution, with relatively little variation between cutting force. The REI values for tool rotation frequency will have small values, as can be seen in Figure 6.14, which presents the results for tests carried out at a spindle speed of 500 rpm, feed rate of 100 mm/min and 1mm depth of cut using a four teeth cutter on a vertical axis milling machine.

(a)　　　　　　　　　　　　　　　　(b)
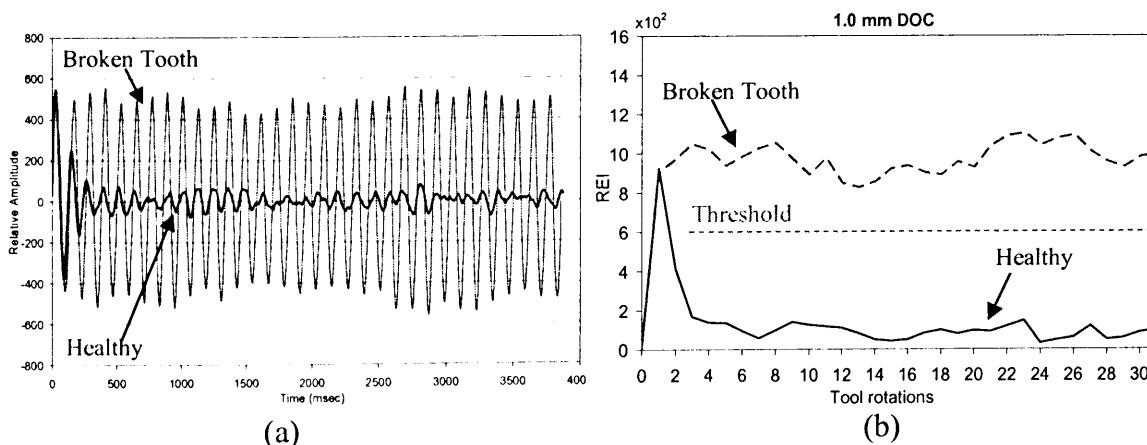
Figure 6.14: (a) The filter output for a healthy and broken cutter at 1 mm depth of cut.

(b) REI at 1 mm depth of cut.

Figure 6.14(a) shows the 8.33 Hz filter's output for a healthy and broken cutter at 1 mm depth of cut. It is obvious that, for a broken cutter, the frequency strength increases. This is due to the fact that previously tool rotation alone was responsible for generating this frequency whereas now the once per revolution action occurring when using the broken cutter is also adding to the strength of this frequency. By monitoring the amplitude or REI of this filtered frequency component, the tool breakage can easily be detected. This ensures that the monitoring technique focuses on the filter's optimum performance to ensure the best possible results with the minimum number of possible false alarms.

To further support the same concept, Figure 6.14(b) presents a much clearer picture. The value of REI of 8.33 Hz filter for a broken cutter is significantly higher (around 9–10 times) than the normal value of REI for a healthy cutter. It must be noted that, due to the impulse response of the filter, there is some settling time before reliable results may be obtained. This settling time occurs once, at the start of monitoring system and in this particular design the settling time is less than 3 tool rotation (280 ms for 500rpm). The increase in REI, when confirmed by changes to the frequency components, has been used as a signal for an alarm signal to warn of tool breakage. This is an important feature of the deployed system.

There are many one-off events, such as machining an inclusion, breaking-in or breaking-out of a workpiece and step changes in the depth of cut that could cause a significant variation in tool force, but they will not cause similar changes to frequency based analysis of the load, since they are not cyclic. This can be confirmed from Figure. 6.15 (a, b) which show the filter's output and REI for a healthy and broken cutter at 2 mm depth of cut. The change in depth of cut causes an overall change in REI magnitude, but the changes associated with the operation of the broken cutter are still apparent.

The above process operates continuously; while the data for a tooth rotation is being acquired, the calculations on the previous acquisition are carried out in parallel and the results are compared against parameter dependent thresholds for decision making. Given the memory considerations appropriate to even the dsPIC microcontrollers, this process requires the application of careful data management. Using the architecture

shown in Figure 6.4, the data acquired by first tier nodes will either have to be communicated to the second level or discarded. In order to prevent data overload and the data becoming obsolete, it will usually be classified, summarized and discarded if it is commensurate with normal machine behavior. Only selected abnormal data is forwarded for future referencing etc. In the event of any abnormal indications, the observant node communicates to other first tier nodes over the CAN bus for verification.
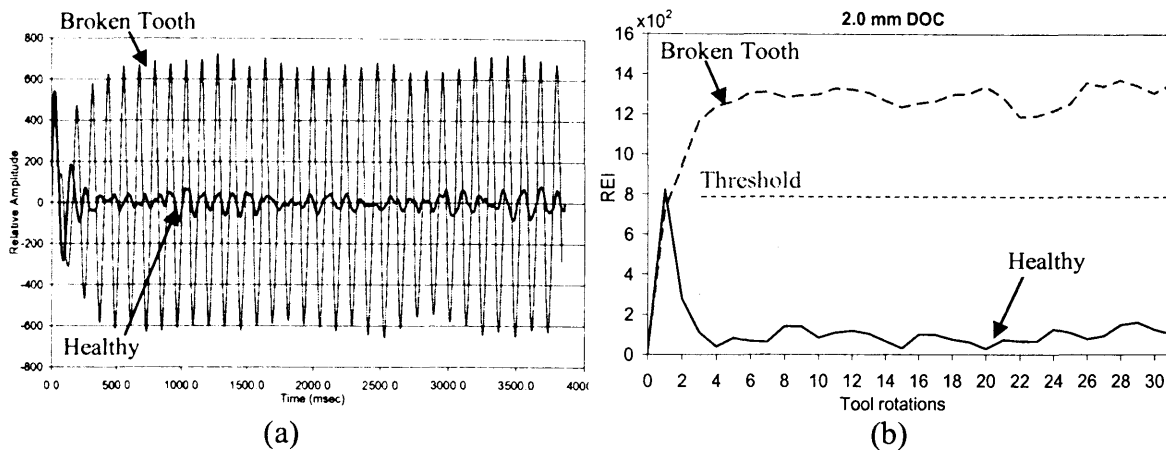

Figure 6.15: (a) The filter output for a healthy and broken cutter at 2 mm depth of cut.

(b) Relative energy index at 2 mm depth of cut.

6.8.2 Cutting Tests

To perform the analysis for various conditions the pre-recorded signals from actual tests with known/pre-determined parameters were again used. The Matlab program read the recorded signal from an excel file and processed the signal to perform the signal conditioning steps including removing DC components by using a high pass filter, amplifying the signal and applying a DC offset of 2.5 volts. After processing the signal, the sampling rate of the signal was increased (using an interpolation filter) and final data was fed to DAQ card which generated the analogue spindle load signal which was fed to dsPIC-based IIR filtering system. Test for healthy (new), healthy (worn) and broken cutters were performed for different depth of cuts. Figure 6.16 shows a typical output obtained during cutting tests. The filters' output in time-domain is shown in left column and REI for three frequencies is shown in middle column while frequency domain view is given in right column. As explained earlier, REI for tool rotation frequency and tooth passing frequency gives clear picture of the health of the cutter.

151

Since the filter output in time domain is not directly used for decision making, this will not be included in further discussions.

(a) Filter output   (b) Relative Energy Index   (c) Frequency Domain View
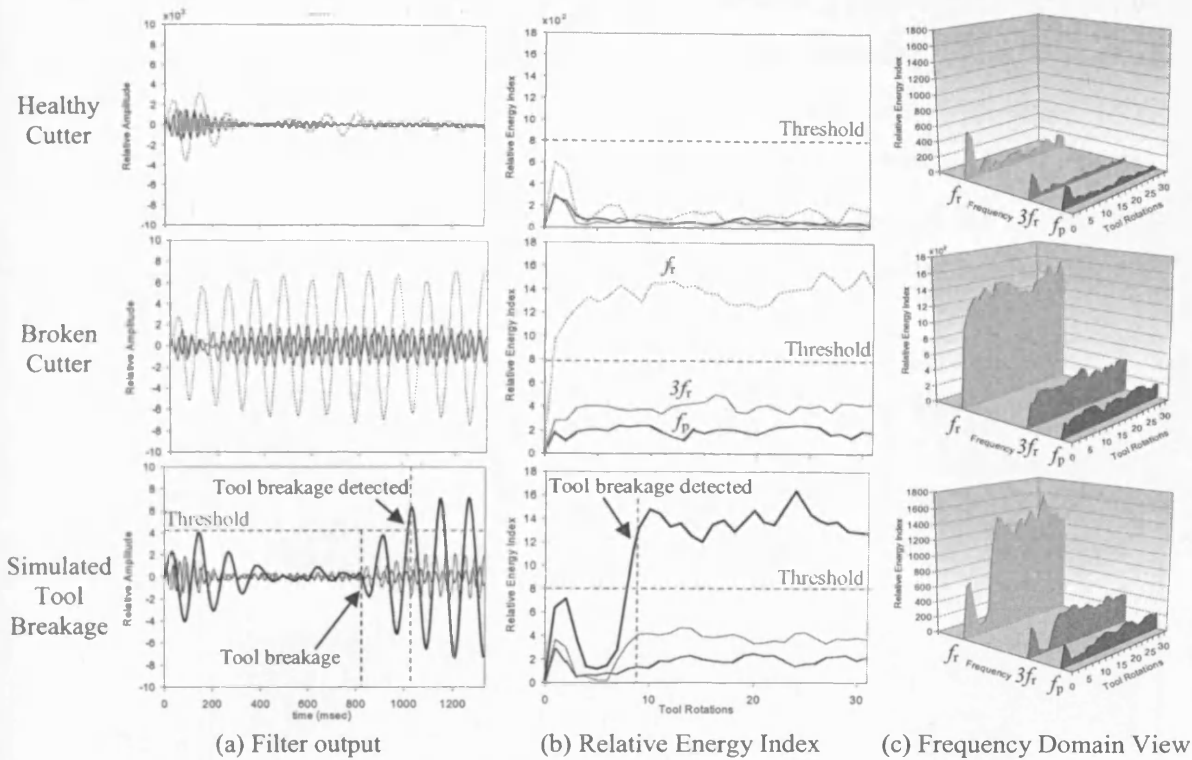
Figure 6.16: Typical output of the system for healthy, broken and tool breakage cases.

6.8.3 Depth of Cut Variations

Cutting forces in milling are dependent on the amount of metal being removed and metal removal rate is directly proportional to the depth of cut. Therefore it was necessary to test the system for the effect of depth of cut variations. Cutting tests were performed for different depth of cuts (0.5mm, 1.0mm, 1.5mm, 2.0mm) for new, worn and broken cutter (with one tooth broken) cases. The REI profiles for three frequency components are shown in Figure 6.17. The left hand column shows the REI for a new cutter, the centre column shows the REI for a worn cutter and right hand column shows the REI for broken cutter. The REI profiles for new and worn cutters are almost same except for the 0.5mm DOC case. The broken cutter can be easily identified by large REI values for the tool rotation frequency and its 3rd harmonic as compared to new and worn cutter REI values.

The REI for the broken cutter increases for all frequency components with increase with depth of cut. It was deemed important to have an adaptive threshold strategy to

152

allow maximum tool usage during varying DOC and still be able to detect the tool breakage without generating false alarms. This is due to following observations: Since larger cuts are normally used for rough machining operation, a fully worn cutter may be allowed to keep cutting until a convenient pause in the machining cycle. It is more likely for the tool to break during larger DOC. Tool breakage with small DOC (normally during finishing operation) will have a larger adverse effect on the workpiece. The following section describes time domain analysis of the spindle load signal which was made possible because of the effective signal conditioning strategy.
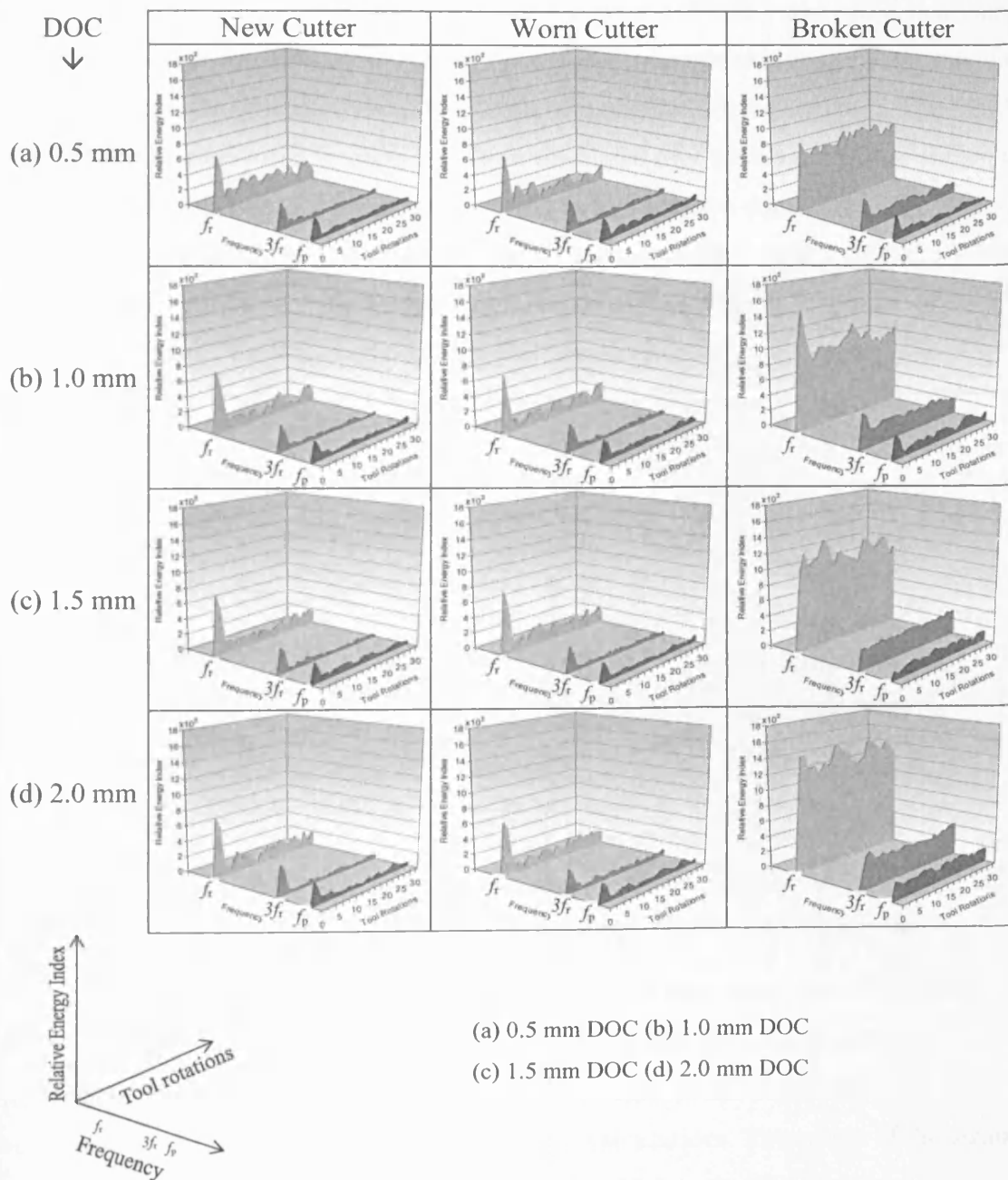
Figure 6.17: Relative Energy Index (REI) for different depth of cut tests

153

6.8.4 Tool Rotation Energy Variations (TREV) Tests

The pre-amplification circuit at the signal conditioning stage included DC blocking high pass RC filter with cutoff frequency of 2.6 Hz. This filtering removed the cutting force variations arising due to tool entry, tool exit and changes in other milling parameters. This variations removal made the signal more stable and reliable for time domain processing. It also made the signal more suitable for interfacing with the dsPIC microcontroller. It was observed that overall signal variations for each tool rotations were very small for new and worn cutter whereas these variations were relatively large for broken tooth cases. Tool Rotation Energy Variations (TREV) was calculated along the same lines as the calculation of REI for frequency components, except that the acquired signal was processed directly instead of using the filtered signal(s). The TREV and REI for the monitored frequencies, for a simulated tool breakage test, are shown in Figure 6.18. In this test tool breakage occurred at tool rotation number 16. The REI for tool rotation frequency (f_r) crossed the threshold at tool rotation number 18 whist TREV crossed the threshold at tool rotation number 17. Thus overall response of TREV method was faster than REI method, for a tool breakage case.
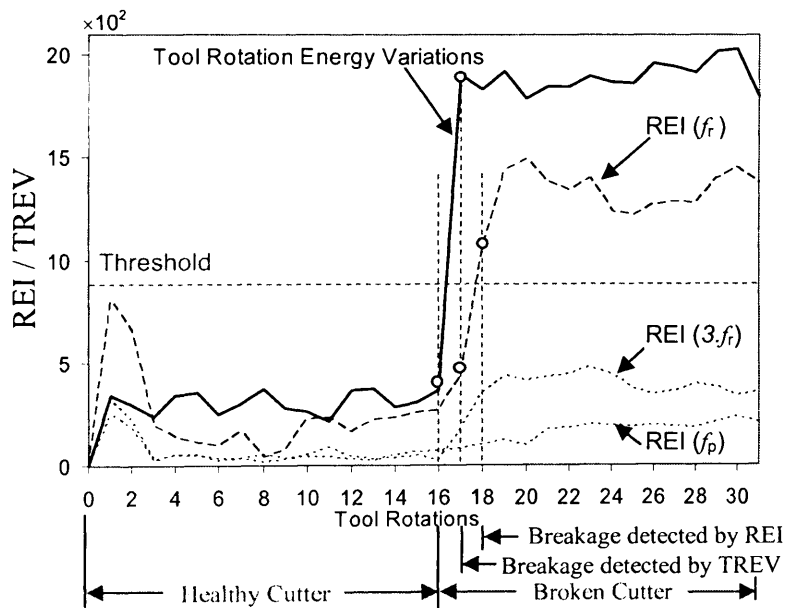
Figure 6.18: Comparisons of Tool Rotation Energy Variations (TREV) and REI

A virtual node was implemented in the system for find this parameter which provided the broken tool indication about one revolution earlier than the filter based REI method which detected tool breakage in two revolutions. This could trigger the sequence to verify tool breakage via the frequency component calculations. The output of the virtual node (implemented within the IIR filter node) to calculate the TREV for cutting tests

performed at different DOC is shown in Figure 6.19. The variations for worn cutter increase as the depth of cut increases but these are still below the threshold level for tool breakage detection. The threshold is set adaptively and increases as the DOC increases.
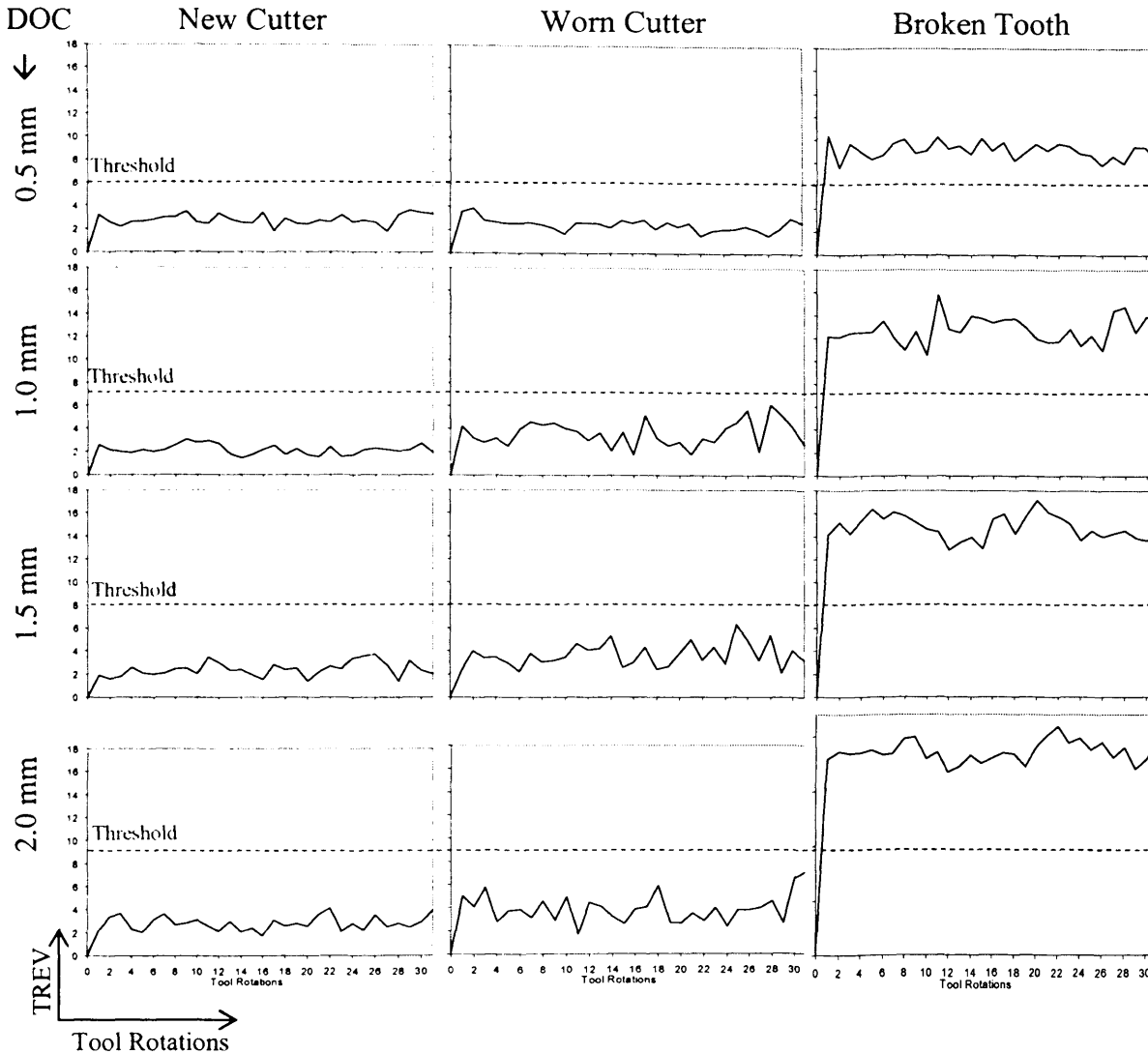
Figure 6.19: TREV for cutting tests at 500rpm spindle speed

6.8.5 Simulated Tool Breakage Tests

After implementing the TREV virtual node, simulated tool breakage tests were carried out for different DOCs. For this purpose the recorded signals for healthy and broken files were joined and played back through the DAQ card. Tool breakage was detected for all cases and results from the filter system are shown in Figure 6.20. The tool rotation frequency f_r and its 3rd harmonic of the increased in case of the tool breakage and the amplitude of the tooth passing frequency f_p behaved randomly. In some cases its

155

amplitude increases while in other cases remains same or increases in very small percentage. As discussed earlier, TREV (shown in left column of Figure 6.20) indicated tool breakage 1 tool rotation earlier than RET (shown in middle column). Thus TREV can be successfully used as an early alarm of tool-breakage and confirmation achieved by REI method. This technique based on combination of TREV and REI will ensure that tool breakage is detected and confirmed in the targeted 2 revolutions.
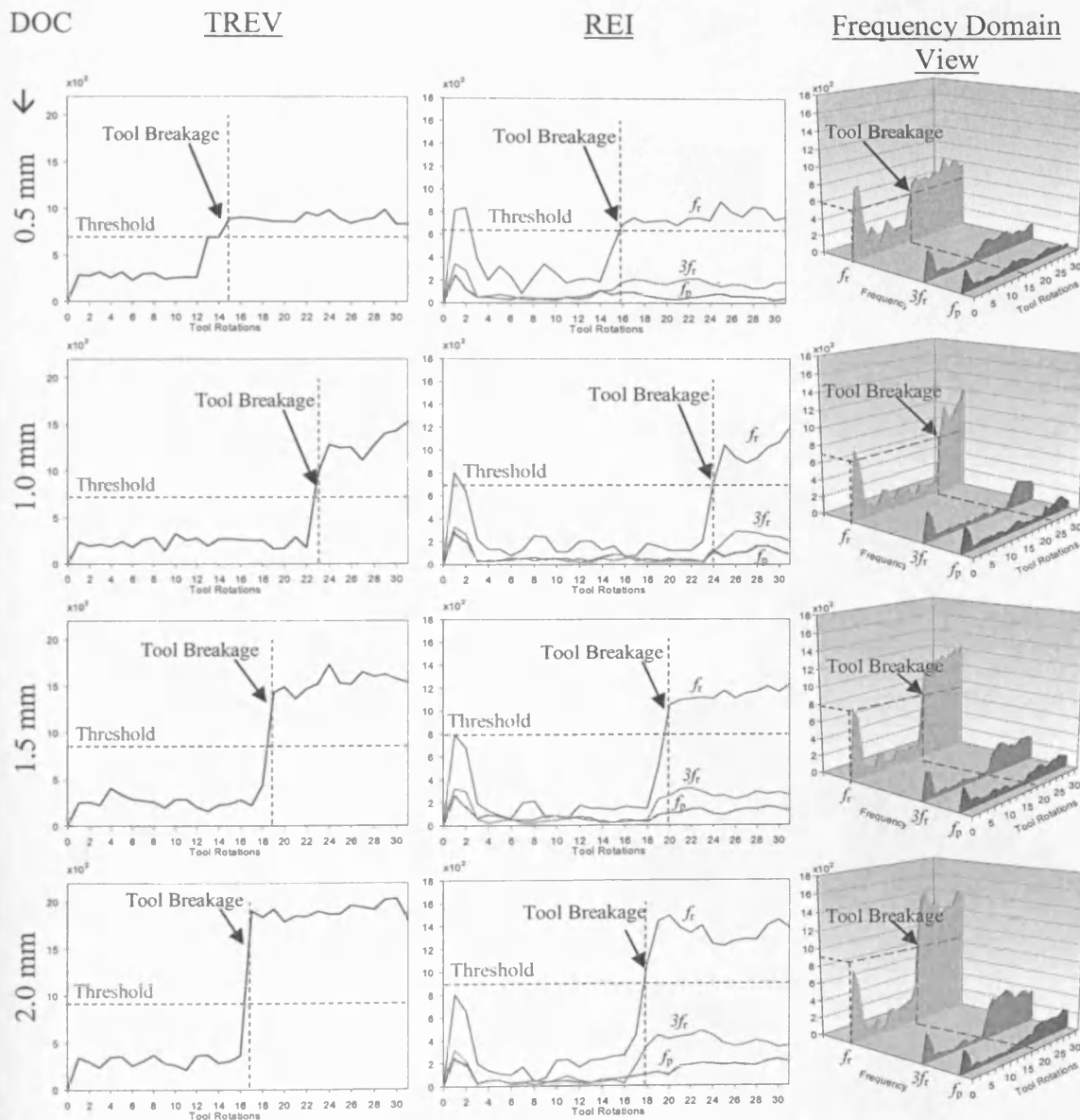
Figure 6.20: Simulated tool breakage tests at different depth of cuts

6.8.6 Cutting Tests at different Spindle Speed

Cutting tests at different spindle speeds were simulated by changing the signal frequency in Matlab before being fed to system and system output for various spindle

speeds is given in Figure 6.21, which shows that system settling time is less than three tool rotations and overall output is same in terms of tool rotations which becomes faster as spindle speed increases.
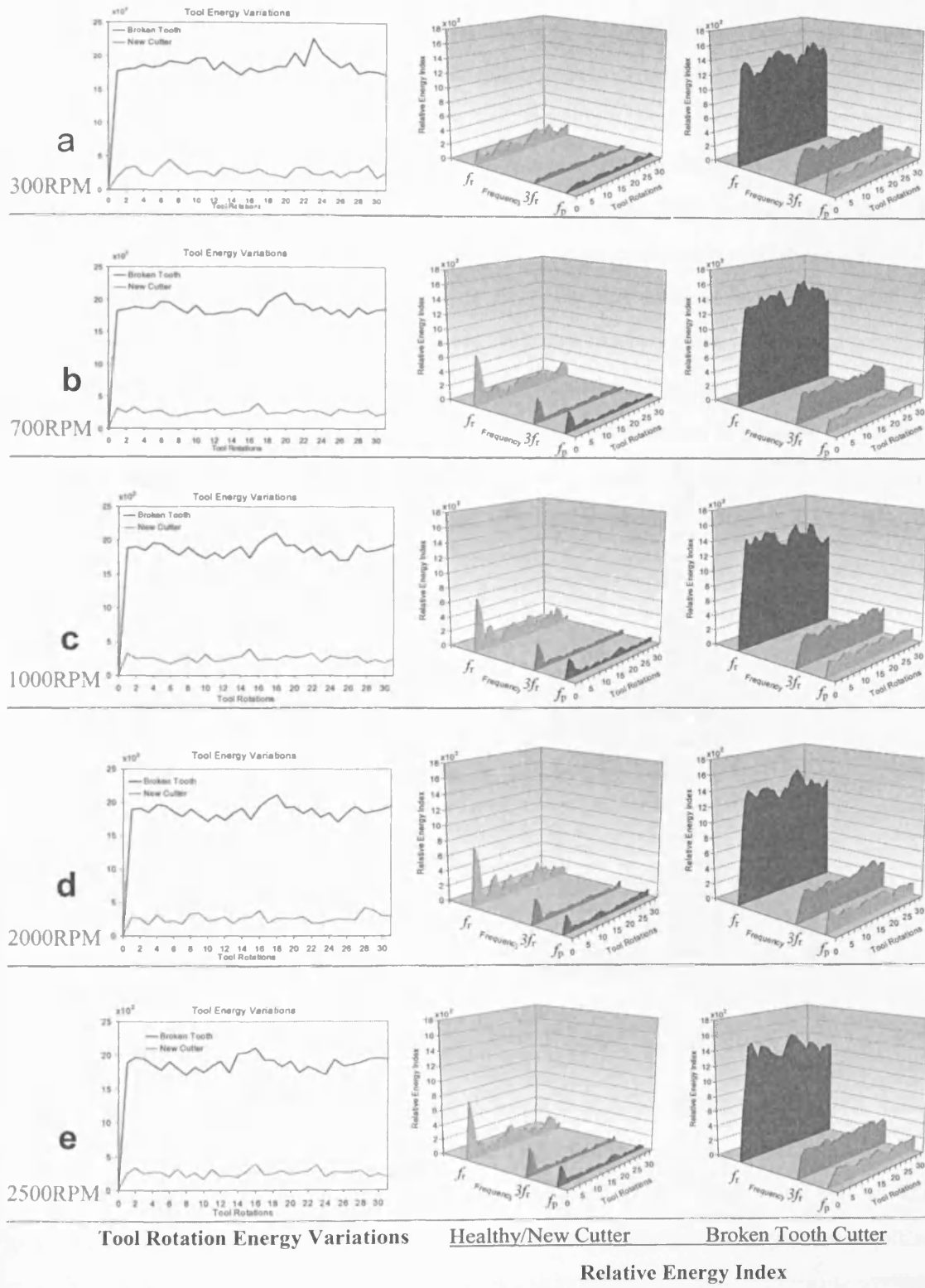
Figure 6.21: Cutting Tests at different spindle speeds (DOC=2.0 mm)

6.9. Decision Making

The extracted features TREV and REI for three frequency components (f_r, $3f_r$ and f_p) has been analysed and shown effective for detecting tool breakage. Although TREV can indicate tool breakage earlier than REI method, counter verification, which can be provided by REI, is required to avoid false alarms. When combined according to Table 6.3, these features can indicate more than tool breakage. For example a blunt tool for which TREV is large but REI of f_r and $3f_r$ would not cross the threshold. In this table '1' indicates that threshold has been crossed and 'X' denotes "don't care" condition. An advanced diagnosis can also be requested for unexpected cases. In these cases the parameter monitoring node will initiate an advance diagnosis sequence and send the acquired data to the second tier for analysis. When a broken tooth is detected a broken tooth message is sent to parameter monitoring node which then combines this decision with decisions from other FENs and make a final decision about the health of the tool. Upon a possible blunt tool detection a blunt flag message is sent which is used for process management function and the tool can be checked after the machining cycle finishes.

Table 6.3: Decision Making Table

| TREV | REI | | | Decision |
	f_r	$3f_r$	f_p	
0	0	0	X	Healthy
0	1	X	X	?
0	X	1	X	?
1	1	X	X	Broken tooth
1	X	1	X	Broken tooth
1	0	0	1	Blunt tooth
1	0	0	0	Wait for next Frame

? = Unexpected : request for advanced diagnosis

6.10. Conclusions

This chapter has outlined the design and implementation of a digital filter based frequency domain signal analysis technique. This research was undertaken to support the monitoring of the milling machining process. The implementation of this application on a dsPIC microcontroller has been successfully achieved and the resulting module was deployed as the first level node in a distributed process monitoring system. The nature of the dsPIC module is such that it can be re-configured using software to

suit a wide range of monitoring tasks and its use in this context is part of an on-going research program.

In the IPMM research particular emphasis is placed upon the ability of the monitoring module to make an instant but accurate diagnosis of a fault condition. This is facilitated by the integration of modules which may all be monitoring the same process, and can support the fault diagnosis procedure. This is very much seen as being a synergistic approach; the overall capabilities of such a system are more than the sum of the individual elements. The nature of the deployed frequency domain analysis techniques and the dynamic digital filtering methodology allow the microcontroller devices to perform a number of sensing functions simultaneously using multiple frequency estimation applications which would normally be judged to be beyond their capabilities. This can provide a very powerful and flexible sensor system, which can be economically deployed to monitor a wide range of machines and processes.

The main benefit comes from the smart operation of this system, in that data is analysed and packaged within the sensor system. Data considered to be of interest can be automatically referred to more powerful analysis systems, but data indicating a normal operation is summarized and then discarded. This reduces traffic on the integrating network, and removes the data saturation effect which has hampered the take up of such monitoring systems in many industrial situations. The same technology and approach is applicable to a wide range of process and machine based applications.

References

[6.1]   Steven W. Smith, "Introduction to Digital Filters", Chapter 14, "The Scientist and Engineer's Guide to Digital Signal Processing", California Technical Publishing 1997, ISBN: 0966017633, pp. 261-276.

[6.2]   Steven W. Smith, "Filter Comparison", Chapter 21, "The Scientist and Engineer's Guide to Digital Signal Processing", California Technical Publishing 1997, ISBN: 0966017633, pp. 343-346.

[6.3]   Wagner, Brian and Michael Barr. "Introduction to Digital Filters", Embedded Systems Programming, December 2002, pp. 47-48.

[6.4]   Douglas L. Jones, "IIR Filter Structures", [WWW] <URL: http://cnx.org/content/m11919/latest/ > (accessed on 21 Apr. 2008)

[6.5]   W. Amer, Q. Ahsan, R.I. Grosvenor, P.W. Prickett, "Machine tool signal analysis using sweeping filter technique", *In the proceeding of the 5th International Conference on Quality, Reliability, and Maintenance* (QRM 2004), Oxford, 2004, pp. 189-192.

[6.6]   "Digital Filter Design/Digital Filter Design Lite Product Overview", [WWW] < URL:http://ww1.microchip.com/downloads/en/DeviceDoc/01033B%2033.pdf > (accessed on 05 May. 2008)

Chapter 7

Depth of Cut Monitoring System

7.1. Introduction

Milling operations are almost always controlled by a computerized controller, with perhaps a supervisory role being played by a human operator. This leads to several operational problems, one of which is the potential for an unexpected cutting tool breakage, which may be due, among other reasons, to incorrect estimation of tool life. There are many modes of possible tool failure, from minor to catastrophic, and the response of the system to each mode may be further conditioned by the nature of the task being undertaken [7.1]. The situation is further clouded by the occurrence of numerous events within a normal machining cycle which can lead to symptoms, such as sudden increases in tool force, which may "fool" inadequate tool monitoring systems into incorrectly diagnosing a tool problem.

Tool wear monitoring and detection plays a critical role in guaranteeing an automatic cutting process [7.2]. Tool wear is found to have direct impact on the quality of the surface finish, dimensional precision and ultimately cost of the finished product [7.3]. Timely and accurate estimation of the tool life is critical. Over-estimation of tool life, results in degraded product quality and damaged parts (in the case of early tool breakage), while under-estimation leads to frequent stoppages (of the machining process) and increased cost of production [7.4]. Thus real-time tool life estimation is deemed to be the key to automated machining. It has been shown in section 3.5 that tool life and tool wear estimation required depth of cut (DOC) information to be known. This chapter describes development of a dsPIC microcontroller-based depth of cut monitoring system utilizing ultrasonic sensors. The sensors had been analysed for accuracy and resolution before being incorporated into the system. The developed system has been installed on milling machine and used for monitoring of DOC during machining tests.

7.2. Depth of Cut Measurement

Depth of cut is the perpendicular distance between the original (uncut) surface and final (cut) surface of the workpiece being milled. A depth of cut from 3 to 8 mm is common for roughing cuts and is less than 1.5 mm for finishing cuts [7.5]. Previously deployed monitoring systems to measure tool wear and tool life, have relied on an assuming a constant value of depth of cut (or have totally ignored it) [7.6]. True tool wear/life can only be sensibly estimated when the volume of metal removed is known; hence providing a measure of how much work has been done by the cutting tool during its lifetime. The volume V of metal removed can be calculated via equation 7.1, if the instantaneous depth of cut h_i is known.

$$V = \sum_{i=1}^{N} W \times \Delta L \times h_i \quad [\text{mm}^3] \tag{7.1}$$

$$\text{with} \quad \Delta L = \frac{feedrate}{60} \times T_{DOC} \quad [\text{mm}] \tag{7.2}$$

where

W is the width of the cut in mm (and is equal to tool diameter in slot milling operation)

feedrate   is amount of metal fed into the cutter in mm.min^{-1}

ΔL is metal fed into the cutter in mm for i^{th} increment (and is constant for constant feederate)

h_i is the measured DOC in mm for i^{th} instant in time and T_{DOC} is update interval in seconds.

Instantaneous DOC information can potentially be used as an extra input to a TCMS (for tool breakage detection). Otherwise, a change of DOC during machining results in changes in the cutting forces and the associated signal values may be mistaken as tool breakage cases, with false alarms being generated. If the object profile is known in advance it can be used to calculate the upcoming change in depth of cut and warn the TCMS so that it can compensate for the changes and adapt accordingly.

Collision detection can also potentially be performed if the object (workpiece) profile is measured. Then by detecting any approaching unusual change in object shape, the TCMS and machine tool controller can be warned and corrective action can be taken.

7.3. System Description

The system architecture as discussed in Chapter 4 is shown in Figure 7.1 with the integrated DOC monitoring system highlighted. A Signal Conditioning Board is used to isolate and condition the signal so that it can be fed to the PIC/dsPIC microcontroller based data acquisition and processing node, which forms the Front End Node (FEN) of the system. These nodes are connected to each other and to the Connectivity Node via CAN Bus Communications. In this architecture the DOC monitoring systems works in collaboration with other monitoring nodes, which exchange information to achieve increased reliability. It gets the required information such as feedrate and tool offset, from parameter monitoring node and provides predicted and calculated DOC information to other nodes.

* Other sensor is behind spindle housing in this view
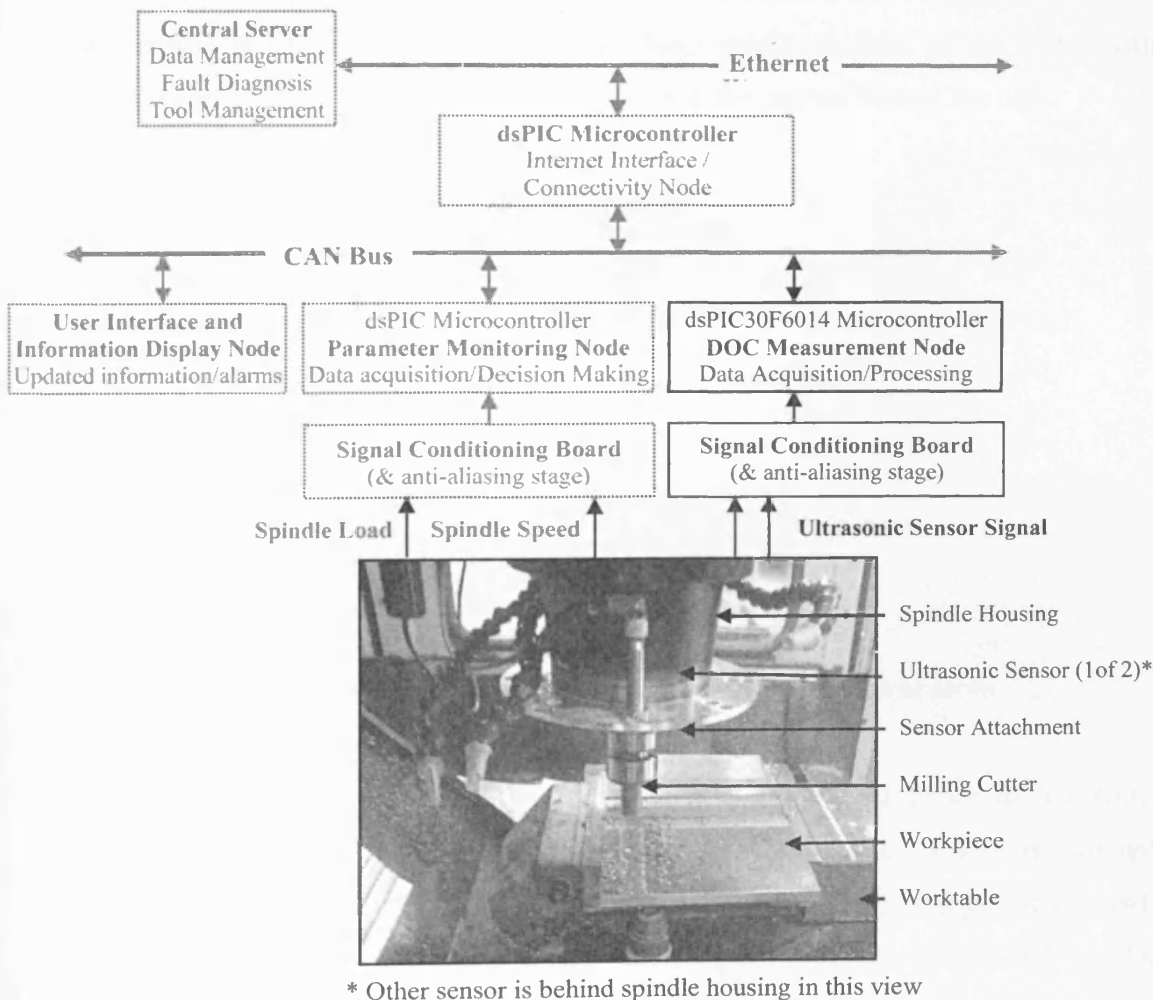
Figure 7.1: System Architecture - DOC Measurement System integrated into TCMS

The Internet Interface/Connectivity Node is connected to a central server via Ethernet. The central server hosts data management and tool management software. Earlier TCMS developed in IPMM centre utilized PIC microcontrollers to implement the Monitoring nodes [7.7]. In this research these have been replaced with dsPIC microcontroller, which offer more processing power. The feasibility of the dsPIC devices for e-Monitoring applications has previously been reported by Siddiqui et al. [7.8].

The developed DOC Measurement System utilized two ultrasonic analog distance sensors mounted on either side of the cutter as shown in Figure 7.2. Both sensors were attached to the spindle housing with a specially designed attachment ("Appendix D") which allowed the sensors to be mounted in different positions and configurations. One sensor (sensor1 in Figure 7.2) measured the object profile in front of the cutter path during machining whilst the second sensor measured the profile behind the cut.
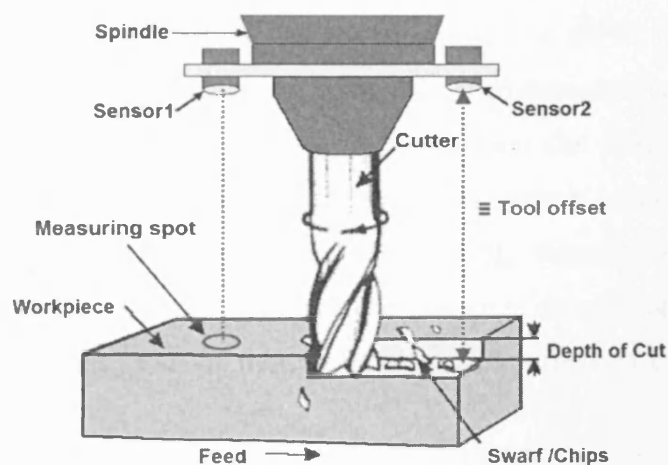
Figure 7.2: Measurement of DOC using two ultrasonic sensors

The sensors were connected to a signal conditioning board and hence to the ADC module of the dsPIC30F6014 microcontroller. The ADC was set to sample the voltage signals from the ultrasonic sensors at a rate of 50sps/channel (a throughput of 100sps). The ADC values were stored in memory from where they were accessed by the different data processing algorithms (discussed in section 7.8) to calculate the instantaneous DOC information. This information was communicated to the other nodes via the CAN bus. The different nodes of the TCMS then used this information in a variety of ways:-

- The tool breakage detection node adapts the various thresholds used in the wider system according to the DOC information, resulting in better detection performance and the avoidance of false alarms.

- The tool life/wear estimation system uses this information to calculate, in an on-going manner, the material volume removed. The cumulative work performed by the tool is then calculated and the residual tool life can be more accurately estimated.

- The object/workpiece profile information can be used for collision detection and avoidance of any accidental damage to the cutter and the machine tool it self.

The system is required to be aligned in the cutting direction. There are two options available to deal with this requirement; multiple sensors and an alignment device. The attachment assembly has been developed such that multiple sensors can be incorporated using the same microcontroller and intelligently processing the data and deciding which sensors are providing meaningful data at the moment. The dsPIC microcontroller can measure data from upto 16 sensors using the ADC. The other alternative, given the fact that the sensors are relatively expensive, is to develop the alignment device. This alignment device could be based upon intelligent interrogation of cutting axis data such that the sensor could align itself along the axis of cutting. Some research work has been carried out by the author in last stages of the research on utilization of feed motor currents for this purpose; detail of this preliminary assessment is given in "Appendix E".

7.4. Ultrasonic Sensors

Ultrasonic sensors are known for their robust performance in harsh and problematic environments where precise detection is essential. They are commonly used for a wide variety of non-contact presence, proximity, or distance measuring applications. The devices typically transmit a short burst of ultrasonic sound toward a target, which reflects back to the sensor. The system then measures the time for the echo to return to the sensor and computes the distance to the target using the speed of sound in the medium [7.9]. This sensing method ensures reliable operation regardless of the object's

color or opacity [7.10]. The sensors that were selected and evaluated for this research were as follows:

- PING)))™ Ultrasonic Sensor
- UNAM 12I9914/S14 Ultrasonic Analog sensor.

7.4.1 Ping Ultrasonic Sensor

Parallax's Ping ultrasonic sensor provides a low-cost and easy method of distance measurement and is often used in robotic applications. The ping sensor measures distance using an ultrasonic (40 KHz) pulse, transmitted from the unit and then distance-to-target time is determined. The processed output from the ping sensor is a variable-width pulse that corresponds to the distance to the target. A single (shared) I/O pin is used to trigger the Ping sensor and for the echo return pulse. The simple construction of the device is shown in Figure 7.3(a) and the required interface connections are shown in Figure 7.3(b). Other parameters from the technical specifications [7.11] for ping sensor are as follows:

- Measurement range : 2cm to 3m
- Supply voltage: 5V +/-10%
- Supply current: 30mA typical, 35mA maximum
- Power consumption: 20mA
- Input trigger: positive TTL pulse; 2 μsec minimum, 5μsec typical.
- Echo pulse: positive TTL pulse; 115 μs to 18.5 ms
- Echo hold-off: 750 μs from fall of Trigger pulse
- Size: 22 mm H×46 mm W×16 mm D (0.85" ×1.8"× 0.6")
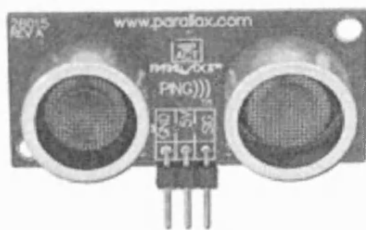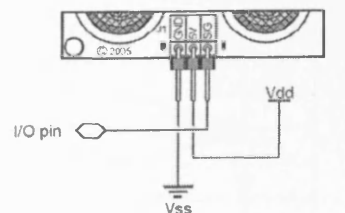
(a) Ping Sensor [7.12]   (b) Connection diagram [7.13]

Figure 7.3: Ping)))^{TM} Ultrasonic Sensor

7.4.2 UNAM 12I9914/S14 Ultrasonic Analog sensor

This sensor has a sensing range of 20-200mm with a stated resolution of <0.3mm which can be improved by selecting a smaller measuring range with the external (Ext) Teach-in facility provided in the sensor (as explained later in section 7.4.3). It has a sonic frequency of 380 KHz and response time of less than 30msec. It requires a supply voltage of 15-30V DC and its output is a 0-10mA signal, which was converted into a 0-5V signal (by adding a load resistor of 500Ω) in this research in order to interface with the dsPIC microcontroller. This sensor and its connection diagram are shown in Figure 7.4.
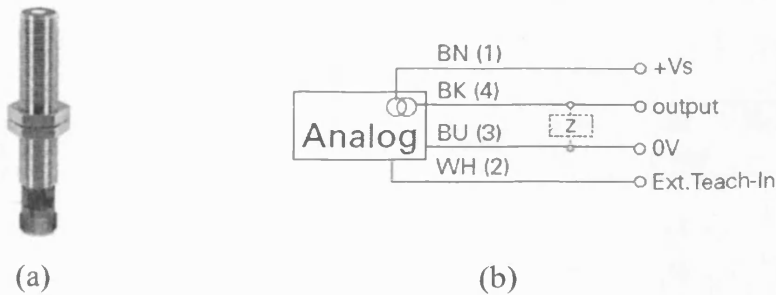
Figure 7.4: (a) Ultrasonic Analog Sensor, (b) Connection diagram [7.14]

It has narrow beam angle (6°) which provides a relatively small foot print (area covered by the beam on striking the object). For typical distance (as used in this research) of 110mm the foot print is only 11.5mm in diameter. It has a narrow sonic cone profile, as shown in Figure 7.5, which makes the sensors capable of reliably measuring the distance in restricted spaces. Thus the sensor can be mounted very close to the cutting tool to measure the DOC. According to the manufacturer this sensor can be used as an alternative to optical distance sensors [7.15].
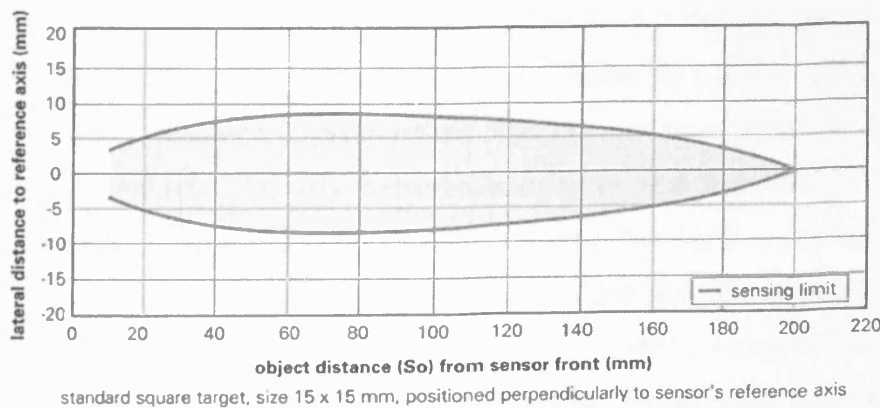
Figure 7.5: Sonic cone profile of the ultrasonic analog sensor [7.16]

7.4.3 UNAM Sensor Resolution Improvement

As mentioned earlier sensor's resolution can be improved with the help of External Teach-in facility provided in the sensor. With this facility, end limit (*Sde*) and close limit (*Sdc*) of sensor's measuring range, $Sd = Sde - Sdc$, can be selected between 20-200mm. To do this, the teach-in input of the sensor is set to high for a specified interval and sensor enters in the teach-in mode. After placing an object at *Sdc*, teach-in input is set to high again and sensor registers the measured distance as *Sdc* value. Then value *Sde* is set in the same way. Default values for *Sdc* and *Sde* are 20 and 200 respectively. Different values of *Sdc* and *Sde* are mapped to minimum and maximum level of the output as shown in the Figure 7.6 and output range (hence measuring range *Sd*) is divided into a constant number of intervals.

Case	Sd (mm)	Resolution (mm)
a	18	0.03
b	36	0.06
c	54	0.09
d	72	0.12
e	90	0.15
f	108	0.18
g	180	0.30
h	18	0.03

(a)   (b)
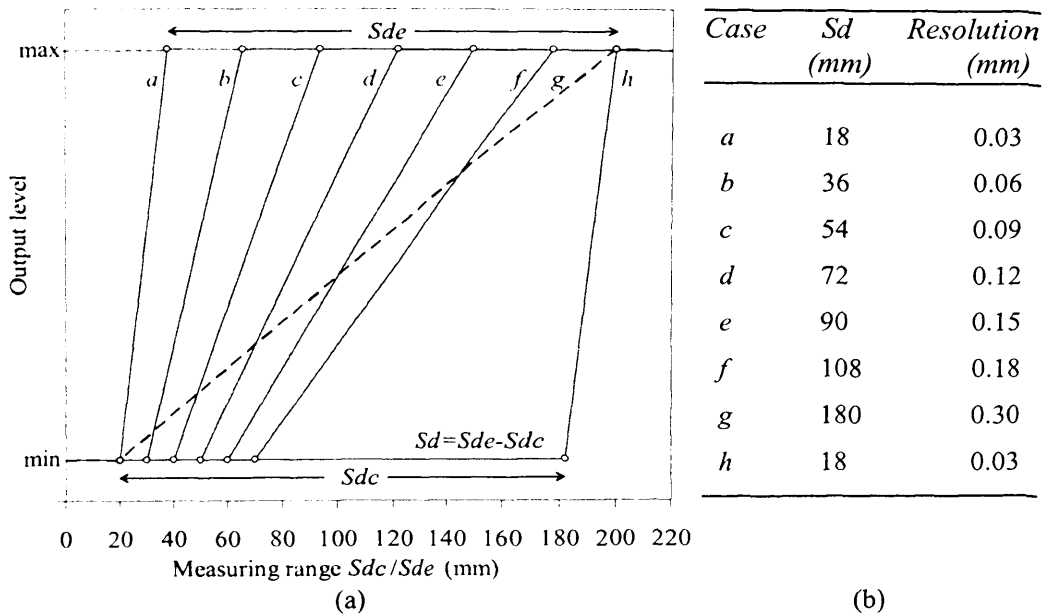
Figure 7.6: (a) Sensor response and (b) resolution for different values *Sd*

For example, in case g of Figure 7.6(a), *Sde* and *Sdc* have default values. The sensor's output is at minimum level for measured distances smaller than *Sdc* and is at maximum level when measured distance is greater than *Sde*. For distances between *Sdc* and *Sde* the sensor's output varies linearly between minimum and maximum level with a resolution, which is less/better than $0.3 \times Sd / 180\,mm$. Similarly cases *a-h* of Figure 7.6(a), show several scenarios with selected values of *Sde* and *Sdc* to provide different values of *Sd* and resolution (as tabulated in the Figure 7.6(b)), which is proportional to the measuring range. Thus resolution can be improved by carefully selecting the *Sde* and *Sdc* which in turn determine the measuring range.

168

Both sensors were accessed for accuracy, resolution and linearity. During this testing sensors were connected via a conditioning board to the dsPIC microcontroller (hosted on a dsPICDEM1.1 General purpose development board). Appropriate software was written and deployed on the dsPIC, such that the distance measurements were communicated back to a PC. Data was stored in CSV file format suitable for import to Excel and/or Matlab for off-line data analysis.

7.5.   PING)))^{TM} Ultrasonic Sensor

7.5.1   System Operation

As stated, the ping sensor detects objects by emitting a short ultrasonic burst and then "listening" for the echo. Figure 7.7(a) shows the sensor operation and associated signals during communication with sensor while Figure 7.7(b) shows operational and communication parameters which were considered during software design. A trigger pulse (duration $t_{OUT} = 5\mu sec$) was sent from the dsPIC via a digital I/O line configured as an output. After sending the trigger, the dsPIC reconfigured the same I/O pin an input. The input capture module (as discussed in Chapter 4) then obtained the characteristics of the sensor's output pulse, with the width (t_{IN}) of this pulse corresponding to the distance to the target.
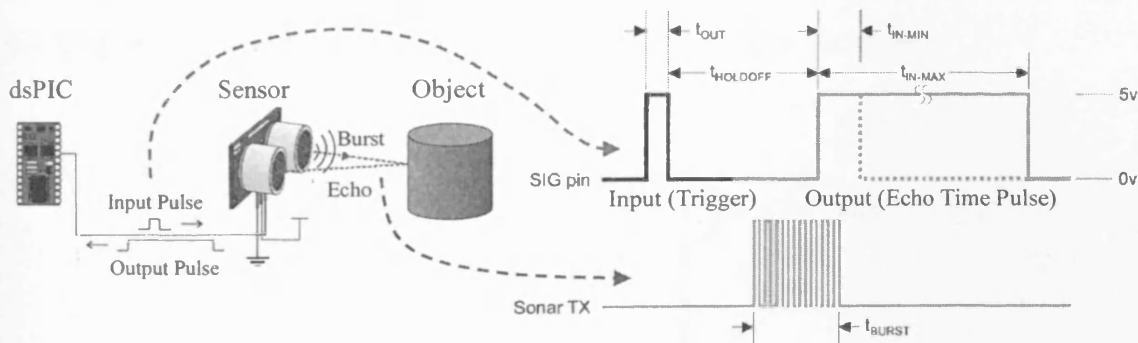
(a) Sensor connections, operation and associated signals

	Host Device	Input Trigger Pulse	t_{OUT}	2 µs (min), 5 µs typical
	PING))) Sensor	Echo Holdoff	$t_{HOLDOFF}$	750 µs
		Burst Frequency	t_{BURST}	200 µs @ 40 kHz
		Echo Return Pulse Minimum	t_{IN-MIN}	115 µs
		Echo Return Pulse Maximum	t_{IN-MAX}	18.5 ms
		Delay before next measurement		200 µs

(b) Communication and operation parameters

Figure 7.7: Ping sensor operation for distance measurement [7.13]

169

In particular input capture reads Timer values (TMR_{RISE} and TMR_{FALL}) on the rising and falling edge of the output pulse from sensor and calculates the time lapse t_{IN} according to equation 7.3.

$$t_{IN} = \frac{TMR_{FALL} - TMR_{RISE}}{F_{cy}} \quad [\text{sec}] \quad (7.3)$$

where F_{cy} is the dsPIC system clock frequency.

Object distance from the sensor is calculated according to equation 7.4 and 7.5.

$$Distance = \frac{t_{IN}}{2} C_{air} \quad [\text{m}] \quad (7.4)$$

where C_{air} is speed of sound in air which can be calculated according to equation 7.3 [7.13]. Speed of sound at ambient/ room temperature T_C (which is assumed to $20^{o}C$) is 343.5 m/s.

$$C_{air} = 331.5 + (0.6 \times T_C) \quad [\text{ms}^{-1}] \quad (7.5)$$

7.5.2 Analysis

A test setup as shown in Figure 7.8 was used for testing the sensor's resolution and linearity. Different metric slip gauges, in combination with a calibrated dial gauge setting, were used to provide a range of known distances between the sensor and a flat (and sufficiently sized) metal target. For these tests the range of sensor-to-target distances was 45-155mm with results being obtained at 1mm increments
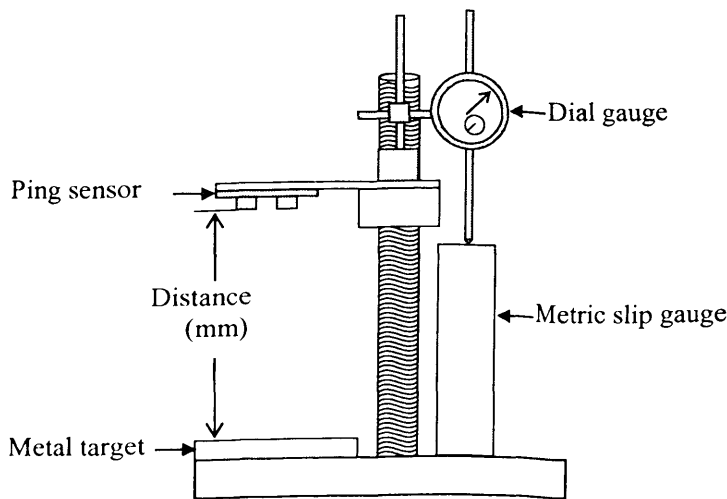
Figure 7.8: Test setup

At each distance setting, 100 measurements were obtained and recorded on the PC. The results of subsequent analysis are shown in Figure 7.9. The resolution of the sensor was found to be less than 6 mm.

(a) Measured distance

(b) Measuring Error
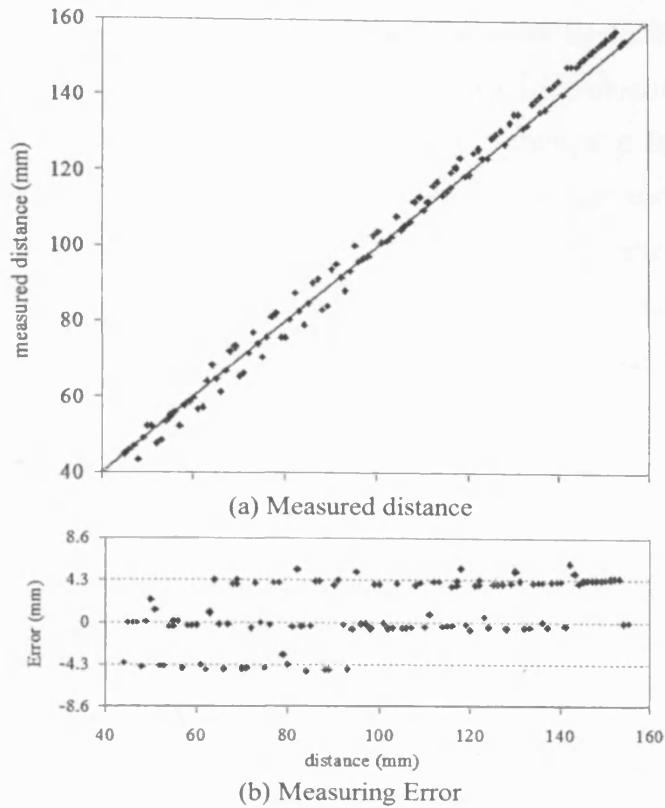
Figure 7.9: Resolution test for PING Sensor

The test described above was performed twice for each of the two Ping sensors and the responses were compared as shown in Figure 7.10. The result showed that the individual sensor responses were different from each other, but both sensors showed a similar degree of repeatability. This means that each sensor has different characteristics which need to be determined before incorporating them into the monitoring system.
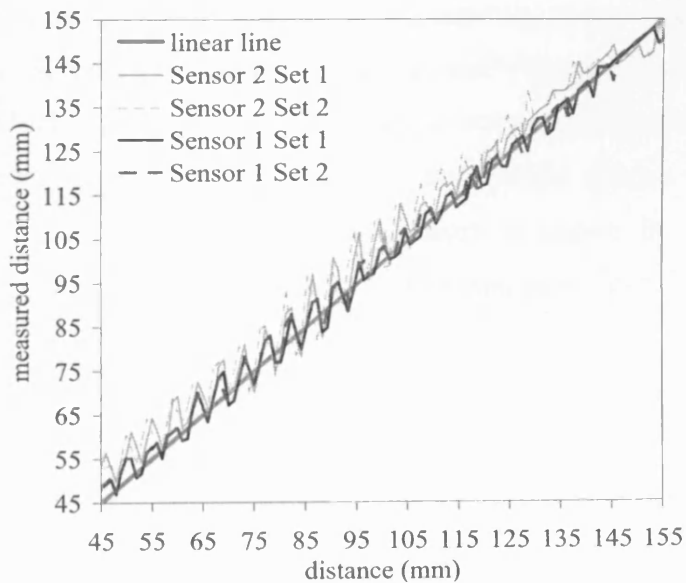
Figure 7.10: Comparison of two sensors

In next test two sensors were used to measure the simulated DOC varying from 9-19mm. The sensors were calibrated to allow for their individual characteristics. Two flat surfaces offset by predefined height (simulating a change in DOC) were used side by side. Each sensor measured the resulting change in height and the difference was calculated. The results in Figure 7.11 show the measured difference. On investigations it was determined that the identified DOCs were grouped on one of the three linear lines which are separated by λ/2 where λ is the wavelength of the 40 KHz ultrasonic is burst transmitted.

$$\lambda = C_{air}/f_{burst}$$
$$= 343.5ms^{-1} / 40\ Khz$$
$$= 8.58\ mm$$
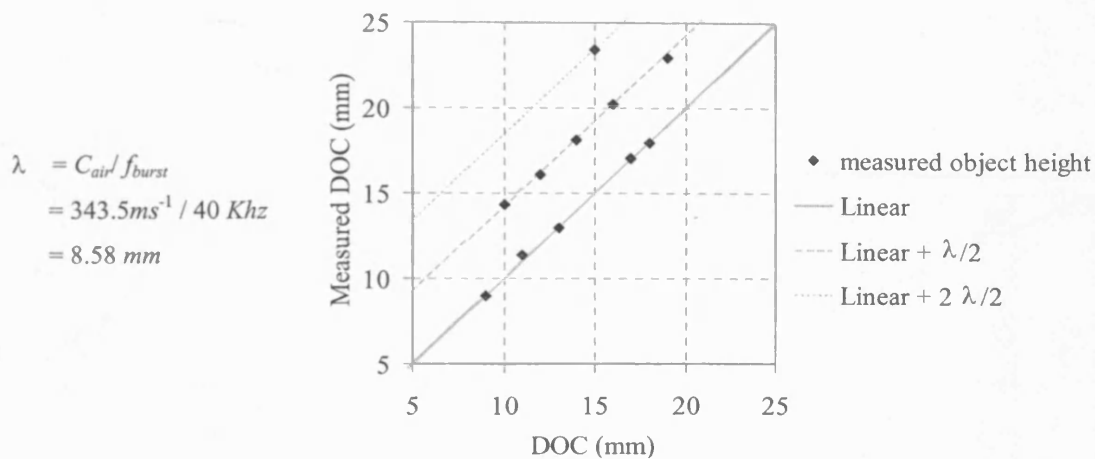
Figure 7.11: Simulated DOC (object height) measurement

This sensor was considered for this application because of its low cost and easy controllability from microcontroller. Because of low cost sensor it was decided that eight sensors will be used with the aim to enable the DOC monitoring in any direction, without the need for aligning the sensors, by intelligently processing the data from all eight sensors. Eight sensors were mounted on a specially designed attachment assembly ("Appendix D") which was then attached to spindle housing of the milling machine and the sensor response was measured by moving the spindle (hence sensors) in 1mm increments. The response of the best three sensors is shown in Figure 7.12. The remaining five sensors have response similar to the responses shown in Figure 7.10.

The selected sensors' responses, shown in Figure 7.12(a), have large measuring errors in the shaded (red) area. There were two ranges, 100-130mm and 155-200mm, where error was relatively small. One of these measuring zones (155-200mm) was further analyzed, by calibrating the sensor response through linear regression and deploying a correction factor. This is shown in Figure 7.12(b) with the calculated errors shown in

172

more detail in Figure 7.12(c). It was apparent that even within the selected range there were error zones (shaded areas in Figure 7.12(c)) of 3 to 4mm. Any measuring error greater than 0.5 mm was deemed to be unacceptable for the DOC monitoring System. There were some segments typical of 7 to 9mm range, which could potentially be used as safe ranges. Based on the test results it was concluded that this sensor could not meet the system requirements and was thus deemed to be unsuitable for the DOC monitoring application.
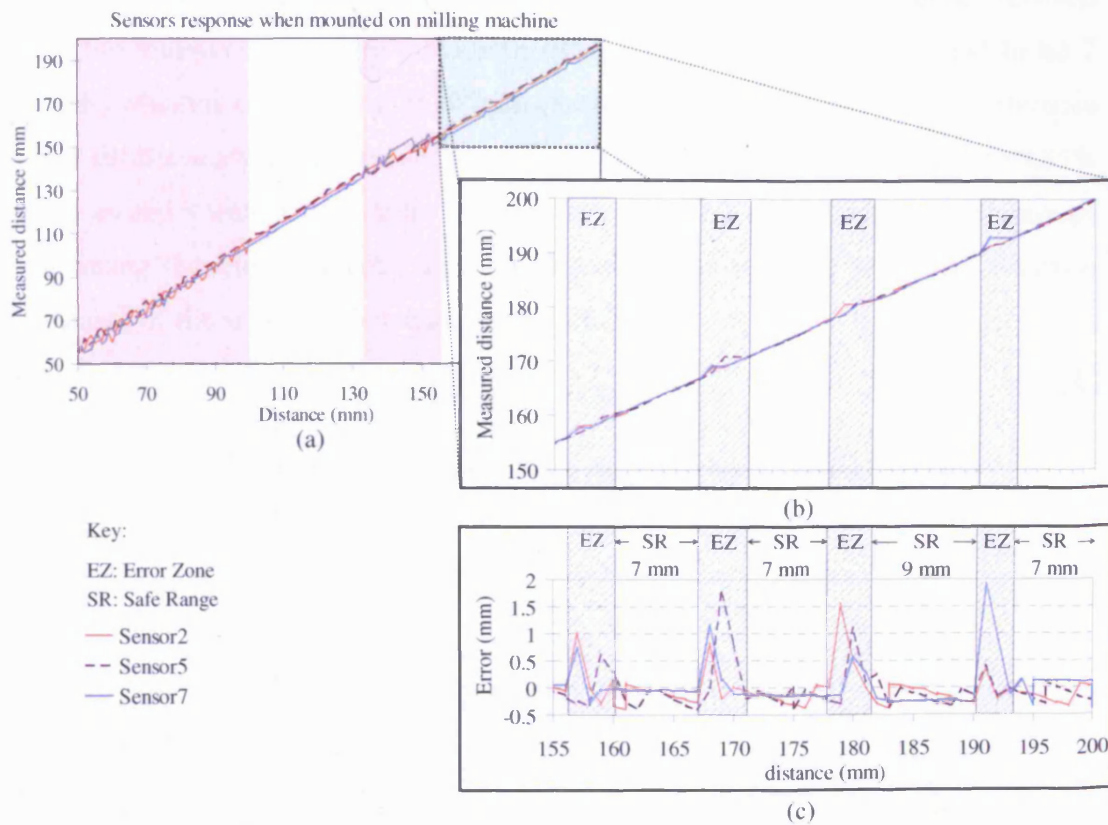
Figure: 7.12 (a) Sensor Response on milling machine (b) Calibrated Response for 155-200mm range (c) Measuring Error after calibrating sensors' response

7.6 UNAM 12I9914/S14 Ultrasonic Analog sensor

7.6.1 System Operation

The sensor's output was converted into 0-5 volts at the conditioning stage and ADC was used to measure the analog voltage. Test software was deployed on the dsPIC microcontroller. ADC measured the voltage which was communicated back to PC. Data was analyzed for various stated parameters.

7.6.2 Sensor Resolution

Resolution is the most basic requirement for this application. It is impossible to measure to an accuracy smaller than the resolution [7.17]. The resolution corresponds to the smallest possible distance change which causes a detectable change to the output signal [7.18]. For the resolution test, the sensor was connected to a test rig where a 25mm×20mm metal object was moved at constant speed towards the sensor and then moved away. Data was collected at 200sps. Figure 7.13(a) shows the data acquired during this test. The bar chart in Figure 7.13(b) shows the difference between consecutive measurements. The maximum difference (resolution) was found to be 7 ADC units which is equivalent to 0.307mm (according to equation 7.4). The difference data was further analyzed and results showed that resolution was <0.27 mm for 99.85% of the cases and it was <0.21 mm for 99% of the cases. This resolution can be improved by narrowing the measurement range by choosing *Sde* and *Sdc* with Ext Teach-in functionality of the sensor as discussed in section 7.4.3

$$d = \frac{ADCValue}{2^{12}} \times (Sde - Sdc) \tag{7.6}$$

where *Sde* is end limit of measuring range (maximum distance) = 200mm

Sdc is close limit of measuring range (minimum distance) = 20mm

(a) Acquired data for resolution analysis

(b) Difference between consecutive samples
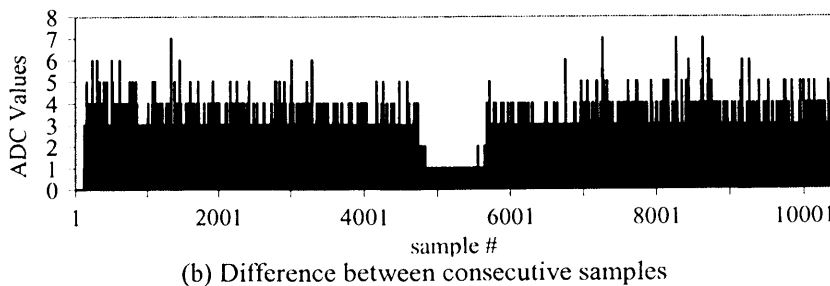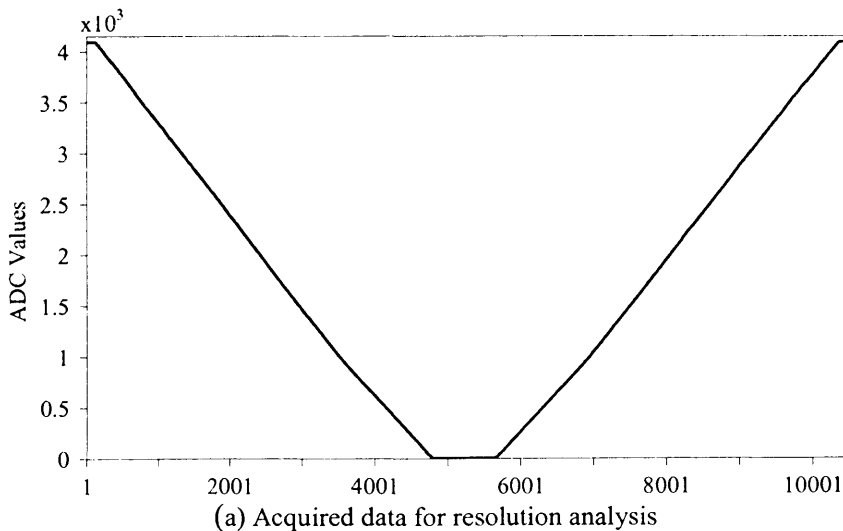
Figure 7.13: Sensor resolution analysis

7.6.3 Linearity

The output from a displacement sensor is proportional to the measuring distance and is shown as an almost perfect straight line. Linearity means the range of deviation from the ideal line [7.17]. It is given as a percentage of the upper-limit of the measuring range i.e. Full Scale (FS.) [7.18]. For this test a 25mm×25mm metal object was placed at measured distances with 1mm increments. A dial gauge, in conjunction with metric slips (Figure 7.8), was used to measure the actual distance. Output voltage was measured with a voltmeter and converted into the measured distance. The measured distance plotted against actual distance is shown in Figure 7.14(a). Measuring Error is plotted against the actual distance in Figure 7.14(b). The measuring error (which is measure of linearity) was less than ±0.2% of FS.
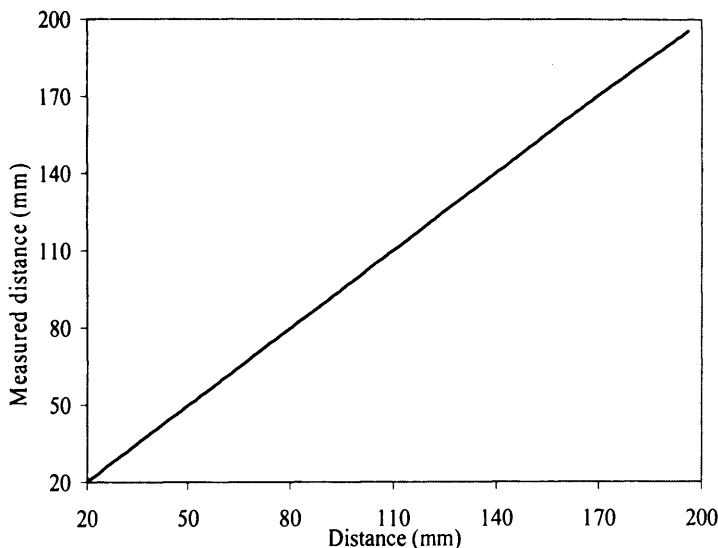
(a) Measured Distance
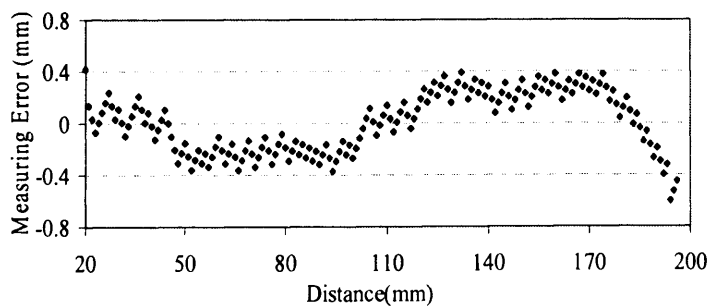
(b) Measuring Error

Figure 7.14: Linearity Analysis

The resolution and linearity tests were performed twice for two sensors and matching results were obtained. Both sensors showed identical response with high degree of repeatability.

175

Following the promising results of these initial tests the sensors were subjected to further machining process based experiments.

7.6.4 Gap and Hole Measurement

The purpose of this test was to investigate the minimum amount of gap/inclusion which can be detected by the sensor. An object with various gaps was created by placing the metal pieces such that seven gaps with gap widths of between 1 and 7mm were created. This object was put on a moving platform and passed underneath the ultrasonic sensor at a constant speed. The object profile was measured by the sensor and data was communicated back to PC. The acquired profile is shown in Figure 7.15. The location and their relative widths are overlayed to identify the sensors' response to various gap sizes. Analysis show that 1 and 2mm gaps were not detected by the sensor, where as 3 and 4mm gaps were detected but the difference in measured height was very small and of the order of sensor resolution. Gap sizes of 5mm and greater widths were detected with confidence.
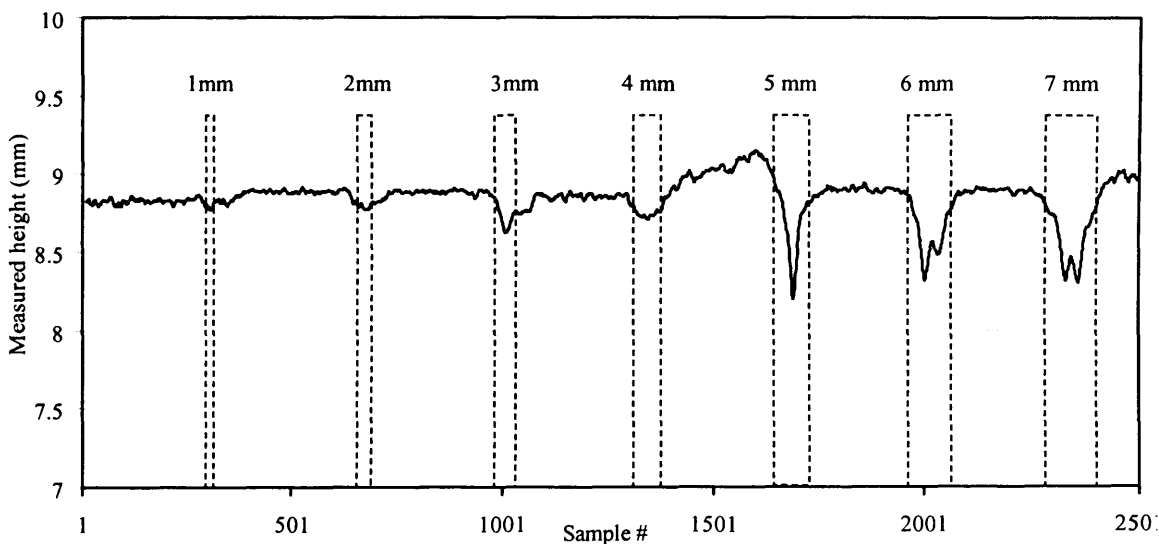
Figure7.15: Gap Measurement

Another test was carried out to measure a hole of 10mm diameter and the sensor was able to detect the location of the hole. This test shows the capability of the sensor to detect hole like features and slots in the workpiece during milling operations. The sensors were thus deemed to have features that could be integrated into the milling cutting monitoring system being developed. Some additional sensor analysis tests are given in "Appendix F".

7.7. System Operation

The ultrasonic sensors provide 0-10mA current signal proportional to the measured distance. This signal was converted to 0-5V and interfaced with ADC of the dsPIC microcontroller using two analog pins. The ADC module was configured to capture the data from both pins at a fixed sampling rate. Figure 7.16 shows the software model of the developed system. Although there is only one ADC module in the dsPIC, it can capture signals from up to 16 inputs. Therefore it could be configured to provide an ADC block for each input. Data for both sensors is processed according to the block diagram shown in Figure 7.16. The algorithms developed will be discussed in next section. Spike removal and block average is applied to both sensors' data. In the subsequent discussion, the sensor in front of the cutter will be referred as sensor 1 and sensor behind the cutter as sensor 2. Since sensor 1 measures the object profile before the cutting, the predicted DOC is calculated utilizing the sensor 1 data and tool offset information and communicated over CAN bus.
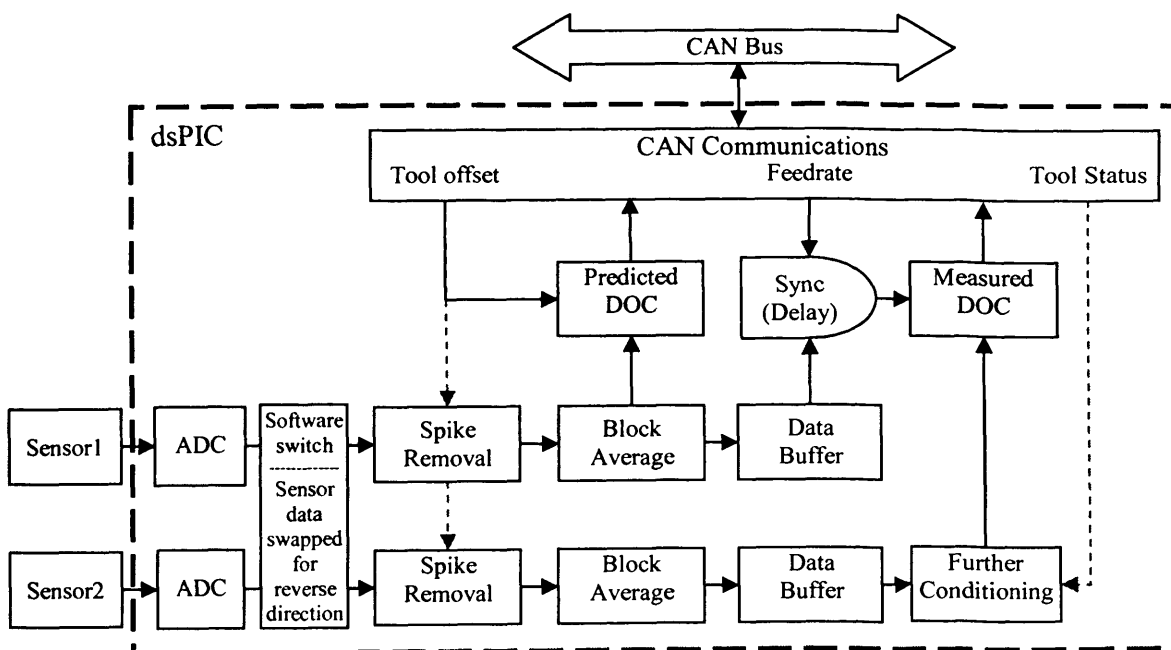
Figure 7.16: Software model of the DOC monitoring System

Data is buffered for subsequent analysis and DOC calculations as the workpiece is being machined. For this purpose Sensor 1 data is delayed by using a synchronization algorithm taking into account the feedrate information provided by parameter monitoring node. Sensor 2 data is further conditioned using the fact that cutting has

actually been carried out, and is combined with synchronized sensor 1 data to calculate the measured DOC. The result is also communicated over the CAN bus. Information relating to the actual cutting operation such as feedrate, tool offset and cutting direction are communicated to the FEN and it transmits the DOC information which is used by other nodes for tool condition monitoring. The next section provides the details of the signal processing algorithms developed for the DOC monitoring system.

7.8. Signal Processing Algorithms

The algorithms were tested for effectiveness on a PC before deployment on the dsPIC microcontroller. The realization of these algorithms for real-time performance was made possible by the DSP features of dsPIC as discussed in Chapter 4.

7.8.1. Moving Average Filter

Let $x(m)$ be the input signal, h(k), $0 \leq k < K$ be the coefficients of FIR low pass filter and $y(m)$ be the output filtered signal then

$$y(m) = \sum_{k=0}^{K-1} h(k) \cdot x(m-k) \qquad (7.7)$$

For the moving average filter (the simplest form of FIR Filter) all filter coefficients are set equal to $1/K$ i.e.

$$h(k) = 1/K, 0 \leq k < K \qquad (7.8)$$

By substituting equation 7.8 in 7.7:

$$y(m) = \frac{1}{K} \sum_{k=0}^{K-1} x(m-k) \qquad (7.9)$$

Figure 7.16 shows the results of a 20 point moving average filter applied to the raw sensor data. Two sensors were attached to spindle housing as shown in Figure 7.2 and the profile of a flat workpiece was measured by feeding the workpiece without any cutting. The unfiltered signal (Figure 7.17(a)) shows some noise in measurement which may be due the machine vibrations. This assumption is based on the static laboratory tests where sensors showed no such variations. The output filtered signal (Figure 7.17(b) shows that the noise has been removed by the application of moving average filter.
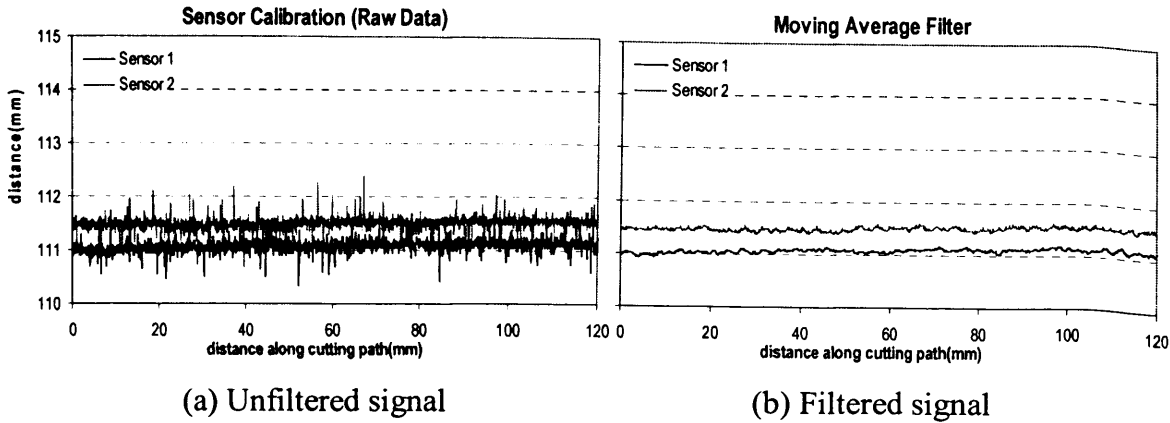
| (a) Unfiltered signal | (b) Filtered signal |

Figure 7.17: Moving Average Filter (K=20)

7.8.2. Block Average

In this algorithm the decimation and moving average algorithms are combined. Decimation is a process of reducing the sampling rate of a signal [7.19]. A moving average filter replaces the low pass filter according to equation 7.8. Let $x(m)$ be the input signal sampled at f_s, the output signal after the decimation be $y(r)$ where the sampling rate f_m is reduced by a factor M i.e. $f_m = f_s / M$ then

$$y(r) = \frac{1}{K}\sum_{k=0}^{K-1} x(rM - k)$$ (7.10)

Thus the operations of decimation/down-sampling and the moving average filter have been embedded in such a way that the moving average filter is operating at the reduced data rate and the average number of computations to generate one output sample is reduced by factor M. The division operation is optimized and replaced by a n-bit shift operation by making $K=2^n$. If K=32 we can shift 5 bits right to divide the sum by K.

This algorithm is used to reduce the data and to remove the effect of noise in the sensor data. The sampling rate of 2sps is deemed sufficient for DOC information where as the sensor itself is capable of updating information at a rate greater than 33sps. Thus if we sample the sensor output at 64sps and do the block average with M=32 and $K \geq M$ sampling rate of 2sps can be achieved while reducing the noise by square root of M [7.20] or about 5.7 (-15dB) in this case.

179

7.8.3. Sensor Data Synchronization

The two sensors were mounted on the machine as shown in Figure 7.2. They were separated by a distance D. This effectively meant that there was a lag of distance D from sensor 1 in sensor 2 data. To calculate the DOC, sensor 1 data needs to be synchronized with sensor 2 data. For this purpose a time shifting technique was utilized.

Let $x_1(r)$, $x_2(r)$ be the distance signals from sensor 1 and sensor 2 respectively sampled at a sampling rate of f_m after block average, the separation between sensors D and $y_1(r)$, $y_2(r)$ be the output signals after synchronization then:

$$\left.\begin{array}{l} y_1(r) = x_1(r - N) \\ y_2(r) = x_2(r) \end{array}\right\}$$

(7.11)

where N is number of samples representing the separation between sensors and is dependent on *feedrate*.

$$N = \frac{60 \cdot D \cdot f_m}{feedrate}$$

(7.12)

7.8.4. Spike Detection & Removal

A noise spike is a single point that deviates from the preceding and following values by a large amount. Noise spikes can seriously bias the calculations of any of the basic statistical properties of a time series if they are not identified and removed.

The simplest method to remove spikes is to clip the trace to fall within an interval defined by upper and lower bounds. An adaptive upper bound method is used to remove the spikes from the sensor 2 data according to the following condition.

$$y_2 = \begin{cases} tool\_offset & if & x_2 > tool\_offset & \& \\ & & x_2 \geq (x_1 + calibration\_factor) \\ x_2 & otherwise \end{cases}$$

(7.13)

Fundamental premise for this condition is the fact that if the cutter is cutting, the distance can not be greater than the tool offset. Tool offset information is only valid once the cutting has been performed. Therefore this algorithm can only be applied to sensor 2 data because of its dependence on tool offset information.

A more sophisticated algorithm was utilized to remove the spikes from for sensor 1 data. This algorithm works as following [derived from [7.21]:-

- Let $x(i)$ be the current point of input signal and let first difference of x at point i be

$$diff(i) = x(i) - x(i-1) \qquad (7.14)$$

- Calculate the first difference of the points in window length of n to both left and right of the current point i.e. for range [i-n,i-1] and [i+1,i+n]

- Determine the absolute median first difference in each window

$$mal = |Median(diff(i-n):diff(i-1))| \qquad (7.15)$$

$$mar = |Median(diff(i+1):diff(i+n))| \qquad (7.16)$$

- Calculate difference between current point and points immediate left and right of current point [$diff(i)$, $diff(i+1)$]

- Calculate the output according to equation below

$$y(i) = \begin{cases} y(i-1) & if & |diff(i)| > q \times mal & \& \\ & & |diff(i+1)| > q \times mar & \& \\ & & diff(i) \times diff(i+1) < 0 \\ x(i) & otherwise \end{cases} \qquad (7.17)$$

where q is multiplier for maximum expected change and its typical value is 3-5

The latter algorithm was applied to the sensor data which measured the object profile at the edge of the workpiece. The raw data (top-left plot of Figure 7.18) shows the spikes present in the data. The centre-left plot shows the output after spikes have been removed and bottom-left plot shows output of the moving average filter applied to the raw data and the spikes removed data. All four signals are shown together on right hand plot. The spike removal algorithm has removed the localized variations in the data which would have been created by the moving average filter if the spikes were not removed.
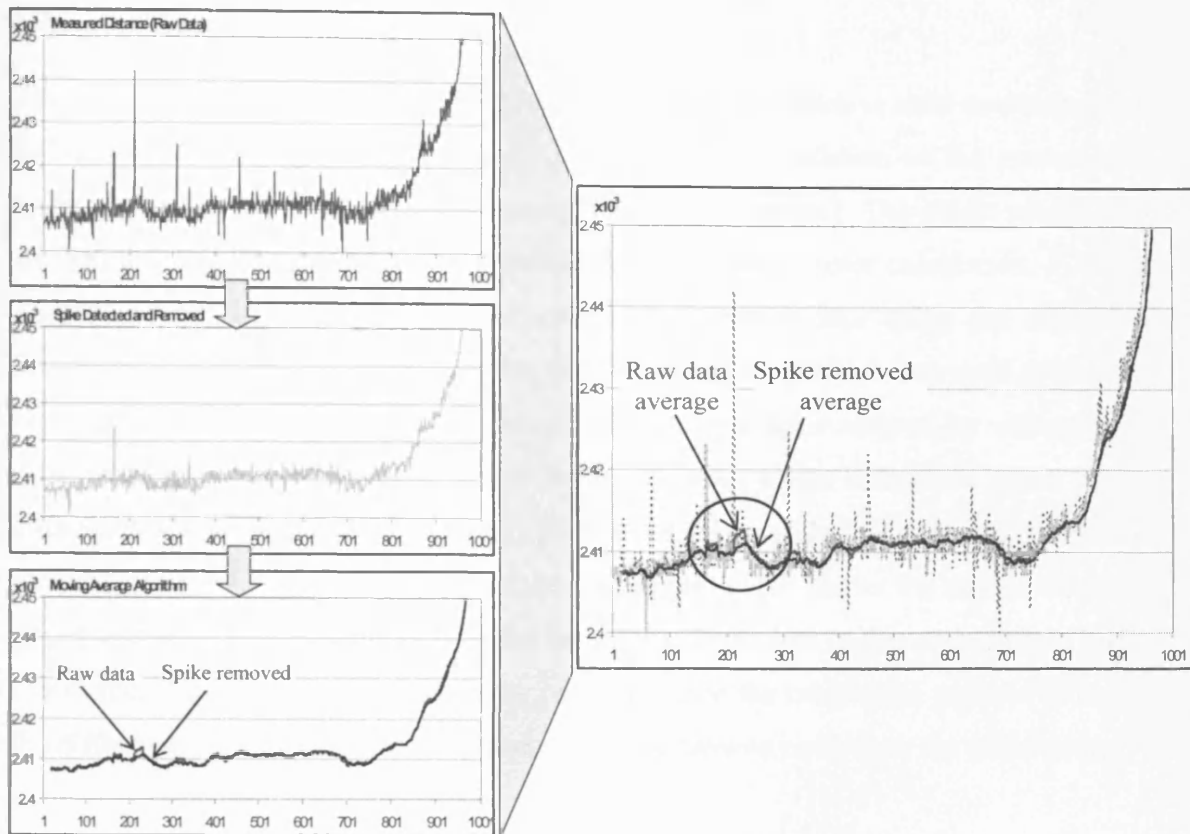
Figure 7.18: Spike removal and moving average algorithm

7.9.   Machining Tests

As described earlier, the two sensors were attached to milling machine spindle using a specially designed attachment assembly as shown in Figure 7.2. This arrangement allowed one sensor to measure the object profile in front of the cutter and other sensor to measure behind the cutter. Before any sensible measurements could be taken, it was necessary to ascertain that both sensors were calibrated to provide the same measurement for a particular distance. Analysis of the sensors showed that sensor response remained same for different sensor units. The main area of concern was the difference in the sensors' height during installation to the spindle housing via the attachment assembly. To make the installation process easy and error free, this difference was compensated for in the software by performing a calibration test after each installation. The calibration process did not require any cutting to be performed and any available workpiece could be used for calibration.

182

7.9.1. Calibration Test

This test was designed to calculate the calibration factor which is used to compensate for the difference in sensor position in z-plane. After installation of the sensors, the work piece was moved under the sensors at a constant feed rate. The object profile was measured with both sensors and processed for calibration factor calculation. For this purpose sensor 1 data was synchronized with sensor 2 data using the algorithm described in section 7.8.3. After this the moving average algorithm was used to remove noise from the signal and the difference between profiles measured by sensors was calculated. The calibration factor is the statistical mean of the difference signal where difference is less than certain threshold (2.0mm in this application). This factor is used for calibrating the sensor output for future tests. Figure 7.19 shows the signals acquired and processed for calibration factor calculation which is -0.41 in this case. Figure 7.19b shows that the object was not perfectly leveled. Since the calibration process relies on the difference signal, the workpiece shape will not have any effect on the calibration.

(a) Raw data   (b) Processed data & calibration factor
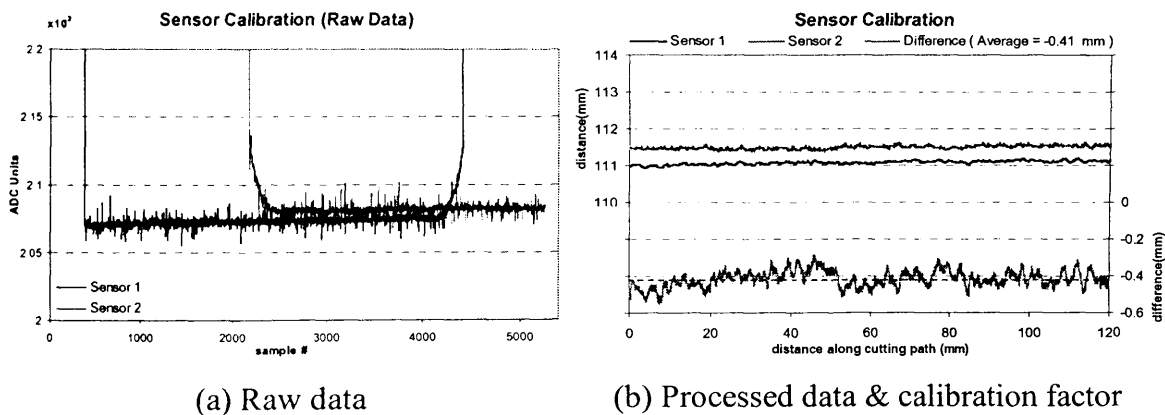
Figure 7.19: Sensor Calibration (Test 1)

Figure 7.20 shows the results of a calibration test carried out with a workpiece having two slots of 20mm $\times$ 2.2mm size each, which were orthogonal to the cutting path. These slots were cut to simulate the change in depth of cut while cutting tests described in section 7.10. The object profiles calculated by sensors (Figure 7.20(a)) show the slots detected at different times because of the physical separation between the sensors. This separation was catered for by synchronization algorithm and Figure 7.20 shows the synchronized profiles where the slots detected by both sensors coincided. This again

shows the flexibility of the system calibration process which does not require any special experiment. The calibration factor calculated in this test was -0.15mm.
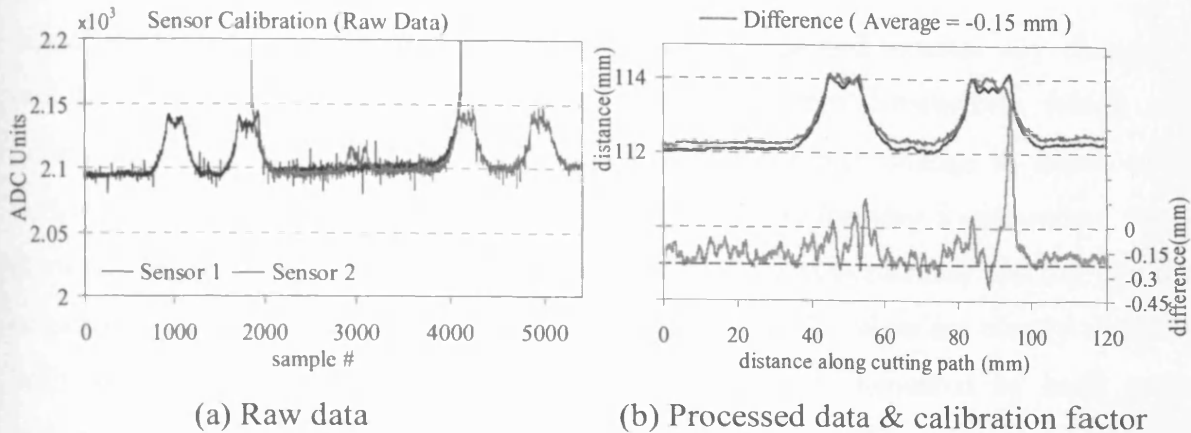

(a) Raw data   (b) Processed data & calibration factor

Figure 7.20: Sensor Calibration (Test 2)

7.9.2   Height Measurement Test

This test was performed to ascertain the linearity of the sensors while mounted on the machine. A number of distance measurement sets were recorded at different values of z (spindle height) by feeding the flat workpiece. First measurement was taken at an arbitrary value of z. Subsequent measurement sets were recorded for z+1mm, z+2mm, z+5mm, z+10mm and z+15mm. Sensor data was calibrated using the calibrating factor calculated earlier. The measurement sets are plotted in Figure 7.21 show that the sensors have measured the distance with an accuracy indicated by the measurement error which was less than <0.1mm. These results show the linear behavior of the sensors, which was required for DOC monitoring System.

(a) Measurement with Sensor 1   (b) Measurement with Sensor 2
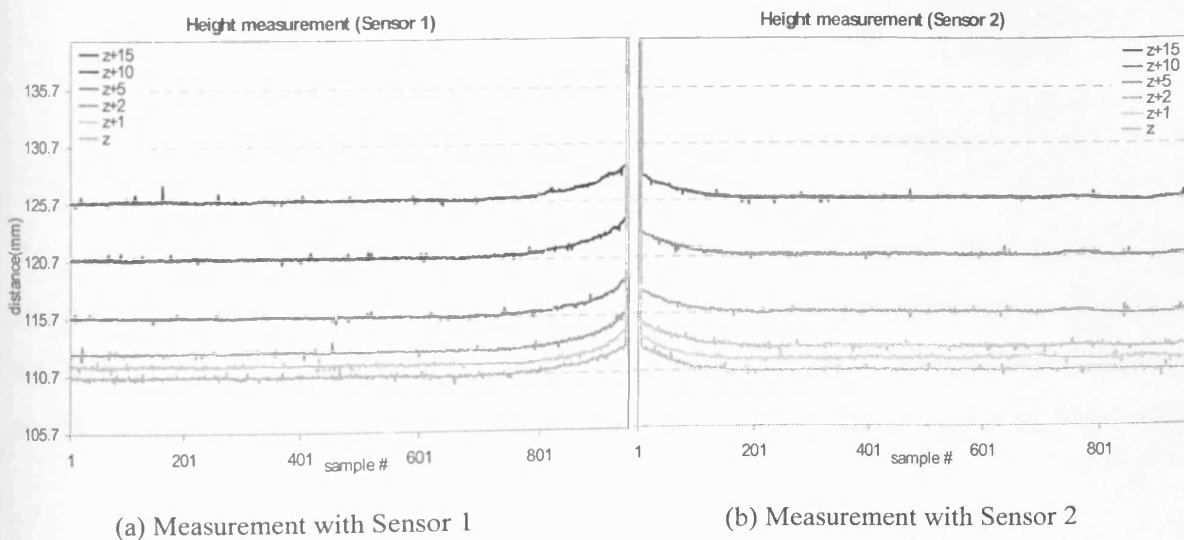
(which was 110.8mm) information is used for the calculation of the DOC. The processed data is shown in Figure 7.23.

The results show the DOC measured by system to be decreasing along the cutting axis. This was subsequently found to be due to the workpiece surface not being perfectly level. There was small slope along the cutting path, which was be confirmed by the object profile measured by sensor 1 before cutting and the DOC measured offline (with a micrometer) shown in Figure 7.23. The developed system was thus able to accurately measure the DOC online within an acceptable tolerance. The resolution was greatly improved (<1mm) with the deployment of different signal processing algorithms.
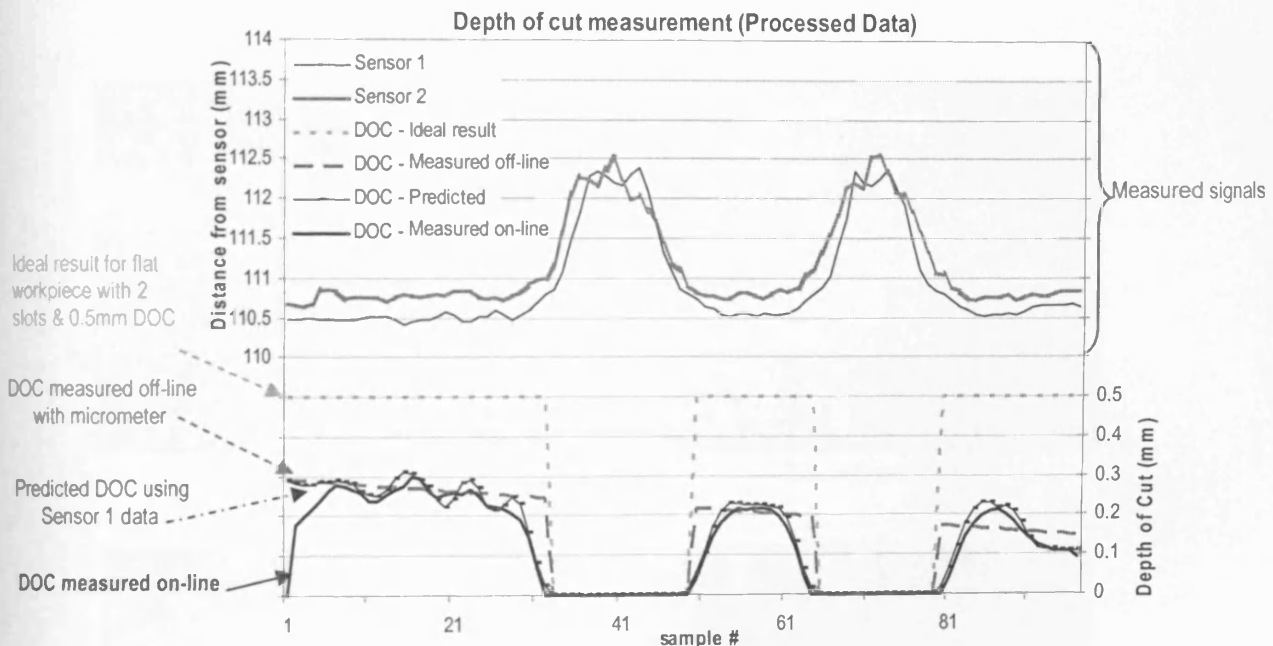
Figure 7.23: Processed data and calculated depth of cut

It not only measured the DOC with sufficient accuracy but also, for the particular test reported, revealed the slope in the workpiece and the slots present in the cutting path. This revealed that the work piece was not set perfectly flat. If this happened during the machining of an actual component it would decrease the dimensional accuracy and in some cases rendered the part useless. In this way the system has shown the potential of monitoring the correct setting of the workpiece. Similarly by monitoring the slots it had enabled the avoidance of false alarms which could have been generated because of
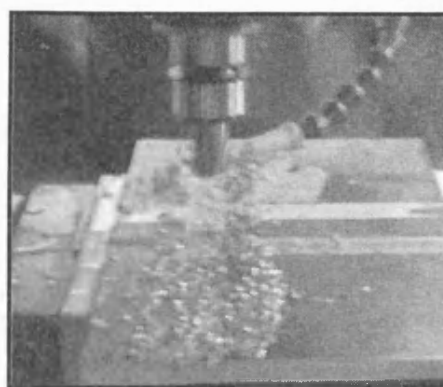
DOC change. This clearly shows the ability of the system to monitor any changes in the DOC in real-time.

7.10.1 Effect of Swarf

Further tests were carried at 0.5mm, 1.0mm, 1.5mm and 2.0mm DOC. Tests revealed that with the presence of cooling fluid and increasing volumes of swarf as shown in Figure 7.24, the sensor data behind the cutter became very noisy. Further, at times the sensors could not make any sensible measurements as the sonic burst was lost due to reflection from the swarf at wide angles. For example, Figure 7.25(a) shows a noisy signal acquired by sensor 2 at 1.5 mm DOC.

(b) 0.5 mm DOC (no coolant)   (b) 1.0 mm DOC
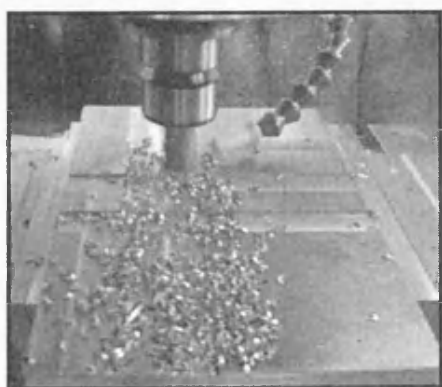
(c) 1.5 mm DOC (no coolant)   (d) 2.0 mm DOC
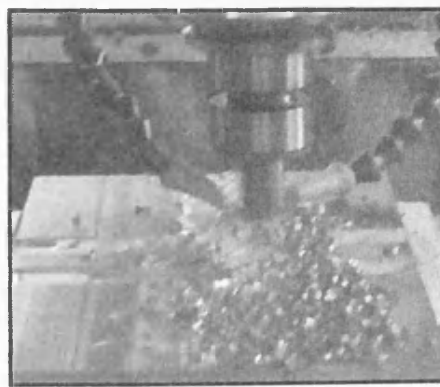
Figure 7.24: Swarf generated during cutting tests

To handle this situation the signal processing regime was modified and tool offset information was used in the spike removal algorithm as previously described in section

7.8.4. The resultant signal is shown in Figure 7.25(b). The sensor 2 data was conditioned via the calculation of the running maximum of the signal to remove the effect of swarf in the measured signal. The results of this are shown in Figure 7.25(c). The other algorithms were as before and with the full set of signal processing algorithms used the DOC was calculated with sufficient accuracy even for 2.0mm DOC Test, which obviously produced greatest amount of swarf.
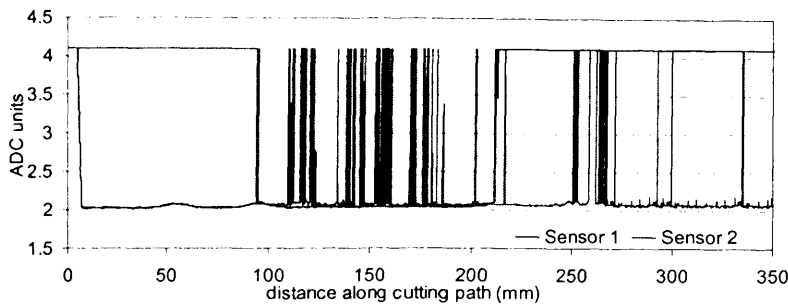

(a) Raw data from Ultrasonic Sensor
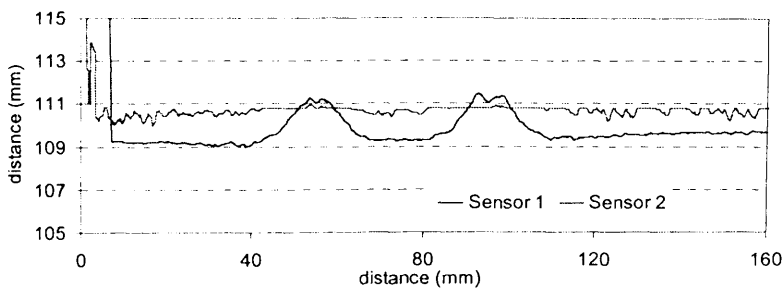
(b) Processed Data
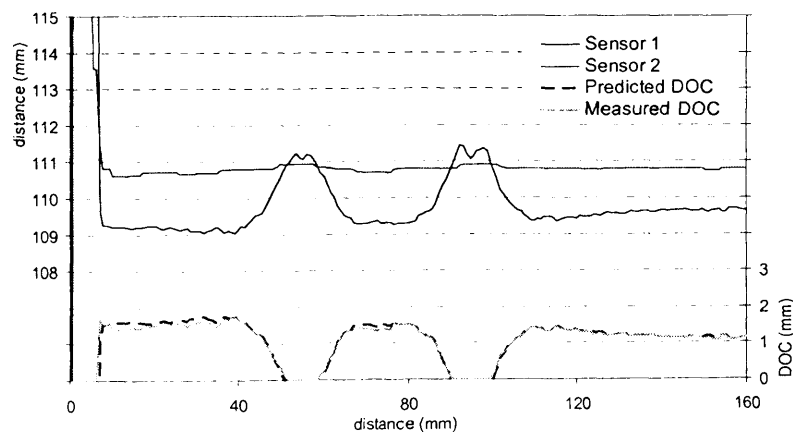


(c) DOC Calculation after further data processing

Figure 7.25: Depth of Cut Measurement for Cutting Test with 1.5 mm DOC

7.10.2 Results and Discussion

Tests carried out at different DOCs show that swarf and coolant fluid have adverse effect on the senor data as shown in Figure 7.26(a—d). In their presence it is not possible to measure the object profile correctly. During the tests the workpiece was

cleared from any swarf before each test. This helped the system to accurately measure the object profile in front of the cutter which results in better prediction of the DOC for tool breakage system. However the measured DOC using sensor 2 data is dependent upon how efficiently the data is processed to calculate the profile.

DOC	Raw data	Processed Data & Calculated DOC
0.5 mm	(a)	(e)
1.0 mm	(b)	(f)
1.5 mm	(c)	(g)
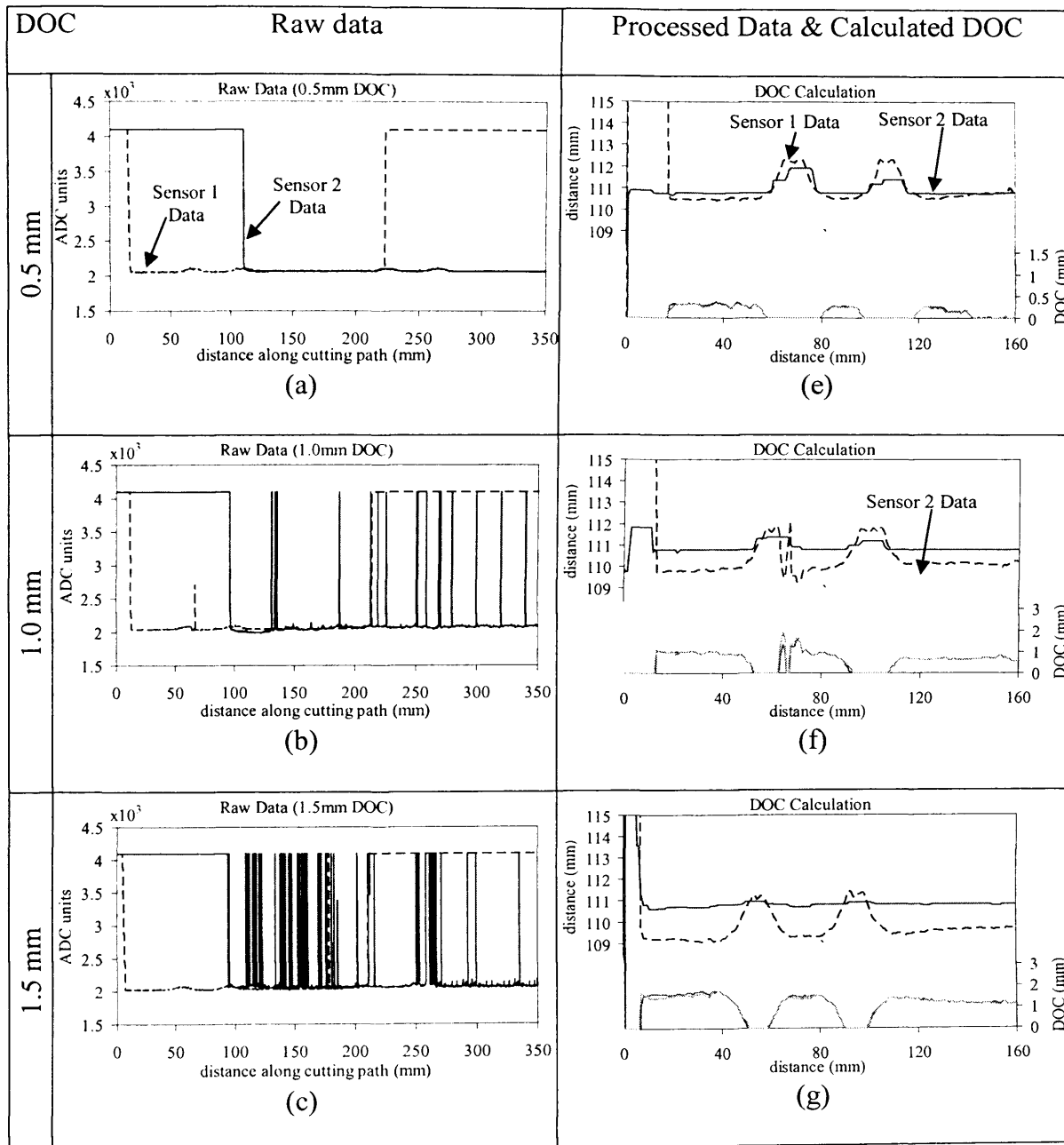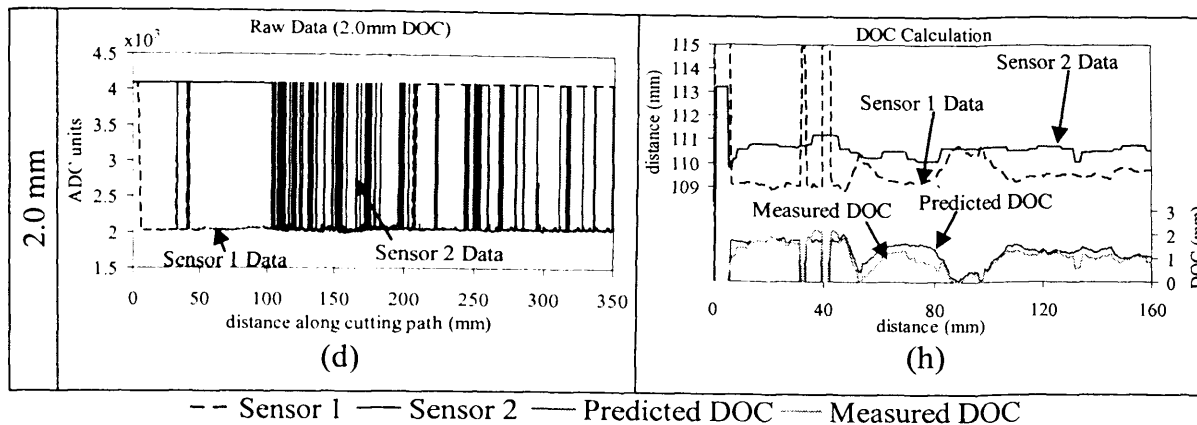
Left Column: Raw Data - Distance from Sensor(s) – (a) 0.5mm (b) 1.0mm (c) 1.5mm (d) 2.0mmDOC

Right Column: Processed Data and Measured DOC – (e) 0.5mm (f) 1.0mm (g) 1.5mm (h) 2.0mmDOC

Figure 7.26: Comparison of DOC Measurements Tests

Figure 7.26(e—h) shows the processed sensor data measured DOC using the modified algorithms as discussed in the previous section. The measured DOC is shown according to the scale on right hand side of each plot.

Integration of the system with tool breakage system will enable to monitor the DOC in a more sophisticated way. DOC monitoring system will predict DOC using sensor 1 data and the known tool offset and communicate the information for tool monitoring (breakage detection). The tool breakage detection system will adapt itself to the changing DOC and correctly monitors the tool breakage. This, in return, provides feedback about the health of the process. When it is conformed that cutting has been performed for particular portion of the workpiece the system can calculate the DOC more accurately by using the fact that object distance behind the cutter should be equal to the tool offset. If no cutting has been performed i.e. the tool is missing or broken, this system, will adjust its calculations to incorporate the fact resulting in reliable calculation of DOC.

7.11 Conclusion

The developed measurement system has been able to measure the DOC with <0.1mm accuracy. The deployed signal processing algorithms and their effectiveness have confirmed the capabilities of the dsPIC devices for eMonitoring tasks. With this research the focus has been shifted from solutions minimizing the signal processing towards more sophisticated DSP algorithms which promise better monitoring solutions.

The system has measured DOC with the assistance of the removal of swarf from the workpiece before cutting. It is recommended that further work should be focused on methods of removing the swarf in an effective way which will not only improve the effectiveness of DOC measurement system but also enhance the tool life in terms of avoiding chip adhesion and better heat dissipation.

References

[7.1] R.A. Siddiqui, W. Amer, Q. Ahsan, R.I. Grosvenor, P.W. Prickett, "Multi-band Infinite Impulse Response Filtering using Microcontrollers for e-Monitoring applications," *International Journal of Microprocessors and Microsystems*, vol. 31, 2007, pp. 370-380.

[7.2] Xingxue Tao, Changqing Liu, Zhejun Yuan, Yong Li, "Robustness improvement of tool life estimation assisted by a virtual manufacturing cell," *International Journal of Materials Processing Technology*, vol. 172, 2006, pp. 445-450.

[7.3] B. Sick, "Online and indirect tool wear monitoring in turning with artificial neural networks: a review of more than a decade of research," *International Journal of Mechanical Systems and Signal Processing*, vol 16(4), 2002, pp. 487-546.

[7.4] P. Bhattacharyya, D Sengupta, S. Mukhopadhyay, "Cutting force-based real-time estimation of tool wear in face milling using a combination of signal processing techniques," *International Journal of Mechanical Systems and Signal Processing*, vol. 21, 2007, pp. 2664-2683.

[7.5] N. Parashar and R. Mittal, "Elements of Manufacturing Processes," Prentice Hall 2004, p 151.

[7.6] K. Szwajka, "Laboratory versus industrial cutting force sensor in tool condition monitoring system," *Journal of Physics: Conference Series*, vol. 13, 2005, pp. 377-380.

[7.7] W. Amer, R. Grosvenor, and P. Prickett, "Machine tool condition monitoring using sweeping filter techniques," *Journal of Systems and Control Engineering*, vol. 221, 2007, pp. 103-117.

[7.8] R.A. Siddiqui, Q. Ahsan, R.I. Grosvenor, P.W. Prickett, "The role of emerging technologies in eMonitoring," *17th International congress on Condition Monitoring and Diagnostic Engineering Management (COMADEM)*, Cranfield, 2005, pp. 263-271.

[7.9] Donald P. Massa, "Choosing an Ultrasonic Sensor for Proximity or Distance Measurement ," [WWW] <URL: http://www.sensorsmag.com/sensors/artide/ Article/detail/ 321383> (accessed on 01 Mar. 2008)

[7.10] Joan Kassan and Jerry Morelli, "Ultrasonic sensing for challenging environments," *Sensors*, 1 July 2005, [WWW] <URL: http://www.sensorsmag.com/sensors/artide/Article/ detail/178903>(accessed on 01 Mar. 08)

[7.11] Parallax Inc., "Ping))) Ultrasonic Sensor Introduction" [WWW]<URL: http://www.parallax.com/Store/Microcontrollers/BASICStampModules/tabid/134/List /1/ProductID/92/Default.aspx?txt Search = PING))) & SortField =ProductName %2c Product Name> (accessed on 14 Apr. 2008)

[7.12] Parallax Inc., "Ping))) Ultrasonic Sensor" [WWW]<URL: http://www.parallax.com/desktopmodules/catalookstore/ImageViewer.aspx?link=Images%2fProd%2 f2%2f280 %2f 28015-L.jpg & desc=PING))) + Ultrasonic + Sensor&PortalID= 0&viewerid=-1&mid=-1> (accessed on 14 Apr. 2008)

[7.13] Ping))) Ultrasonic Sensor (#28015) Datasheet from Parallax Inc. California 95765 USA published June 2005.

[7.14] Baumer Electric., "UNAM 12I9914/S14 Ultrasonic sensor Data sheet," [WWW] URL: http://sensor.baumerelectric.com/productnavigator/downloads/ Produkte/PDF/Datenblatt/Ultraschall_Sensoren/UNAM_12I9914_S14_web_EN .pdf> (accessed on 17 Mar. 08)

[7.15] Baumer Electric., "Application Report: with Distance Measurably better," [WWW] < URL: http://www.baumerelectric.com/shared_data/forms_layout/ baumer/839_029en_mit_abstand_measurably_internet.pdf> (accessed on 10 Mar. 2008)

[7.16] Baumer Electric., "UNAM 12UI9914/S14 Ultrasonic Analog sensor Specifications," [WWW] <URL: http://sensor.baumerelectric.com/ productnavigator/downloads/Produkte/Bilder/Schallkeule/E-Zchn-4156.gif > (accessed on 17 Mar. 2008)

[7.17] "Displacement Sensors: Expert Techniques & Applications to improve Productivity," [WWW] <URL: http://www.keyence.co.uk/dwn/lt_tech_guide _ku.pdf > (accessed on 10 Mar. 2008)

[7.18] "Technical definitions of measuring sensors," [WWW] <URL: http://www.brodersen.dk/products/sensor/baumer/inductive/manuals/E_Flyer_D istSens.pdf> (accessed on 11 Mar. 2008)

[7.19] Jerry E. Purcell, "Multirate Filter Design - An Introduction," [WWW] < URL: http://www.mds.com/tech/filter/multirate_article.pdf > (accessed on 10 Apr. 08)

[7.20] Steve Smith, "It was suppose to be a 12 bit converter? DSP to Rescue," [WWW] <URL: http://www. dspguide.com/appexam.htm> accessed on 12 Apr. 2008)

[7.21] Raymond J. Walker, "Time Series Analysis: Facing Reality," [WWW] <URL: http://lucid.igpp.ucla.edu/lessons/ess265/2005/Lecture_8_Facing_Reality.pdf> (accessed on 10 Apr. 08)

Chapter 8

System Integration:

A Process Management System

8.1. Introduction

If a cutting tool on a machine is used, there are many events that can occur at any time. While tool wear is an ongoing phenomenon, things like tool breakage often occur without any warning. The developed system can be used for the monitoring of events other than tool breakage when integrated in the architecture as described in Chapter 4. The research described in this dissertation will enable the construction of the architecture as shown in Figure 8.1. Each element has been described in previous chapters. This chapter brings together these components and describes how the system will work and identifies contributions made by the individual elements.

System integration refers to combining together two or more subsystems or elements into one system. Systems integration combines the capabilities of the subsystems into one system in a way which is much more superior to the sum of the individual elements. It is thus concerned with value-adding to the system, with capabilities that are possible because of interactions between subsystems. The integrated system for this research has the capabilites of monitoring system performance and combining the monitoring results to reach a definitive conclusion about process health and also provides information for process management.

8.2. System Overview

The integrated tool condition monitoring system consists of three FENs in the first tier, as shown in Figure 8.1, to monitor the cutting process and tool health. Two FENs monitor tool breakage by analysing the spindle load signal in time and frequency domains using different signal processing methods as described in Chapter 5 and 6. The

depth of cut (DOC) monitoring FEN provides on-line information ahead of the cutting process as discussed in Chapter 7. In addition there is a parameter monitoring node which plays a central role in system level decision making about tool health. A user interface and information display node communicates with the local operator and provides real-time cutter/process health information (typically on a display). This node can be part of the process monitoring node. In future applications the system could be integrated into the CNC consol to provide seamless operation and real-time communication.
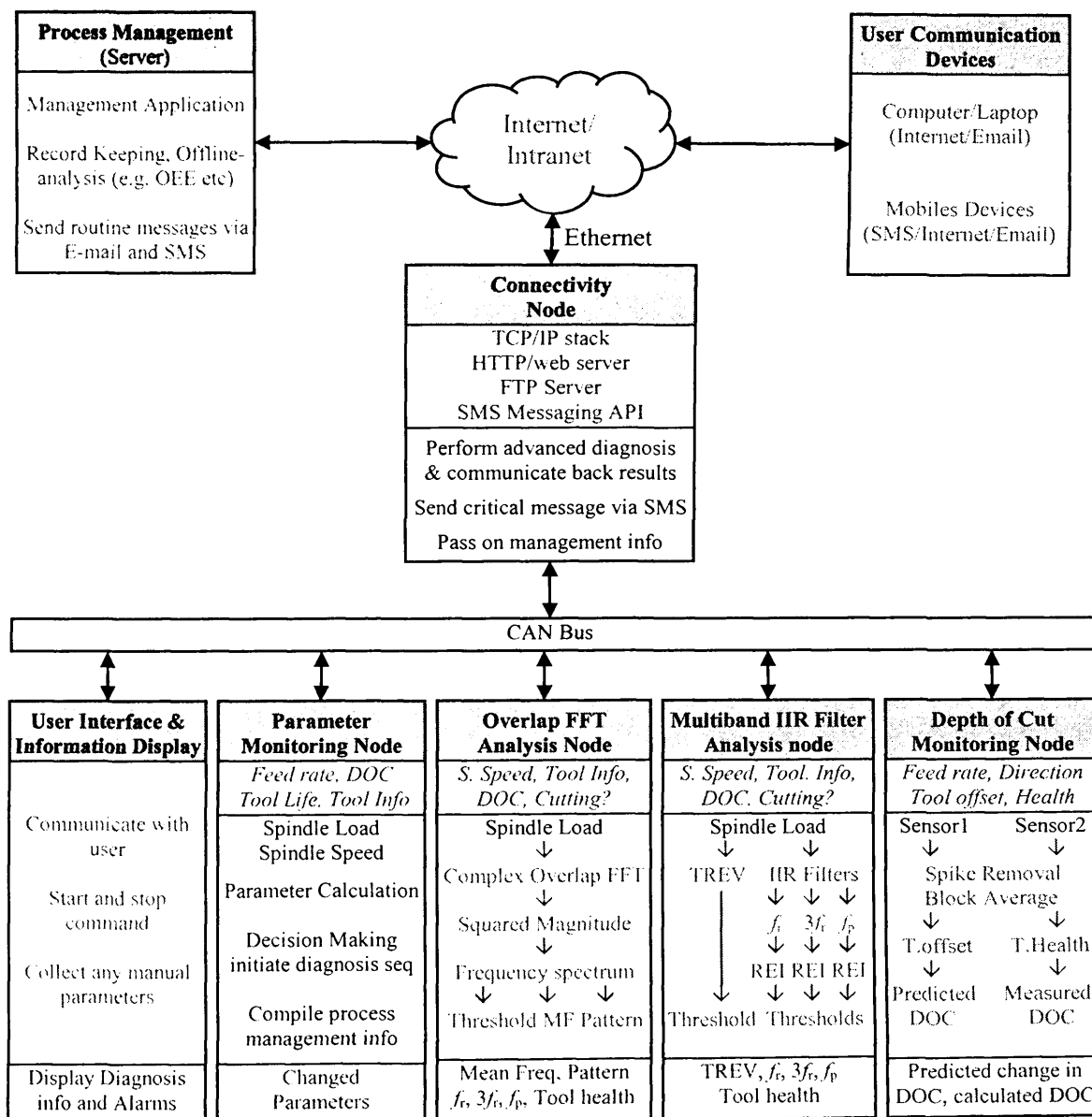

Figure 8.1: Architecture of Integrated Process Monitoring and Management System

196

These nodes are connected to a CAN bus and communicate to each other by message passing. Messages are identified by message identifiers. Each node sends messages at regular intervals when the process is under normal conditions to announce its presence and provide the status of process. When an abnormality is detected by a node, it communicates the information immediately. In this way a tool breakage and critical DOC information is communicated to the parameter monitoring node for immediate combined diagnostics to verify the decisions. At the second tier, the dsPIC-based connectivity node provides an advanced diagnosis platform for analysing the signals when referred by first tier. It also hosts a web server which provides web pages related to the process. Finally it transfers the process management related information to the server. Each of these elements shown in Figure 8.1 is considered in the following sections.

8.3. Parameter Monitoring node

The parameter monitoring node monitors the signals and calculates the system parameters at the initialization stage and communicates this information to all FENs. Before starting the actual process, operational parameters and threshold values for local decision making are set. The start of cutting operation is detected when the average spindle load exceeds the cutting threshold as shown in Figure 8.2. Similarly this threshold indicates when there is no cutting being carried out. This node sends this information over the network using a "start monitoring" message when the loads exceeds threshold and a "suspend monitoring" when the load drops below the threshold. In this way tool breakage is monitored when the cutting is being carried out. This information will also be augmented by the DOC monitoring node which will indicate a coming change in DOC.

The monitoring of spindle load also confirms cutting tool and workpiece interaction i.e. that neither of them is missing. The parameter monitoring node also monitors these signals in real-time to detect any changes. If any change (for example any change in spindle speed, feed rate etc) is detected by this node, it communicates these changes to the FENs. The concerned FEN receives the information and adjusts its parameters dynamically. It is worth noting that there is potential for developing a method allowing the parameters at this node to be acquired form the CNC controller (such as current

cutting direction through G codes). At the same time tool information such as tool offset could be obtained from the database at the management application, which can be downloaded and stored locally.
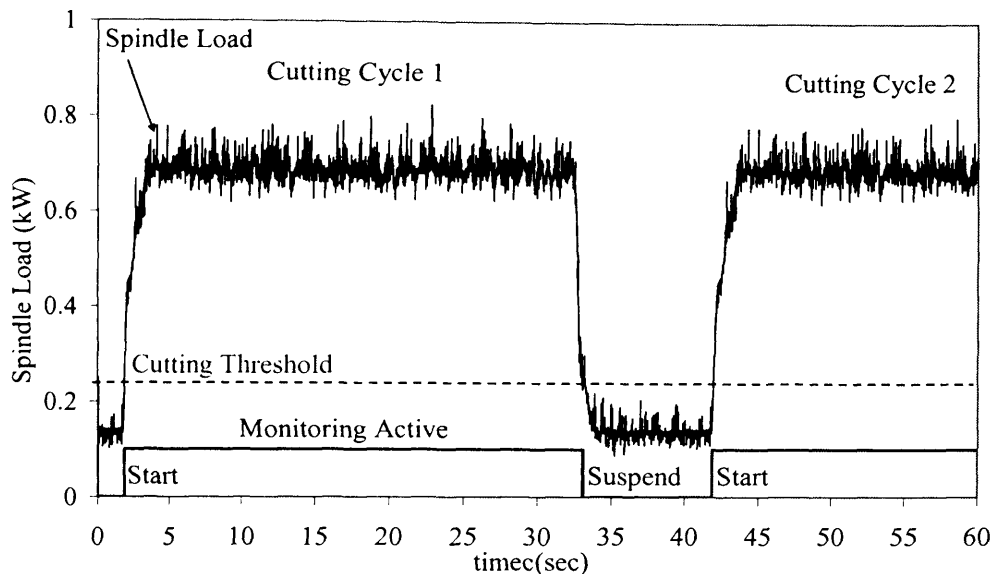

Figure 8.2: Spindle load based cutting cycle determination for tool monitoring.

8.3.1. Decision Making at the First Tier

Decisions about the health of the cutter are made in two phases at the first tier. Firstly the monitoring nodes have local decision making logic programmed into them based on the signal processing methods they are using and the characteristic of the process being monitored. This technique has been discussed in Chapters 5 and 6. This allows the nodes to reduce the network communication by sending a message only when it is absolutely necessary. In the second phase, the parameter monitoring node is responsible for decision making regarding tool health by integrating the information provided by other monitoring nodes. It receives messages from three FENs and may be programmed to combine the health status according to the example rule-base as shown in Table 8.1. In this Table '1' means that a threshold is crossed or a possible tool breakage detected by a node and X denotes a "Don't care" condition. Other warnings generated by the monitoring nodes, such as chipped or blunt tool are not shown in this Table. These will be flagged and appropriate advanced analysis will be initiated to verify the tool health.

198

Table 8.1: Combined Decision Making at First Tier

Frequency		Time		Average Load	Status
FFT	IIR	ΔDOC	TREV	↑Load	
1	0	X	X	X	AD
0	1	X	X	X	AD
1	1	0	1	X	Broken Tooth
0	0	0	1	1	Flag this event *
0	0	1	1	1	Query Entry/Exit/Inclusion
1	1	1	1	X	Broken Tooth *
-	-	-	-	1	Request data from Nodes

* Mark tool for later inspection.

AD=start advanced diagnosis sequence.

8.3.2. Data Communication for Advance Diagnosis

As mentioned in Chapter 4 more than 90% of the faults regarding tool breakage will be dealt with at the first tier. However there are cases when the acquired signal (like spindle load and speed) are communicated to the second tier for advanced analysis. For most effective analysis, the maximum possible amount of data should be used. To achieve a 1 Hz FFT resolution with advanced analysis, it was decided to always buffer 1 second of data so that the data relating to an abnormal condition is available. It was also decided to acquire another second of data after the abnormal condition is detected. To effectively monitor the tool breakage for entire range of spindle speed (up to 6000rpm) for a 4 tooth cutter, the sampling rate was set to 1Ksps. Therefore, 2000 data samples (12-bit) required to be transmitted to second tier for each signal. Each CAN message can carry 8 bytes of data or in this case 4 data samples as each sample requires 2 bytes. Thus there would be 500 CAN messages to be transmitted for one signal. If we send the spindle speed signal as well then a total of 1000 messages need to be transmitted. This would require about 1.07 seconds with a CAN speed of 125Kbps. The time can be reduced by increasing the CAN bus speed up to 1Mbps but this will reduce the effective length of the network and all nodes on the network may not work properly. The other solution is to reduce the amount data by using data compression techniques discussed in Chapter 4. These techniques provide up to 50% compressing ratio and help reducing the total data transmission time. This not only improves the network efficiency but also enables the system scalability allowing more devices to be added if required.

8.3.3. Advanced Diagnosis Sequence

As soon as an abnormality is detected by one of the monitoring nodes or when the parameter monitoring node finds that advanced diagnostics are required for decision making, it starts the diagnostics sequence. It acquires and monitors spindle speed and spindle load signals and always buffers the signals for the last 1 second. The stored information includes data prior to abnormality. If required, the node sends the buffered spindle load and speed data to the second tier, via CAN communications for advanced analysis. It also acquires another second of data and sends it along with other parameters such as DOC and feed rate information. Upon receiving the decision from the second tier, it raises the alarm in case of confirmation tool breakage. Based on the advanced diagnostics of the signals over time, the rule base (shown in Table 8.1) will be updated through the built in run-time self programming (RTSP) facilities provided in dsPIC devices, to incorporate the lessons learnt from the analysis of process abnormalities. The same is true for other monitoring nodes. This node also compiles the process management information and sends it to higher tier.

8.4. Internet Connectivity

Internet connectivity was realized by deploying the Microchip's TCP/IP stack on the connectivity node. The dsPICDEM.net 1 connectivity board, used for this purpose, has a Realtek Ethernet controller which has a unique Media Access Control (MAC) address. It was given an IP address from Cardiff School of Engineering Information Technology (IT) department. File Transfer Protocol (FTP) and HTTP servers were programmed to run simultaneously for data communication. Both of the FTP and HTTP servers were programmed to listen to the connection on different ports. Each connection started a new session to handle a particular request. The WebPages were created using Hyper Text Mark-up Language (HTML). These pages were converted to a Microchip File System (MPFS) image file and uploaded to the EEPROM on the board by communication to FTP server on a command prompt. The access to the FTP server was authenticated by username and password. HTTP server was used to present the information to ordinary users through hosted WebPages. It generated the part of webpage dynamically to display the current process information form stored variables. Since an automated pushing of information is not possible through Internet Explorer (IE), this page was programmed to refresh its contents after a pre-programmed interval.

(2 seconds in this application). Figure 8.3(a) shows the webpage that displays the process status relayed to the internet by connectivity node. In this case it is showing the tool status and system operational status using simulated data. The healthy status is shown as 'h' and white background. Figure 8.3(b) shows the information for a broken tool as 'B' with red background applied to status area. The change in background colour is utilized for easy identification of the tool status. The architecture of the webpage allows the user to see the process information while visiting other pages such as help page as displayed in Figure 8.3(b).
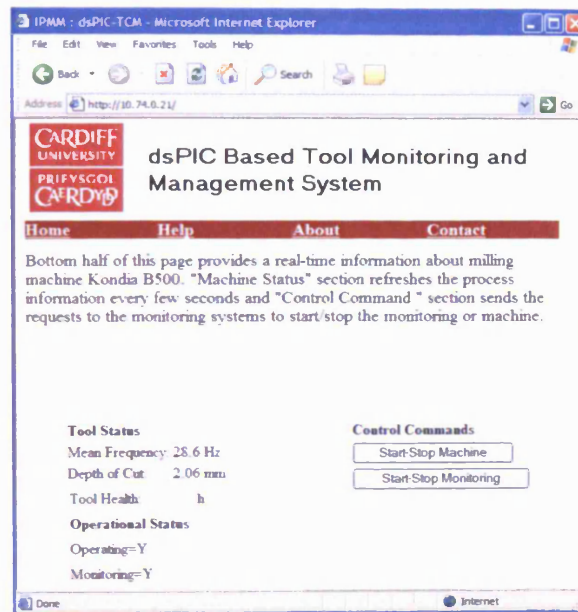
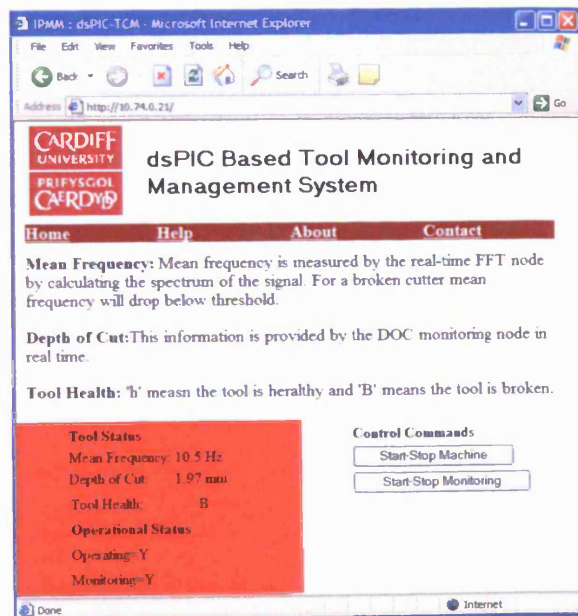Figure 8.3(a): Webpage information for a healthy cutter

Figure 8.3(b): Webpage information for a healthy cutter

Provided control command buttons on the page as shown in Figure 8.3 send the request to the connectivity node, which can be programmed to act accordingly. In this application these are provided to demonstrate the web-based control capability of the system. The HTTP authentication is also implemented so that only registered users, with valid username and password, can interact with the process or monitoring system. In this case, when the webpage is opened in the web browser, the user is prompted to provide a valid username and password for authentication as shown in Figure 8.4. After successful authentication, a session is opened and the required webpage is displayed (Figure 8.3). This session remains valid until the browser is closed. In this way the user is required to authenticate only once at the start of session.
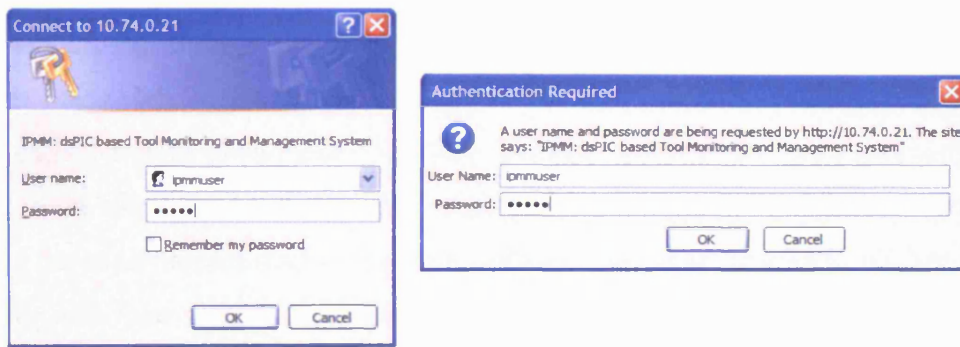

(a) Internet Explorer   (b) Mozilla Firefox

Figure 8.4: Authentication request prompt

Mobile devices have small display screens and can display limited amount of information. In such cases, the status page can be opened directly by appending '/status.htm' to the main URL (e.g. *http://10.74.0.21/status.htm*). The status page has the same behaviour (Figure 8.3) as described previously and is shown in Figure 8.5 for a healthy and broken cutter cases.
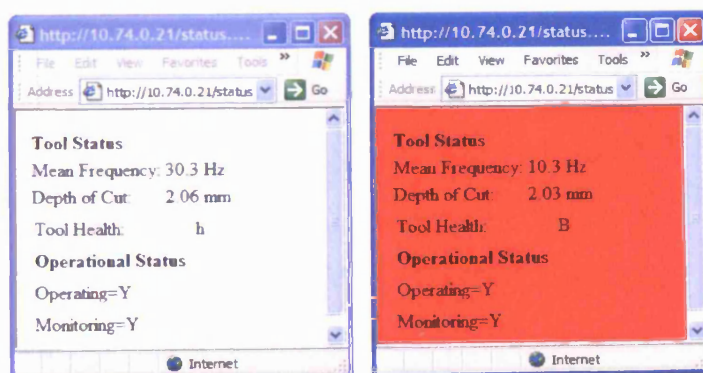
(a)   (b)

Figure 8.5: Status page showing information for (a) healthy cutter (b) broken cutter

202

8.5. Response to Normally Occurring Machining Events

Another common problem with tool force monitoring is the entry/exit of work piece and milling into a shoulder. These events are clearly capable of confusing most existing monitoring systems. The researched system for tool breakage monitoring successfully identified the new and broken cutter for different depth of cuts and spindle speeds and it also identified the simulated breakage in all the cases. Based on these results the system is expected to correctly identify tool condition under different commonly occurring events such as tool entry, tool exit, change in DOC and contact between the tool and an inclusion. Figure 8.6 shows a spindle load signal for a complete cutting cycle. At start, the load is at the "idle level". As the tool starts to enter the workpiece the load starts to increase and crosses the cutting threshold. At this point the parameter monitoring node sends a message alerting the "start of cutting". The load keeps increasing until the tool is fully engaged with workpiece. Halfway through cutting the tool encountered a slot/hole in the workpiece and load decreased considerably and went back to previous level after duration proportional to the width of slot. This is analogous to milling out of a shoulder and then milling into the shoulder. At the end the tool exits from the workpiece and load drops below the cutting threshold. At this point the parameter monitoring node alerts the other nodes to suspend monitoring.
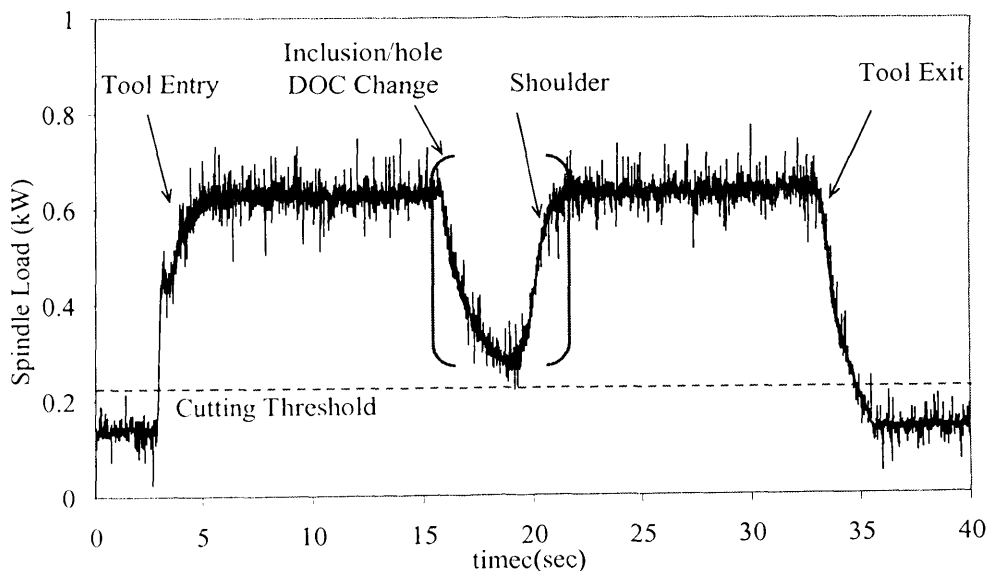

Figure 8.6: Different Events in a Machining cycle.

As it can be seen that load varies according to the cutting conditions, it is not possible to find tool condition directly from this signal. However after intelligently filtering the load signal as shown in Figure 8.7, it was possible to almost eliminate the effects of

these events from the signal and the filtered signal relating to the tool condition was obtained. This signal was further processed by IIR filtering node and FFT node to establish the tool condition. Figure 8.7 shows the filtered signal obtained for a healthy tool. It is clear that the signal carries the information which is almost independent of those events described above. Coupled with the information, when the load is greater than the cutting threshold, the tool condition can be correctly identified. Moreover the system was unaffected by these events and did not generate any false alarm.
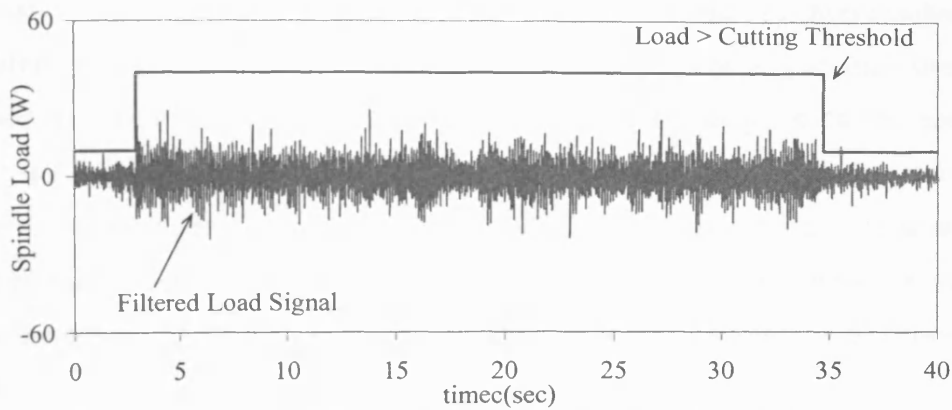

Figure 8.7: Filtered Spindle Load Signal for a Healthy Cutter

Similarly Figure 8.8 shows a signature for a broken tool which looks similar to the healthy cutter profile but is differentiable from the healthy cutter signal using signal processing techniques described in Chapter 5 and 6. It was observed that the variations of the filtered signal increase with increase in depth of cut. So the thresholds for detecting the tool breakage required the depth of cut information, which is being provided by the DOC monitoring node. Thus incorporating the DOC information can aid the system when trying to reliably detect the tool breakage.
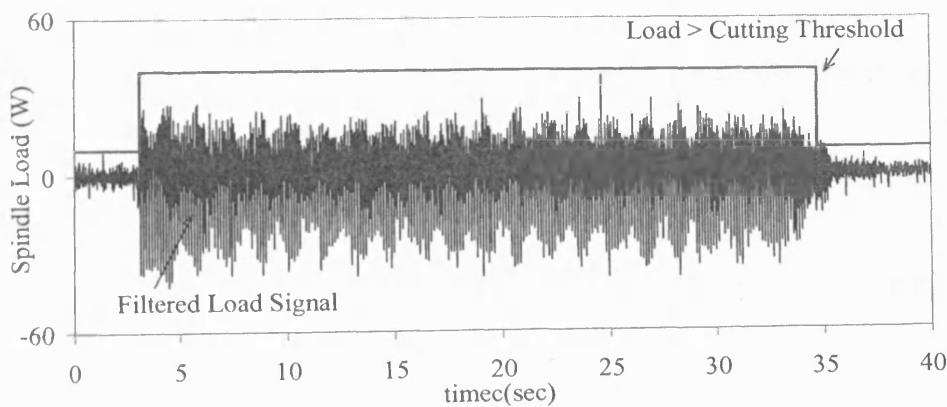

Figure 8.8: Filtered Spindle Load Signal for a Broken Cutter

204

It is quite common to actually encounter hard piece of material in a workpiece. There will be sudden increase in tool force and many existing tool breakage systems will possibly identify this event as being due to tool breakage. Because of the frequency based nature of the process, the developed system will not generate the false alarm. Further diagnostics is enabled by the fact that the integrated system will actually monitor/read out what the DOC was and establish if it had changed recently. Knowing that DOC has not changed, it can actually be assumed that it must be due to "something else". That "something else" could be related to tool wear. If the situation resolves itself and conditions come back to normal then the chances are there was an inclusion in the workpiece or some other cause of the disruption. That's the diagnostics the researched system has made possible. It wouldn't signal tool breakage because at the integration level all monitoring decisions are combined together, all the information is analysed and determined whether it's either the tool wear or it's a hard piece of material. Because conditions revert back to normal again, it's not tool wear, it's possibly a hard piece of material.

The system may be configured to flag up the fact that the tool has machined hard piece of material because it may have damaged the tool. There may be a crack or some other fault with tooth which has yet to indicate itself as broken tooth, but will do so if it continues to cut. In this way if a particularly high force is recorded, the operator can be asked to inspect the tool, because the tool might break a lot sooner than it should. It is almost impossible even using the most advanced tool condition monitoring methods to actually detect cracks in teeth. But it is not impossible to look carefully when it is sent for calibration to determine whether that's the case.

The developed system is not affected by the entry and exit events, but it records an increase in machine load. This is also confirmed by the fact that DOC system will report that there is an entry or exit event. Entry events will be distinguished from shoulder/increase in DOC by the fact that at an entry event the load is at its idle level before entering into workpiece and for the shoulder it will be greater than cutting threshold before entering into the shoulder.

8.6.   Process Management Strategy

Having discussed the tool breakage monitoring system, it is finally worth considering how the other currently available IPMM modules and elements such as the DOC monitoring system developed in this thesis, can be integrated in order to provide a better overall process management tool. Within this scenario, tooth breakage will be covered by individual modules. There will be times when the module thinks that perhaps the tool is broken. When it can make access to the information such as DOC, it can improve its decision accuracy. But integrating it into a higher level will also provide more information.

Under normal conditions, when a tool is cutting workpiece, tool load will be equally spread during each rotation of the tool. There will be some variations due to tool wear. Although this system only alarms when sensing a broken tooth, tool wear may also be monitored using the same information. The system uses the average load and its variation components for tool health monitoring. This component is potentially useable to measure and monitor tool wear and tool life. There is parallel research work going on in IPMM centre on tool wear and tool life [8.1] and there is a clear link between this work and the research reported in this thesis. The previous work is still based on previous generation of PIC microcontrollers and would benefit from this research. It would be worth developing a tool wear monitoring system on the same hardware as the current system for possible easy integration, exchangeability and interchange-ability with enhanced signal processing.

It is perfectly possible for symptoms similar to broken tooth being generated by events in milling process such as shoulder milling, milling an inclusion and change in DOC. These can be eliminated by the researched system because they are not frequency based and are one off events (and frequency components will come to normal conditions). That diagnostics could be confirmed from DOC monitoring system. DOC and Tool Breakage systems will work together. The parameter monitoring node might think that DOC might have changed when tool force suddenly increases. So it will query: has the DOC changed? DOC monitoring is working ahead of cutting. It should have already sent the information if it detected a change in DOC. It will track the latest position of cutter based on feed rate information. However, information about change in DOC can

be requested and the system will re-access the information and send the latest diagnostics of data taken from near the cutter location. If the module replies that there is no DOC change then it means something else might have happened. If something happens, the system does not stop the machine, until final decision about the tool breakage is confirmed.

Of more interest is the detection of sudden increase in force due to machining an inclusion. When the tool encounters a hard piece of material the parameter monitoring node will record a sudden increase in load. The tool failure/breakage monitoring node reports that tool is not broken, but that a higher than normal cutting force occurred. This can then initiate the tool inspection process identified in Section 8.5 and also from the basis of subsequent tool management strategies.

8.7.   Summary

By monitoring all the events during the milling operation, the monitoring system provides the benefit of actually having always the record of the entire tool life. If a record of these events is kept it can be used for tool management and OEE strategies based around the following data:

- How many entrances and how many exits the tool made
- How many shoulders milled by the tool
- What was the cutting speed
- For how long the tool was actually cutting
- What DOC was it working on etc
- How many times tool a hard piece of material or an inclusion has been machined

This analysis helps build up a picture of the cutting performed by a tool over entire tool life and provide a more accurate description of what tool life really means. The tool management system accordingly will utilize the new learnt tool life meaning to develop an even more robust tool condition monitoring strategy.

References

[8.1] P.W. Prickett and R.I. Grosvenor, "A Microcontroller-Based Milling Process Monitoring and Management System," *Proceedings of the Institution of Mechanical Engineers, Part B: Journal of Engineering Manufacture*, vol. 221, 2007, pp. 357-362.

<div align="right">

Chapter 9

Conclusion and Future Work

</div>

9.1   Main Contributions of the Research

This research was aimed at developing advanced signal processing techniques and algorithms for implementation on dsPIC microcontrollers for a machine tool condition monitoring system and thus exploring the potential of the dsPIC technology for the realization of an e-Monitoring system. The research has produced the following important contributions: -

- **Signal Processing Techniques.** The development of novel signal processing and analysis techniques which are optimized for deployment on microcontroller devices. These are capable of real-time feature extraction to detect tool breakage for entire range of spindle speed. These techniques include:-
    - o A novel implementation of the overlap FFT technique on microcontrollers for real-time frequency analysis for tool health monitoring.
    - o A novel variable sampling rate implementation exploiting the on-chip features of the dsPIC technology in an intelligent way.
    - o The development of a Multiband IIR filtering technique to eliminate the requirement for analogue hardware filters. This enhances reliability and makes the system compact and thus suitable for embedded applications.
    - o The development of a novel Dynamic Coefficient Selection technique for enhancing the effectiveness of the monitoring system.
    - o A virtual node implementation of the TREV technique in time domain for tool breakage detection.
- Tool breakage detection within 1½ revolutions and verification within 2 revolutions by using the developed techniques and existing machine tool signals thus eliminating the requirement of additional sensors for real-time tool breakage detection.

<div align="right">

209

</div>

- A novel depth of cut monitoring system development and implementation for on-line measurement of DOC information, which enhances the system robustness and reliability. The DOC information enables the approach to identify events which were not possible in the absence of it.

- The development of a future proof monitoring system architecture which welcomes the advancements in technology and provides an infrastructure for easy integration of new devices.

- The development of embedded distributed monitoring system solely based on dsPIC technology.

- The use of dsPIC microcontrollers to implement the techniques in addition to providing CAN bus and internet connectivity to the proposed system.

- The use of integrated system strategy for decision making which enhances the system reliability and enabled a process management strategy using the information provided by the researched system especially the DOC monitoring system.

- Capture of all significant events for off-line analysis and subsequent diagnosis. Exception reporting allows diagnostic system development.

9.2 Conclusions

The most important conclusions drawn from the research can be summarized as follows:-

- The dsPIC microcontroller has the capability of running overlap FFT, analysis and decision making for maximum operational spindle speed and still utilizes only 50% of the processing time when operating at 29.49MIPS.

- The main frequencies of interest in a machine tool condition monitoring system are tool rotation frequency, its third harmonic and tooth passing frequency. These frequencies are dependent on number of teeth and spindle rotation speed.

- The strength of these frequencies for healthy and broken tools is significantly different and these variations can reliably be used to detect a broken tool.

- The mean frequency and unique pattern are significantly different for healthy and broken cutter. These features can improve the reliability of the broken tool detection system.

- The tool rotation energy variations for a healthy and broken cutter are significantly different and can used to detect a broken tool.

- The depth of cut measurement and its integration enhanced the system robustness and reliability.

- The DOC information enabled the approach to identify events which were not possible in the absence of it.

- The system integration increases the overall system efficiency and reliability.

- A process management strategy is made possible using the information provided by the researched system especially the DOC monitoring system.

- The dsPIC microcontrollers are reliable and flexible devices for implementation of reliable and cost effective e-Monitoring system.

- The dsPIC technology is capable of providing internet connectivity and can host multiple services simultaneously. It can be used to realize a web-based monitoring and control system.

Considering these conclusions it is evident that cutting process information can be extracted from machine tool signals. By analysing them using the developed signal processing techniques, it is possible to detect tool breakage. The incorporation of the depth of cut information and the combination of the process status generated by the FENs can be used in an integrated way to cross verify the results. This provides high reliability and reduces the false alarms. It also enables the system to monitor and record the events a cutting tool has experienced during its life cycle which will enhance the understanding of tool life phenomenon from a new perspective.

The dsPIC microcontroller not only fulfils the requirements of the embedded machine tool monitoring system but also has the capability to incorporate more signal processing algorithms in future if required. These may be added as a result of advanced analysis of unexpected conditions. The dsPIC microcontroller has multiplexed input and output

functions and is capable of implementing the proposed monitoring system. Based on the testing and verification of the proposed signal processing, data analysis techniques and DOC measurement techniques it is possible to conclude that the dsPIC technology is capable of providing an effective low-cost tool condition monitoring system. The proposed monitoring system fulfils the main requirements by providing information for monitoring and maintenance activities.

9.3   Recommendations for Future Work

Based on the analysis of the research presented in this thesis and an investigation of the various options for enhancing the effectiveness of the system, the following areas are identified as possible further research work.

The DOC monitoring system is affected by swarf generated during cutting operation. It is therefore recommended that further work should be focused on methods of removing the swarf in an effective way which will not only improve the effectiveness of DOC monitoring system but also enhance the tool life in terms of avoiding chip adhesion and better heat dissipation.

The DOC monitoring system was developed to explore the possibility of measuring this important parameter in real-time and has been shown to produce a viable solution. The developed system was tested for fixed axis cutting where as in actual machining the cutting direction can change based on the machining requirements and shape of the product. Therefore to realize a fully automated system, the development of an alignment device for aligning the sensors in the cutting direction is recommended.

A preliminary study and analysis of feed motor current signals has shown the potential of developing the tool condition monitoring system based on feed motor current analysis. These signals contain information about feedrate, cutting force and cutting direction. The signal processing and analysis techniques presented in this thesis can be applied to the indirect cutting forces, extracted from the motor current signals, to detect the tool breakage. The cutting direction can be estimated by measuring the feedrate in horizontal axis utilizing the feed motor current signals as discussed in Chapter 7.

The developed system has enabled a process monitoring strategy which requires the storage of the events detected by the system for long term analysis such as tool life estimation and trend analysis. The implementation of the process management system elements is recommended to utilize the full potential of the developed techniques and monitoring strategies presented in this research. This will need investigation into the hardware, software and communication requirement. By utilizing the system architecture and communication capabilities provided by the developed system, any computer connected via Ethernet or the internet can be utilized for this purpose.

Two tool breakage monitoring nodes utilizing different signal processing and analysis techniques have been developed and implanted in this research to show the potential of dsPIC in handling variety of DSP algorithms. Both nodes can detect tool breakage in real-time. It is possible to detect tool breakage using either of them independently. Therefore, it is recommended the further research be conducted to define criteria for selection of an algorithm for tool breakage detection node based on further testing of these algorithms.

The dsPIC Technology has all the ingredients such as microcontroller and DSP core, memory, peripherals, timers, interrupts and communications modules suitable for a System-on-a-Chip (SoC) design. The recent dsPIC33F microcontrollers provide added features such as increased processing power (40 MIPS), Direct Memory Access (DMA) module, increased program and data memory and 2 ADC units each with up to 1.1MSps speed and 4 S/H buffers. This can provide facilities to acquire 8 analogue signals simultaneously and up to 32 analogue signals using one chip. Similarly Microchip's latest 32-bit microcontroller PIC32 provides 80MHz clock speed and up to 1.5 MIPS/MHz (i.e. 120 MIPS) throughput. It hosts a DMA, a 32-bit single cycle multiply and divide module, MAC unit, a bus matrix operating at processor clock speed and Joint Test Action Group (JTAG) interface. The DMA capability will enable the capture of a large amount of data before the MCU is interrupted for data analysis. This will reduce the software overhead and save the MIPS for additional monitoring tasks. The increased processing capabilities of these devices and communication capabilities make them ideal for implementing a SoC for a tool condition monitoring system. Thus further research in this area, utilizing the developed algorithms, SoC concepts and recent 16 and 32-bit embedded devices, is recommended.

dsPIC Related Details

Selected Manuals are provided in attached CD in folder "Appendix A"

Schematic Block Diagram for dsPIC30F6014
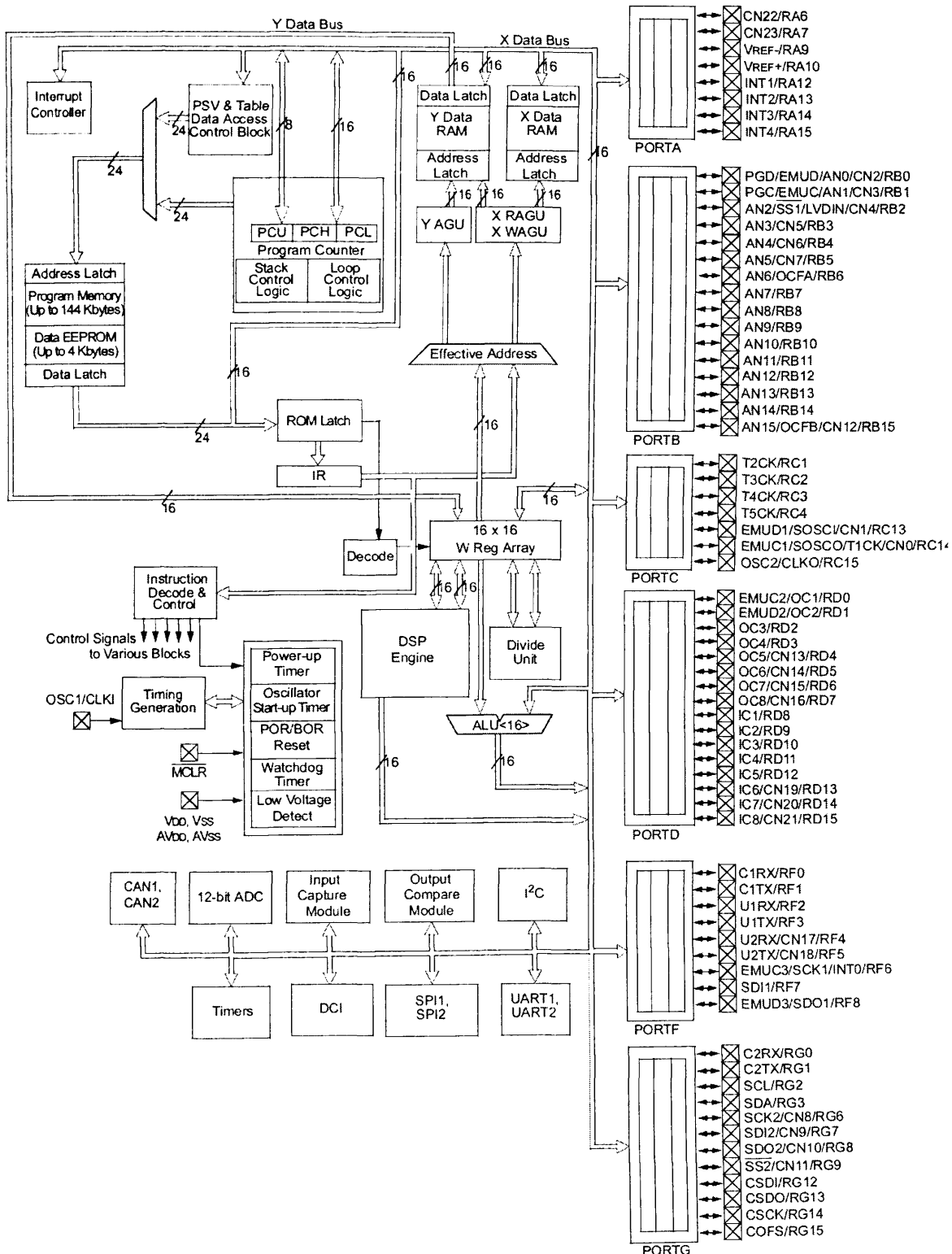
dsPIC30F6014 Features

High Performance Modified RISC CPU:

- Modified Harvard architecture
- C compiler optimized instruction set architecture
- Flexible addressing modes
- 84 base instructions
- 24-bit wide instructions, 16-bit wide data path
- Up to 144 Kbytes on-chip Flash program space
- Up to 48K instruction words
- Up to 8 Kbytes of on-chip data RAM
- Up to 4 Kbytes of non-volatile data EEPROM
- 16 x 16-bit working register array
- Up to 30 MIPs operation:
  - DC to 40 MHz external clock input
  - 4 MHz-10 MHz oscillator input with PLL active (4x, 8x, 16x)
- Up to 41 interrupt sources:
  - 8 user selectable priority levels
  - 5 external interrupt sources
  - 4 processor traps

DSP Features:

- Dual data fetch
- Modulo and Bit-reversed modes
- Two 40-bit wide accumulators with optional saturation logic
- 17-bit x 17-bit single cycle hardware fractional/ integer multiplier
- All DSP instructions are single cycle
  - Multiply-Accumulate (MAC) operation
- Single cycle ±16 shift

Peripheral Features:

- High current sink/source I/O pins: 25 mA/25 mA
- Five 16-bit timers/counters; optionally pair up 16-bit timers into 32-bit timer modules
- 16-bit Capture input functions
- 16-bit Compare/PWM output functions:
- Data Converter Interface (DCI) supports common audio Codec protocols, including I^2S and AC'97
- 3-wire SPI™ modules (supports 4 Frame modes)
- I^2C™ module supports Multi-Master/Slave mode and 7-bit/10-bit addressing
- Two addressable UART modules with FIFO buffers
- Two CAN bus modules compliant with CAN 2.0B standard
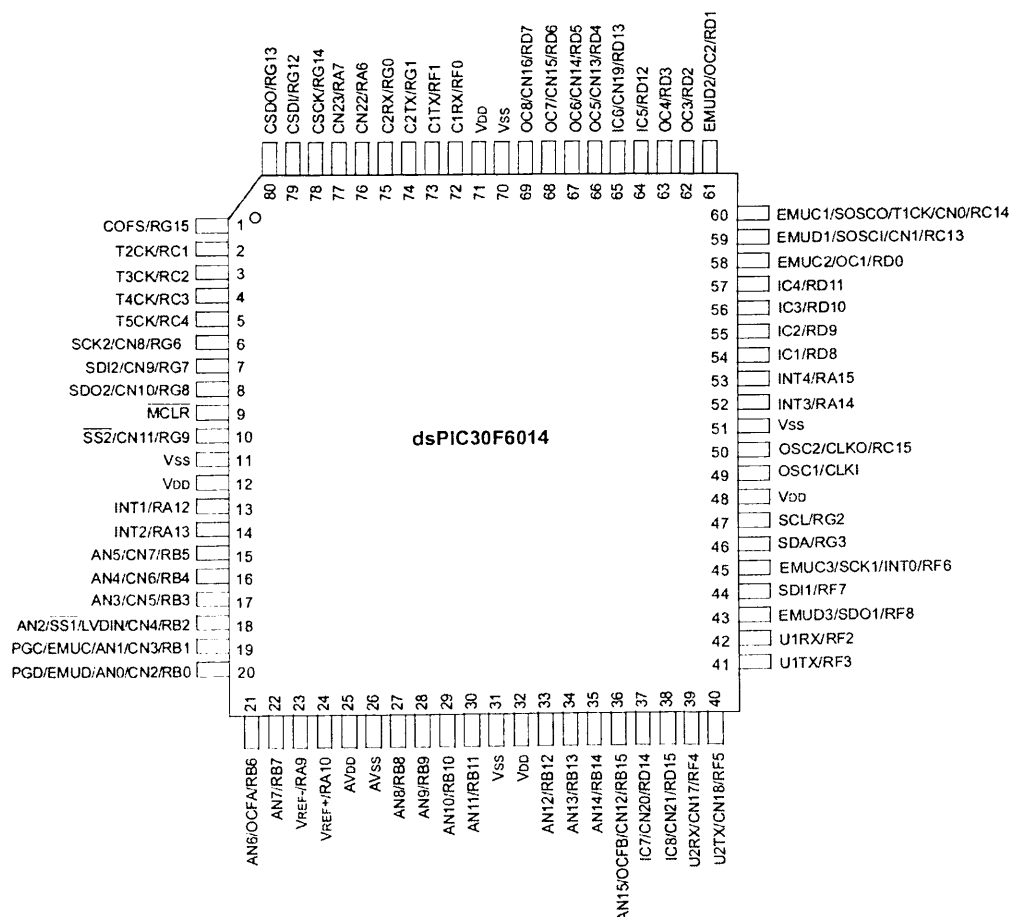
Analog Features:

- 12-bit Analog-to-Digital Converter (A/D) with:
  - 100 Ksps conversion rate
  - Up to 16 input channels
  - Conversion available during Sleep and Idle
- Programmable Low Voltage Detection (PLVD)
- Programmable Brown-out Detection and Reset generation
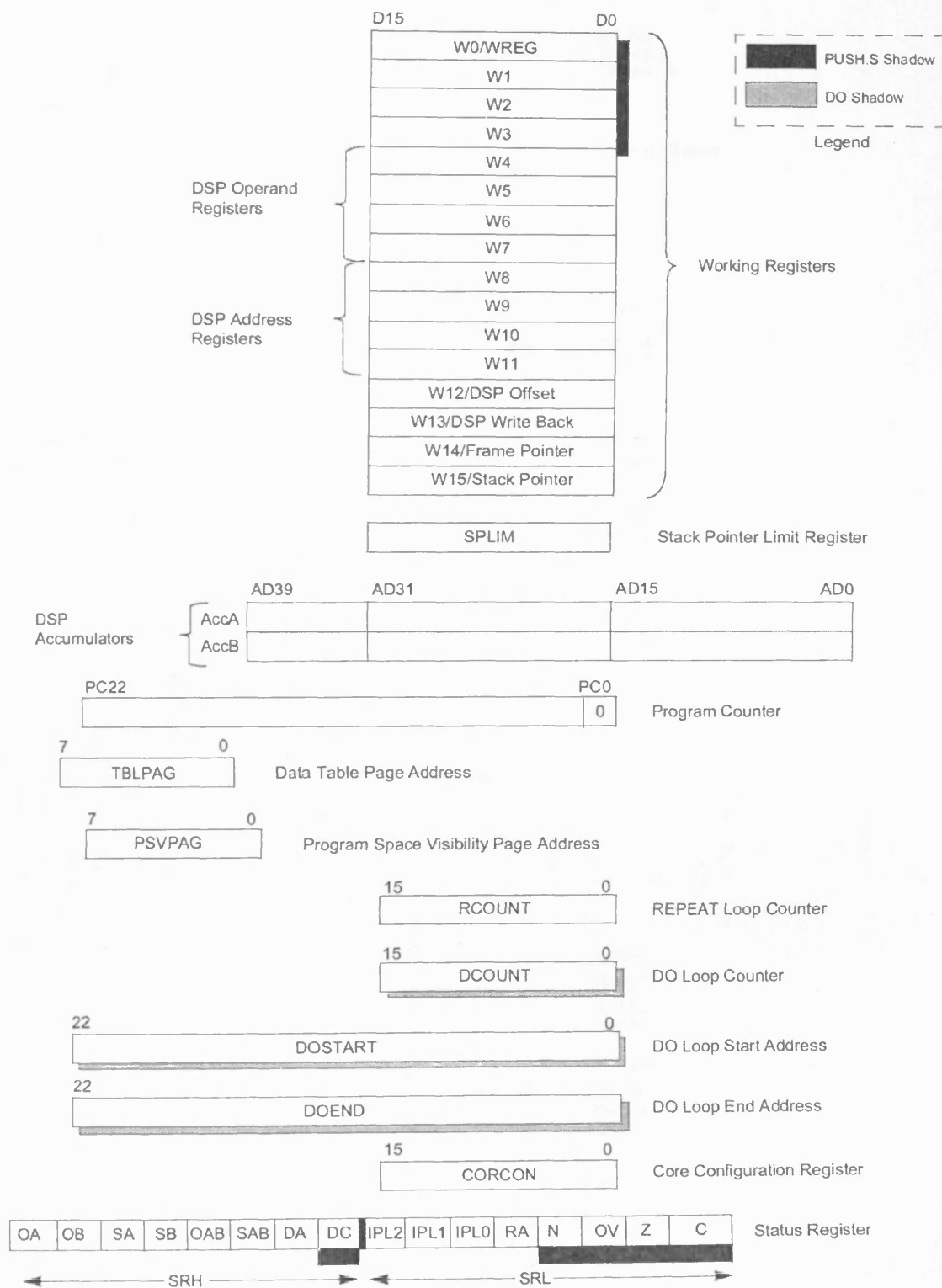
Special Microcontroller Features:

- Enhanced Flash program memory:
  - 10,000 erase/write cycle (min.) for industrial temperature range, 100K (typical)
- Data EEPROM memory:
  - 100,000 erase/write cycle (min.) for industrial temperature range, 1M (typical)
- Self-reprogrammable under software control
- Power-on Reset (POR), Power-up Timer (PWRT) and Oscillator Start-up Timer (OST)
- Flexible Watchdog Timer (WDT) with on-chip low power RC oscillator for reliable operation
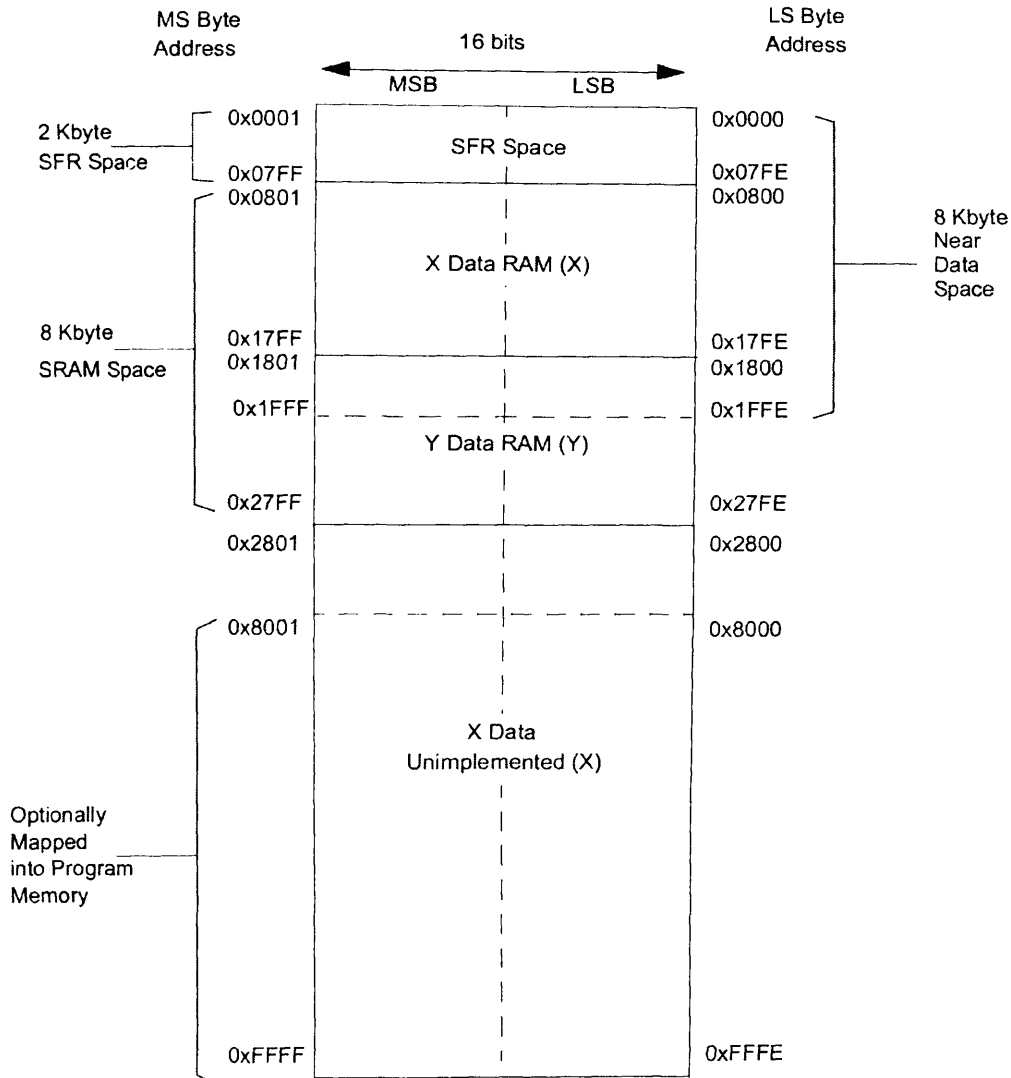
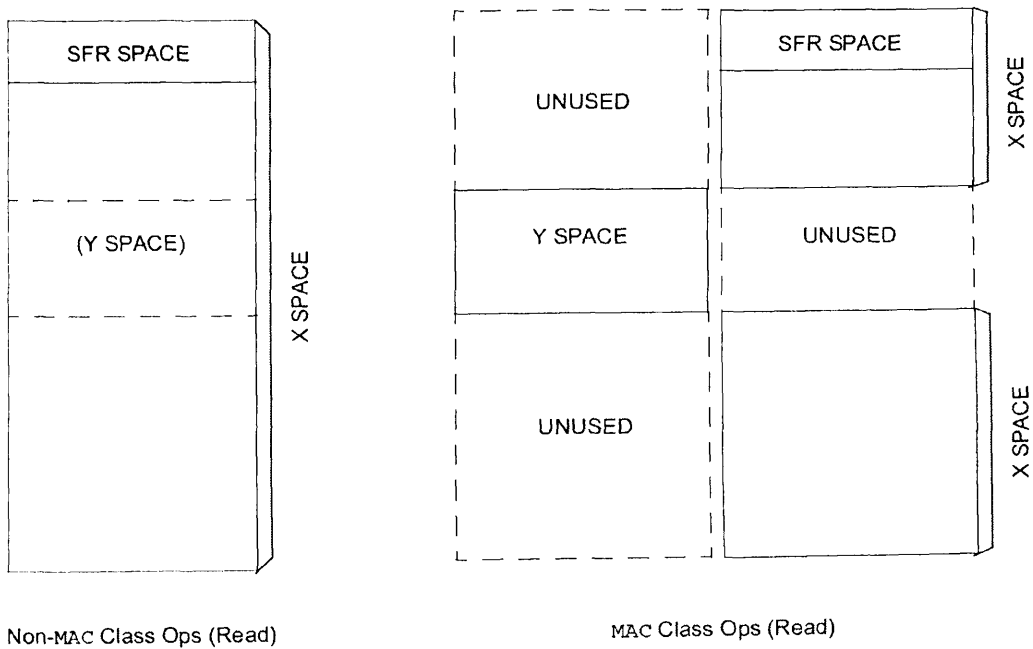# Pin Diagram of dsPIC30F6014

Programmer's Model for dsPIC30F

Program Space Memory Map for dsPIC30F6014

Reset - GOTO Instruction	000000
Reset - Target Address	000002
	000004
Interrupt Vector Table	
	00007E
Reserved	000080
Alternate Vector Table	000084
	0000FE
User Flash Program Memory (48K instructions)	000100
	017FFE
Reserved (Read '0's)	018000
	7FEFFE
Data EEPROM (4 Kbytes)	7FF000
	7FFFFE
	800000
Reserved	
	8005BE
UNITID (32 instr.)	8005C0
	8005FE
Reserved	800600
	F7FFFE
Device Configuration Registers	F80000
	F8000E
	F80010
Reserved	
	FEFFFE
DEVID (2)	FF0000
	FFFFFE

Vector Tables (000004 – 000080)

User Memory Space (000000 – 7FFFFE)

Configuration Memory Space (800000 – FFFFFE)

Data space Memory Map for dsPIC30F6014

MS Byte
Address

16 bits

MSB   LSB

LS Byte
Address

2 Kbyte
SFR Space

0x0001

SFR Space

0x0000

0x07FF

0x07FE

8 Kbyte
Near
Data
Space

0x0801

0x0800

X Data RAM (X)

8 Kbyte
SRAM Space

0x17FF

0x17FE

0x1801

0x1800

0x1FFF

0x1FFE

Y Data RAM (Y)

0x27FF

0x27FE

0x2801

0x2800

0x8001

0x8000

X Data
Unimplemented (X)

Optionally
Mapped
into Program
Memory

0xFFFF

0xFFFE

Data space for MCU and DSP (MAC class) Instructions

SFR SPACE
(Y SPACE)

X SPACE

UNUSED
Y SPACE
UNUSED

SFR SPACE
UNUSED

X SPACE

X SPACE

Non-MAC Class Ops (Read)

MAC Class Ops (Read)

219

Schematic diagrams dsPICDEM 1.1 Development Board

CAN and Serial Communication Interfaces

R16 CHART 1%
R17 CHART 1%
R18 CHART 1%

REVISIONS
ZONE	REV.	DESCRIPTION	DATE	APPROVED

Q1 CHART
Q2 R42

R19 CHART 1/2W

C4 CHART 50V
C5 CHART 50V

U4 CHART

RX 14
FILT 15
FILT2 16
REF 11
DCT 2
VREG 9
VREG2 10
REXT 13
REXT2 12
IGND 3

QB 7
QE 8
QE2 1

RNG1 5
RNG2 6

RNG1 RNG2

R15 10ohm 4 C18

3000V UF? C3

PSTN

R27 CHART   R28 CHART
R26 CHART
C9 CHART 50V

C10 CHART 50V   C11 OPEN 50V   Z2 CHART

R29 CHART   R30 36K

Q3 R42

R31 CHART 1%   R32 CHART 1%   R33 CHART 1%

R34 CHART
C12 CHART 50V

R42 Q4

R20 CHART 1%

R24 CHART 1%   R25 CHART 1%

C6 CHART 50V   R21 CHART 1%   R22 CHART 1%   C7 .1uF 50V   C8 .1uF 50V   R23 CHART 1%   Z1 5.6V   D1 MMBD7000

C13 CHART 250V   MOV1 CHART

IGND I+

3000V UF? C15

Note: For JATE support C11 should be populated with a 0.1 uF, 16V
Tant/Elec/X7R, +/-20% and R23 should be populated with a
2.7nF, 16V, X7R, +/-20% capacitor

	Si3035	Si3034
C5	1.0uF,16V	.1uF,16V
C5	OPEN	.47uF,25V
C13	15nF,250V	10nF,250V
C4	OPEN	.22uF,35V
C6	OPEN	.68uF,16V
C12	OPEN	.01uF,16V
C10	OPEN	1800pF,50V
Q1	OPEN	BCP56T
R19	51ohm,1/2W	OPEN
R22	15ohm,1/4W	402ohm
R27,R28	301ohm	OPEN
R34	36K	120K
R23	OPEN	10K
R20	OPEN	78.7ohm
R21	OPEN	215ohm
R26	301ohm	2.2K
R29	OPEN	150ohm
R24	0ohm	OPEN
R25	OPEN	0ohm
R16,R17,R18	OPEN	4.87K
R31,R32,R33	OPEN	4.87K
MOV1	240V MOV	OPEN
U4	Si3012	Si3014
Z2	18V	43V

PARTS LIST

| QTY FSCH | PART OR | NOMENCLATURE | MATERIAL |
| REQD NO. | IDENTIFYING NO. | OR DESCRIPTION | SPECIFICATION |

UNLESS OTHERWISE SPECIFIED
DIMENSIONS ARE IN INCHES
TOLERANCES ARE:
FRACTIONS DECIMALS ANGLES
XX
XXX

MATERIAL

FINISH

NEXT ASSY   USED ON

APPLICATION   DO NOT SCALE DRAWING

CONTRACT NO.
1552

DIVERSIFIED ENGINEERING
& MANUFACTURING, INC.

MICROCHIP
dsPICDEM.net 1 DEMO BOARD
dsPICDEM.net 2 DEMO BOARD

APPROVALS	DATE
DRAWN D ROSS	4/4/02
CHECKED	
ISSUED	

SIZE FSCM NO.   DWG. NO. 03-01679   REV. B
C
114102

SCALE   SHEET 5 OF 11

Schematic diagrams dsPICDEM.net Board

10 base-T MAC/PHY interface

Block Diagram of CAN module of dsPIC30F

CAN Buffers and Protocol Engine

BUFFERS

TXB0	TXB1	TXB2
MSGREQ · TXABT · TXLARB · TXERR · MTXBUFF · MESSAGE	MSGREQ · TXABT · TXLARB · TXERR · MTXBUFF · MESSAGE	MSGREQ · TXABT · TXLARB · TXERR · MTXBUFF · MESSAGE

Message Queue Control

Transmit Byte Sequencer

Acceptance Mask RXM1

Acceptance Filter RXF2

Acceptance Mask RXM0

Acceptance Filter RXF3

Accept

Acceptance Filter RXF0

Acceptance Filter RXF4

Accept

Acceptance Filter RXF1

Acceptance Filter RXF5

RXB0 — Identifier — MAB — Identifier — RXB1

Data Field   Data Field

PROTOCOL ENGINE

Transmit Shift	Receive Shift
CRC Generator	CRC Check

Receive Error Counter — RERRCNT

— TERRCNT

Transmit Error Counter — Err Pas — Bus Off

Protocol Finite State Machine

Transmit Logic

Bit Timing Logic

Bit Timing Generator

CiTX[1]   CiRX[1]

Note 1: i = 1 or 2 refers to a particular CAN module (CAN1 or CAN2).

Tool breakage Simulation
(Electronic Appendix)

Please refer to the attached CD (folder "Appendix B") for the animation.

Some Screen shots are given below:-
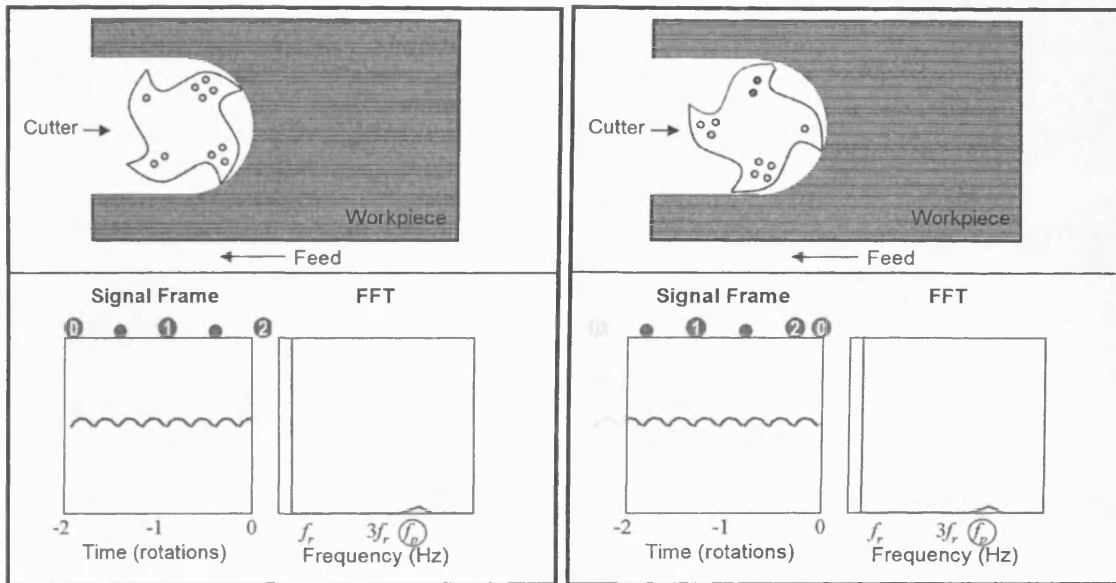
(a) Healthy Tool

(b) At tool breakage
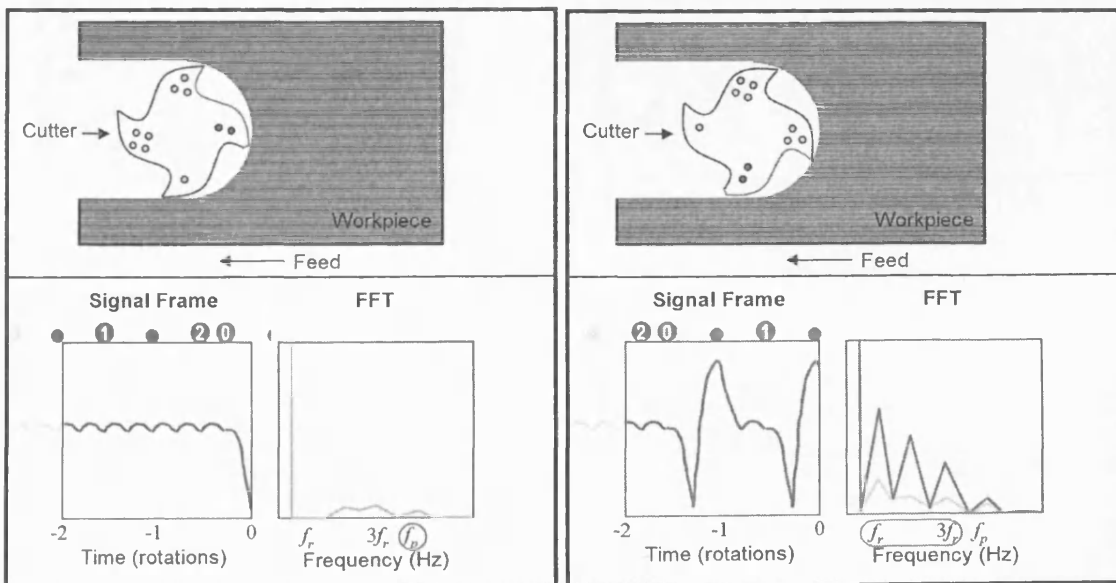
(c) First FFT after tool breakage

(d) Tool breakage detection in 1.5 rotations

225

Additional Tool breakage Test Results

Modelled Cutting Forces and FFT for 4 and 8 teeth Cutters

4 Teeth cutter	8 Teeth cutter

New Cutter

FFT

New Cutter

FFT

Broken Cutter

FFT

Broken Cutter

FFT
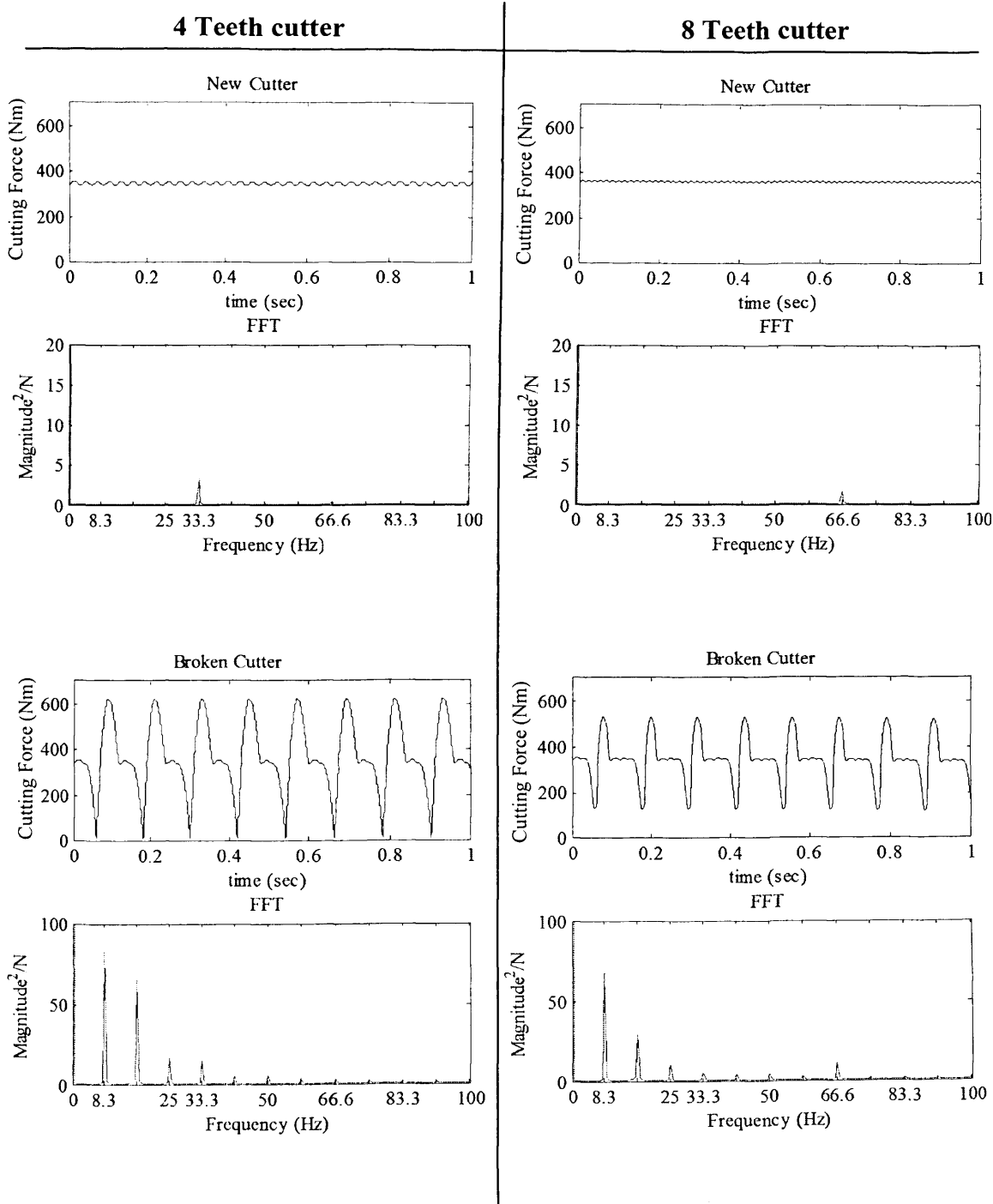
Overlap FFT analysis of simulated tool breakage

(a)   0.5 mm DOC
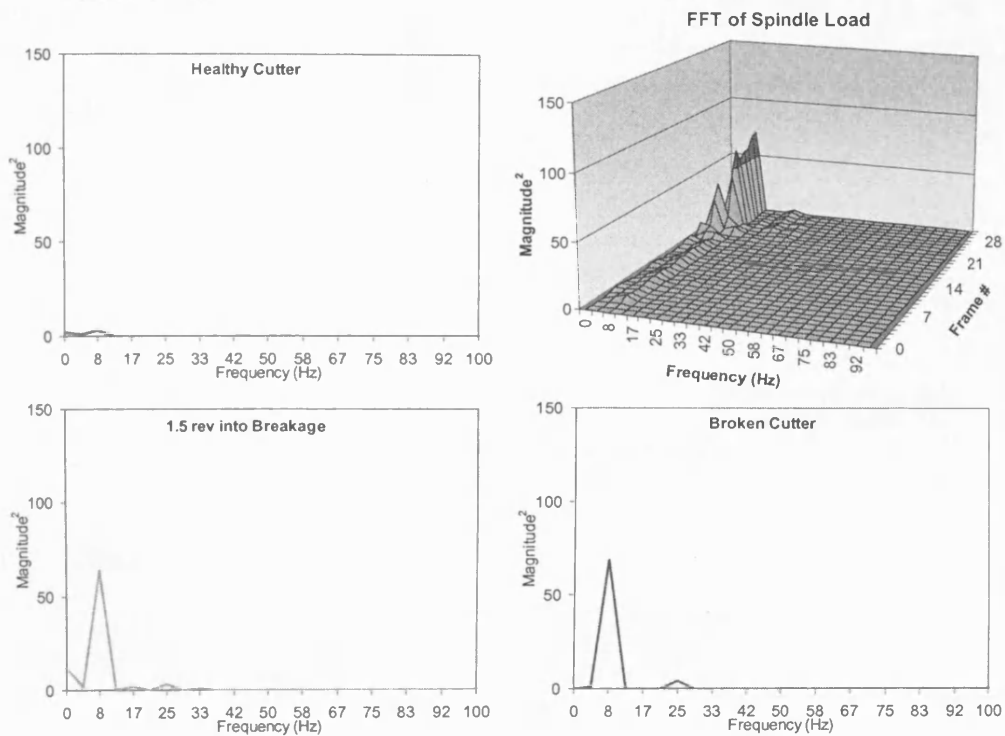
(b)   1.0 mm DOC
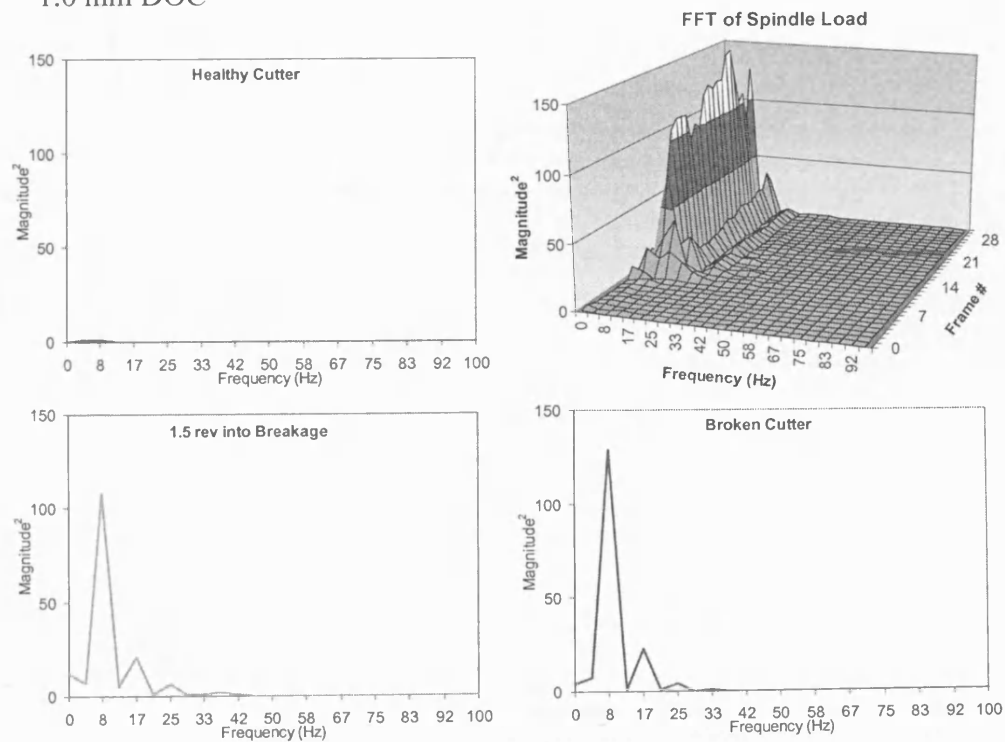
Mean Frequency for simulated tool breakage Tests

(a) 0.5 mm DOC
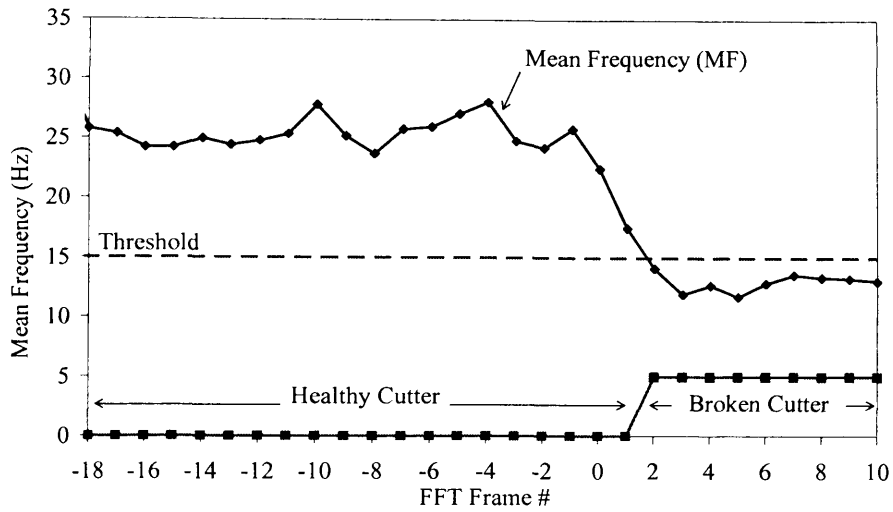
(b) 1.0 mm DOC
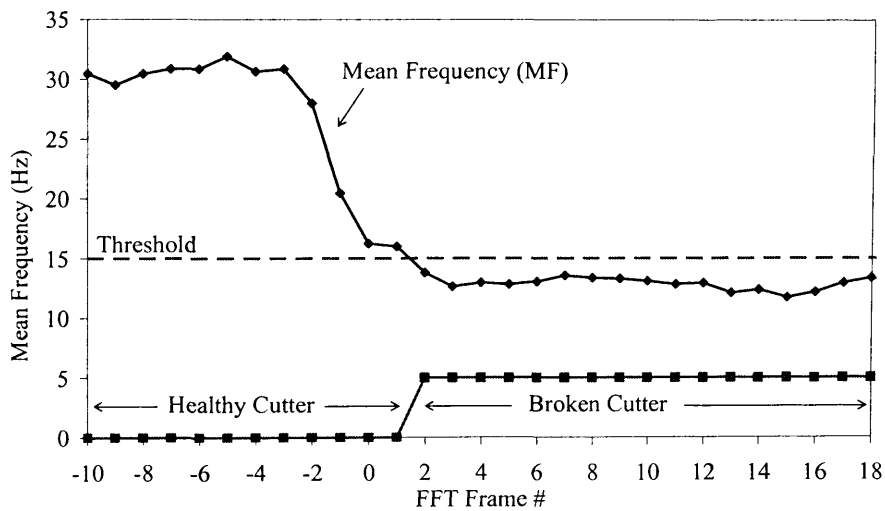
(b) 1.5 mm DOC
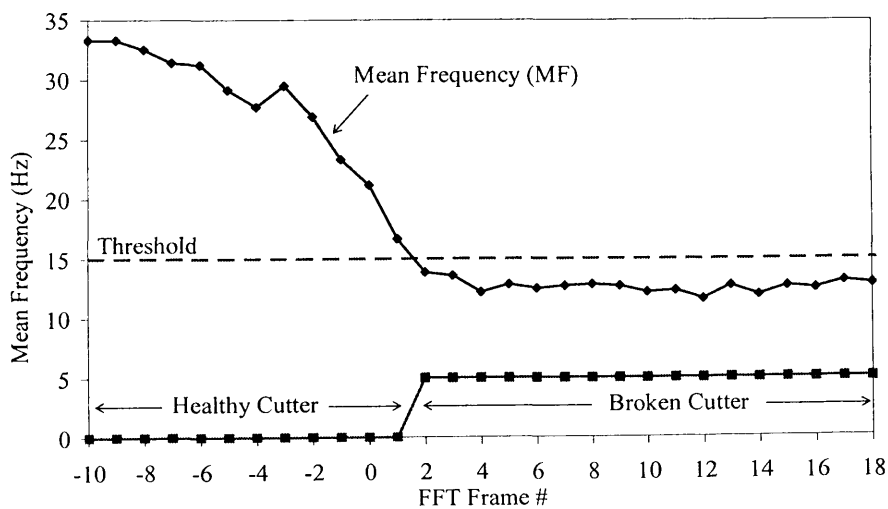
Tool Entry & Exit (DOC=1mm, DOC, feed rate =200mm/min, Ns=500rpm)

New Cutter

Spindle Load (Watts)

Tool Entry

Processed Signal

Spindle Load

Tool Exit

Spindle Load (Watts)

Spindle Load

Small peak to peak for new cutter

Spindle Load (Watts)

Tool Entry

Spindle Load

Processed Signal

Tool Exit

Broken Cutter

Spindle Load (Watts)

Spindle Load

Large peak to peak for broken cutter

Time (sec)

229
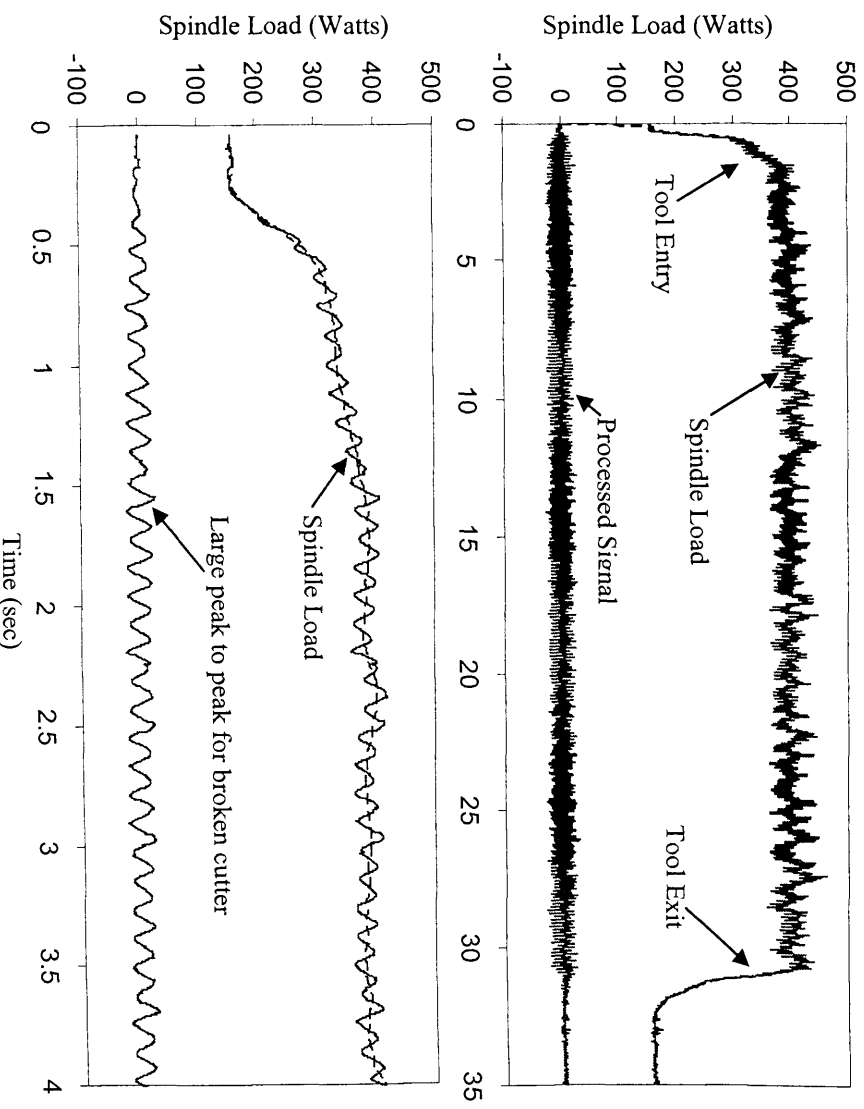
Tool Entry & Exit (DOC=2mm, DOC, feed rate =150mm/min, Ns=450rpm)

New Cutter
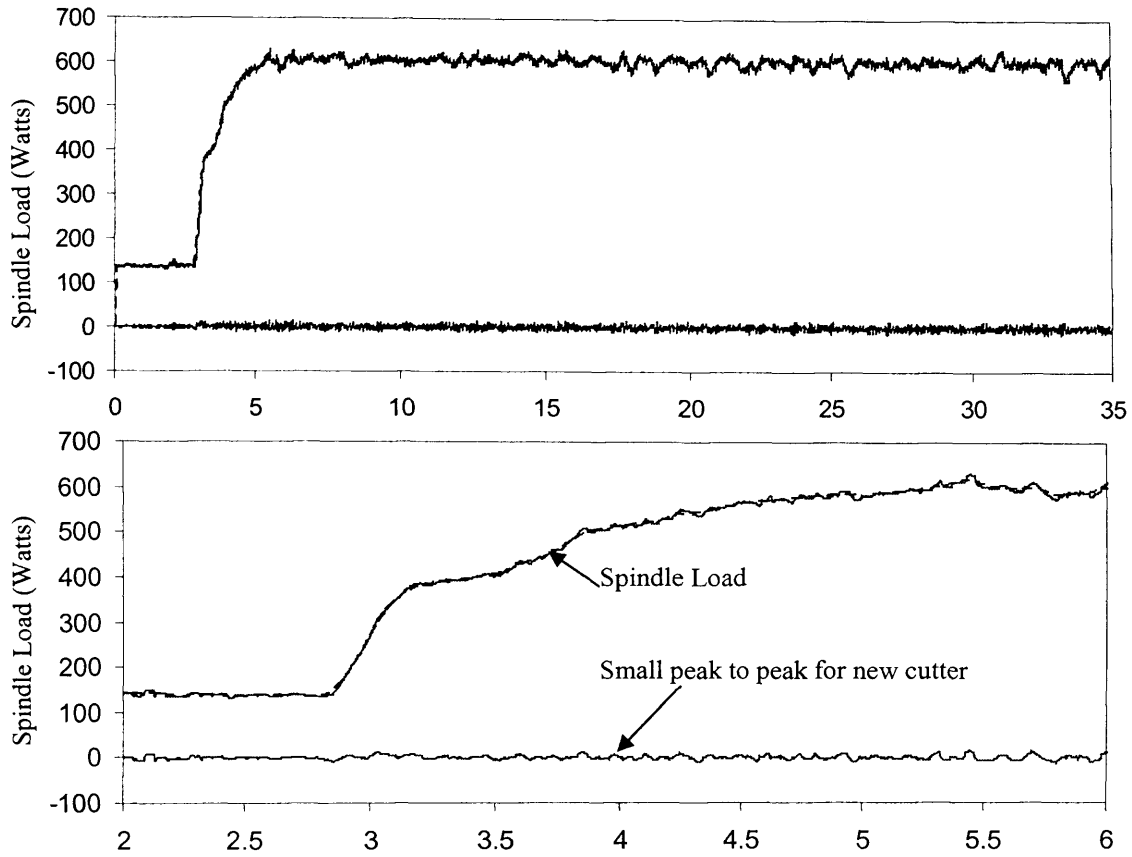
Broken Cutter
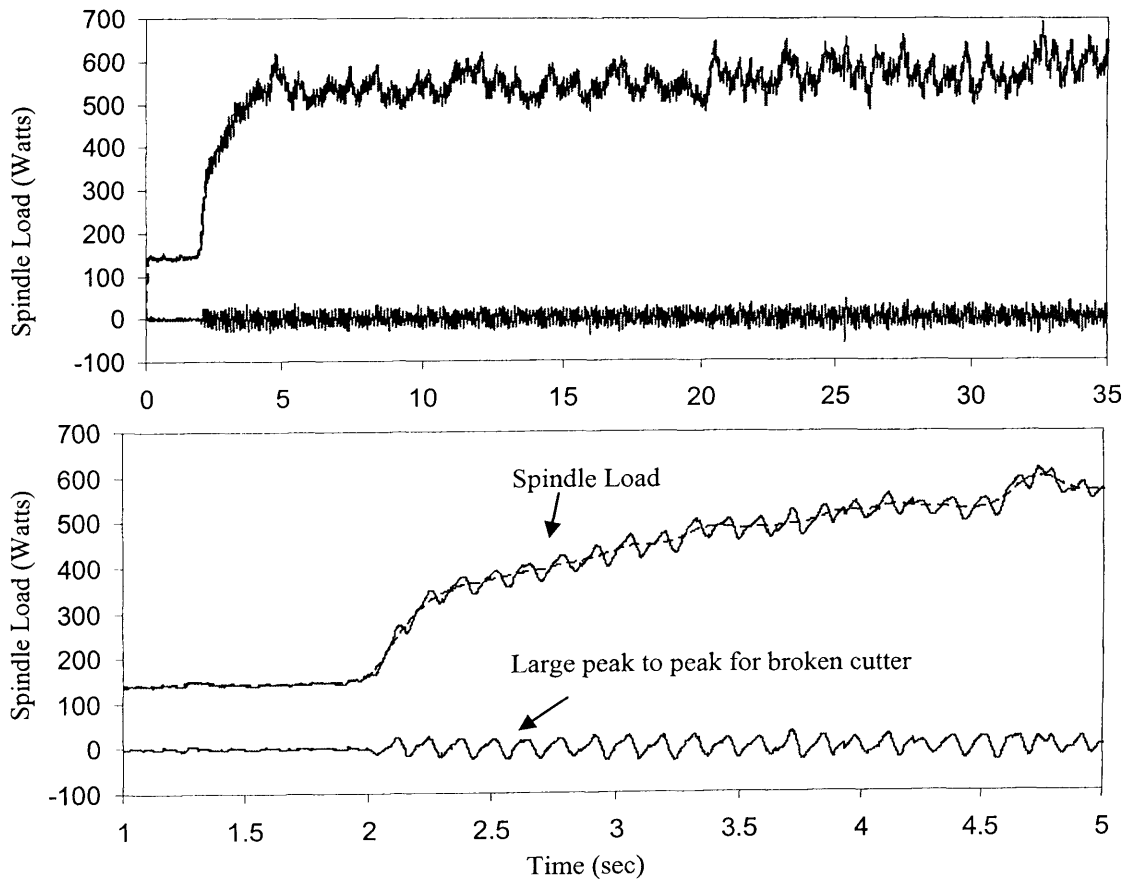
Tool Entry & Exit (DOC=1mm, DOC, feed rate =150mm/min, Ns=500rpm)
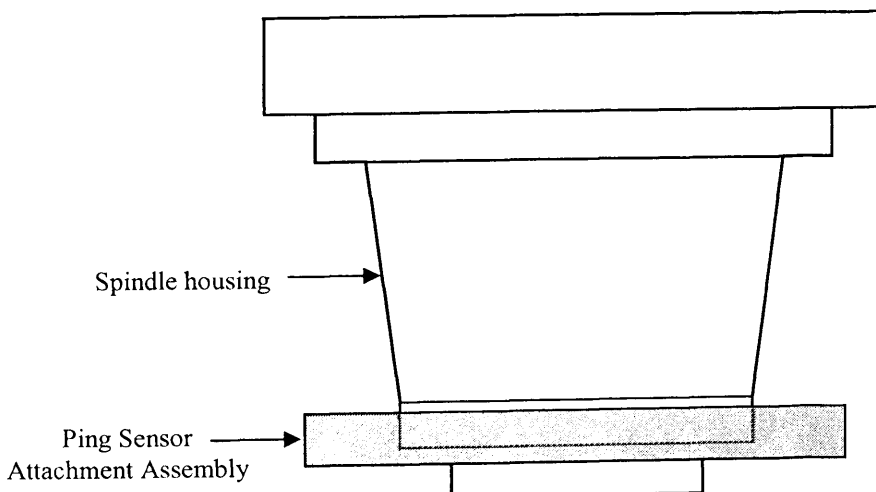
New Cutter
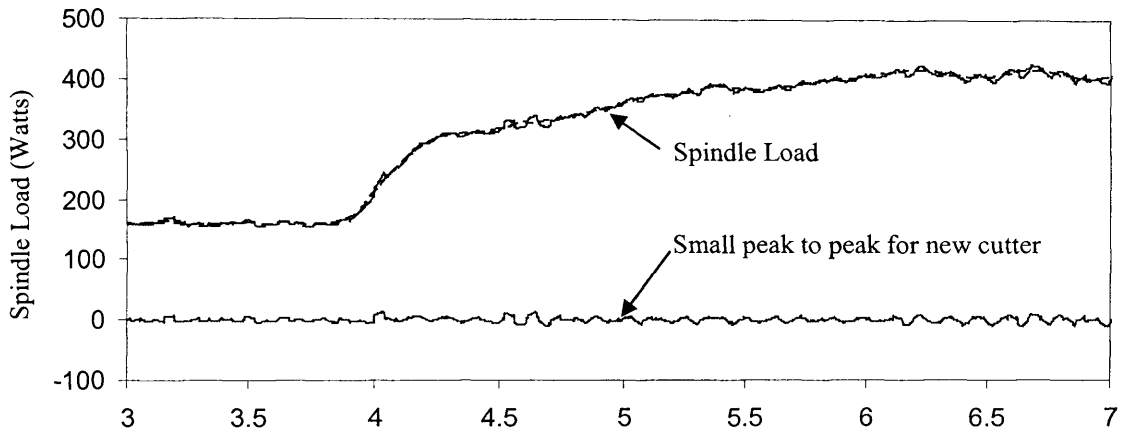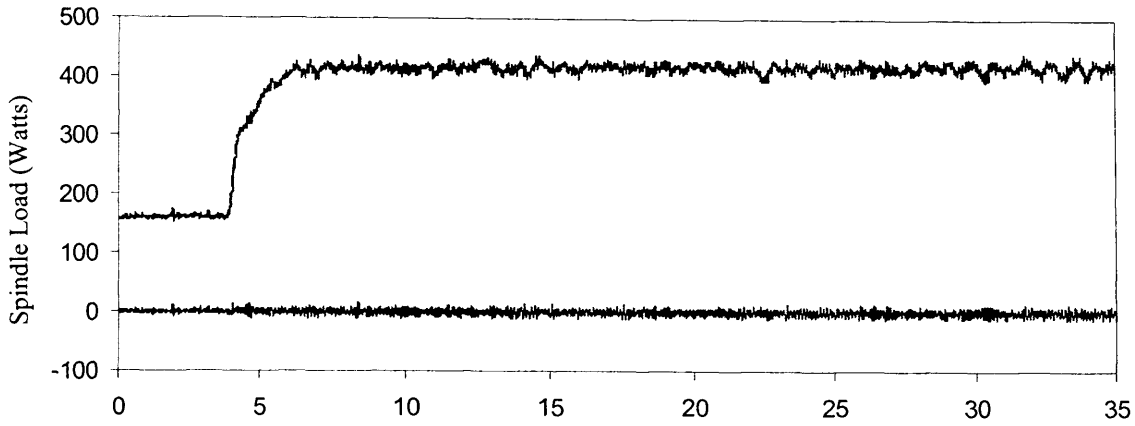
Broken Cutter
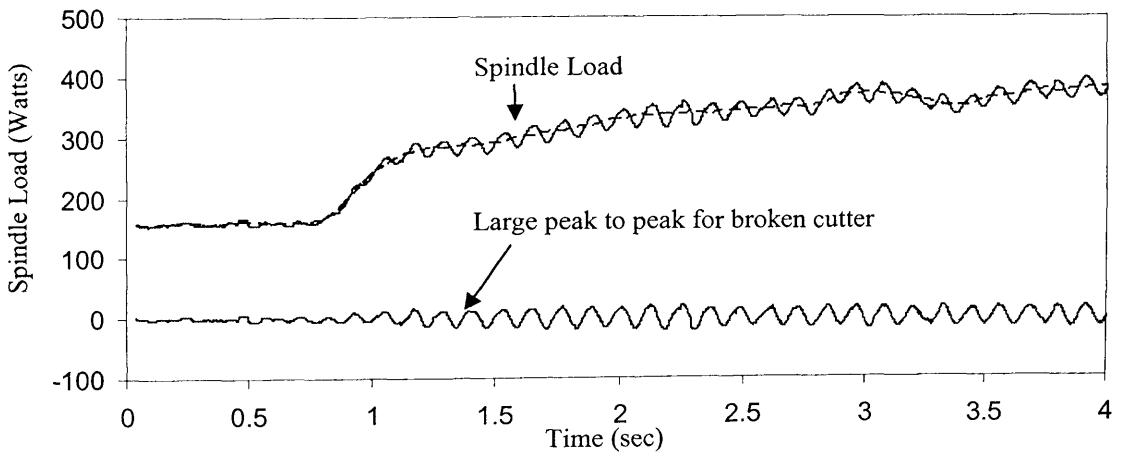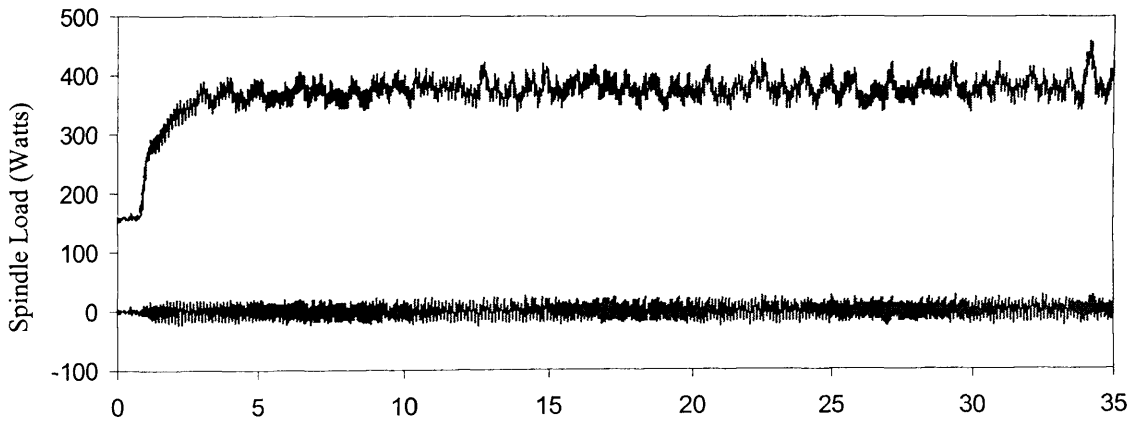
Sensor Attachment Assembly

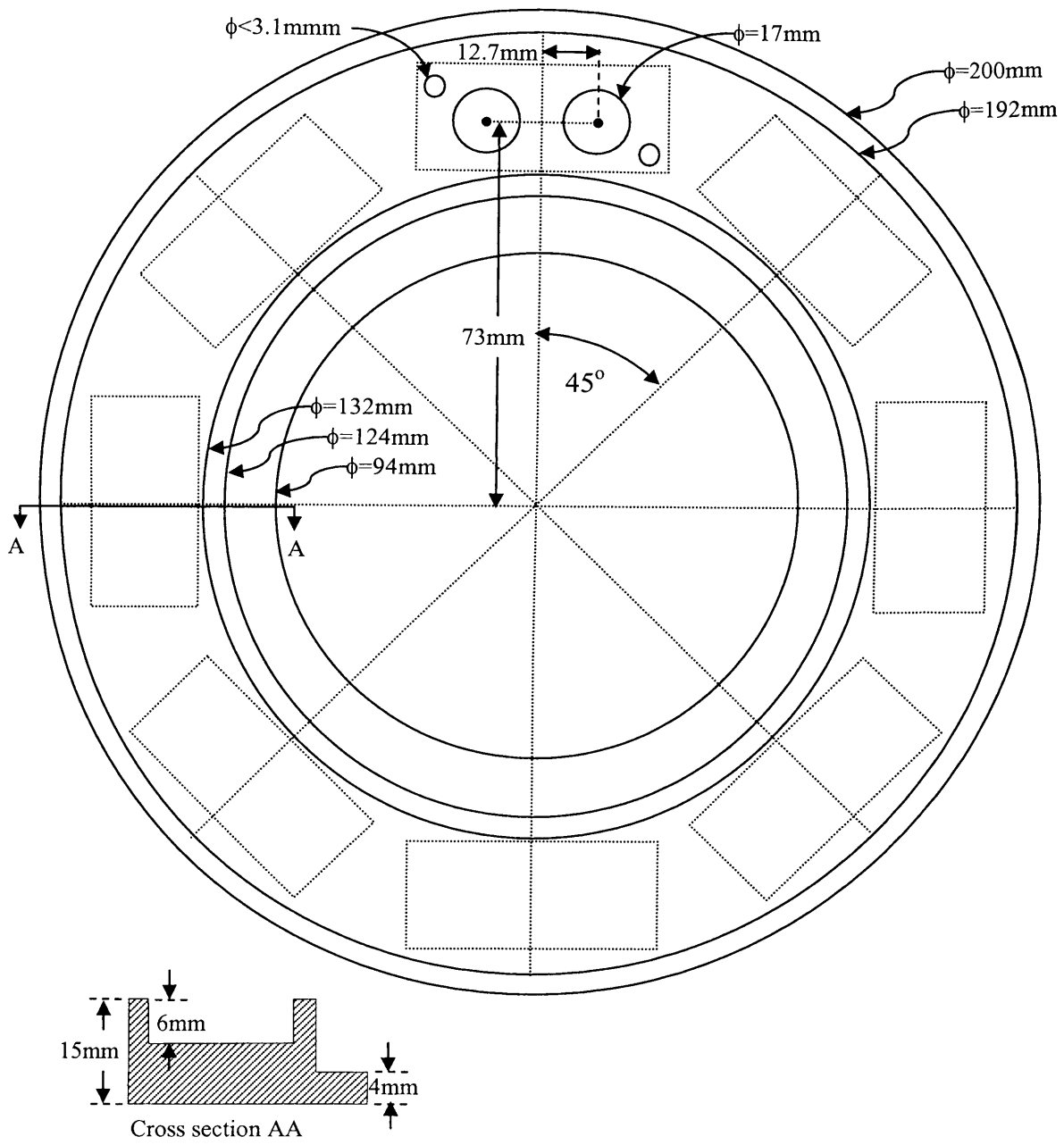*Sensor's Data Sheets are provided in attached CD in folder "Appendix D"*
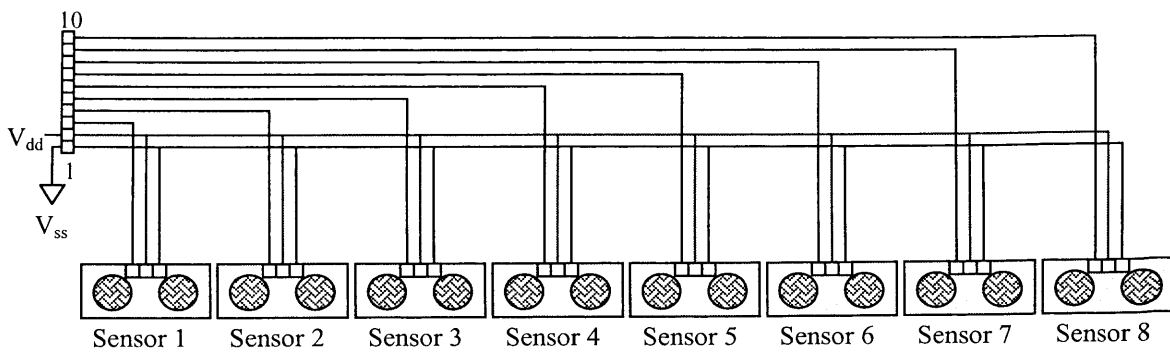
Spindle Housing Dimensions
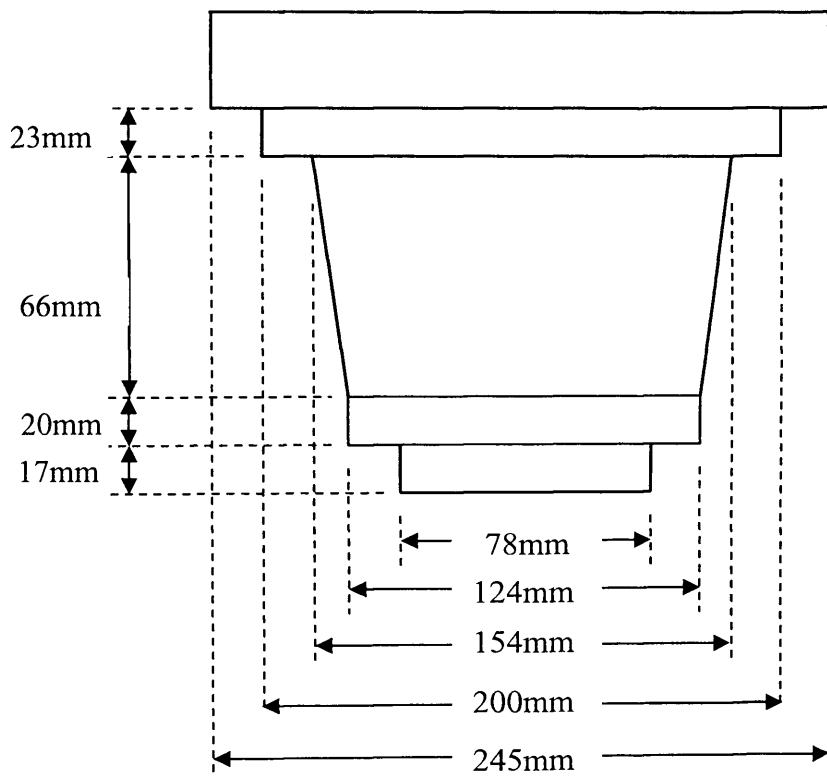
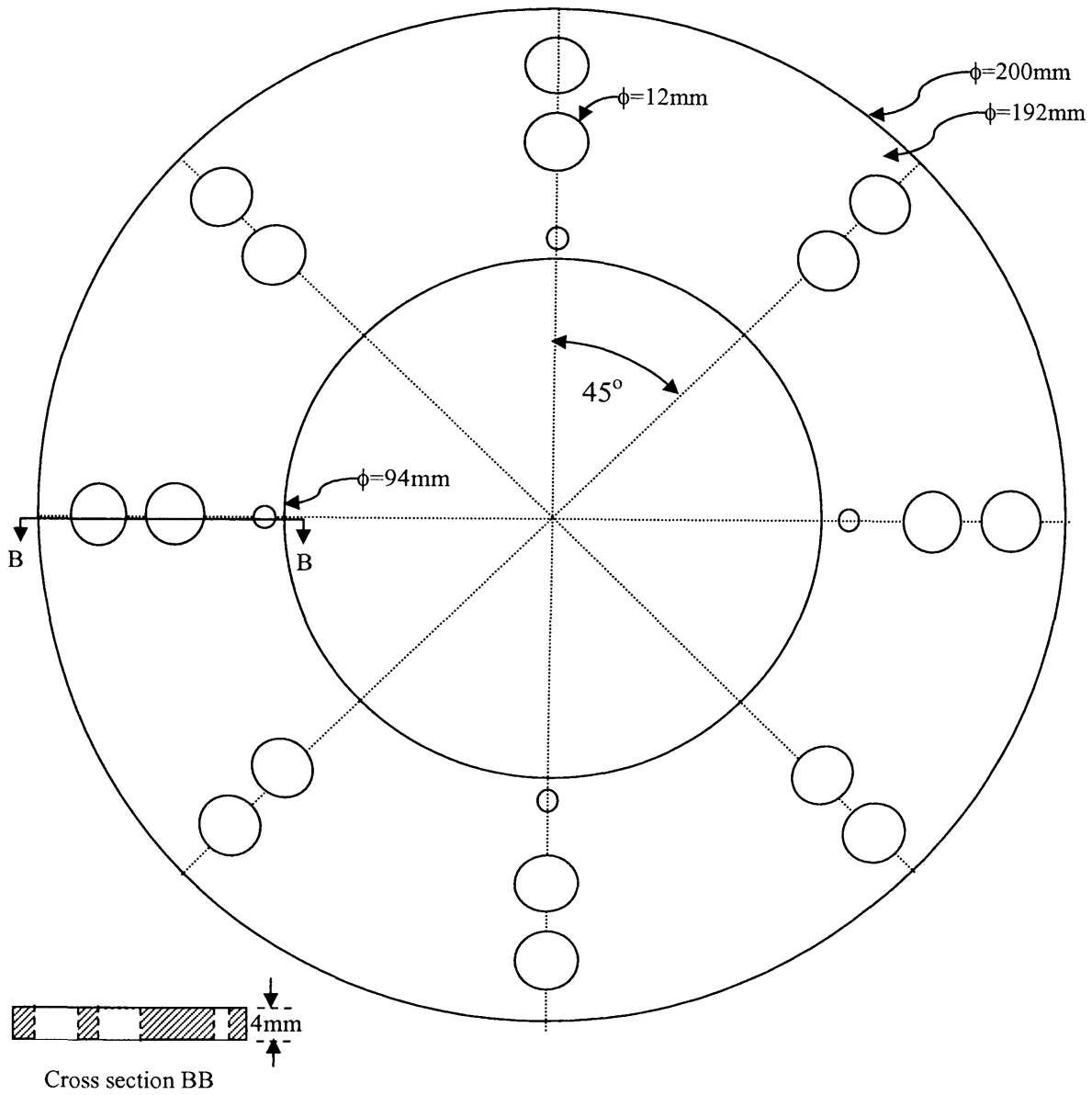## Location of Sensor Attachment Assembly

Ping Sensor Attachment Assembly

φ<3.1mmm
φ=17mm
12.7mm
φ=200mm
φ=192mm
73mm
45°
φ=132mm
φ=124mm
φ=94mm
A
A

15mm
6mm
4mm
Cross section AA

Connection Diagram

10
V_{dd}
1
V_{ss}

Sensor 1   Sensor 2   Sensor 3   Sensor 4   Sensor 5   Sensor 6   Sensor 7   Sensor 8

233

UNAM Sensor Attachment Assembly

ϕ=200mm
ϕ=192mm
ϕ=12mm
45°
ϕ=94mm
B
B
4mm

Cross section BB

Location of Sensor and Attachment Assembly

Spindle housing

UNAM Sensor
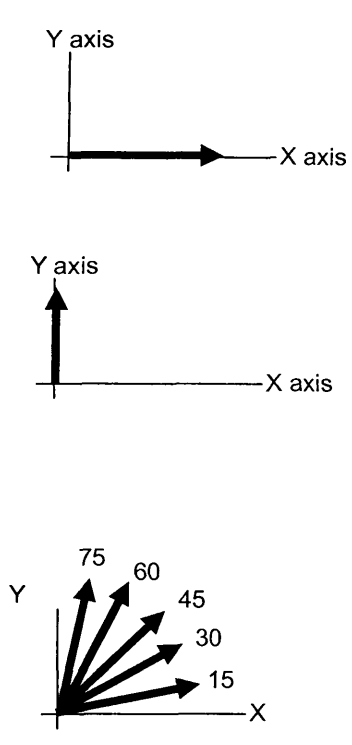
Attachment Assembly

234
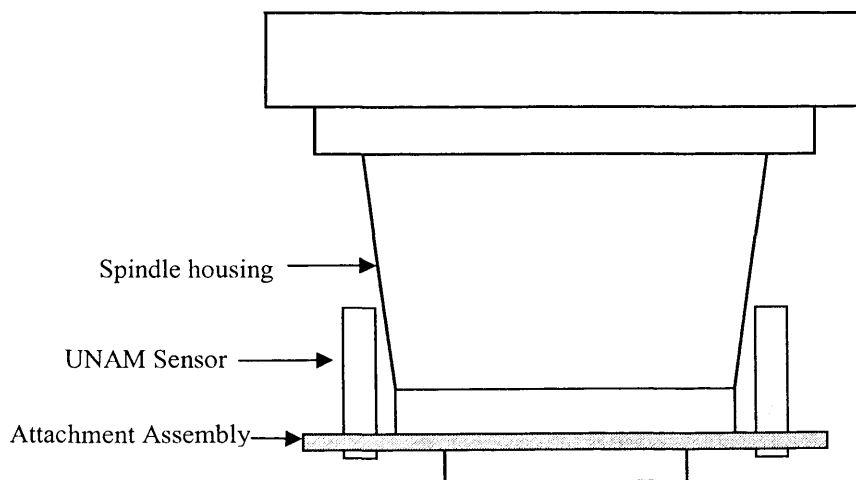
Direction of Cut and Feedrate Estimation

Cutting Tests

Following tests were performed to establish relationship between X and Y feed dive motor current for feedrate and Cutting direction

TEST	Feed Rate	Cutting Angle
1	100	0
2	150	0
3	200	0
4	250	0
5	300	0
6	100	90
7	150	90
8	200	90
9	250	90
10	300	90
11	100	15
12	100	30
13	100	45
14	100	60
15	100	75
16	200	15
17	200	30
18	200	45
19	200	60
20	200	75

For these tests appropriate G Codes were written to specify the start and stop position to make the work piece move in desired direction.

For example for Test 11:

Start position = (0, 0) mm

Stop position = (50, 13.4) mm and so on.

This provided bout 30 seconds of data for analysis

The feed motors are 3 phase motors. Therefore only two current components (R and S phase) were acquired and third component was calculated via following equation.
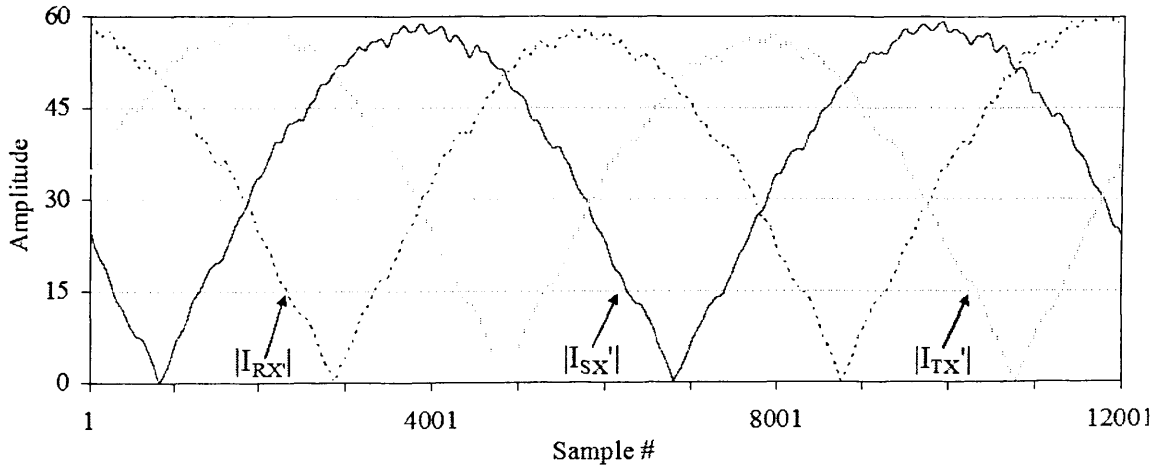
$$I_{TX} = -I_{SX} - I_{QX}$$ since $I_R + I_S + I_T = 0$ for 3 phase motor.

Processing of the acquired current signals (at 8Ksps) is shown in following figures.
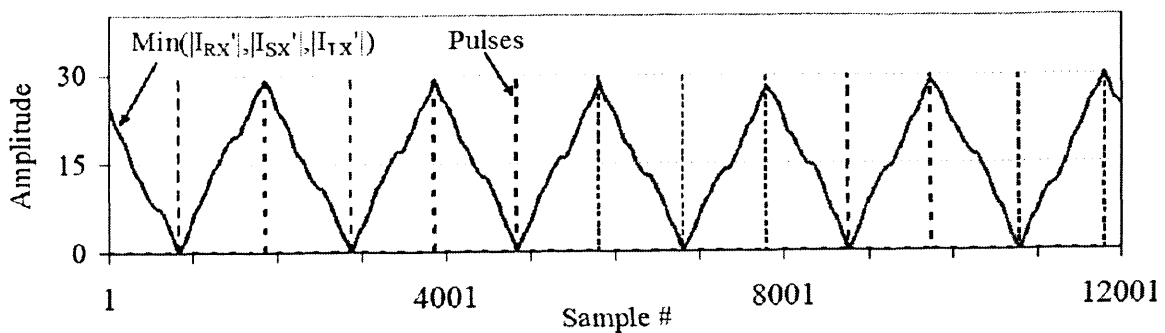
The X axis feed motor currents:
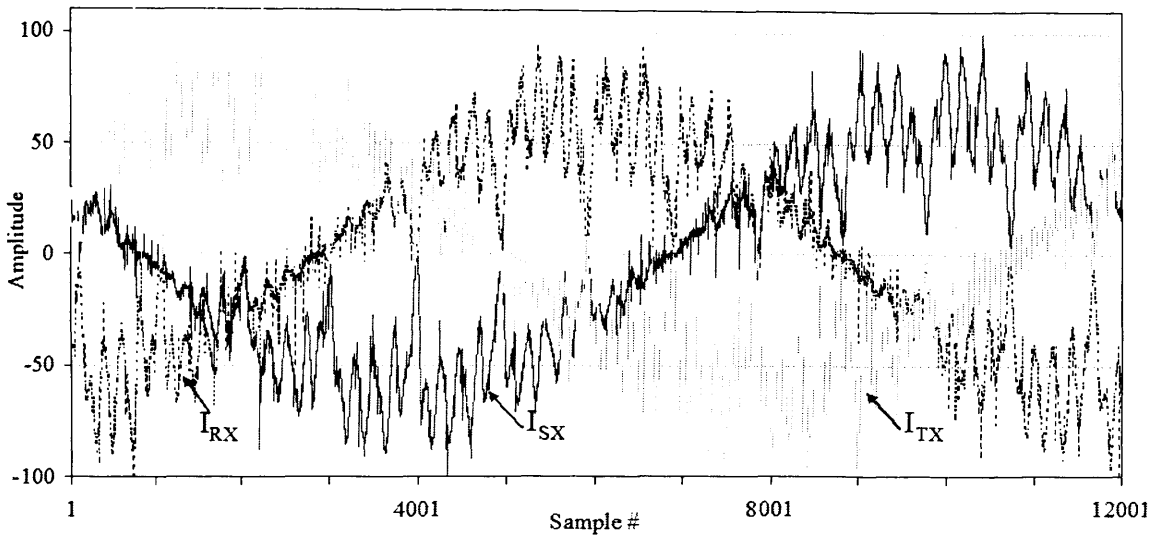
Filtered and Absolute Valued Signals:

Further processing and Generated pulses on min and max values for exact time period measurement which are used to calculate feedrate

236

The pulse rate f_1 is number of pulses in one second.

Also, $f_1 = 1/\Delta T$

Where, ΔT is time between consecutive pulses. These two methods are used to calculate the frequency of the signal (f)

$$f = f_1/12$$

$$feedrate = \frac{120 \times pitch \times f}{P} \text{ [mm/min]}$$

P is number of poles in the motor (in this case $P=8$).

Pitch is the distance between consecutive threads on the drive shaft (in this case *pitch* = 10 mm).

Therefore

$$feedrate = \frac{120 \times 10 \times f_1}{8 \times 12} = 12.5 \times f_1 = \frac{12.5}{\Delta T} \text{ [mm/min]}$$

Let *xfeedrate* and *yfeedrate* be the feedrate in X and Y direction then the direction/ angle θ is calculated using following equation

$$\theta = \tan^{-1}\left(\frac{xfeedrate}{yfeedrate}\right) \text{ [degrees]}$$

Calculations of feedrate and Direction of cut

Test No	X feedrate (mm/min)	Y Feedrate (mm/min)	Resultant Feedrate (mm/min)	Cutting Direction (degrees)
1	100	0	100	0
2	150	0	150	0
5	0	100	100	90
6	0	150	150	90
11	96.59	25.88	100	15
12	86.60	50	100	30
13	70.71	70.71	100	45
14	50	86.60	100	60
15	25.88	96.59	100	75
16	193.19	51.764	200	15
17	173.21	100	200	30
18	141.42	141.42	200	45
19	100	173.21	200	60
20	51.764	193.19	200	75

Application of Technique for whole cutting cycle

At Tool Entry

At Tool Exit

These plots show that the technique described is capable of finding the feedrate under all varying cutting condition and different events such as tool entry, tool exit and milling into shoulders.
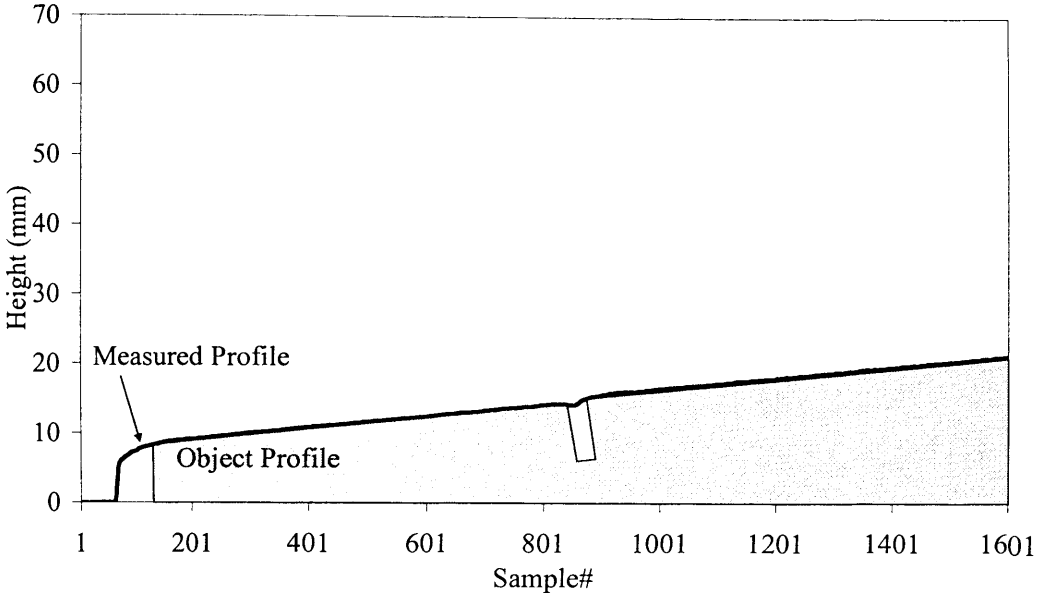
Additional Sensor Analysis Tests

PING Sensor Analysis Tests

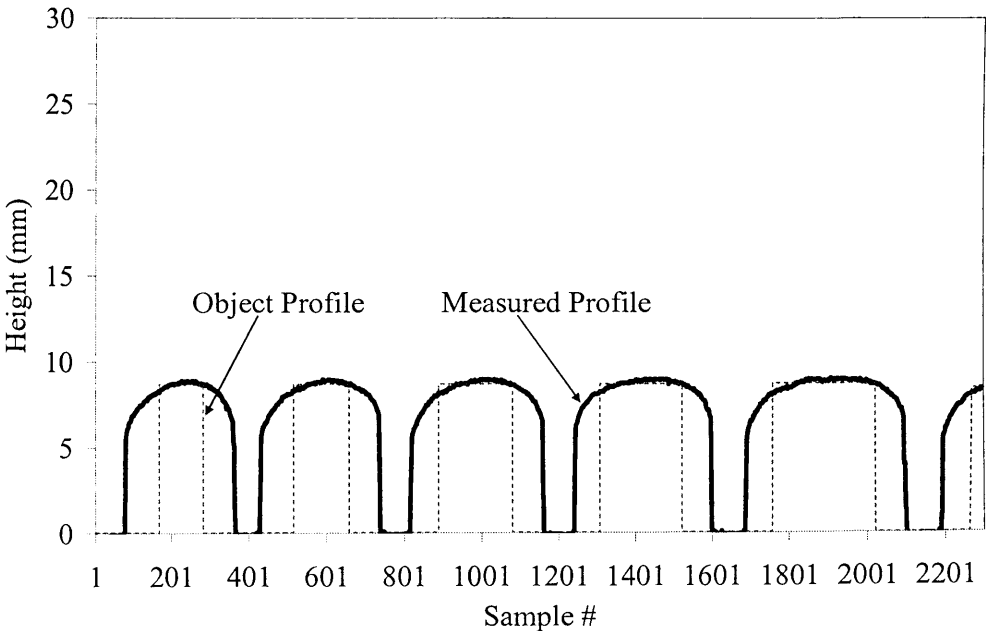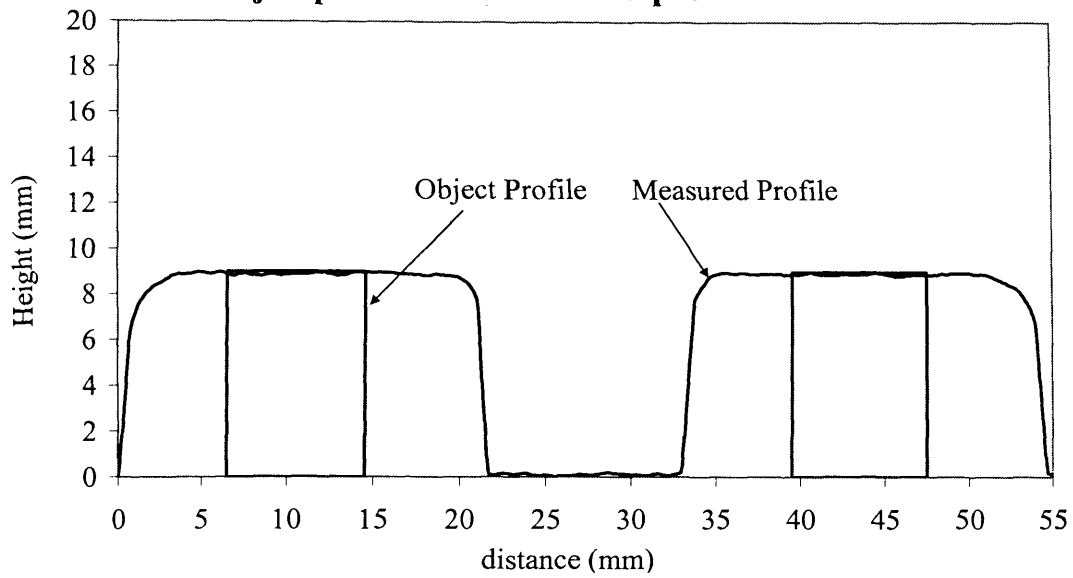**Restricting and focusing the ultrasonic signal**
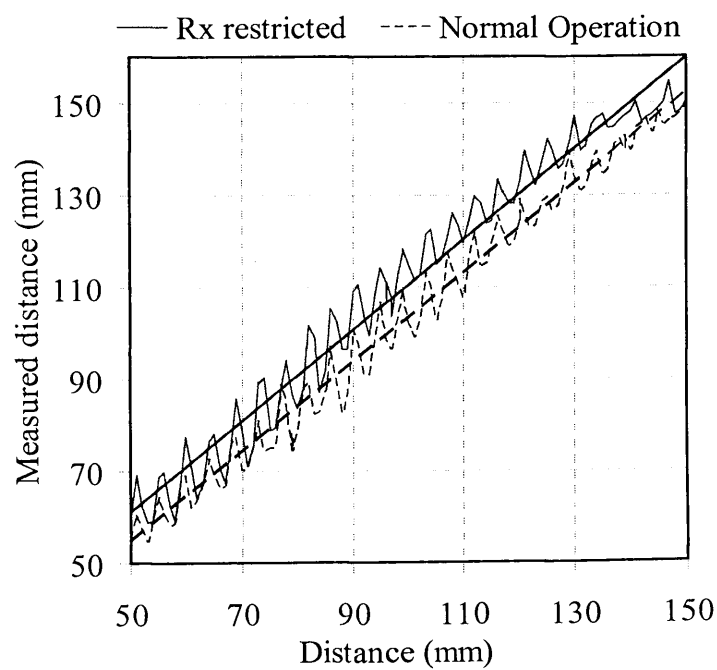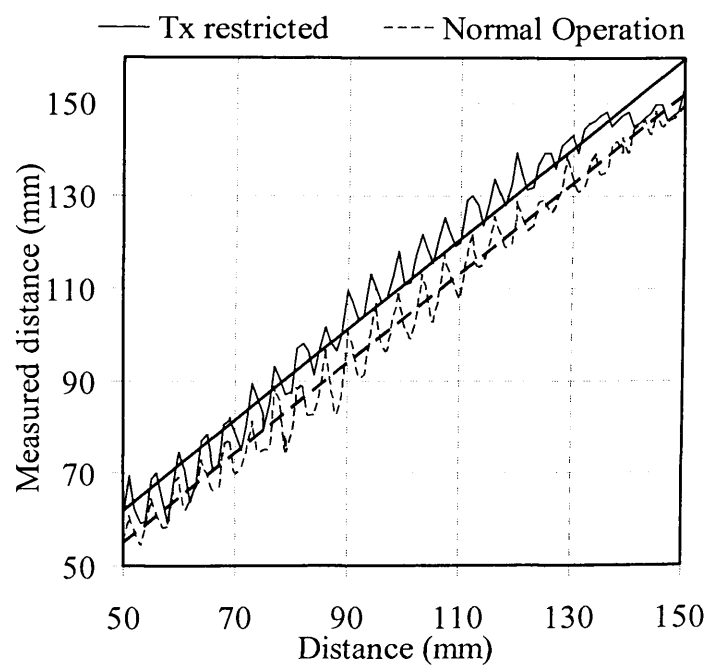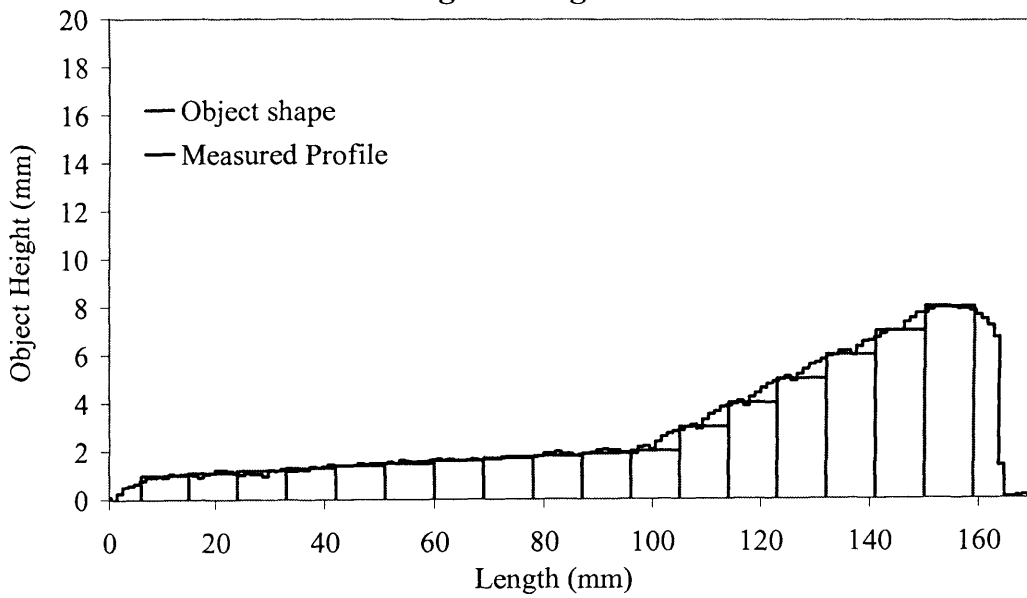
UNAM Sensor Analysis Tests

Measurement on Slope

Measurement on the Object Edges

Determination of Object profile from Sensor Output

Object Profile   Measured Profile

y-axis: Height (mm), 0 to 20
x-axis: distance (mm), 0 to 55

Measurement on Incremental changes in height

— Object shape
— Measured Profile

y-axis: Object Height (mm), 0 to 20
x-axis: Length (mm), 0 to 160

11mm hole detection and object profile measurement

Object Profile   Measured Profile

hole   hole

y-axis: distance(mm), 0 to 20
x-axis: height(mm), -10 to 120

6.25mm   6.25mm   6.25mm

φ=11mm   75mm   φ=11mm   25mm

241
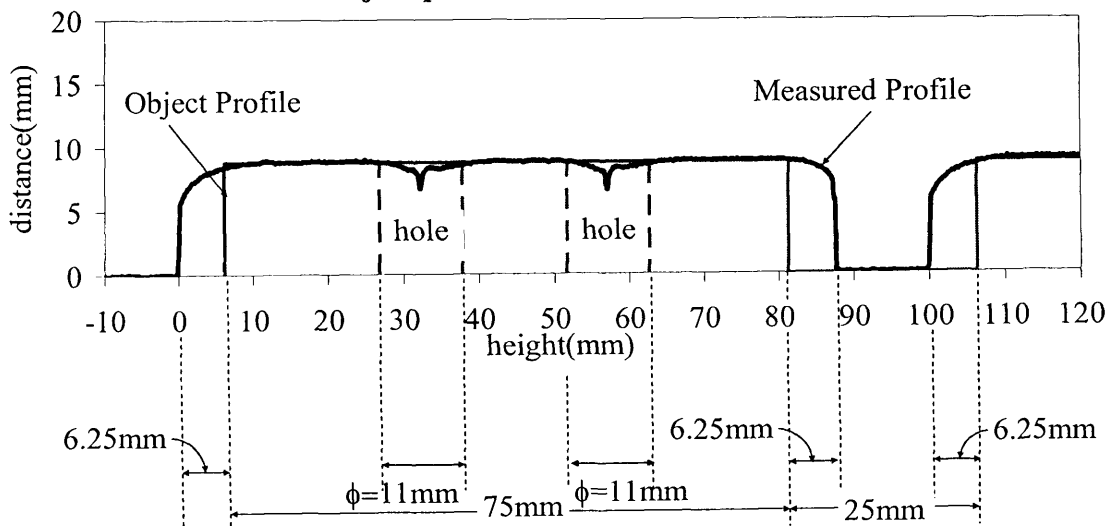
Appendix G

List of Publications from Research Work

Full Text of these publications is provided in attached CD in folder "Appendix G"

1. R.A. Siddiqui, Q. Ahsan, R.I. Grosvenor and P.W. Prickett, "The role of Emerging Technologies in e-Monitoring," *in proceeding of COMADEM 31st August – 2nd September 2005, 18th International Congress on Condition Monitoring and Diagnostic Engineering Management, Cranfield UK.* Cranfield University Press, UK ISBN 1871315913, pp. 263–271.

(Oral presentation in the 18th International Congress on Condition Monitoring and Diagnostic Engineering Management, Cranfield, UK)

2. Q. Ahsan, R.A. Siddiqui, R.I. Grosvenor and P.W. Prickett, "Adaptable e-Monitoring System for Multi-Loop," *in proceeding of COMADEM 31st August – 2nd September 2005, 18th International Congress on Condition Monitoring and Diagnostic Engineering Management, Cranfield UK.* Cranfield University Press, UK ISBN 1871315913, pp. 211–220.

(Oral presentation in the 18th International Congress on Condition Monitoring and Diagnostic Engineering Management, Cranfield, UK)

3. R.A. Siddiqui, Q. Ahsan, W. Amer, M. Al-Yami, R.I. Grosvenor and P.W. Prickett, "Distributed Process Monitoring and Management," *In proceeding of IEEE International Conference on Engineering of Intelligent Systems, ICEIS 2006,* 22-23 April 2006. Islamabad, Pakistan. Pp 336-341.

(Oral presentation in the IEEE International Conference on Engineering of Intelligent Systems, 2006, Islamabad, Pakistan)

4. R.A. Siddiqui, M. Al-Yami, R.I. Grosvenor and P.W. Prickett, "On-line Measurement of Process Parameter for e-Monitoring Applications" *in proceeding of COMADEM 10-13th June 2008, 21st International Congress on Condition Monitoring and Diagnostic Engineering Management, Prague Czech Republic.* ISBN 978 80 254 2276 2, pp. 435–444.

5. M. Al-Yami, R.A. Siddiqui, R.I. Grosvenor and P.W. Prickett, "A Pressure-based Approach to the Monitoring of a Pneumatic Parallel Gripper" *in proceeding of COMADEM 10-13th June 2008, 21st International Congress on Condition Monitoring and Diagnostic Engineering Management, Prague Czech Republic.* ISBN 978 80 254 2276 2, pp. 33–42.

Journal Paper

6. R.A. Siddiqui, W. Amer, Q. Ahsan, R.I. Grosvenor, P.W. Prickett, "Multi-band Infinite Impulse Response Filtering using Microcontrollers for e-Monitoring Applications," *International Journal of Microprocessors and Microsystems,* vol. 31, 2007, pp. 370–380.